MONASH University

The Interplay of Cytokines in the Pathogenesis of Female Reproductive Cancer

A thesis submitted for the degree of
Doctor of Philosophy

by
Irene Papageorgiou
B.Science (Honours)

Faculty of Medicine, Nursing and Health Sciences,
Department of Molecular and Translational Sciences,
Centre for Innate Immunity and Infectious Diseases,
Hudson Institute of Medical Research,
Monash University, Australia,
August 2018

Under the Supervision of
Assistant Professor Nollaig Bourke
&
Professor Paul Hertzog

HUDSON INSTITUTE OF MEDICAL RESEARCH | CENTRE FOR INNATE IMMUNITY AND INFECTIOUS DISEASES | MonashHealth

Table of contents

Copyright Notices

General Declaration

This thesis contains no material which has been accepted for the award of any other degree or diploma at any university or equivalent institution and that, to the best of my knowledge and belief, this thesis contains no material previously published or written by another person, except where due reference is made in the text of the thesis.

Signature: 

Print Name: Irene Papageorgiou

Date: 23/08/2018

Thesis Including Published Works Declaration

I hereby declare that this thesis contains no material which has been accepted for the award of any other degree or diploma at any university or equivalent institution and that, to the best of my knowledge and belief, this thesis contains no material previously published or written by another person, except where due reference is made in the text of the thesis.

This thesis includes 1 original paper published in peer reviewed journal. The core theme of the thesis is to examine the roles of cytokines in the pathogenesis of female reproductive cancers. The ideas, development and writing up of all the papers in the thesis were the principal responsibility of myself, the student, working within the Centre for Innate Immunity and Infectious Diseases, Hudson Institute of Medical Research Hudson Institute of Medical Research, Faculty of Medicine, Nursing and Health Sciences, under the supervision of Professor Paul Hertzog and Dr Nollaig Bourke.

The inclusion of co-authors reflects the fact that the work came from active collaboration between researchers and acknowledges input into team-based research.

I have not renumbered sections of submitted or published papers in order to generate a consistent presentation within the thesis.

In the case of Chapter 2, my contribution to the work involved the following:

Thesis Chapter	Publication Title	Status	Nature and % of student contribution	Co-author name(s) Nature and % of Co-author's contribution*	Co-author(s), Monash student
2	Expression of nodal signalling components in cycling human endometrium and in endometrial cancer	Published	Involved in project conception, design, performed experiments, as well as data analysis and prepared the manuscript. 80%	1) Peter K. Nicholls: participated in immunohistochemistry studies. **2%** 2) Fang Wang: involved in PCR studies. **4%** 3) Martin Lackmann: provided the Cripto monoclonal antibodies. **1.5%** 4) Yogeshwar Makanji: revised the manuscript. **0.5%** 5) Lois A. Salamonsen: provided endometrial tissues and intellectual input. **1%** 6) David M. Robertson: involved in the project design and intellectual input. **1%** 7) Craig A. Harrison: involved in project conception, provided intellectual input, and manuscript editing. **10%**	**No**

Student signature: [redacted] **Date:** 23/08/2018

The undersigned hereby certify that the above declaration correctly reflects the nature and extent of the student's and co-authors' contributions to this work. In instances where I am not the responsible author I have consulted with the responsible author to agree on the respective contributions of the authors.

Main Supervisor signature: [redacted] **Date:** 23/08/2018

Publications

Papageorgiou I, Bourke N, Antony Y Matthews AY, Lim S, de Weerd NA, Hertzog PJ. The Anti-Tumourigenic roles of Interferon Epsilon in Endometrial Cancer. *Prepared for submission*. August 2018.

Papageorgiou I, Lackmann M, Harrison CA, Robertson DM. Monoclonal Antibody Treatment Targeting Nodal Signalling Reverses Cancer Cell Tumourigenesis. *Prepared for submission*. August 2018.

Bourke NM, Achilles SL, Huang SU, Cumming HE, Papageorgiou I, Gearing LJ, Thakore S, Mangan NE, Mesiano S, Hertzog PJ. Human IFNε: Spaciotemporal expression, hormone regulation and innate immunity in the female reproductive tract. *bioRxiv*. October 16, 2018.

Papageorgiou I, Nicholls PK, Wang F, Lackmann M, Makanji Y, Salamonsen LA, Robertson DM, Harrison CA. Expression of nodal signalling components in cycling human endometrium and in endometrial cancer. *Reproductive biology and endocrinology*. 2009 October 29; 7: p. 122.

Conference Proceedings and Presentations

Oral Presentations

2016

Careers Development Week, St Raphael's Greek Language, High School, Brighton, Melbourne, Australia, May.

Presentation titled: *"Medical Research at the Hudson Institute and Female Reproductive Tract Cancer"*.

2007

Prince Henry's Institute (14th) Student Symposium, Monash Medical Centre, Clayton, Melbourne, Australia, November.

Abstract title: *"The Role of Nodal Signalling in Tumourigenesis"*.

2006

Prince Henry's Institute (13th) Student Symposium, Monash Medical Centre, Clayton, Melbourne, Australia, November.

Abstract: *"The Role of Cripto in Tumourigenesis"*.

TGF-β Family Meeting, Prince Henry's institute, Monash Medical Centre, Clayton, Melbourne, Australia, May.

Presentation title: *"The role of Cripto in Tumourigenesis"*.

Poster Presentations

2017

Monash Health Translation Precinct Research Week, Monash Medical Centre, Clayton, Melbourne, Australia, November.

Abstract title: *"The anti-tumourigenic properties of IFNε in endometrial cancer".*

Victorian Infection and Immunity Network Symposium. Walter and Eliza Hall Institute, Parkville, Melbourne, Australia, October.

Abstract title: *"Interferon epsilon regulates proliferation and apoptosis of reproductive tract epithelium".*

2009

Southern Health Research Week, Monash Medical Centre, Clayton, Melbourne, Australia, February.

Abstract title: *"The Role of Nodal Signalling in Tumourigenesis".*

2008

The 20th Lorne Cancer conference, Lorne, Victoria Melbourne, Australia, February.

Abstract title: *"The Role of Nodal Signalling in Tumourigenesis"*

Awards and Prises Arising from this Thesis

2009

Highly Commended Poster Award in Cancer Research Category, Southern Health Research Week Poster Competition, Monash Medical Centre, Clayton, Melbourne, Australia, February.

2006

Novo Nordisk, Award for Student Excellence, First Year PhD, Novo Nordisk, Prince Henry's Institute 13th Student Symposium, Monash Medical Centre, Clayton, Melbourne, November. Received the prize of $100.00 Borders voucher.

Acknowledgements

I would like to extend my immense gratitude to my supervisors, **Assistant Professor Nollaig Bourke**, and **Professor Paul Hertzog** for giving me the opportunity to finalize my PhD at the Regulation of Interferon and Innate Signalling (RI&IS) laboratory. Your patience and understanding regarding my CFS/ME condition was paramount to my progress and instrumental towards thesis completion. I have been very blessed by your guidance, mentorship and enthusiasm. Paul's optimistic approach boosted my confidence and helped me get through all the difficulties. Paul, you are an extraordinary scientist, but above all, an amazing human being. Nollaig, you've been a remarkable supervisor and have extended your support above and beyond the human constraints of distance, from the other side of the world. You have always been there for me, even during the day of my e-thesis submission, emailing me and constantly encouraging me. You are an incredible scientist and a beautiful person.

I would also like to thank all CiiiD (Centre for Innate Immunity and Infectious Disease) members for welcoming me in their laboratory. A special thank you to all members of the RI&IS group including: **Anthony Matthews, Dr San Lim, Dr Nicky De Weerd, Stephanie Huang, Dr Helen Cumming, Jodee Gould, Zoe Marks, Dr Ross Chapman, Dr Jamie Gearing, Dr Michelle Tate, Dr Evelin de Geus, Dr Niamh Mangan, Isaac Woodhouse, Dr Rebecca Smith, Dr Deborah Bianco and Madelynne White,** for creating such a lovely working and collaborative scientific environment to carry out research. I am extremely appreciative for all their technical assistance and valuable feedback during our group meetings. I am especially grateful to **Anthony Matthews** for his incredible dedication to our laboratory and for his help especially afterhours. I would like to thank **Dr Evelin de Geus,** for all her help with the FACS analysis experiments.

I would also like to thank my Honours supervisor **Professor Martin Lackmann,** who is sadly missed! You were an inspiring scientist and mentor and sparked my interest in cancer research. I will always remember our philosophical discussions fondly. Thank you for all of your valuable input towards the chapter 2 and 3 studies and especially for producing the monoclonal antibodies. These studies would have not existed, without your support. You will live forever in my memories!

I thank **Associate Professor David Robertson** and **Associate Professor Craig Harrison** for supervising all studies carried out in chapter 2 and chapter 3. I appreciate your guidance and support.

I am especially grateful to the Monash Graduate Education (MGE) administration team and especially to **Victoria Kasapidis** for all her advice throughout my PhD. I am very appreciative to the MGE for their understanding during my illness, and for allowing me to resume my PhD work and continue part time, after 4 years of absence. A big thank you to **Zuzana Quinn** for her valuable advocacy which helped me overcome my study conundrums. I also thank the disability support services team for their assistance.

I am very thankful to all my Doctors: **Professor Stephen Holdsworth, Dr Jacques Joubert, Dr Marian Miller, Dr Anne Applebe, Dr John Sweica, Associate Professor Jack Gerschman, Dr Leonid Handjsuk,** and **Dr Kim Hayes** for overseeing me during the worst state of my health and helping me manage my chronic illness and resume my PhD. I can't thank them enough for their perseverance in dealing with a mystery illness with unknown to date aetiology.

To all my friends and family: **Bimps, Stella, Julian, Nikos, Theodore, Helen, Stavros, Svetlana, Christina, Akis and Jenny, Nick, Ritsa, John, Dimitra, Alex, Anitoula, Jimmie,**

Lynette, Elias, as well as **Maria and Stefanos Baltatzis,** a big thank you for all your patience and encouragement throughout my PhD journey.

I would also like to thank all the people involved in proofreading my thesis: **Assistant Professor Nollaig Bourke, Professor Paul Hertzog, Dr Helen Cumming,** and **Stella Lumb.**

In memory of my lovely grandmother **Irene** and grandfather **Nickodimus** to whom I owe an enormous sense of gratitude for raising me and encouraging my scientific curiosity as a kid.

Lastly, I would like to thank my wonderful husband **George** for being my rock throughout this long journey. I am very fortunate for your love and support and for always providing me with a much-needed comic relief! I apologise for all the long nights you had to wait up for me and for the endless scientific discussions which you have grown to now appreciate.

"And if you find her poor, Ithaka won't have fooled you. Wise as you will have become, so full of experience, you will have understood by then what these Ithakas mean."
-C.P. Cavafy, Collected Poems, 1911

List of Abbreviations

ARC 105	Activator recruited cofactor 105
ALK4	Activin type I receptor
ActRIIB	Activin type II B receptor
ActRII	Activin type II receptor
APS	Ammonium persulfate
ANOVA	Analysis of variance
AVE	Anterior visceral endoderm
APC	Antigen presenting cells
Balb/C	Albino, laboratory-bred mouse strain
bp	Base pairs
BCL-2	B-cell lymphoma 2
BMM	Bone marrow-derived macrophage
BMPs	Bone morphogenetic protein
BSA	Bovine serum albumin
°C	Degrees Celsius
CSC	Cancer stem cell
$C0_2$	Carbon dioxide
CASP1	Caspase-1
CEBPh	CCAAT/ enhancing protein h
CDC20	Cell-division cycle protein 20
CXCL10	Chemokine (C-X-C motif) ligand 10
CSF1	Colony stimulating factor 1
Co-Smad	Common mediator-Smad
cDNA	copy deoxyribonucleic acid

Ct	Cycle threshold
cGAS	Cyclic GMP-AMP synthase
CMV	Cytomegalovirus
dUTP	2'-Deoxyuridine 5'-Triphosphate
DAPI	4’,6-diamidino-2-phenylindole,
DAMPs	Damage-associated molecular patterns
dH_20	Deionized water
DC	Dendritic cell
DNA	Deoxyribonucleic acid
DHFR	Dihydrofolate reductase
DMSO	Dimethyl sulfoxide
DVE	Distal visceral endoderm
DTT	Dithiothreitol
dsDNA	Double-stranded DNA
dsRNA	Double-stranded RNA
ExE	Trophectoderm-derived extra-embryonic ectoderm
ESCs	Embryonic stem cells
EU	Endotoxin units
ECL	Enhanced chemiluminescence
ELISA	Enzyme-linked immunosorbent assay
ELISA	Enzyme-linked immunosorbent assay
ERBB2	Epidermal growth factor (EGF) 2
EGF-CFC	Epidermal growth factor-Cripto-FRL1-Cryptic
CDH1	Epithelial cadherin
EMT	Epithelial mesenchymal transition
EGTA	Ethylene glycol tetraacetic acid
EDTA	Ethylenediaminetetraacetic acid

Ets	E-twenty six
FoxH1	Homolog of Xenopus forkhead activin signal transducer-1
FIGO	International Federation of Gynaecology and Obstetrics
FRT	Female reproductive tract
FCS	Fetal calf serum
FITC	Fluorescein isothiocyanate
FACS	Fluorescence activated cell sorting
FAST2	Forkhead activin signal transducer 2
FoxH1	Forkhead box H1
GAS	Gamma-activated sequence
g	g-force
GRP78	Glucose regulated protein 78kDa
GPI	Glycosylphosphatidylinositol
G	Gram
GDF	Growth and differentiation factor
HSV	Herpes Simplex Virus
HGSC	High Grade Serous Carcinoma
HRP	Horseradish peroxidase
Hr	Hour
hESC	Human embryonic stem cells
HER2	Human epidermal receptor growth factor 2
hIFN	Human IFN
HIV-1	Human immunodeficiency virus-1
IgG	Immunoglobulin G
IP	Immunoprecipitation
ICM	Inner cell mass
IFN	Interferon

IFNα	Interferon alpha
IFNAR	Interferon alpha receptor
IFI27	Interferon alpha-inducible protein 27
IFNβ	Interferon beta
IFNε	Interferon epsilon
IFNGR	Interferon gamma receptor
IRG	Interferon regulated gene
IRF	Interferon regulatory factor
ISG	Interferon stimulated gene
ISGF3	Interferon stimulated gene factor 3
ISRE	Interferon stimulated response element
ISG12	Interferon-stimulated gene 12a protein
ISG15	Interferon-stimulated gene 15
IL	Interleukin
IU	International units
JAK	Janus Kinase
Kb	Kilobases
kDa	Kilodaltons
L	Litres
MTT	[3-(4, 5-Dimethylthiazol-2-yl)-2, 5-diphenyltetrazolium bromide
$MgSO_4$	Magnesium sulfate
MRI	Magnetic resonance imaging
MMMT	Malignant Müllerian Mixed Tumour
mRNA	Messenger ribonucleic acid
µl	Microgram
µg	Microgram
µM	Micromolar

mg	Milligram
ml	Millilitre
mM	Millimolar
MQ water	Milli-Q purified water
Min	Minute
MAPK	Mitogen activated protein kinase
MAb	Monoclonal antibody
SMAD	Mothers against decapentaplegic/drosophila homolog
MMTV	Mouse mammary tumour virus
MXA	Myxovirus resistance protein 1
NaCL	Sodium chloride
NK	Natural Killer
NLR	NOD-like receptors
LDS	Nonreducing lithium dodecyl sulfate
NFkB	Nuclear factor κB
OAS	Oligoadeylate synthetase
PACE	Paired basic amino acid residue-cleaving enzyme
PAMP	Pathogen associated molecular pattern
PRR	Pattern-recognition receptor
P/S	Penicillin/Streptomycin
PMSF	Phenylmethane sulfonyl fluoride
PBS	Phosphate buffered saline
PI3K/Akt	Phosphatidylinositol-3-kinase/protein kinase B
pDCs	Plasmacytoid dendritic cells
PDGF	Platelet-derived growth factor
PCR	Polymerase chain reaction
PVDF	Polyvinylidene fluoride membrane

PET-CT	Positron emission -computed tomography
PS	Primitive streak
PRE	Progesterone receptor response element
PI	Propidium iodide
PKR	Protein kinase R
qRT-PCR	Quantitative polymerase chain reaction
RIPA	Radioimmunoprecipitation
r-hIFNβ	Recombinant human interferon beta
r-hIFNε	Recombinant human interferon epsilon
r-mIFNε	Recombinant mouse interferon epsilon
r-Cripto	Recombinant-Cripto
RIG	Retinoic-acid inducible gene
RT	Reverse transcriptase
RT-PCR	Reverse transcription polymerase chain reaction
RNA	Ribonucleic acid
rRNA	Ribosomal RNA
RLR	RIG-like receptors
RPMI	Roswell Park Memorial Institute
SB-431542	4-[4-(1,3-benzodioxol-5-yl)-5-(2-pyridinyl)-1*H*-imidazol-2-yl] benzamide
Sec	Second
STI	Sexually Transmitted Infections
STAT	Signal transducer and activator of transcription
ssRNA	Single stranded RNA
SE-HPLC	Size exclusion-High performance liquid chromatography
Smad	Small mothers against decapentaplegic
SDS	Sodium dodecyl sulfate
SDS-PAGE	Sodium dodecyl sulfate-polyacrylamide gel electrophoresis

SPC	Subtilisin-like proprotein
SPC	Subtilisin-like proprotein
SOCS	Suppressor of cytokine signalling
TDGF1	Teratocarcinoma-Derived Growth Factor
TDGF-1	Teratoma-derived growth factor 1
TUNEL	Terminal deoxynucleotidyl-transferase-mediated dUTP-biotin nick end-labeling
TEMED	Tetramethylethylenediamine
TβRII	TGF-β type II receptors
T	Thymus
TLR	Toll-like receptors
TGF-β	Transforming growth factor-beta
TAP1	Transporter associated with Antigen Processing 1
Tris-HCL	Tris hydrochloride
TBS	Tris-buffered saline
TNF	Tumour necrosis factor
TP53	Tumour protein
TYK2	Tyrosine kinase 2
USP18	Ubiquitin Specific Peptidase 18
VEGF	Vasoactive endothelial growth factor
VE	Visceral endoderm
v/v	Volume/Volume
WB	Western blot

Abstract

Understanding the mechanisms involved in malignant pathogenesis is fundamental to the development of targeted cancer therapies. One of the most common gynaecological cancers, endometrial cancer, is the main focus of this thesis. There is no early detection test for this disease, with highly invasive treatments (hysterectomy, radiotherapy, chemotherapy), associated with fertility repercussions. Although survival rate is very good when detected at early stages, late stage diagnosis is associated with poor survival. Thus, development of new diagnostic and treatment options are of vital importance. This thesis examines how pro-tumourigenic Nodal/TGF-β cytokine signalling is utilized to facilitate tumour development. Additionally, dysregulated anti-tumourigenic cytokines are also implicated in tumourigenesis. As such, the anti-cancer properties exhibited by a type I interferon (IFN) specific to the reproductive tract, IFNε, was also investigated.

Nodal is rarely expressed in non-embryonic adult cells (except regenerative tissues), and re-emergence contributes to cancer pathogenesis. This thesis (Chapter 2) aimed to investigate the expression of Nodal signalling components in cancerous and healthy human endometrium. We were the first to report, cyclical expression patterns of Nodal signalling components within healthy endometrial tissue. These results implicate Nodal signalling as a regulator of remodelling events occurring within the proliferative phase of the menstrual cycle. We were also the first group to detect overexpression of both Nodal and Cripto in human endometrial cancer samples. Furthermore, expression of Nodal and Cripto increased dramatically within the epithelial tumour compartment, in the histological transition of Grade 1 to Grades 2 and 3. Concurrently, Lefty (antagonist) expression was low or absent eluding to unrestricted Nodal signalling in these tumours. Furthermore, this data strongly suggests that dysregulated Nodal and Cripto expression

positively correlates with the degree of endometrial cancer aggressiveness, corroborating with various other types of malignancies such as melanoma and breast cancer.

Additionally, this thesis further aimed to study the effects of Nodal signalling blockade on cancer cell behavior (Chapter 3). In these studies, neutralising Cripto monoclonal antibodies were employed to specifically block Nodal signalling. We demonstrated that 6E10 MAb treatment significantly suppressed *in vitro* cancer cell proliferation and migration reflecting NODAL/CRIPTO expression levels. Furthermore, the reversal of tumourigenic phenotype by *in vitro* 6E10 MAb treatment was accompanied by abrogated Smad 2/3 phosphorylation levels. These results correlate with previous studies confirming that Nodal/Smad signalling promotes cancer cell growth and metastasis.

In order to broaden the study to include other cytokines present in the FRT we also investigated type I IFN, IFNε. IFNε is emerging as an important FRT cytokine with distinguished characteristics from other type I IFN members. As such IFNε is constitutively expressed by epithelial cells of the FRT and is hormonally regulated, exclusively within the endometrium. Therefore, the final aim of this thesis was to investigate the *in vitro* anti-tumourigenic effects of IFNε in FRT epithelial cancer cells (Chapter 4). In this study we observed that IFNε down-regulated anti-apoptotic, and up-regulated pro-apoptotic, IFN stimulated genes (ISGs); in vaginal, cervical and endometrial, cancer cell lines. Interestingly, IFNε significantly suppressed proliferation of vaginal, cervical and endometrial, cancer cell lines. Additionally, we demonstrated that IFNε induces early, as well as late stage apoptosis of epithelial cancer cells.

Collectively the body of evidence in this thesis highlights pro-tumourigenic Nodal, and anti-tumourigenic IFNε, cytokine activities. The findings of this thesis support both Nodal and Cripto as diagnostic and prognostic biomarkers of endometrial cancer as well as attractive molecular targets for anti-cancer therapy. As such we demonstrated that 6E10 Cripto monoclonal antibody could be utilized as potential therapeutic agent. Subsequently this thesis further supports the use of IFNε in the development of endometrial cancer therapies.

Chapter 1

General Introduction

"Either we shall find what it is we are seeking or at least we shall free ourselves from the persuasion that we know what we do not know".

-Plato, Republic, Book VII

Chapter 1: General Introduction

1.1 Tumourigenesis

1.1.1. Historical Origins of Cancer Biology

Contrary to the misbelief of a modern world affliction, archaeological evidence suggests that cancer may have existed as early as the pre-historic era. The oldest malignant metastatic disease on earth, identified by CT (computerized tomography) of dinosaur vertebrae (cretaceous hadrosaurs; duck-billed dinosaurs), dates approximately 70 million years ago (1). Further use of modern technological advancements has led to the discovery of the oldest case of human malignancy using micro-CT imaging. According to Odes E., *et al.,* (2016) the toe bone fossil discovered in Swartkrans cave, near Johannesburg, belonged to a hominin (human relative) that was diagnosed with osteosarcoma and estimated to have lived on earth 1.7 million years ago. *in vivo*

The term cancer is derived from the Greek word *"karkinos"* (καρκίνος) which translates to a crab, was first used by the "*father of modern medicine"* Hippocrates (460-370 BC). It is postulated that Hippocrates associated the appearance of a dissected solid tumour, with protruding veins stretching from all sides, analogous to a crab that adheres to its surroundings with its claws (2). The medical book known as the Hippocratic Corpus is devoted to diseases that produce masses "onkos" (Greek: όγκος) and *"karkinos"* is described as non-ulcer forming and ulcer-forming tumours. According to Hippocrates *"that which medicine does not heal, the knife frequently heals; and what the knife does not heal, cautery often heals; but when all these fail, the disease is incurable"* (3). His treatment approaches on advanced malignancies were that *"occult cancers should not be molested. By attempting to treat them, they quickly become fatal. When unmolested, they remain in a dormant state for a length of time"* (4).

Although cancer has coexisted alongside human evolution, its prevalence has increased in the new era. Rapidly aging populations, unhealthy lifestyles, as well as the overwhelming presence of environmental carcinogens are among numerous causative factors contributing to this increase.

1.1.2. Cancer Hallmarks

Cancer is a major cause of illness globally, with devastating socio-economic impacts on individuals, families, and the community. 134,174 new cancer diagnoses have been estimated to occur in Australia for the year 2017, which equates to approximately one new cancer case detected every 4 minutes. The Australian Institute of Health and Welfare (AIHW) estimated there were 47,753 of cancer related deaths in 2017 (5). Fortunately, prognosis has improved, with the overall 5-year survival rate increasing considerably over the years. However, this is largely dependent on multiple factors such as age, gender, cancer type and staging (5).

Cancer should not be viewed as a single disease, but more importantly as a cluster of complex diseases that share common characteristics. More importantly, it constitutes a chain of events with intricate communication networks, acting both intracellularly as well as via the microenvironment, to sustain the acquired tumourigenic status. From Hippocrates's time to the current technologically advanced era of research, cancer biology has culminated to the notion of a multistage heterogeneous disease. Tumourigenesis involves the acquisition of a complex network of dysregulated molecular processes.

To provide a framework of key molecular mechanisms associated with malignancy, Hanahan D., and Weinberg R.A., (2011), proposed the ten hallmarks of pathogenic

development, as portrayed in **Figure 1** (6, 7). To rationalise the intricacies of cancer biology, according to the authors, the hallmarks initially comprised the following characteristics: 1) sustaining proliferative signalling, 2) evading growth suppression, 3) cell death resistance, 4) replicative immortality, 5) angiogenesis, 6) invasion/metastasis (6). The authors subsequently revisited this phenomenon and added: 7) reprogramming energy metabolism, 8) evading immune response, 9) genome instability/mutation, and 10) tumour-promoting inflammation; as subsequent carcinogenic traits (7). The multistep machinery allows cells to evolve progressively by acquiring these qualities successively, to maintain and aid the malignant transformation.

During carcinogenic development normal cells are recruited to form the "*tumour-associated stroma"* or mesenchymal cells adjacent to the cancer cell epithelium, or parenchyma (refer to **Figure 2**). The stromal cells are in constant communication with the cancerous cells to and facilitate transformative events. Hence the tumour microenvironment is an essential framework that supports the cancerous phenotype and contributes to cellular heterogenicity (7).

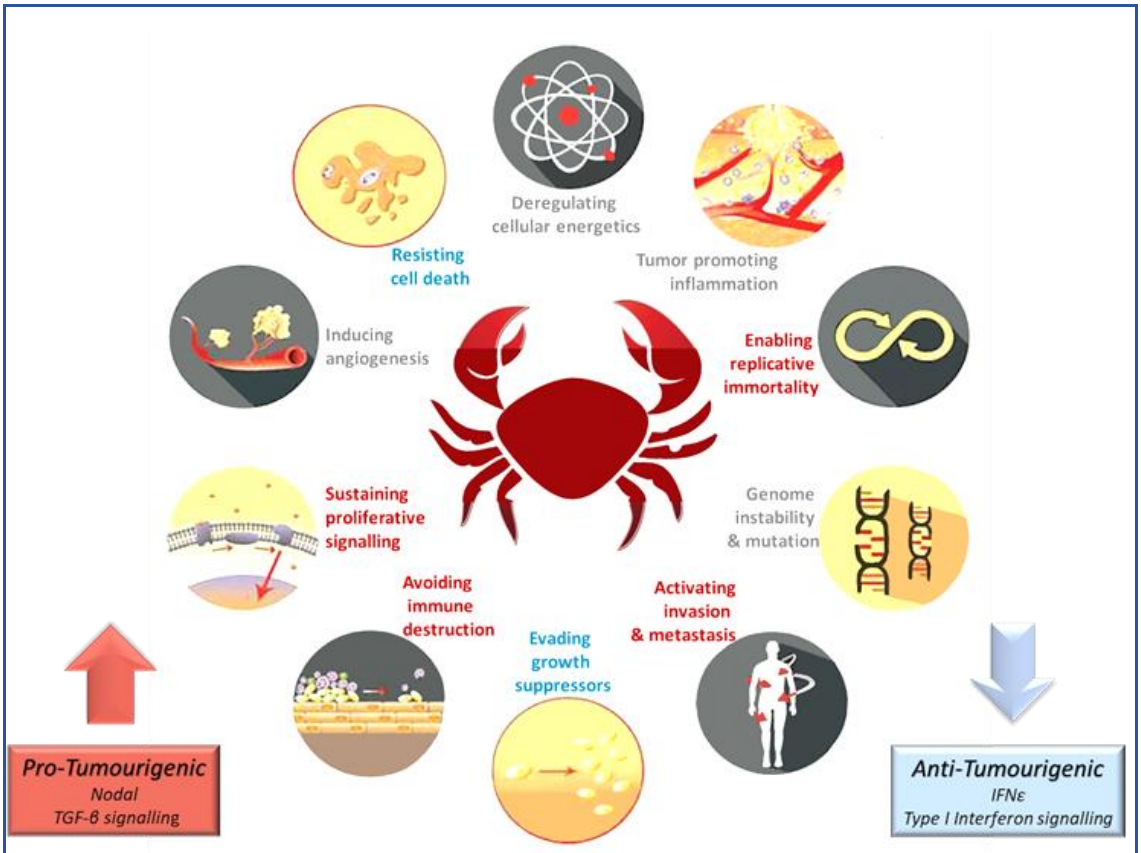

Figure 1. Hanahan and Weinberg's Cancer Hallmarks.
Acquired capabilities leading to cancer development. Highlighted Nodal signalling (red) as part of the pro-tumourigenic machinery and IFNε signalling (blue) exhibiting anti-tumour functions. Adapted from (6, 7).

Cytokines are cell signalling molecules that can be involved in neoplastic development. These molecules are aberrantly expressed and can display pro-tumourigenic properties such as the TGF-β family member of growth factors, Nodal (see **Figure 1**). In contrast cytokines exhibiting anti-tumourigenic properties are dysregulated as a mechanism to promote malignancy. An example of the latter is type I interferon, IFNε (**Figure 1**). As

this thesis intends to examine how these two cytokines are utilized to favour cancer development, this introduction will discuss in detail their biological significance.

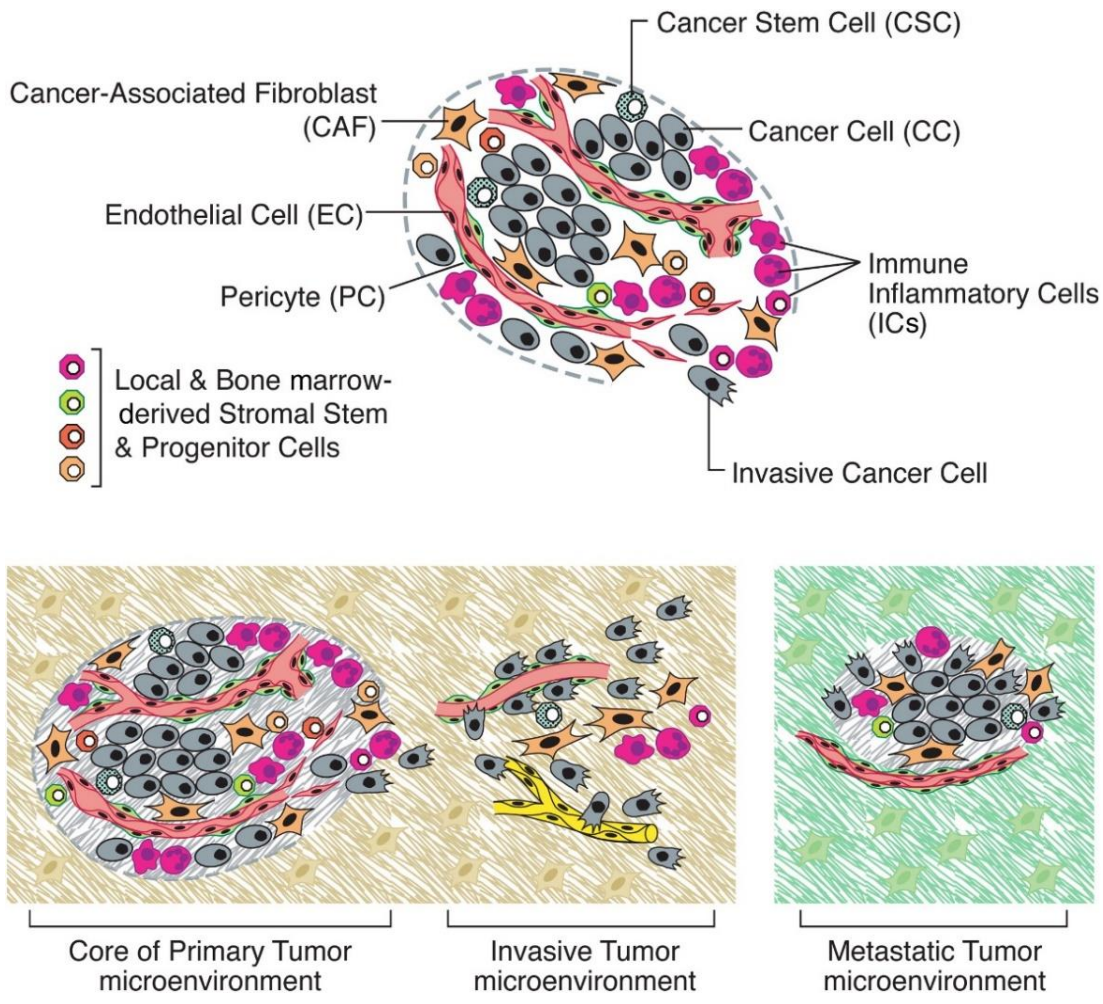

Figure 2. Solid Tumour Microenvironment Architecture.
Distinct cell types constitute a solid tumour supported by a specialised microenvironment according to dissemination status. Adapted from (7).

1.2 Female Reproductive Cancer

Gynaecological cancers of the upper and lower female reproductive tract (FRT) are an important cause of morbidity and mortality worldwide (8). In Australia, 1,763 gynaecological cancer related deaths are estimated for 2017 (9). FRT cancers including the most commonly: ovarian, cervical, uterine (endometrial); as well as the rarer: vulva, vaginal, placenta; comprise the third most common diagnosed female malignancy (5). Emphasis will be given to endometrial cancer in this introduction.

1.2.1 Biology of the Female Reproductive Tract

The FRT comprises of ovary, fallopian tubes, uterus, endocervix (projecting into the uterus), ectocervix (protruding into the vagina), and vagina as illustrated in **Figure 3**. The FRT is primarily important for successful reproduction. The mucosal lining of upper and lower FRT is morphologically and functionally diverse. While the upper FRT (including uterine tubes, uterus, and endocervix), is covered by the columnar epithelium which is essential for embryo implantation (10); the lower reproductive tract (comprising of ectocervix and vagina) is lined with stratified squamous epithelium, serving additional protective function against infections (11).

1.2.1.1 Endometrial tissue Anatomy

The uterus is a pear-shaped organ (**Figure 3**), approximately measuring: 8 cm long, 5 cm wide and 2.5 cm thick (during nulliparity); and located in the pelvic cavity. The uterine corpus, opens into the cervix, followed by the vagina (12). Lining the uterus is the highly regenerative endometrial mucosal tissue, where fertilization occurs. Structurally the endometrium is composed of the upper functionalis layer (or zona functionalis, refer to (**Figure 4**), in which the morphological changes occur, and the lower basalis layer

(otherwise known as zona basalis) (13). Surrounding the endometrium is the smooth muscle layer of myometrium. The endometrium consists of glandular and luminal epithelial cells, surrounded by stromal cells (see **Figure 4**). Paracrine activities of stromal cells facilitate growth and differentiation of endometrial epithelial cells. It has been postulated that stem/progenitor cells identified in glandular and stromal zona basalis, might contribute to the great regenerative capacity of the endometrium (14).

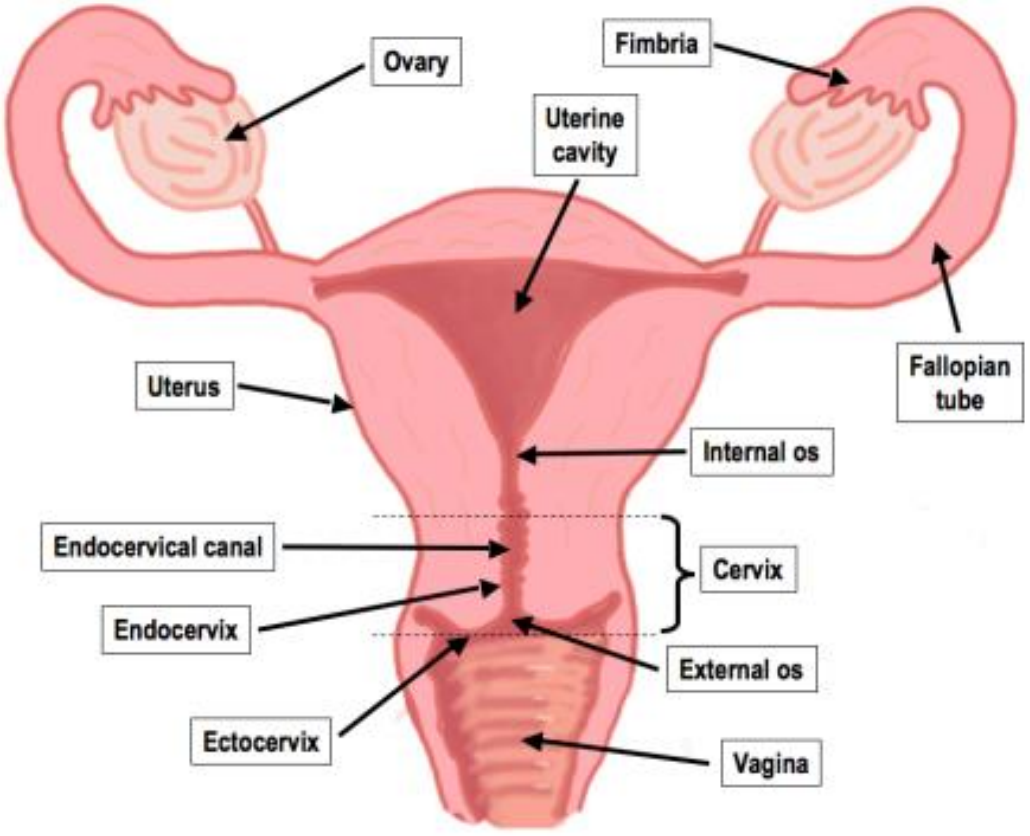

Figure 3. Anatomy of the Female Reproductive Tract.
Adapted from (15).

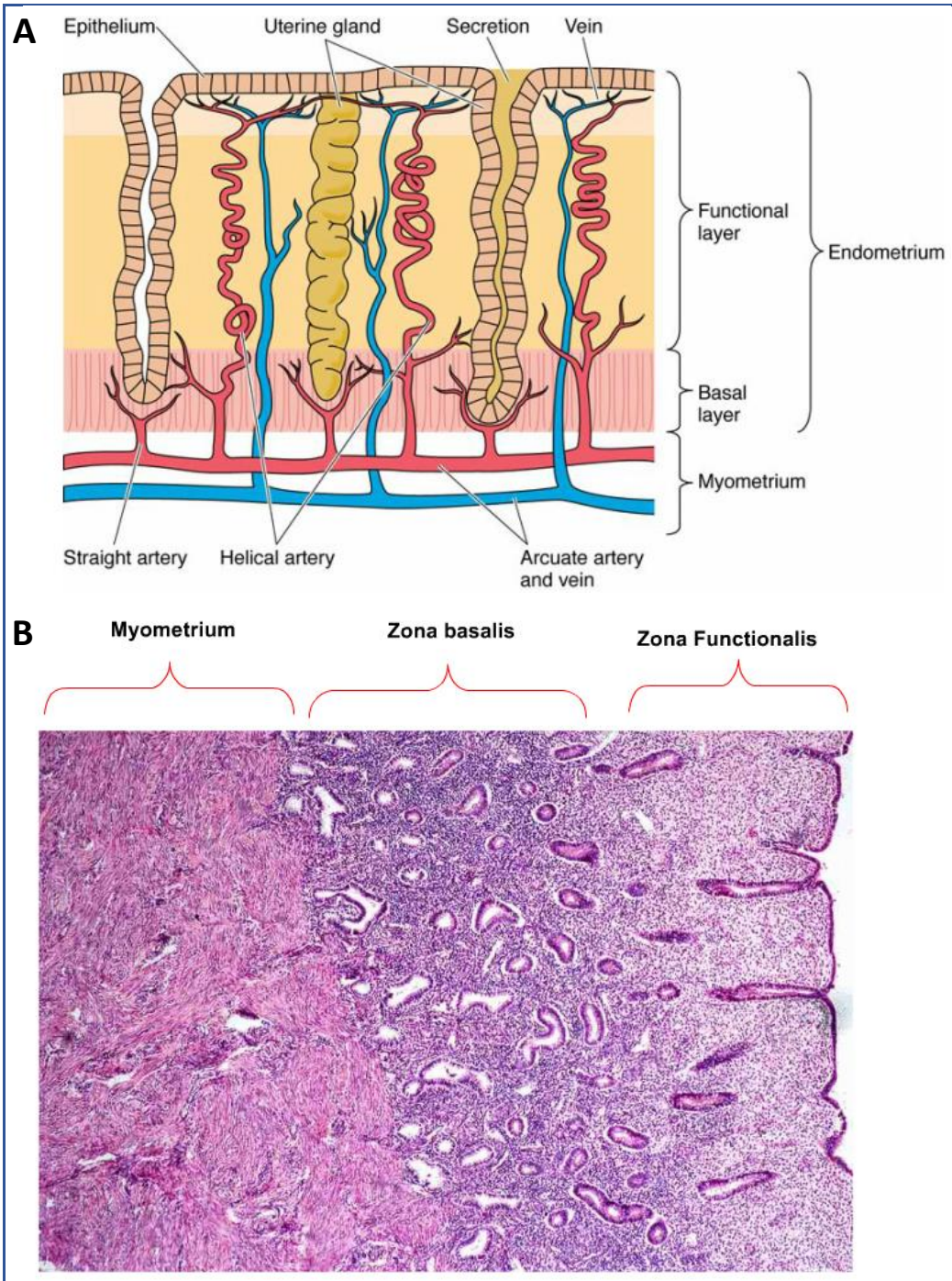

Figure 4. Structural Organisation of the Human Endometrium.
A) Graphical illustration of the different cell types comprising the human endometrial tissue. B) Histology of the endometrial compartments. Adapted from (16).

1.2.1.2 The Menstrual Cycle

The human endometrium undergoes cyclical processes of growth, differentiation, and regression in response to ovarian hormonal fluctuations of oestrogen and progesterone as indicated in **Figure 5** (17, 18). These processes are crucial in preparation of embryo implantation. The menstrual cycle which lasts for approximately 28 days, is divided into three main phases: proliferative, secretory and menstrual; with ovulation occurring on approximately the fourteenth day (19). At day 5 of the cycle, oestrogen levels rise to initiate the proliferative phase (20, 21). Under the influence of oestrogen, dominating the proliferative phase, the endometrium undergoes rapid cellular proliferation, glandular thickening and elongation as well as angiogenesis (21). During this phase narrow, short, glands thicken, and elongate forming branched glands, to adopt a convoluted morphology by the late proliferative phase of the endometrium.

Following ovulation at cycle day 14, under the influence of progesterone the secretory phase is characterized by marked epithelial differentiation, in preparation for embryo implantation. Progesterone antagonises oestrogen mediated proliferation of glands and stroma. In the presence of progesterone, stromal cells undergo decidualization associated with an epithelial-like morphology. In addition, stromal cells become enlarged and secretory whereas spiral arterioles begin to coil (19). In the absence of implantation, progesterone and oestrogen levels decrease, allowing for the menstrual phase to occur. Endometrial regression and shedding of the functionalis layer, follows in days 1-5 of the cycle (19). Subsequently the cycles continue sequentially until pregnancy occurs or menopause is reached (**Figure 5**).

Menopause commences with the cessation of oestrogen and progesterone from the ovaries, with concurrent anovulation and termination of the menstrual cycle. During menopause the endometrium becomes inactive and atrophic. For most women

menopause normally occurs between 45-55 years of age although premature menopause may result from cancer treatment or surgery, as well as from unknown aetiology (22).

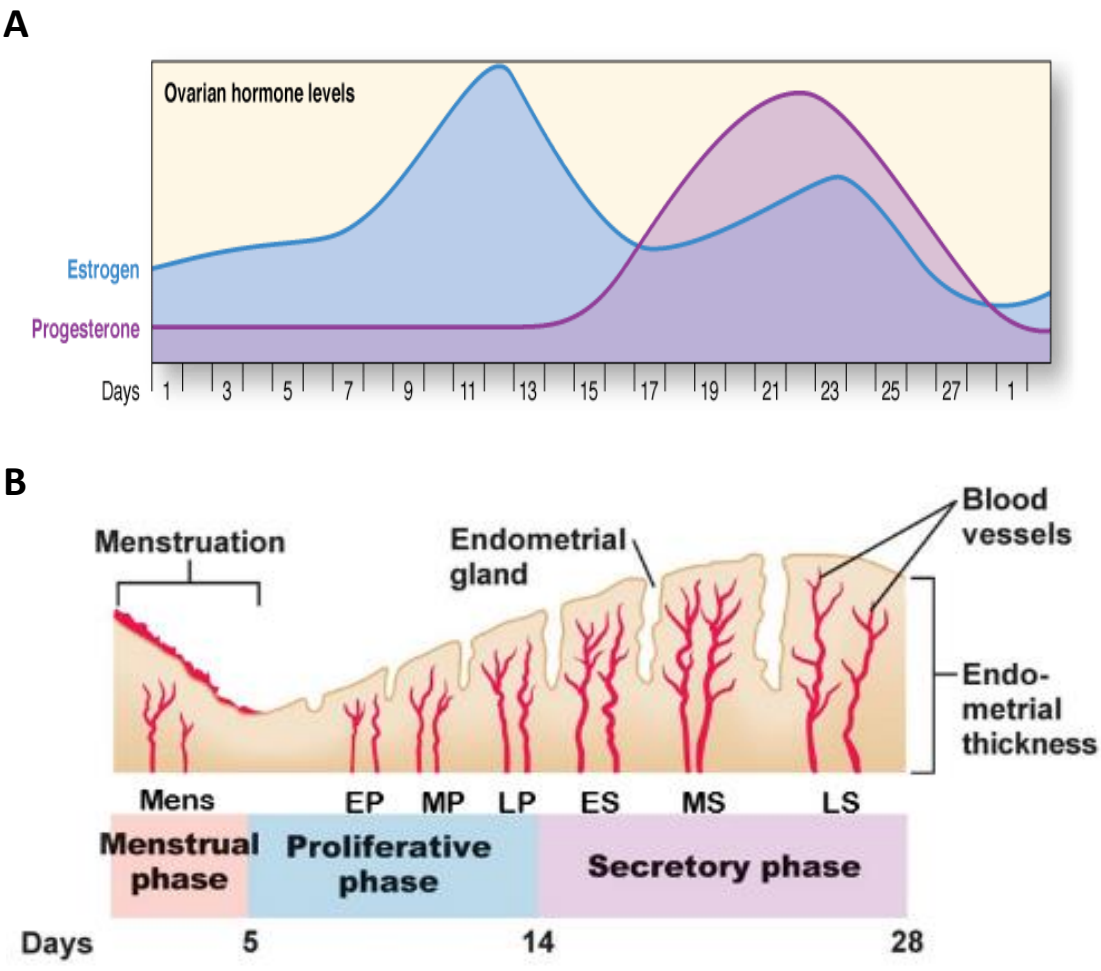

Figure 5: Cyclical Changes of the Human Menstrual Cycle.
A) Oestrogen and progesterone fluctuations following the menstrual cycle in women. B) Human endometrium undergoing cyclical changes. Adapted from (17, 18).

1.2.2 Endometrial cancer

Endometrial cancer, or malignant neoplasm of corpus uteri, is the most common invasive gynaecological malignancy in the developed world (23). An estimated 2,861 of new uterine cancer cases were diagnosed in Australia in 2017, with the occurrence of 453 endometrial cancer related deaths (23). Early stage endometrial malignancies usually have a favourable prognosis compared to advanced disease, characterized with poorer clinical outcomes and associated deaths (5).

1.2.2.1 Risk Factors

Nearly 90% of diagnosed uterine cancers are sporadic, while the remaining 10% are hereditary, typically in women with familial Lynch syndrome (24). Alarmingly, endometrial cancer incidence rates have substantially risen in the last decade, due to increased aging population and obesity prevalence (23).

Risk factors for endometrial cancer include anovulation, nulliparity, polycystic ovarian syndrome, early age menarche and diabetes mellitus (25-29). It has been suggested that these factors contribute to unopposed oestrogen exposure, which stimulates endometrial cell proliferation, leading to predisposition of endometrial hyperplasia or malignancy. Moreover, treatments such as oestrogen-only hormonal therapy; tamoxifen chemotherapy for breast cancer; and pelvic irradiation; have also been associated with increased endometrial cancer risk (28-30). In addition, tobacco smoking and hypertension constitute significant endometrial cancer risk factors (31).

1.2.2.2 Pathology and Prognosis

According to Bokhman's dualistic model of pathogenesis, sporadic endometrial cancer is categorised into type I and type II (32-34). Additional clinicopathological features,

including histological and morphological characteristics as well as grading, are employed to facilitate diagnosis (as summarized below in **Tables 1** and **2**) (32, 35, 36). Patient prognosis is dependent upon the cancer type and disease progression. Diagnosis of at early stage endometrial cancer, with localised malignancy (FIGO staging I/II), has an overall five-year survival rate of 69-88% (37). In a contrast five-year survival rates of advanced disease are drastically reduced to 47-57 % and 15-20 for the highly aggressive stage III and IV respectively (38).

Table 1. Endometrial Cancer Sub-type Clinicopathological features

	Type I	*Type II*
Histology	Endometrioid adenocarcinoma	Non-endometrioid carcinoma, serous, clear cell
Oestrogen Dependence	Dependent	Independent
ER or PR	Positive	Negative
Tumour Grade	Low grade (grade 1)	High grade (grades 2, 3)
FIGO Staging	Early (FIGO stages I or II)	Advanced (FIGO stages III /IV)
Invasiveness	Minimal myometrial invasion	Deep myometrial invasion
Genetic Mutations	Microsatellite instability, *PTEN*, *KRAS, CTNNB1, PIK3CA*	*HER-2* amplification, *p53, CDH1*
Menopause Status	Pre /Peri-menopausal	Post-menopausal
Prognosis	Favourable	Unfavourable

ER: oestrogen receptor; PR: progesterone receptor; FIGO: International Federation of Gynaecology and Obstetrics. PTEN (phosphate and tensin homolog); KRAS (Kirsten ras sarcoma viral oncogene homolog); CTNNB1 (beta-catenin); PIK3CA (phosphatidylinositol-4,5-bisphosphate 3-kinase catalytic subunit alpha); of HER2(epidermal growth factor receptor tyrosine kinase); TP53 (tumour protein); CDH1 (epithelial cadherin);

Modified from (32, 36).

Type I endometrial cancer also known as endometroid, is the most common, occurring in 70-85% of cases, and generally afflicts younger pre/peri-menopausal women (39). Grading of type I endometrial cancer is based on tumour differentiation status (summarized in **Table 2**). The majority of type I endometrial cancers are oestrogen sensitive and display high to moderate differentiation morphology (32,39).

Table 2. Histopathological Classification of Endometrial Cancer Sub-types.

FIGO Grading	
Grade 1	*well-differentiated, ≤ 5% non-squamous solid growth pattern*
Grade 2	*moderately differentiated, 6- 50% of non-squamous growth pattern*
Grade 3	*poorly-differentiated, > 50% of non-squamous growth area*
Type II non-endometrioid	
Serous carcinoma	*atypical cells, complex pattern of papillary features*
Clear cell carcinoma	*clear or hobnail cells with clear cytoplasm*
Malignant Müllerian Mixed Tumour (MMMT)	*high grade pleomorphic nuclei, mixture of epithelial and mesenchymal malignant components, papillary*

Adapted from (32,35,36,40)

Whereas type II tumours represent 10-20% of endometrial carcinomas, are typically diagnosed in older postmenopausal women (32,35). They present a distinct molecular profile from type I endometrial cancers, involving amplification of *HER2/ERBB2* [epidermal growth factor (EGF) receptor family of receptor tyrosine kinases]; as well as genetic mutations of *TP53* (tumour protein), and *CDH1* (epithelial cadherin) genes (34). Type II malignancies are highly aggressive with frequent relapses and metastasis, thus accompanied by less favourable prognosis (32, 36, 40).

Furthermore, FIGO (International Federation of Gynaecology and Obstetrics) surgical staging of endometrial cancer describes a *"four stage disease progression"*, as outlined in **Table 3** (30, 35, 36, 41). Surgical staging is based on tumour size and dissemination status, to further complement diagnosis, and is essential in determining prognosis of the disease.

Table 3. FIGO Surgical Staging of Endometrial Cancer

Stage I		
IA	*tumour invasion < 50% of the myometrium*	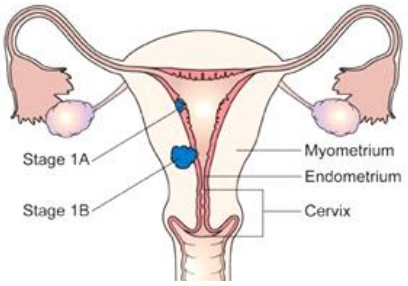
IB	*tumour invasion ≥ 50% of the myometrium*	
Stage II		
tumour invades cervix, but does not extend beyond the uterus		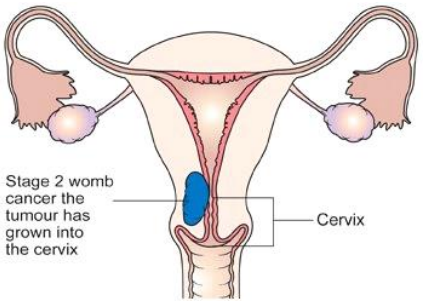
Stage III		
IIIA	*tumour invades the serosa of the corpus uteri and/or adnexae*	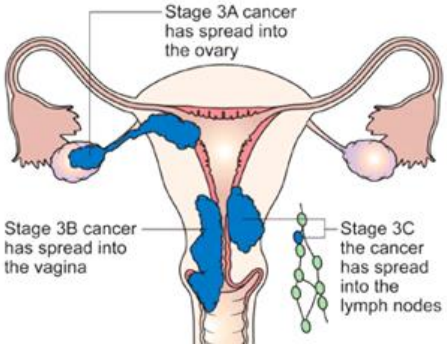
IIIB	*vaginal and/or parametrial involvement*	
IIIC	*metastases to pelvic and/or para-aortic lymph nodes*	
Stage IV		
IVA	*tumour invasion of bladder and/or bowel mucosa*	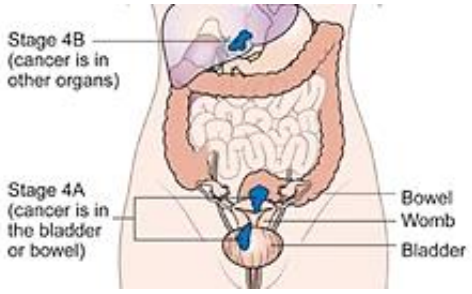
IVB	*distant metastases, including intra-abdominal metastases and/or inguinal lymph nodes*	

Adapted from (30, 35, 41, 42).

1.2.2.3 Diagnosis and treatment

Postmenopausal vaginal bleeding is commonly present in endometrial cancer patients (43). Other symptoms may also include vaginal discharge (pyometra), in this group of women (40). Premenopausal women diagnosed with endometrial cancer may present with irregularities in menstruation. However, there is currently no early detection test for endometrial cancer and diagnosis is often carried out by histopathological examination of endometrial biopsies (30). Further diagnostic tools such as transvaginal ultrasound, dilatation and curettage, and hysteroscopy may also be utilized in combination, to confirm endometrial malignancies (29, 44). Tumour metastasis can be monitored by magnetic resonance imaging (MRI) for elucidation of myometrial and cervical invasion. In addition, lymph node dissemination can be determined by PET-CT (positron emission -computed tomography) scan (44, 45).

Surgery including hysterectomy and bilateral salpingo-opherectomy remains the current treatment to date (40). Extensive surgery may be required for advanced FIGO stage disease and high-risk histological subtypes, in conjunction with radiation therapy (either external beam radiation or vaginal brachytherapy) or chemotherapy (most commonly: cisplatin, carboplatin, paclitaxel, doxorubicin) (44). Subsequently, chemotherapy and radiotherapy target cancer cells, as well as healthy cells, by causing irreversible DNA damage leading to cellular death. Furthermore, these cancer therapies are associated with severe side effects (40,44).

Alarmingly, advanced FIGO stage endometrial cancer survival following treatment is currently less than one year (23). Furthermore, disease recurrence within three years of treatment, is very common for either late or early stage endometrial cancer (28,29). To add to the complexity of therapeutic approaches, aggressive and recurrent endometrial malignancies develop resistance to chemotherapy and radiotherapy (36). Additionally,

young women diagnosed with endometrial cancer will suffer grave ramifications to their fertility. Non-surgical, fertility-sparing therapy options are limited to progestogen hormonal treatment, with an associated risk of cancer progression in 80% of the cases (28).

It is evident that development of less invasive diagnostic and treatment options are of vital importance for endometrial cancer patients. Hence, understanding the precise dysregulated molecular mechanisms contributing to the pathophysiology of endometrial cancer is paramount to the development of new diagnostics and targeted therapies. This chapter will further discuss the involvement of pro-tumourigenic, Nodal, and anti-tumour IFNε as well as providing relevant introductory themes of both cytokines.

1.3 TGF-β Superfamily

The transforming growth factor-β (TGF-β) superfamily of cytokines comprises of over 40 members subcategorized according to structural identities or functional properties (46). TGF-β was discovered in 1983, as the first member of the TGF-βs subgroup (47). Others members include: activins / inhibins; Nodal; BMPs (bone morphogenetic proteins); GDFs (growth and differentiation factors); as illustrated in the phylogenetic tree below [**Figure 6,** (48)].

TGF-β superfamily ligands as well as their associated signalling components are highly evolutionary conserved among different invertebrate and vertebrate species. TGF-β cytokines regulate **pleotropic cellular processes** including cell growth, apoptosis, differentiation, adhesion, and migration, morphogenesis, essential in embryogenesis and adult tissue homeostasis. Dysregulated TGF-β signalling has been implicated human disease such cancer, fibrosis, cardiovascular, reproductive, and wound healing disorders (49, 50).

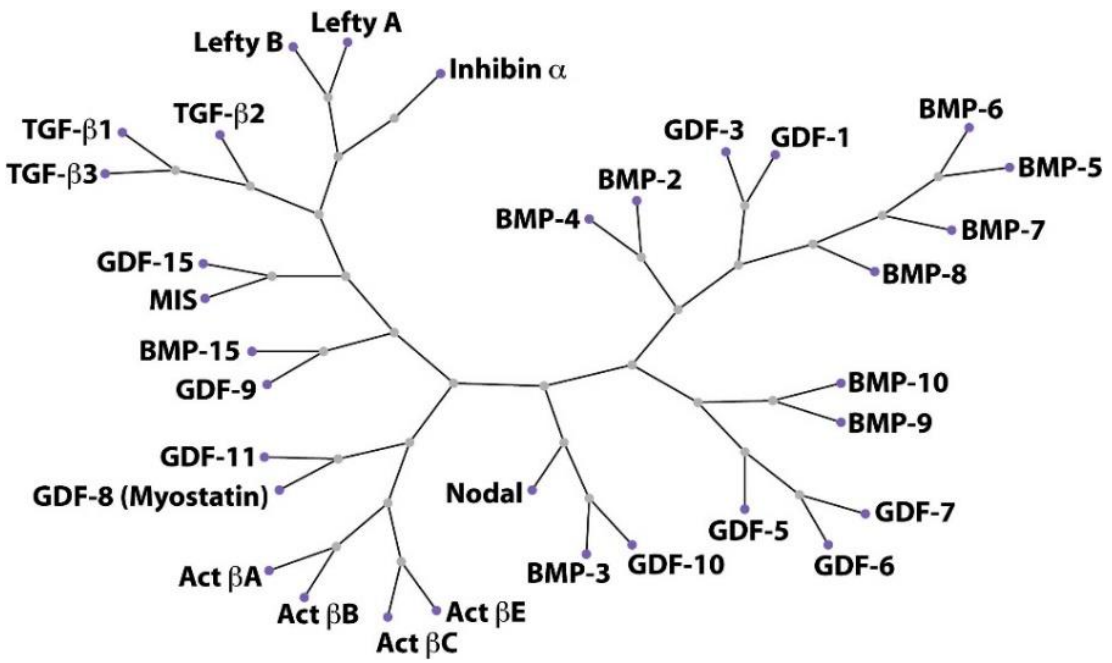

Figure 6. TGF-β Phylogenetic Tree.
The TGF-β phylogenetic tree, according to Hinck, A.P., et al., (2012), is derived from alignment of human mature C-terminal domain family proteins. Adapted from (48).

1.3.1 Structure

All TGF-β mature ligands share a common structural motif known as the "*cysteine knot"* formed by intramolecular disulphide bonds interlocked between conserved Cys residues (46). According to Allendorph *et al.,* (2007), TGF- β protein structure resembles a butterfly-shaped configuration, as illustrated in **Figure 7** below (51). Ligands are synthesized intracellularly as large dimeric precursor forms containing pro-domains that require cleavage by proteases prior to secretion of the dimeric mature protein (52).

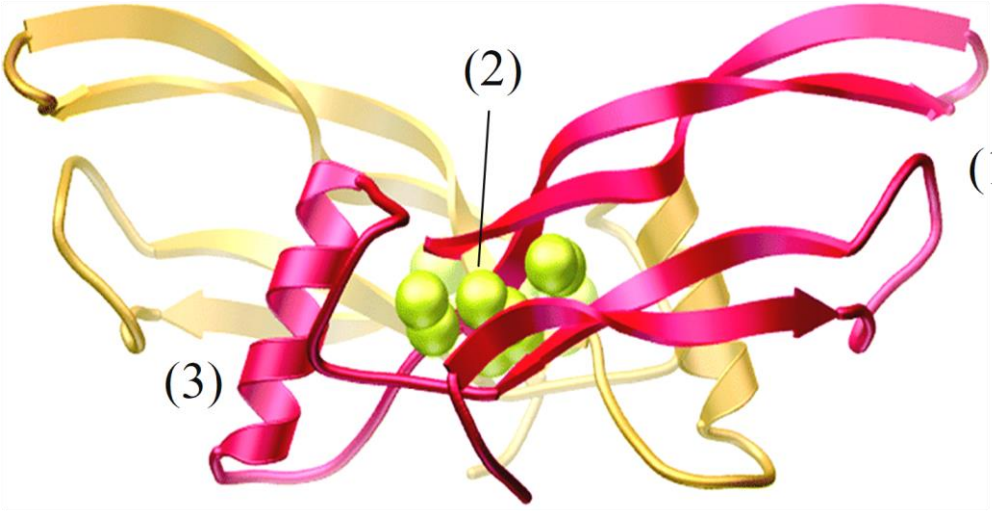

Figure 7. Structure of TGF-β Superfamily Ligands.
"Butterfly shaped" or "open hand" Illustration of BMP3 dimer structure highlighting conserved motifs across the TGF-β superfamily. (1) demonstrates 'fingers' formed by two pairs of anti-parallel β-sheets interlocking with (2) the "cysteine knot" core. (3) consists of the "wrist" domain, formed by the α-helix of one monomer and the "fingers" of the second monomer. Adapted from (51).

1.3.2 Mode of Action

TGF-β signal transduction is initiated by ligand binding to transmembrane serine/threonine kinase receptors. Twelve TGF-β receptor members have been discovered in mammals classified as type I receptors, ALK (activin receptor-like kinases) 1-7; and TGF-β type II receptors (TβRII, ActRIIA, ActRIIB, BMPRII); (53-56). Recruitment of such a specialized network of receptors with ligand interaction dictates downstream signalling via the Smad pathway (see **Figure 8**, below) (57). Nodal and activin share signalling receptors ALK4 and ActRIIA, activating Smad2/3, whereas TGF-β isoforms

interact with TβRII and ALK1/4 mediating phosphorylation of Smad2/3 or Smads 1/5/ 8. In addition, co-receptors have been recognized to facilitate TGF-β ligand accessibility to receptors in a highly regulated manner. These accessory proteins are commonly transmembrane, or GPI (glycosylphosphatidylinositol)-membrane bound such as Cripto, (depicted in **Figure 8**, below) utilized by Nodal mediated signalling (58). This will be further discussed below. Another example of co-receptor activity is betaglycan, known to enhance TGF-βII and inhibin signalling (46, 59).

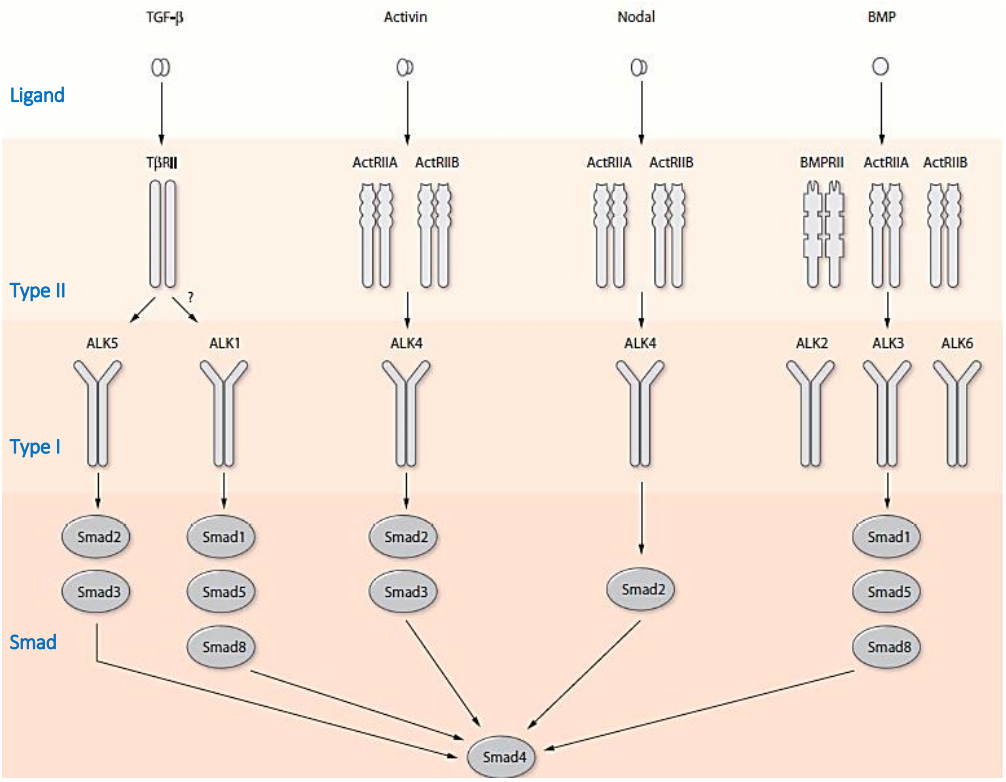

Figure 8. TGF-β Superfamily Ligand Interactions with Receptors.
Summary of key binding components accompanying TGF-β isoform, activin, Nodal and BMP, ligand-receptor complex initiation. TGF-β ligands bind to type I (ALK 1-7) and type II (TβRII, ActRIIA, ActRIIB, BMPRII) receptors to mediate Smad signalling transduction. Adapted from Kitisin K, et al., (2007), (57).

1.3.3 Canonical TGF-β Signalling Pathway

TGF-β family ligands orchestrate myriads of biological responses, initiated by binding to cognate type II and type I receptors, mediating signal transduction via the canonical TGF-β/ Smad cascade. **Figure 9**, demonstrates differential TGF-β ligand/receptor binding to form specific active heterotetrametric complexes, leading to recruitment and phosphorylation of receptor-regulated Smads (R-Smads) (46, 60).

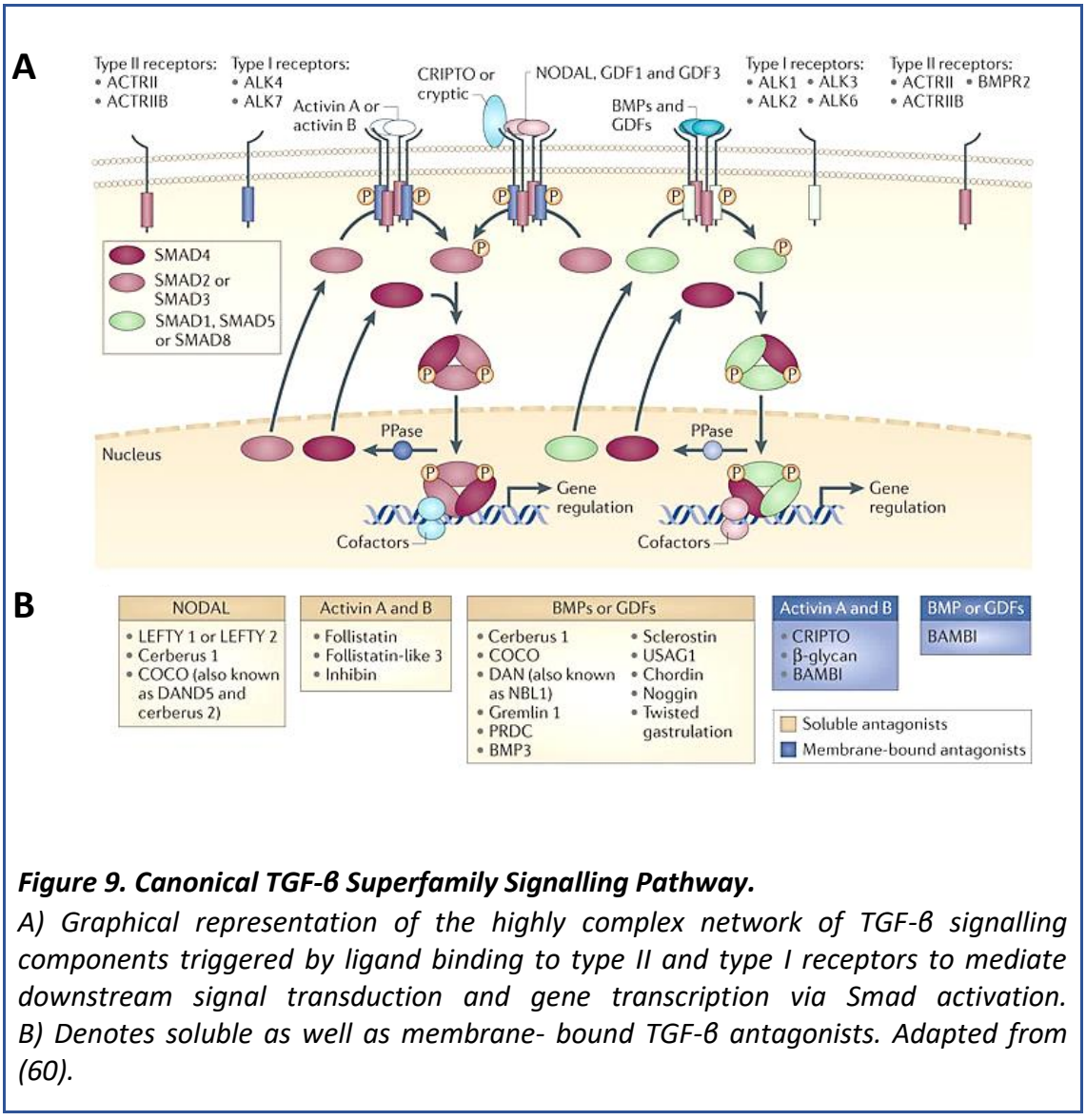

Figure 9. Canonical TGF-β Superfamily Signalling Pathway.
A) Graphical representation of the highly complex network of TGF-β signalling components triggered by ligand binding to type II and type I receptors to mediate downstream signal transduction and gene transcription via Smad activation. B) Denotes soluble as well as membrane- bound TGF-β antagonists. Adapted from (60).

Activated R-Smads form complexes with Smad 4, which translocate to the nucleus to regulate gene expression (61). Endogenous inhibitors, such as Nodal antagonist, Lefty, are key regulators of TGF-β signalling studied extensively during embryonic development (57). Another example is Nodal co-receptor Cripto which antagonizes activin A/B signalling (60).

1.3.4 Nodal

According to Conlon, F.L. *et al.,* (1991), **morphogenic** TGF-β protein, Nodal was originally discovered by retroviral mutation studies in transgenic mouse models, displaying **embryonically lethal phenotypes** (62). Additional murine genetic characterization gave rise to the nomenclature of Nodal, reflecting spatial expression localization within "*the node"* of the gastrula embryonic organizer (63).

Nodal is located on chromosome 10q22.12 of the human genome, consisting of three exons, that translate into 347 amino acid residues to constitute the 26 kDa Nodal protein (64). Similar to other TGF-β family members, Nodal is also **evolutionary conserved** among different species, exhibiting central activities such as mesoderm specification, anterior-posterior axis establishment as well as maintaining stem cell pluripotency during embryonic development (65). **Aberrant reactivation** of Nodal has also been implicated in **carcinogenesis** (66). Integral to understanding the pleotropic biological actions of Nodal in health and disease is the underlying mode of action.

1.3.4.1 Canonical Nodal signalling axis

Nodal is initially biosynthesized in the form of a dimeric pro-protein followed by proteolytic processing which serves as an inherent regulatory mechanism of TGF-β activity (65). Proteolytic processing also regulates Nodal's biological activity (65). However, in contrast to other TGF-β ligands, studies conducted during embryonic development indicate that Nodal is enzymatically processed extracellularly. Cleavage by subtilisin-like proprotein (SPC) enzymes including FURIN (or SPC1) and PACE 4 (or SPC4) activates Nodal (67). It has also been reported that co-receptor **Cripto** facilitates proteolytic cleavage, by interacting with the Nodal pro-protein and SPC and forming a complex (68, 69). Canonical TGF-β signalling is initiated with mature Nodal ligand binding to type II (ActRIIA/B) and type I (Alk4) receptor transmembrane serine/threonine kinases (refer to **Figure 10**), and co-receptor Cripto (70). Cripto is an essential mediator of Nodal dependent-Smad signalling cascade, facilitating high affinity receptor binding.

Receptor complex activation leads to phosphorylation of receptor type I by receptor type II kinase, as well as Smad2/3 activation (61). This triggers association of cytosolic R-Smads (receptor associated -Smads) Smad2/3, with co-Smad (common mediator-Smad) Smad4 and formation of hetero-oligomeric complexes which translocate to the nucleus (50). The accumulation of active Smad complexes initiates interactions with winged-helix transcription factor FoxH1, and homeodomain protein Mixer which act as co-activators of targeted gene expression (71). Furthermore, active Smad2/3-Smad4 complexes also interact with Mediator transcriptional co-activator complex subunit ARC 105 to further facilitate gene transcription (66).

1.3.4.2 Antagonism

Developmental studies have provided significant evidence of Nodal signalling regulation by secreted antagonists. **Lefty** proteins have been established as TGF-β inhibitors that bind unconventionally to Nodal, or co-receptor Cripto, as monomers instead of dimers, preventing formation of active receptor-ligand complexes and thus blocking downstream signalling (72-74).

Nodal activities are also abrogated by **Cerberus**, which obstructs ligand-receptor interactions by directly binding to Nodal. Cerberus is a multifunctional TGF-β inhibitor that also binds to BMPs (75). In addition, membrane-bound proteins Tomoregulin-1 (76) and Nicalin (77), also attenuate Nodal signalling. Subsequently *Lefty* and *Cerberus-like* genes are transcribed by the Nodal cascade, acting as negative feedback mechanism to regulate Nodal (65, 78). Collectively these processes control spatiotemporal activities of Nodal in embryogenesis and are dependent upon communication with the surrounding microenvironment.

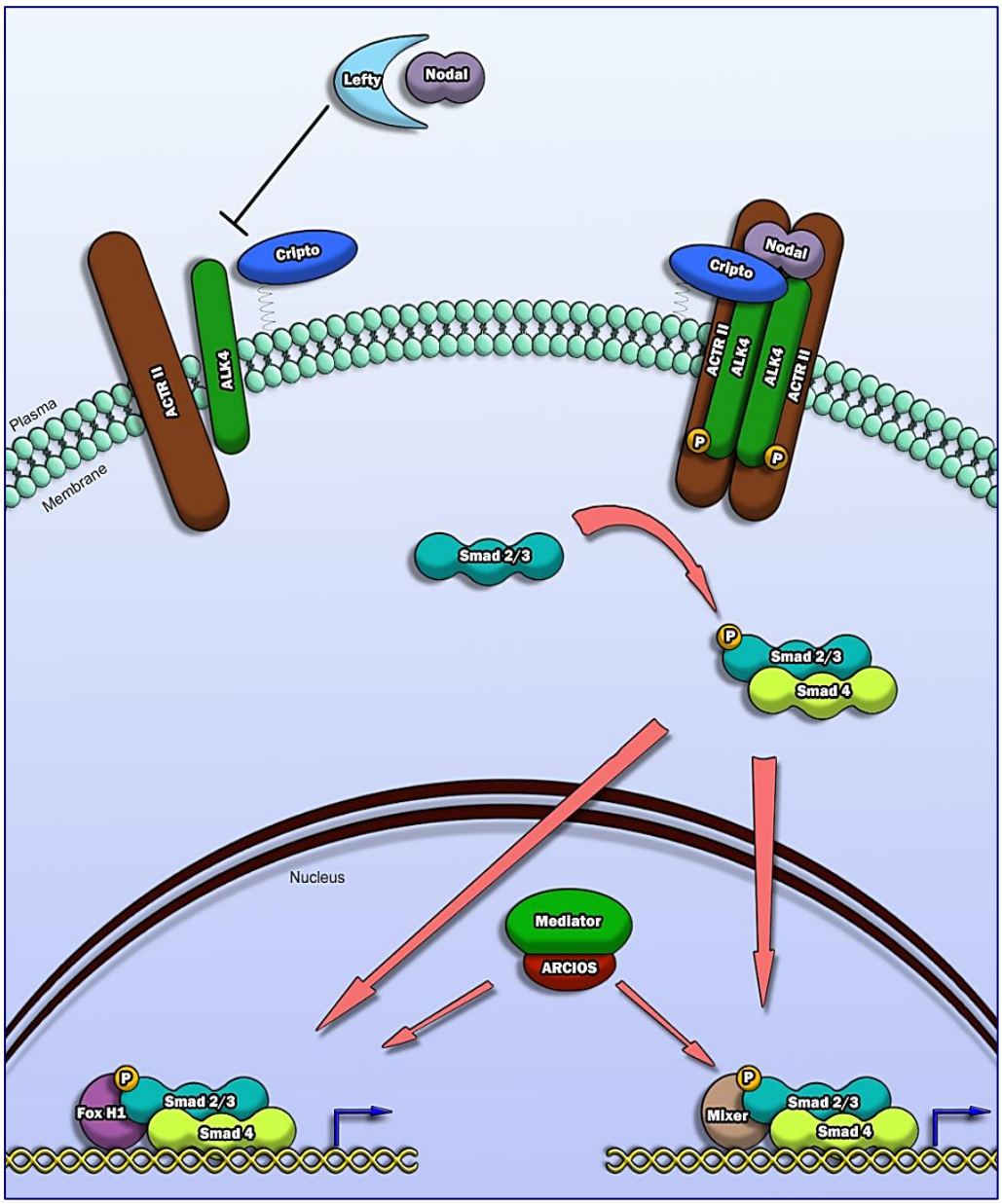

Figure 10. Canonical Nodal Signalling Pathway.
Illustration of the canonical Nodal signalling pathway. Nodal dimers bind to co-receptor Cripto forming an active complex with type II (ActRIIA/B) and type I (ALK4) receptors, leading to Smad 2/3 phosphorylation and complex formation with Smad 4 and translocation to the nucleus. Active Smad complexes within the nucleus, interact with transcription factors (Fox H1, Mixer) and transcriptional co-activator complex (ARC 105, Mediator), leading to transcriptional activation of target genes. Lefty is a soluble antagonist that binds to Nodal and prevents downstream Smad activation.

1.3.4.3 Cripto essential mediator of Nodal signalling

1.3.4.3.1 Structure and canonical signalling

Cell surface **GPI** (glycosylphoshatidylinosytol) anchored protein co-receptor Cripto is an essential mediator of canonical Nodal signalling (79). **Cripto** belongs to the EGF-CFC (epidermal growth factor-cripto-FRL-Cryptic) family of growth factors which consist of an amino-terminal signal peptide, an epidermal growth factor (EGF)-like domain, a cysteine- rich CFC domain and a hydrophobic C-terminus that contains a site for GPI-anchor attachment to the cell membrane, as illustrated in **Figure 11** below (80, 81). A soluble, biologically active form of Cripto, is generated by removal of GPI domain by GPI-phospholipase D (82). Although coexistence of both soluble and membrane bound Cripto has been reported both *in vivo* and *in vitro*, the precise biological effects that they elicit have not yet been clarified in detail (83).

Figure 11. Graphical illustration of Human Cripto Protein.
Human Cripto protein consists of 188 amino acid residues. Key structural motifs include: N-terminus, EGF-like domain, CFC-domain, and the hydrophobic C-terminus containing GPI site.

As previously mentioned, Cripto is an essential **co-receptor** for canonical Nodal signalling and activation of the receptor complex ALK4 and ActRIIA/B (see **Figure 10**). Cripto interacts with Nodal through the EGF like-domain (refer to **Figure 11**) and requires post-translational modification by o-fucosylation (83). Whereas binding of Cripto to

ALK4 is mediated by the CFC domain (81). Direct interaction of Cripto and ALK4 is essential for binding of Nodal to the ALK4/ActRII complex mediating downstream Smad signalling activation, and subsequent transcriptional activation of target genes (49, 50). Cripto also plays an important role in **endocytic trafficking** of Nodal and thus controls signal strength. At the cell surface, Cripto recruits the Nodal precursor and an SPC enzyme (Furin or PACE4), to facilitate cleavage of the prodomain, as well as endocytotic translocation in early endosomes (69, 84). Within the endosomes the Nodal/Cripto complex interacts with the ALK4/ActRII receptor complex to mediate Smad signalling (83, 85, 86). These molecules will eventually proceed to lysosomal recycling (84).

In addition, Nodal endocytotic trafficking can also occur via **Cripto-independent** mechanisms. The Nodal precursor can be cleaved by soluble extracellular protein convertases or associate with unidentified cell surface proteins from the microenvironment, triggering endocytosis (84). However, in the absence of Cripto, Nodal is sequestered on intraluminal vesicles within endosomes triggering transportation to lysosomes. In this regard, Nodal signalling is delayed or inhibited. Alternatively, unprocessed Nodal can interact with its receptor complex on caveolin lipid rafts to further initiate lysosomal degradation (68).

1.3.4.3.2 Alterative signalling pathways

Cripto has been shown to elicit activities **independent** of the classical Nodal/Smad signalling pathway. It has been reported that Cripto can interact with Glypican-1 which is a GPI-anchored heparan sulphate proteoglycan protein attached to microdomains of lipid rafts within the plasma membrane. This activates downstream signalling via c-Src [cellular sarcoma (Schmidt–Ruppin A-2) viral oncogene]/mitogen-activated protein kinase (MAPK) and phosphatidylinositol 3-kinase (PI3K)/Protein Kinase B (Akt) signaling

pathways independent of Nodal (87). The latter downstream signalling pathways are important regulators of cell proliferation motility, and survival. Evidence suggests that Cripto mediated activation of c-Src is involved in cell proliferation and migration of murine mammary epithelia cells (87).

Subsequently, it has recently been shown that **Cripto** also binds to GRP78 (glucose regulated protein 78kDa) at the cell surface (88). This interaction activates both the Nodal-dependent Smad cascade as well as the **Nodal-independent** Src/MAKP/PI3K pathway, to promote cellular proliferation and survival (89). Additionally, Cripto can also function as a chaperone protein to promote Wnt/β-catenin as well **as Notch/Cbf-1** signal transduction pathways (90). These signalling pathways have been shown to modulate stem cell proliferation and differentiation.

1.3.4.3.3 Roles in Embryogenic Development

EGF-CFC homologues have been identified in human (Cryptic), mouse (Cripto-1, Cryptic, cfc1), zebrafish ([oep] one-eyed pinhead), Xenopus (FRL1/XCR1, XCR2, XCR3) and are expressed almost exclusively during embryogenesis (91, 92). Zebrafish and murine genetic studies have shown that EGF-CFC proteins are critical regulators of **mesoderm** and **endoderm** formation as well as the establishment of left/right asymmetry and cardiogenesis during vertebrate development (91). This phenotype is replicated in knock out studies including: *ActRIIA/B* $^{-/-}$; *Alk4*$^{-/-}$; and *Nodal* $^{-/-}$ mice. These are consistent with the overlapping embryogenic properties of Nodal mediated signalling via Activin receptors, facilitated by Cripto triggering TGF-β/Smad signalling (93-95).

Cripto's vital roles in development were further elucidated according to Xu C., *et al*., (1999), by murine *Cripto* knockout (Cr-1$^{-/-}$) models displaying **embryonically lethal** phenotypes, accompanied by gastrulation failure, aberrant morphogenesis, pericardic

mesoderm defects and death at embryonic day seven and a half (96). Furthermore, the morphogenic activities of Cripto extend to also include primitive streak elongation, anterior/posterior axis patterning specification, mesoderm formation and organogenesis (97).

Cripto is crucial in regulating **stem cell maintenance**, pluripotency, and cellular growth during embryonic development and is recognized as a stem cell marker. Cripto is expressed in undifferentiated pluripotential or [induced pluripotent stem cells (iPSC)] human and murine embryonic stem (ES) cells. More specifically, Cripto is detected within a four-day mouse blastocyst, confined in the inner cell mass as well as in extraembryonic trophoblast cells, prior to gastrulation (92). Cripto expression peaks within migrating epiblast cells (via **EMT**) that will compartmentalize to mesoderm and endoderm (98). The Cripto expression pattern is constrained to cardiac progenitor cells following the eighth day of embryogenesis (99).

1.3.4.3.4 Oncogenic properties

The essential functions of stem cell maintenance and pluripotency displayed by Cripto during embryonic development, have also been implicated in **tumourigenesis**. The *CRIPTO* gene was initially isolated from human NTERA 2-D1 testicular, and mouse F9 undifferentiated, teratocarcinoma cells (80). Hence, the *CRIPTO* gene is also known as *TDGF1* (Teratocarcinoma-Derived Growth Factor). Following developmental stages, in the normal adult tissue, the expression of Cripto is significantly reduced and sequestered to either the stem cell niche, or within highly regenerative cellular compartments (100).

Overwhelming evidence support observations collectively validating that **Cripto overexpression** *in vitro* induces a transformed cellular phenotype (101-103). Concurrently, transgenic mice overexpressing Cripto in the mouse mammary gland,

under the control of MMTV (mouse mammary tumour virus), develop mammary tumours (104, 105). Anti-sense inhibition of *CRIPTO* in human cancer cells reverts their transformed phenotype both *in vivo* and *in vitro,* highlighting the essential **tumourigenic properties of Cripto** (106). In addition, use of specific antibodies that target either the EGF-like domain, or the CFC region of Cripto, have resulted in inhibition of tumour growth by 70% in testicular and colon xenograft models, as well as other carcinoma cell lines (107, 108).

Cripto partakes in a variety of signalling pathways to promote tumour development and progression. Both in *in vitro* and *in vivo* reports clearly demonstrate that Cripto enhances proliferation, anchorage independent growth, EMT (epithelial to mesenchymal transition), motility, migration, invasion, vascularization, and angiogenesis of cancer cells, to sustain **malignant progression** (101, 109-113).

Cripto also interacts with other TGF-β family members ligands such as activin A/B and TGF-β1 and antagonizes signalling by preventing complex formation with their cognate signalling receptors (88, 114). In this regard Cripto inhibits activin A/B and TGF-β1 mediated **growth inhibitory** and **cytostatic effects** (115). Concurrently Cripto mediated signalling promotes proliferation migration and plasticity to further favour the oncogenic phenotype (114,115).

Cripto has been detected to be aberrantly overexpressed in human breast, colon, non small cell-lung, testicular, gastric, pancreatic, cervical squamous, ovarian, oesophageal squamous, and hepatocellular carcinomas compared to healthy tissue (116, 117). Interestingly, **increased Cripto** expression plasma levels were detected in early stage breast cancer patients, compared to healthy controls, implicating its use as potential biomarker for early diagnosis of malignancy (118). Further evidence suggests

clinicopathological significance and prognostic value of Cripto associated with advanced disease. Additionally, increased Cripto serum levels were observed in breast, colon, non small cell-lung, cervical squamous, oesophageal squamous and hepatocellular cancers which correlated with **metastatic potential** and **poor prognosis** (119-124).

1.3.4.4 Nodal Mediated Roles in Developmental Biology

TGF-β superfamily members have been extensively characterized to exhibit essential roles during embryonic development. This section focuses on the crucial morphogenic mechanisms mediated by Nodal to better understand re-emergence in tumourigenesis.

1.3.4.4.1 Early Events of Mammalian Embryonic Development

Embryogenesis encompasses a complex interplay of cellular processes such as division and differentiation required for embryonic conception and development. **Figure 12** portrays the homologous developmental events during the pre-implantation stage, among human and mouse (125). However, differences in timing and molecular signalling pathways are distinguishable in these two species. Following human and mouse fertilization, the single diploid, zygote cell undergoes mitotic divisions (cleavage) increasing cell numbers (without cell growth), leading to the formation of the blastocyst (126). The **blastocyst** is comprised of the ICM (inner cell mass) containing pluripotent embryonic cells, and the outer trophectoderm layer (127). Subsequently, pre-implantation epiblast and hypoblast (or primitive endoderm) compartments of the late blastocyst, are derived from ICM. Following implantation, the human embryo exhibits distinct structural characteristics compared to mouse (as seen in **Figure 12**) (128).

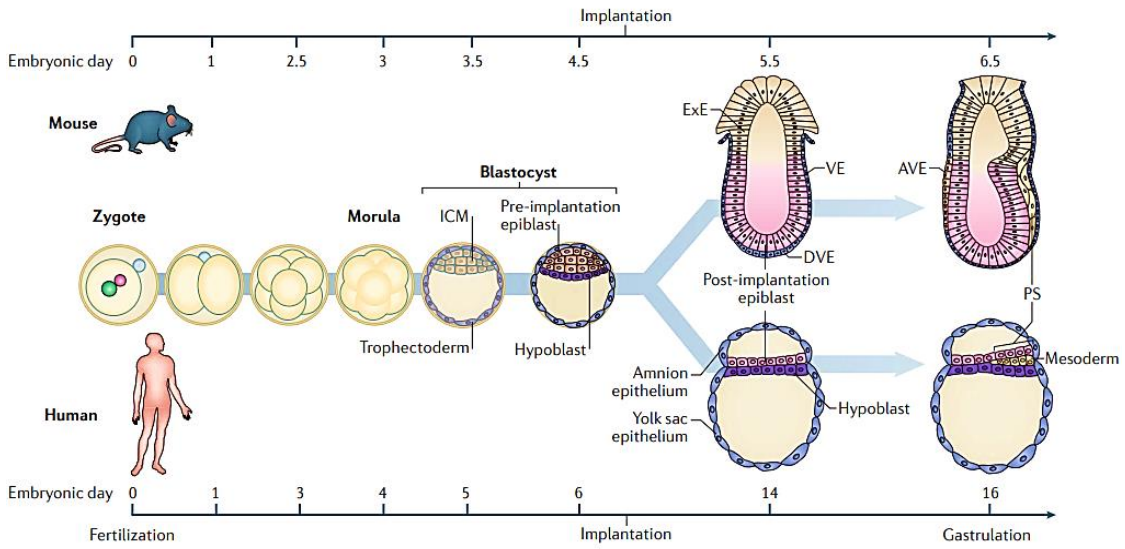

Figure 12. Early Developmental Events in Murine and Human Embryos.
Schematic representation of embryogenic stages occurring in the zygote during fertilization, implantation, and gastrulation. Structural similarities are evident in the pre-implantation stage of both mouse and human embryos. Following implantation and gastrulation human embryonic architecture displays species specialization and patterning, distinct from murine. ExE (trophectoderm-derived extra-embryonic ectoderm); VE (visceral endoderm); DVE (distal visceral endoderm); AVE (anterior visceral endoderm); PS (primitive streak). Adapted from (125).

Gastrulation in the human embryo, commences at embryonic day 16 upon formation of the primitive streak at the posterior end of the embryonic disc. Gastrulation is initiated by gradient morphogenic activity throughout the developing embryo, for germ layer specification. Epiblast cells undergo EMT and migrate between the epiblast and primitive endoderm, forming the mesoderm and ectoderm layers (129). This follows ingression of epiblast cells to give rise to the endoderm layer. This transformation process leads to the establishment of three germ layers (ectoderm, mesoderm, endoderm) for lineage specification and embryonic patterning, as depicted in **Figure 13**

(130). The ectoderm will develop into the following: nervous system (central and peripheral), epidermis, sensory organs (eye, ear, nose) (131). Whilst circulatory system, heart, kidney, reproductive system, skeletal system, smooth muscle, connective tissues, tendons, ligaments, dermis and cartilage are derived from the mesoderm lineage (132). The endoderm is a precursor of the gut tube (including cecum, intestine, stomach); liver; pancreas; lungs; thyroid; prostate (133).

1.3.4.4.2 Morphogenic Properties in Early Embryonic Development

Nodal and members of its signalling pathway play crucial roles during **early embryogenesis**, including germ layer induction as well as anterior-posterior and left-right axis establishment. Nodal is also vital during the implantation stage of embryonic development, with its expression localized in the ICM of the blastocyst and secreted by ESCs to facilitate expansion of progenitor precursor cells (134). Lack of Nodal signalling in mouse mutants has been reported to contribute to premature differentiation of the ICM to neuronal tissue (135). Following implantation, Nodal is imperative in **maintaining pluripotency** and is expressed in the epiblast from which the foetus is derived (134, 136).

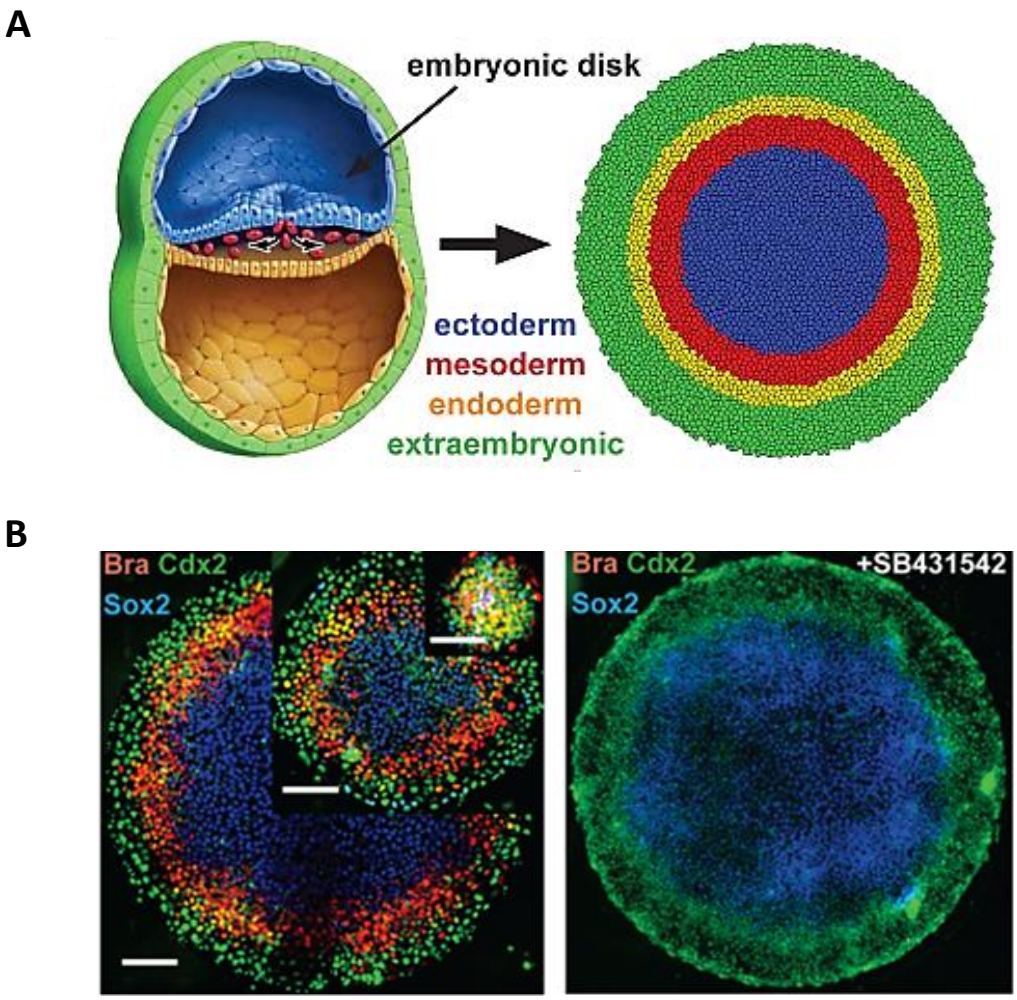

Figure 13. Gastrulation Structure of Embryonic Stem Cells.

A) Architecture of human embryo gastrula (left) and micropatterned hESC cells treated with morphogenic BMP4 for 42 hours, according to Heemskerk, I. and Warmflash, A., 2016.; to simulate embryonic patterning in vitro. B) Immunofluorescence staining of lineage markers including extraembryonic (Cdx2+, Sox17-, Bra-, Sox2-); endoderm (Sox17+, Sox2); mesoderm (Bra+, Sox17-); ectoderm (Sox2 +, [Nanog-, not provided]). The authors treated with the Nodal inhibitor SB431542 (B right panel); resulting in aberrant gastrulation patterning with lack of mesoderm formation and abnormal ectoderm expansion within the mesodermal layer. (B left panel) In comparison control pluripotent cells undergoing specification of ectoderm, mesoderm, and endoderm germ layers. Adapted from (130).

1.3.4.4.3 Mesoderm and Endoderm Induction

Nodal's fundamental developmental roles have been revealed by knockout studies vertebrate models including human, murine, zebrafish, Xenopus; reported to display defects in mesoderm, endoderm, and **primitive streak formation** (63, 78, 136, 137). Primitive streak in the mouse embryo is achieved via "interlinked fast and slow positive regulatory loops" (138). As illustrated in **Figure 14**, unprocessed pro-Nodal protein is secreted from the epiblast and induces expression of FURIN and PACE4 enzymes as well as BMP4 from the neighbouring ectoderm. Subsequently BMP4 activates Wnt3 pathway activation in the epiblast leading to Nodal and Cripto expression (139). Concomitantly Cripto null mouse models present analogous phenotypes to Nodal $^{-/-}$ mice, with primitive streak defects and lack of mesoderm and endoderm patterning (139, 140). Thus, mesoderm is generated upon low Nodal activity responses. While high levels of Nodal signalling, mediated by Mixer homeoproteins, leads to **endoderm specification** (137, 141, 142).

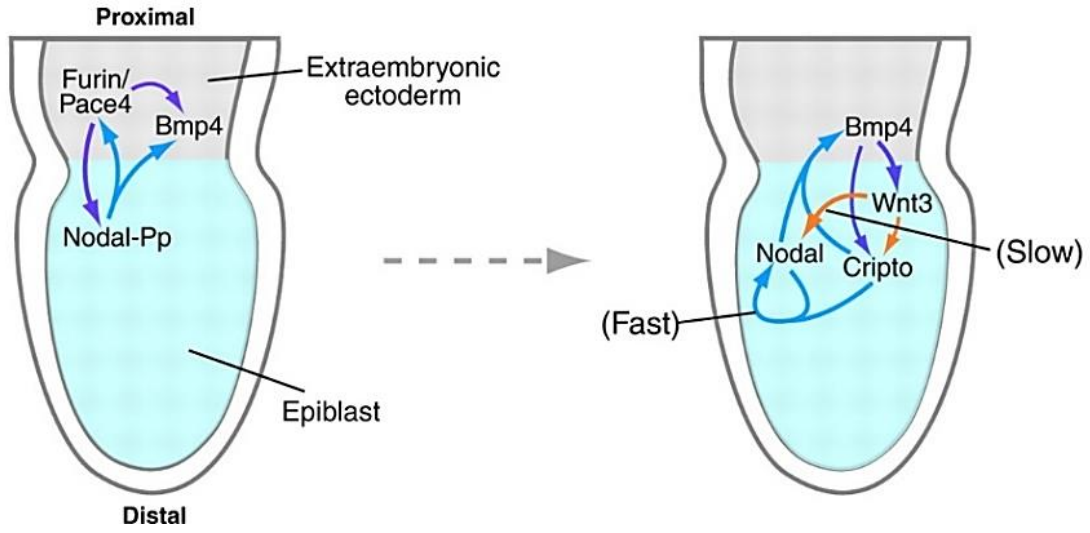

Figure 14. Models of Regulatory Pathways in Murine Mesoderm Induction.
Graphical depiction of the pre-gastrulation stage of embryonic development represented in lateral view. Nodal pro-protein (Nodal-Pp) expressed in the epiblast, activates expression of its convertases (FURIN, PACE4), and Bmp4 in the extraembryonic ectoderm. In turn mature Nodal production triggers both fast acting and slow acting autoregulatory feedback loops to induced primitive streak formation. Adapted from (138).

1.3.4.4.4 Neural Patterning

Nodal signalling is an essential mediator of **neural development** (see **Figure 15**). As previously discussed, Nodal is initially expressed in the ICM and primitive endoderm of the mouse blastocyst at 4.5 dpc (days post-coitum). At 5.5 dpc Nodal expression is confined within the epiblast and embryonic visceral endoderm, to facilitate induction of

the **AVE** (anterior visceral endoderm) (134). Anterior patterning of the adjacent epiblast is mediated by secretion of Nodal's antagonists Lefty and Cerberus within the AVE (143). Modulation of Nodal signalling by Lefty and Cerberus inhibitors is detrimental in anterior neural specification, as excessive Nodal activity contributes to the formation of enlarged or duplicate primitive streaks according to Perea-Gomez *et al.,* (2002), (144). Furthermore, decreased Nodal activity is observed in mutant oep (Cripto homologue) zebrafish as well as in hypomorphic Cripto mouse mutants with phenotypes that resemble human holoprosencephaly[1] (145, 146).

1.3.4.4.5 Left-Right Axis Specification

As murine development progresses to the gastrulation stage, Nodal pathway activity is restricted to the node located at the anterior of the primitive streak (65). Left-right axis specification is initiated from the node (63, 147). **Patterning of the left** side of the embryo results from Nodal signalling through the ventral node as well and this is facilitated by co-receptor Cryptic from the lateral plate mesoderm (68). Whilst in the right side of the embryo the activities of Nodal are restricted by inhibitors (CER1, Lefty1/2). Concurrently, leftwards ciliated action by the node physically confines Nodal within the left side of the embryo (68). Following gastrulation, Nodal is downregulated during somitogenesis, with expression ceasing at 8 dpc (148).

[1] Holoprosencephaly (HPE) is a cephalic birth defect caused by failure of the prosencephalon (embryonic forebrain) to sufficiently develop two hemispheres, resulting in a single-lobed brain accompanied with skull and facial abnormalities. HPE malformations may also include: close eye spacing, small head size, lip cleft, mouth roof. Highly sever cases can be fatal (146).

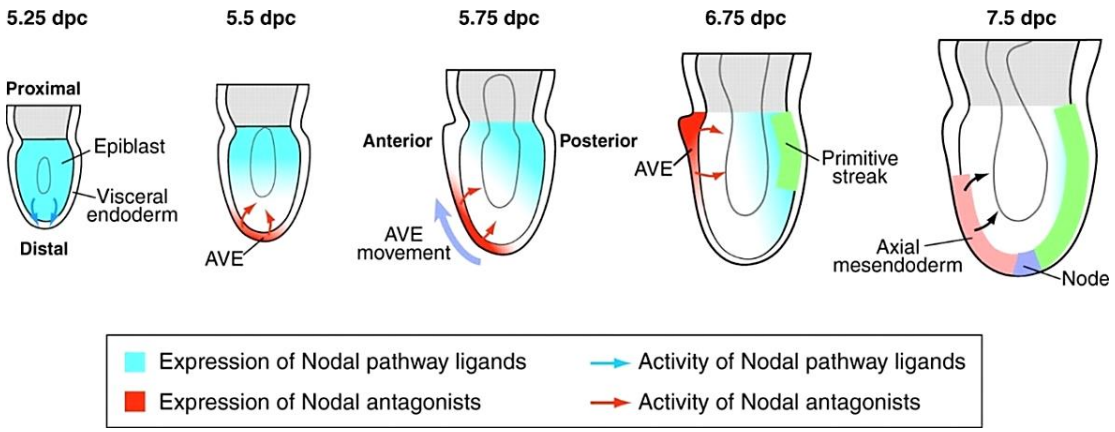

Figure 15. Stages of Murine Neural Specification Mediated by Nodal Signalling. *Regions of Nodal expression are highlighted in blue and areas coloured in red indicate presence of Nodal inhibitors (Lefty and Cerberus). Following implantation at 5.25 dpc (days post-coitum), Nodal signalling throughout the epiblast, is necessary for establishment and movement (purple arrow) of the AVE (anterior visceral endoderm) at the distal end of the developing embryo. Lefty and Cerberus, expressed within the AVE, antagonise Nodal leading to anterior specification in adjacent epiblast at 5.75 dpc. Concurrently, Nodal activity leads to the development of the anterior primitive streak and in turn, the axial mesendoderm accompanied by gastrulation at 7.5 dpc. Finally, the axial mesendoderm conveys important signals (black arrows) for forebrain and neural tube patterning. Adapted from Shen, M. M., et al., (2007), (138).*

1.3.4.5 Regenerative stem cell functions

Nodal displays instrumental morphogenic roles in early embryonic development, as previously discussed, and is functionally restricted in the normal adult tissue. However, Nodal has also been shown to exhibit important functions in non-embryonic tissues that

are highly dynamic and undergo regenerative or remodelling events. Nodal is expressed in the **placenta** although its roles are controversial. Evidence suggests that Nodal supports normal placentation as well as regulating trophoblast differentiation during placental development (149). A study which utilized conditional knockout mice lacking Nodal specifically in the reproductive tract, demonstrated the importance of Nodal for placentation, and full-term pregnancy (150). The authors also reported a defective maternal-foetal interface disrupted placentation, as well as intrauterine growth restriction, accompanied by preterm birth at 17.5 days post coitum and foetal loss (150). However further studies are required to clarify the intricate mechanisms involved and the precise mechanisms regulate by Nodal signalling during **fertilization** and **pregnancy**.

Nodal signalling has also been suggested to regulate **mammary gland** development during lactation. Cyclical expression of Nodal and cognate signalling pathway members was detected in murine mammary gland (151, 152). Accordingly, Nodal, Cripto, ALK-4, and SMAD4 were upregulated during lactation, and downregulated during post-lactational involution of Balb/C mice (151, 152). In this regard Nodal orchestrates mammary gland remodelling events as increased Nodal signalling coincides with proliferative alveola expansion accompanying lactation. In contrast, subsiding of Nodal signalling concurs with apoptotic events of alveolar epithelial tissue, that take place to revert the mammary gland to pre-lactation morphology during involution (153-155).

Furthermore, Nodal signalling is essential in maintenance of **human adult stem cells** parallel to its regulatory functions in pluripotent embryonic stem cell niche during development. Studies suggest that tightly regulated Nodal activities govern the fate of human adult liver and pancreatic **stem cell populations** (156, 157). However, the detailed mechanisms associated have not been fully deciphered yet.

1.3.4.6 Nodal Signalling in Cancer

As discussed previously, Nodal expression is generally restricted to embryonic and dynamic tissues. During late developmental stages upon cellular differentiation, Nodal expression is "*switched off*" and its activity is generally absent from adult tissues (65). However, evidence suggests that **Nodal re-emerges in malignancy** and its morphogenic properties facilitate tumour development (refer to **Figure 16**) (158).

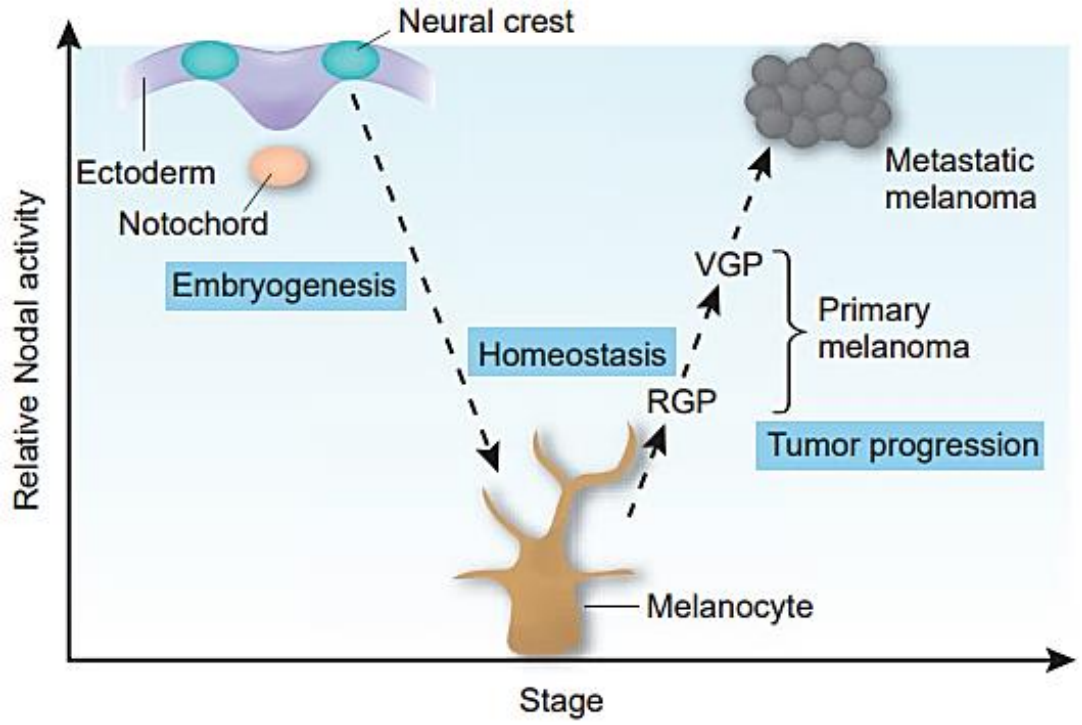

Figure 16. Nodal Re-Emerges during Melanoma Progression.
Illustration depicting Nodal activity during embryogenic and tumourigenic events. In early embryonic development Nodal activity is elevated and is then lost with melanocyte differentiation. Upon malignant transformation Nodal expression and activity rise dramatically with increase disease stage. RGP, radial growth phase; VGP, vertical growth phase. Adapted from (158).

Studies implicate Nodal-mediated maintenance of pluripotency to be associated with increased tumourigenesis and cancer cell aggressiveness (66, 159-161). Morpholino-oligonucleotide inhibition of Nodal *in vivo* reduced plasticity of melanoma cells and significantly reduced tumourigenicity and metastasis (66, 159).

Eloquent studies conducted by Postovit *et al*., employed *in vitro* and *in vivo* a three-dimensional (3D) model enriched by hESCs (human embryonic stem cells), to examine the effects of the **stem cell microenvironment** on melanoma cell behaviour (162, 163). The authors determined that exposure of **aggressive melanoma** cells to the stem cell enriched 3D model (prior to removal of hESCs) lead to reduced tumour growth and proliferation, as well as increased apoptosis (163, 164). It was postulated that the suppressed tumourigenicity of metastatic melanoma cells resulted from Lefty (Nodal inhibitor) secreted by the hESC microenvironment.

Subsequently, Nodal overexpression was detected in highly advanced **melanoma** tissue sections (stages III and V) compared to undetected levels from normal skin samples (66, 165, 166). Further studies demonstrate that Nodal contributes to aggressive melanoma vascular-like phenotype, and Nodal signalling blockade reduced vasculogenic mimicry (167, 168). These findings implicate dysregulated embryogenic processes involving Nodal to promote invasive and aggressive tumour phenotypes. However, additional studies should be conducted to validate the potential prognostic value of Nodal in melanomas.

Nodal signalling has also been shown to play crucial roles in the development of **breast cancer** (169). Knockdown studies have revealed that *NODAL* facilitates growth, proliferation, invasion and cell renewal of triple-negative breast cancer cells. Additionally, xenografts of *NODAL knockdown* breast cancer cells displayed significant

reductions in tumour progression, compared with controls (169). Further studies utilized Nodal inhibitor, Cerberus to block Nodal signalling in breast cancer cells (170). Treatment of these cells with human Cerberus significantly reduced proliferation, migration and invasion of cells that expressed high levels of Nodal (170).

Concurrently, it has been suggested that Nodal facilitates **breast cancer** angiogenesis. In primary breast cancers Nodal protein expression was positively correlated with microvascular density (171). The authors also demonstrated that Nodal mediated vasculature recruitment by promoting expression and secretion of pro-angiogenic factors VEGF (vasoactive endothelial growth factor) and PDGF (platelet-derived growth factor). In addition, it was also reported that *in vivo* Nodal inducible inhibition results in the collapse of the established tumour vasculature (171).

Nodal has also been implicated in the maintenance of the **cancer stem cell** (CSC) signature of breast cancer. According to Meyer *et al.,* (2009) phenotypic switching of invasive breast cancer cell subpopulations was mediated by Nodal signalling both *in vitro* and *in vivo* (172). Thus, Nodal may be important in sustaining tumour-initiating CSC populations, and maintaining breast **cancer cell plasticity** (173).

Further evidence substantiates **clinicopathological correlations** between Nodal expression levels and **breast cancer progression** and **stage**. A study examining 400 patient samples, found that Nodal was positively correlated with advanced breast tumour stage, lymph node status, tumour grade and dissemination (174).

Similarly, in **glioma patients**, Nodal expression has also been correlated with tumour grade and progression (175). Overexpression of Nodal in poorly invasive cell lines increased their invasive potential, in contrast to *NODAL* knockdown of highly invasive

cell lines associated with supressed invasiveness (175). Lee *et al.,* (2010) also reported that Nodal promotes *in vivo* tumour growth and proliferation (175). Further evidence suggests that that Nodal enables tumour growth and vascularization by regulating HIF-1 (hypoxia-inducible factor-1) (176). These findings collectively support the link between aberrant Nodal signalling and **brain cancer progression** (177-180).

Dysregulated Nodal activities may also contribute to the pathogenesis of **hepatocellular carcinoma**. Cavallari *et al.,* (2013) confirmed that human adult liver stem cells secreting Lefty (Nodal inhibitor) were capable of suppressing the tumourigenicity of Nodal-expressing HepG2 cells (181). These findings corroborate the aforementioned observations of aggressive melanoma cell phenotype reversal by the hESC microenvironment (160). Further evidence suggests that high Nodal expression might be a predictor of poor prognosis of hepatocellular carcinoma (182).

Dysregulated Nodal signalling has also been linked to **male reproductive cancers** including testicular and prostate cancer. A study demonstrated that inhibition of Nodal signalling by anti-Cripto antibody treatment significantly inhibited tumour growth of NCCIT **testicular cancer** cells in murine xenografts (107). Increased Nodal levels where detected in advanced prostate cancer stages compared to non-cancerous tissue, indicating a positive correlation of Nodal with **prostate cancer** progression (183). The authors also showed that overexpression of Nodal *in vitro,* increased prostate cancer cell growth (183). Further studies suggest that dysregulated Cripto/Nodal signalling may be associated with the development of **germ cell testicular neoplasia** (184, 185). However additional investigation is required to fully understand the underlying molecular events at play.

Nodal signalling has also been implicated in **pancreatic cancer** development. Low levels of Nodal expression were detected in well-differentiated adherent pancreatic cancer cells, whilst high Nodal levels were expressed in non-adherent pancreatic spheroids, associated with **CSC populations** (186). Subsequently *in vitro* recombinant Nodal treatment increased spheroid formation, size, and invasiveness of CSCs (186, 187). Whereas, Nodal signalling blockade of pancreatic cells, by an ALK4/7 inhibitor, abolished self-renewal of CSCs and tumourigenicity, both *in vitro* and *in vivo* (186). The authors also demonstrated the reversal of CSC xenograft resistance to gemcitabine chemotherapy (186). It has also been shown that Nodal signalling promotes migration and invasion, induces EMT and enhances the expression of (MMP-2) matrix metalloproteinase-2 of pancreatic cancer cells (188). In line with clinical observations from other cancer types, high expression of Nodal correlated with **reduced pancreatic cancer patient survival rates** (189). These observations illustrate the detrimental effects of Nodal in the pathogenesis, CSC maintenance and aggressiveness associated with pancreatic cancer progression (188).

1.3.4.7 Potential Nodal Targeted Therapeutics Applications in Cancer

Given that the expression of embryogenic Nodal is relatively absent in normal tissues and that its re-emergence facilitates the tumourigenic phenotype, it poses as an ideal target for cancer therapy (65,158). A growing body of evidence suggests the potential use of both Nodal and Cripto as biomarkers of cancer progression and clinicopathological prognosis and survival associated with various cancer types (66,165-169,174-178,180,182,183,189). Nodal has been demonstrated to facilitate proliferation, migration, invasion, EMT, angiogenesis, CSC renewal and plasticity of cancer cells (158,159,163,168,171,172,173,175,180,183,186,188). In this regard dysregulated Nodal signalling promotes crucial cellular processes utilized in the maintenance and

progression of the oncogenic phenotype. Furthermore, Nodal signalling has been reported to play key roles in aggressive cancer types which are problematic to treat with the current chemotherapeutical approaches (164,168,170,171,173-175,177-188). For all these reasons Nodal provides quite a promising candidate for targeted cancer therapy which may be relevant to different cancer types.

1.4 Interferon Superfamily

Interferons (**IFN**)s are a superfamily of class II helical cytokines, identified 50 years ago. Their assigned terminology was based on their abilities to interfere with the growth of viral influenza (190). Aside from anti-viral activities, the IFNs have also been extensively characterised as integral regulators of innate and adaptive immunity by exhibiting anti-proliferative, pro-apoptotic and immunomodulatory properties. According to amino acid composition and receptor specificity, IFNs are classified into type I, type II and type III as illustrated in the phylogenetic tree in **Figure 17** (191-195).

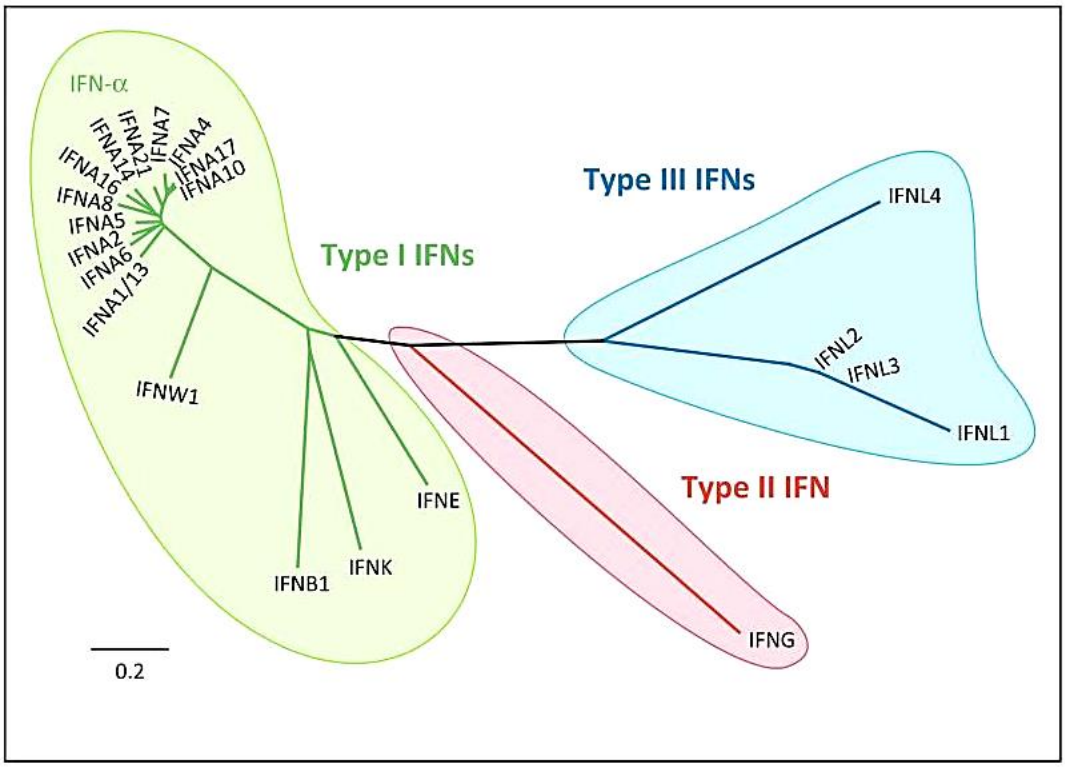

Figure 17. Phylogenetic Tree of Human Interferon Cytokine Family.
IFN superfamily consisting of types I (green), II (red), and III (blue). The scale bar symbolizes amino acid substitutions per site. Adapted from (195).

The **type I IFN** family consists of 8 members including IFNα (14 subtypes), IFNβ, IFNε, IFNκ and IFNω, identified in both human and mice. While members such as IFNδ, IFNτ, and IFNζ (limitin) are exclusively present in porcine, ruminant and mice respectively. The highly evolutionary conserved type I *IFN* family of genes are clustered on human chromosome 9 (196-198) [or mouse chromosome 4 (199-202)] and are all intronless except for *IFNK* (199). Signalling is mediated by the heterodimeric IFNAR receptor complex as illustrated below in **Figure 18** (203).

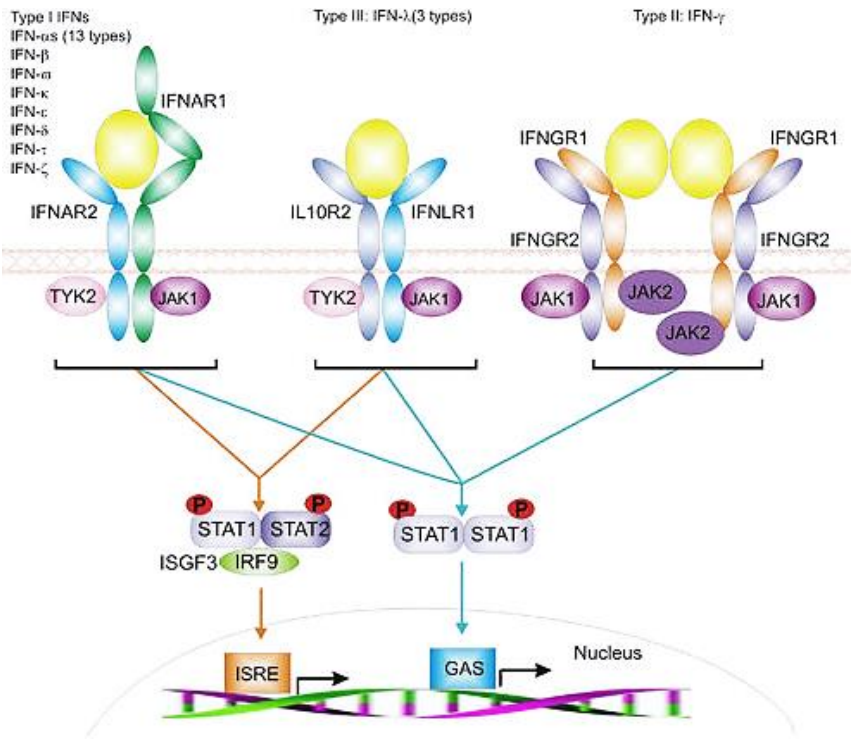

Figure 18. Interferon Superfamily Mode of Action.
Schematic depiction of the differential receptor complex formation IFNs (type I, type II and type III) to mediate signal transduction via the JAK-STAT pathway. STAT complex activation induces specialized gene expression of both ISRE (interferon stimulated response element) or GAS (gamma interferon-activated site) promoter elements (IFN type I and type II) or genes containing exclusively GAS promoter elements (IFN type III). Adapted from (204).

In contrast to type I, the **type II IFN** family consists of a single member only, known as interferon gamma (IFN-γ). Even though IFN-γ is structurally heterogeneous to IFN type I proteins, it has been subsumed to the IFN superfamily, due to exhibiting antiviral as well as immunoregulatory properties (205). Production of IFN-γ is mainly restricted to activated immune cells such as T cells [CD4+T helper cell type 1 (Th1) lymphocytes, CD8+ cytotoxic lymphocytes], NK cells, B cells, and APCs [(professional antigen-presenting cells), including monocytes, macrophages and dendritic cells]; stimulated by mitogens [IL-12, IL-18, IL-2 and phytohemagglutinin (PHA)] (206-208).

IFN-γ signalling is mediated by the IFNGR1/R2 (interferon gamma receptors 1 and 2) tetrameric receptor complex (as shown in **Figure 18**), distinct from the type I IFN signalling mechanism (209). Similar to type I IFNs, IFN-γ signal transduction is facilitated by the JAK-STAT pathway to orchestrate acute host defence mechanisms, as well as adaptive immunity against pathogenic infection (205, 210).

Human **type III IFNs** comprise of four IFN-λ (interferon-lambda) molecules: IFN-λ1 (IL-29), IFN-λ2 (IL28A), IFN-λ3 (IL-28B) and IFN-λ4 (211). **Figure 18** demonstrates that type III IFNs signal via a distinct heteromeric receptor complex composed of IL-10R2 and IFNLR1 (194, 212). The IFN-λs can exert anti-viral activities with cell-type and tissue specificity (213). Type III IFN responses are mainly restricted to lung and intestinal mucosal epithelial tissues due to the restricted expression of IFNLR1 (214, 215).

The widespread immunological properties modulated by interferons to combat bacterial, viral, and fungal infections will not be further discussed as they fall beyond the focus of this thesis. As this thesis will attempt to examine the direct anti-tumourigenic properties exhibited by **type I IFNs** as discussed in **Chapter 4**, this review will attempt to

further elaborate on the associated evidence as well as essential underlying molecular mechanisms.

1.4.1 Type I IFNs

Type I IFNs are produced by all nucleated cell types upon pathogenic infection via the detection of PAMPs (pathogen-associated molecular patterns) of viral or bacterial origin. However, plasmacytoid dendritic cells (pDCs) are specialized in the production of large amounts of type I IFNs (216). Type I IFNs display pleotropic biological functions, crucial in innate and adaptive immunity as well as maintenance of homeostatic mechanisms, as depicted in **Figure 19**. The most commonly characterised type I IFN members include IFNα and IFNβ, which share 30% amino acid sequence identity and are produced in a cell type specific manner. Infected epithelial cells and adjacent fibroblasts produce IFNβ to provide microbial protection by inducing intracellular antimicrobial processes (217).

Concurrently, type I IFNs regulate innate immune responses by facilitating antigen presentation as well as cytokine and chemokine production. Additionally, type I IFN signalling stimulates B cell antibody production and activates T cell function thereby augmenting adaptive immunity (217). Apart from the well characterised anti-viral and anti-bacterial activities, type I IFNs also exhibit anti-proliferative, pro-apoptotic, anti-migratory and immunomodulatory properties via the JAK-STAT signalling transduction cascade. Owing to their anti-tumour activities type I IFNs (α and β) have been clinically utilized in cancer therapy.

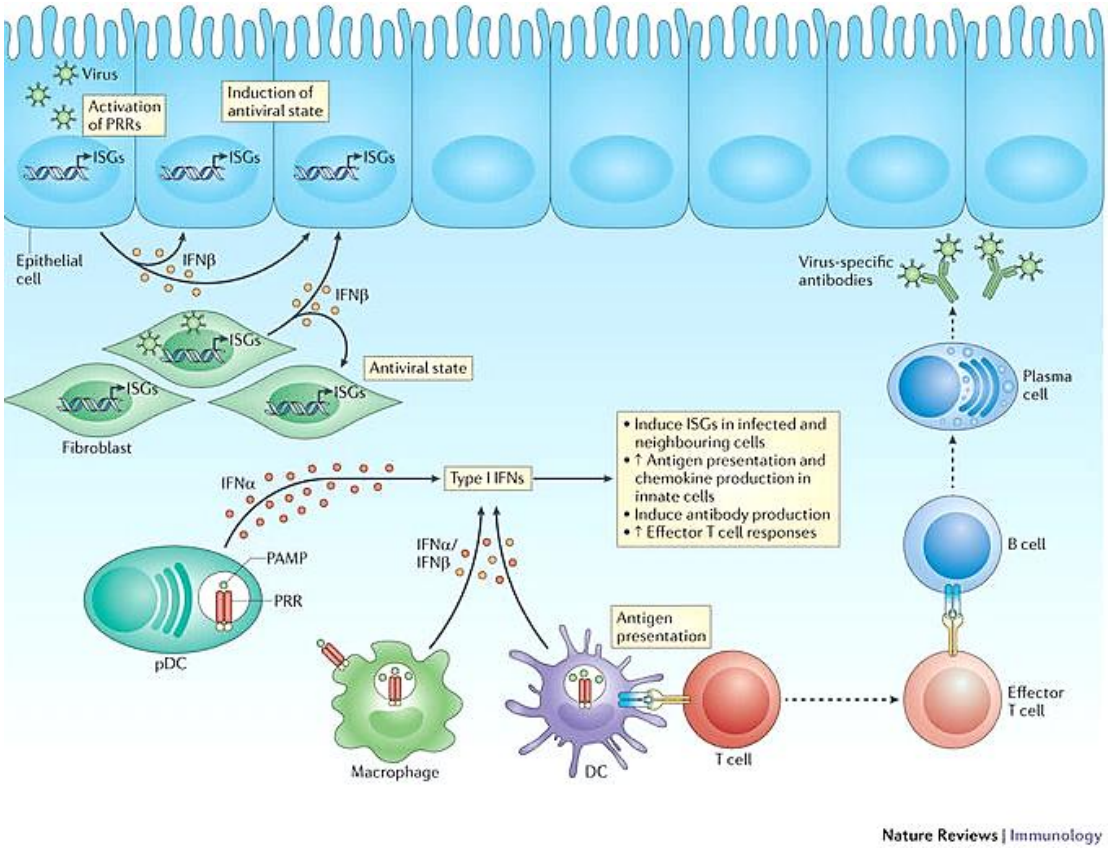

Figure 19. IFN type I mechanisms of Intracellular, Innate and Adaptive Immunity.
Upon infection epithelial cells and neighbouring fibroblasts sense pathogen components via PRRs (pattern-recognition receptor) and secrete type I IFNs (mainly IFNβ). Type I IFN paracrine and autocrine action confines the infection by induction of antimicrobial pathways. Immune cells including DCs and macrophages also produce type I IFNs to facilitate antigen presentation and mediate innate immunity responses. In turn type I IFN signalling triggers B cell antibody production and T cell activation to enhance adaptive immunity. Adapted from (217).

1.4.1.1 Induction of type I IFNs

Production of type I IFNs is initiated by PRRs (illustrated in **Figure 20**), acting as pathogenic sensors. These receptors include Toll-like receptors (TLR), RIG-like receptors (RLR), NOD-like receptors (NLR), and Cyclic GMP-AMP synthase (cGAS); and are localized in the cell surface, cytoplasm and endosome (218). Upon microbial infection, PAMPs or DAMPs (damage-associated molecular patterns) conserved among bacteria and viruses, (such as dsRNA, dsDNA, ssRNA, bacterial lipopolysaccharide) are sensed by the PRR.

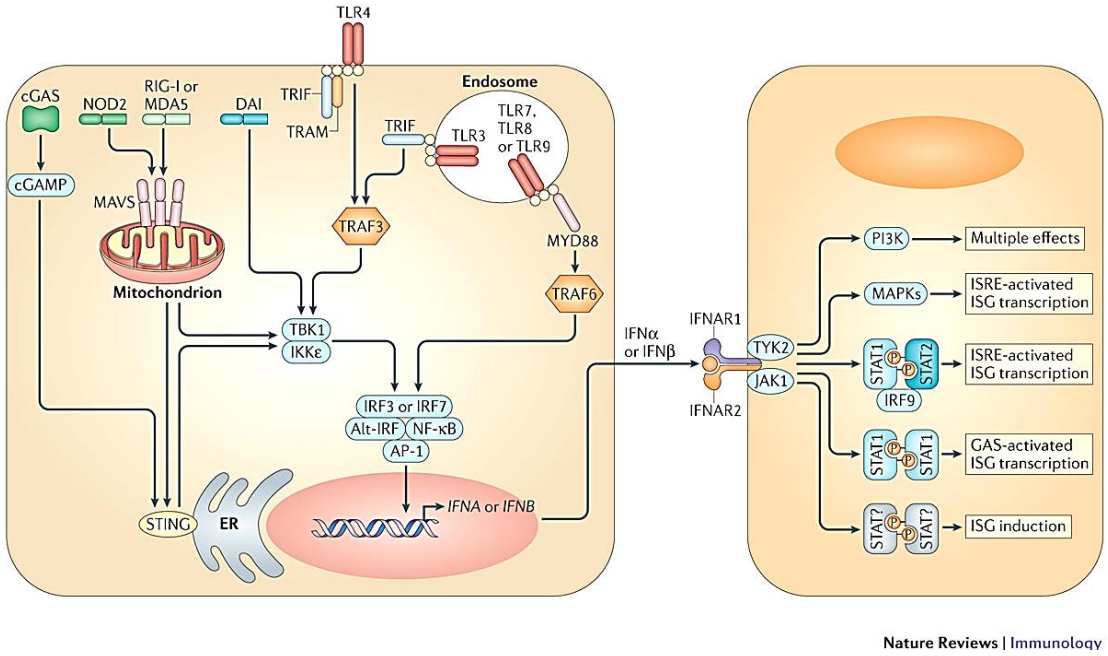

Figure 20. Type I Interferon Induction by Pattern-Recognition Receptors.
Pattern-recognition receptors of infected cells bind to PAMPs and activate downstream signalling pathways leading to transcription of IFNA or IFNB. IFNα/β are then secreted and can mediate either autocrine or paracrine type I IFN signalling. Adapted from (219).

1.4.1.2 Canonical IFN type I signalling

A complex network of IFN type I signalling pathways dictates the precise biological activities in a tightly controlled manner and in accordance with the tissue specific microenvironment. Canonical IFN type I signalling pathway is mediated through activation of the common receptor IFNAR (IFN alpha-receptor), as illustrated in **Figure 21**. Heterodimeric IFNAR consists of two transmembrane glycoproteins IFNAR1 and IFNAR2 (191, 192).

To date, three IFNAR2 isoforms have been identified, as generated by alternative splicing of a commonly transcribed gene (220). Studies conducted in our lab have detected the soluble form, known as IFNAR-2a in serum and attributed both agonistic as well as antagonistic IFN activities (221). However, further studies are required to fully elucidate the function of soluble IFNAR-2a. IFNAR2b is the shortest transmembrane IFNAR2 form lacking the intracellular signalling domain and may act as a dominant negative regulator of type I IFN signalling (222). Whereas IFNAR2c is the long transmembrane form containing the cytoplasmic domain, well characterized for its essential functional requirement within the IFNAR receptor complex, for type I IFN signal transduction (223).

The IFN ligand binds initially to the high affinity subunit IFNAR2 followed by the low affinity subunit IFNAR1 (223). Formation of IFN ligand-IFN receptor complex triggers cross phosphorylation of receptor associated Janus kinase JAK1 and tyrosine kinase TYK2 followed by recruitment and phosphorylation of STATs (Signal Transducer and Activator of Transcription). This leads to STAT dimerization and formation of transcription factor complex ISGF3 [composed of STAT1, STAT2 (or STAT 4, STAT5, STAT6) and IRF9) (224).

The ISGF3 complex then translocates to the nucleus to regulate gene expression, by binding to interferon stimulated response element (ISRE) (225). **IFN type I mediated signalling** can induce transcription of a wide range of interferon stimulated genes (ISGs) encoding for a wide variety of proteins that exhibit cell specific antiviral, anti-proliferative, anti-tumour and immunomodulatory activities (226-228).

Activation of type I IFN signalling leads to the regulation of myriads of ISGs, accounting for over 3,000 identified genes to date. These have been compiled and curated by our group in the Interferome database (229). ISGs that are up- regulated or down-regulated encode effector proteins that mediate broad biological functions, including antiviral, anti-tumour and immunoregulatory (see **Figure 21**). They collectively formulate type I IFN responses based on the cellular microenvironment.

ISGs can also serve as regulators of IFN signalling by providing positive or negative feedback loop mechanisms. PRR and IRFs (interferon regulatory factors) are examples of positive feedback signalling regulation (230). In contrast type I IFNs can also induce the transcription of SOCS (suppressor of cytokine signalling) or USP18 (ubiquitin specific peptidase 18), which act via a negative feedback loop to inhibit JAK-STAT signalling, as a protective mechanism of excessively toxic signalling which contributes to pathology (231). Furthermore, aberrant overexpression of SOCS has been linked to tumourigenesis of melanoma and prostate malignancies (232, 233).

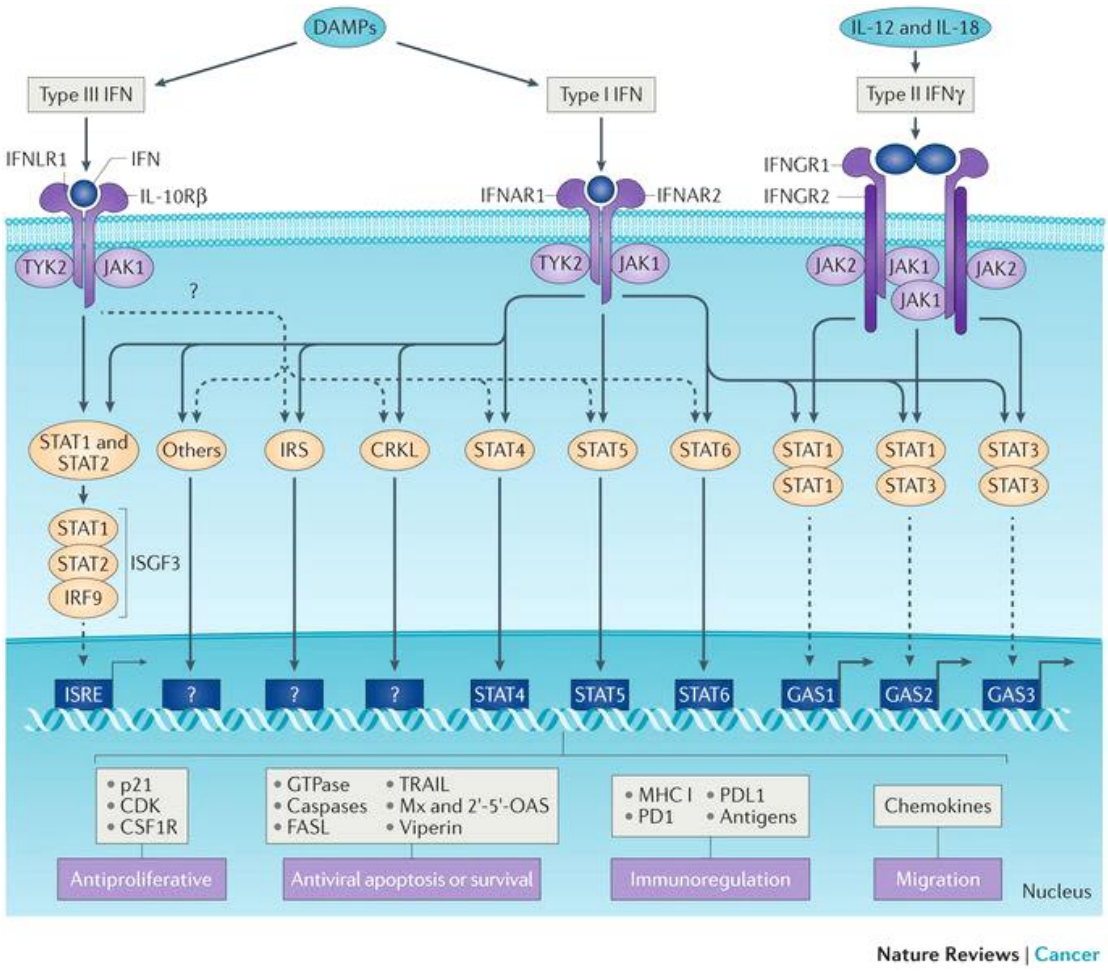

Figure 21. Canonical IFN type I Signalling Pathway.

Cells respond to DAMPs (damage-associated molecular patterns) and produce IFNs. Type I IFNs engage with the IFNAR receptor complex and phosphorylate the JAK1 and TYK2 to initiate the intracellular JAK-STAT pathway. In turn phosphorylation and dimerization of STAT molecules triggers binding to IRF9 and formation of ISGF3 (STAT1/STAT2/IRF9) complex. The latter translocates to the nucleus to induce transcription of interferon regulated genes. Adapted from (234).

1.4.1.3 Non-Canonical type I IFN pathway

Apart from the classical JAK-STAT pathway, type I IFNs can also signal via alternative pathways independent of the JAK-STAT cascade, depending on the cellular context. It has been reported that type I IFNs can also activate p38 mitogen-activated protein kinase (MAPK), phosphatidylinositol-3-kinase (PI3K) and NFkB (nuclear factor κB) pathways (235, 236). Furthermore, type I IFNs have also been shown to facilitate Rap1-CrkL (Ras-proximate-1 -Crk-like protein) pathway associated with repression of p21 (proto-oncogen protein 21) activity. The latter contributing to type I IFN anti-tumour and growth inhibitory effects (237).

1.4.1.4 IFN type I anti-tumour activity

Besides the well characterised host defence properties against pathogens, type I IFNs also exhibit potent anti-tumour effects, by promoting anti-proliferative and anti-apoptotic cellular mechanisms (238). These anti-tumour activities (summarised in **Figure 22**) are executed either directly by intrinsic cellular procedures or indirectly by utilization of host immunosurveillance processes (239). "*As such, the effect of type I IFNs on the reciprocal crosstalk between immune and tumour cells is key to their antitumour potential. The source, inducer, subtype, dose, duration and stability of the endogenous or exogenous IFN also have a major impact on outcome; as does the requirement for IFNα/β receptor (IFNAR) expression*" (234). Type I IFN anticancer effects have been deciphered predominantly for IFNα and IFNβ, compared to the lesser studied IFNε, IFNκ and IFNζ.

1.4.1.4.1 Intrinsic mechanisms

Intrinsic **type I IFN anti-tumour processes** (summarised in **Figure 22**), involve the regulation of proliferation, apoptosis, and differentiation (240, 241). Anti-proliferative

as well as pro-apoptotic efficacies vary according to the cell type and the specific IFN type I subtype (242-244). Type I IFNs exhibit anti-proliferative or growth inhibitory properties. It has been reported that IFNβ reduced BMM (bone marrow-derived macrophage) cell proliferation with CSF1 treatment (colony stimulating factor 1) (245-247). Moreover, BMM cells derived from IFNAR1-null mice proliferate faster than their analogous wild type (247). It has been suggested that IFNs down-regulate proto-oncogenes, such as c-myc leading to growth inhibition (241, 248, 249). Additionally, it was observed that IFNα induction of cell cycle arrest at the G0/G1 phase, correlated with down-regulation of c-myc mRNA in lymphoma cells (250).

Apoptosis is a homeostatic mechanism essential in eliminating infected or damaged cells, or cells that have escaped cell cycle checkpoints and have adopted aberrant proliferative characteristics (251). Evidence suggests that type I IFNs induce apoptosis of transformed cells through the extrinsic apoptotic pathways accompanied by activation of death receptors as well as by the intrinsic apoptotic (or mitochondrial pathway) cascade (252). More specifically, IFNα and IFNβ have been shown to activate caspase pathways and concurrently suppress the expression of anti-apoptotic genes (such as *BCL-2*) leading to programmed cell death (253-255). Furthermore, type I IFNs regulate the expression of various molecules such as: FAS ligand/receptor, caspase-8, p21/waf1, IRF1, STAT1, PKR, RNase L, PML, Daxx, TNF family receptors/ligands, phospholipid scramblase, death-associated protein kinases involved in cell survival and apoptosis (252, 256-261).

1.4.1.4.2 Extrinsic mechanisms

Type I IFNs also utilize extrinsic mechanisms to promote anti-cancer activity of immune cells by activating broad innate and adaptive immune responses, as depicted in

Figure 22 (262). The extrinsic anti-cancer machinery is associated with activation of innate and adaptive immunity including stimulation of T cells, natural killer cells, dendritic cells, innate lymphoid cells; and with inhibition of immunosuppressive cell types which attenuate anti-tumour immunity (such as myeloid-derived suppressor cells and regulatory T cells) (263-265). In addition, type I IFN activate antigen presentation processes (264). Hence tumour infiltrating immune cells can facilitate anti-tumour immunity in response to type I IFN paracrine activities.

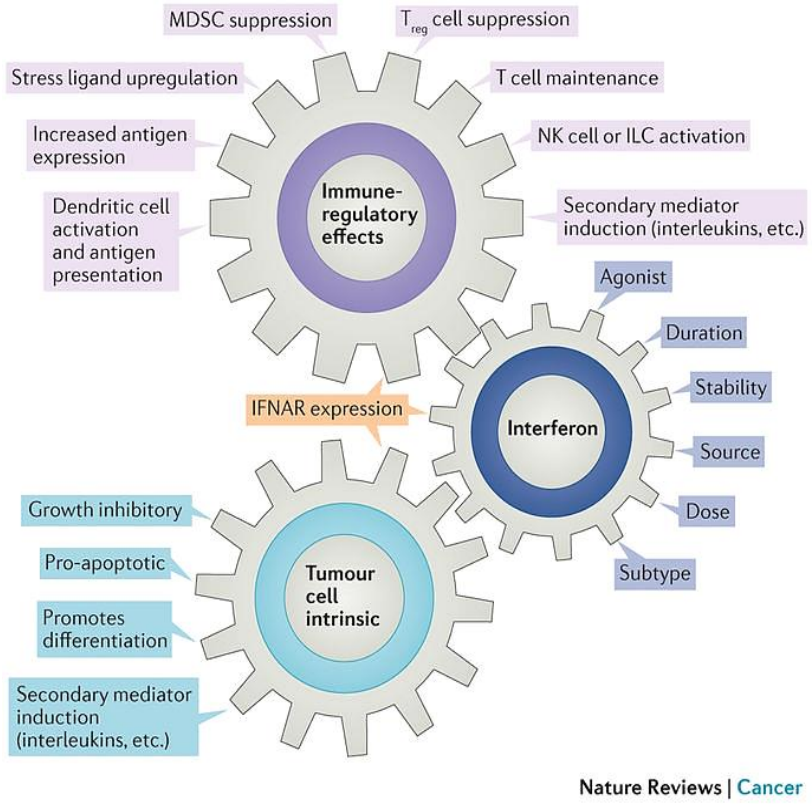

Figure 22. The Interplay of Anti-Tumourigenic Properties Exhibited by type I IFNs. *Schematic representation of the various anticancer processes orchestrated by type I IFNs. Autocrine type I IFN response can trigger intrinsic mechanisms by regulation of cellular proliferation, apoptosis or differentiation. Paracrine type I IFN stimulation involves recruitment and activation of innate and adaptive cytotoxic lymphocytes associated with immunoregulatory functions. Adapted from (234).*

An example of breast cancer evasion through dysregulated type I IFN responses has been described by Bidwell et al., (2012) (266). In this study breast cancer cells obtained from bone metastases revealed a significant reduction in type I IFN regulated gene signatures compared to the corresponding primary tumour mouse model. Restoration of type I IFN signalling by overexpression of Irf7 in tumour cells or systemic administration of IFNa substantially reduced bone metastasis by activation of the critical anti-cancer immune surveillance cells (NK cells and CD8+ T lymphocytes) (266). Thus, activation of type I IFN signalling pathway could trigger an anti-tumour immune response, suppressing breast cancer metastasis to the bone.

1.4.1.4.3 Type I IFN therapeutic applications

Given their multifactorial host defence properties, type I IFNs have been applied as clinical treatments for viral infections, autoimmune disease and cancer. IFNα has been used to treat hepatitis B and C infections (267-269). Whereas IFNβ therapy has shown promising anti-inflammatory effects in multiple sclerosis and constitutes the only currently approved treatment of relapsing remitting disease (RRMS) (270). However, success of IFNβ treatment has not been fully understood in multiple sclerosis clinical trials conducted to date (271, 272).

The first type I IFN cancer therapy was approved in 1985 with the use of IFNα treatment of hairy cell leukaemia (273). Thereafter IFNα therapy was clinically extended to combat other haematological malignancies including chronic myeloid leukaemia and lymphoma; as well as in solid tumours such as malignant cutaneous melanoma, Kaposi's sarcoma, renal cell carcinoma (232, 239, 274-277). Although results from these studies are promising, the major concern with current use of IFNα in long term cancer therapy is that it is often not well tolerated by patients, due to its broad and systemic toxicity (278).

Acute IFNα cancer therapy may include fever, chills, headache, myalgia; as well as delayed responses like nausea, vomiting, fatigue, anorexia, leukopenia, neutropenia, neurotoxicity, retinal haemorrhage; and autoimmune disease with occurrence of hyper/ hypothyroidism, type 1 diabetes mellitus, coeliac disease, autoimmune hepatitis, psoriasis, rheumatoid arthritis glomerulonephritis, sarcoidosis (279). Furthermore, therapeutic success of adjuvant IFNα cancer treatment has been controversial (239).

Subsequently IFNβ adjuvant cancer therapy has also been clinically trialled in glioblastoma, metastatic breast cancer, advanced pancreatic cancer, advanced non-small-cell lung cancer, patients (280-282). Although in these studies IFNβ treatment prolonged the progression-free survival of advanced, breast cancer, glioblastoma, pancreatic carcinoma, patients; this was not reported for advanced non-small-cell lung cancer patients.

1.4.2 IFNε: A Unique Type I interferon

Sequencing of type I IFN locus led to the discovery of the novel interferon epsilon (IFNε), by our lab in 2004 (202). The human IFNε gene is located on chromosome 9p21, within type I IFN locus (202). Consisting of 208 amino acids, human IFNε is homologous to the murine protein (202). Three-dimensional structure modelling predictions suggest that IFNε resembles type I IFN family members, sharing sequence identities of 25% and 30% to IFNα and IFNβ, respectively. IFNε was rightfully classified as type I IFN as it mediates signal transduction via the canonical type I IFN pathway (see **Figure 23**). Further evidence by Stifter, S. A., *et al.,* (2017), suggests that r-mIFNε (recombinant-mouse IFNε) can induce STAT1 phosphorylation as well as down-stream signal transduction via activation of ISRE promoter elements leading to transcription of canonical IRGs (192, 283, 284). Subsequent characterization by our group revealed that IFNε promotes local

innate immune responses within the female reproductive tract (FRT) (283). Furthermore, similar to other type I IFN family members, IFNε has been shown to regulate cell proliferation, activate innate and adaptive immune responses and elicit antiviral and antibacterial properties (284)

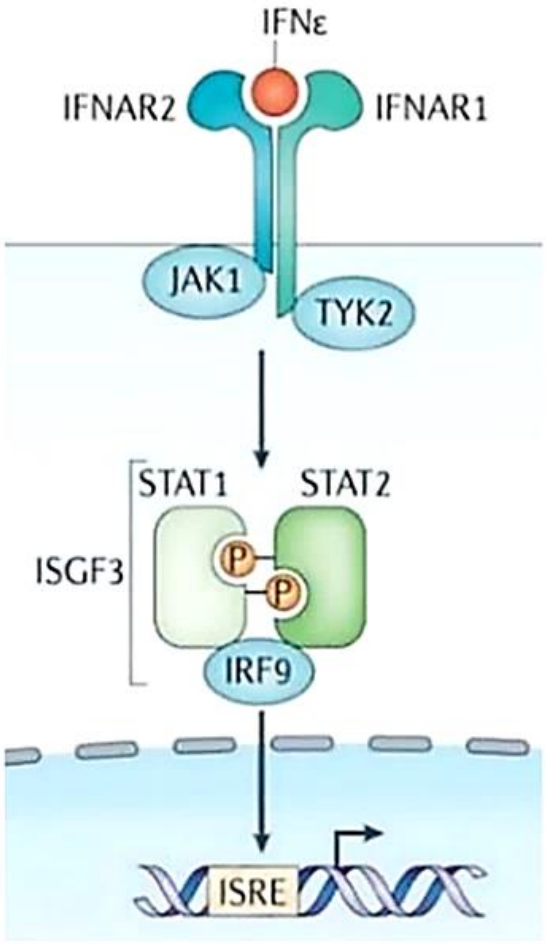

Figure 23. Canonical IFNε (type I Interferon) Signalling Pathway.
Engagement of IFN type I ligand with IFN type I receptor leads to activation of the JAK/STAT pathway followed by induction of IRG transcription. Signal transduction of this pathway elicits pleotropic IFN biological activities. Adapted from (217).

1.4.2.1 Constitutive expression IFNε in the FRT

Our lab has also demonstrated that in contrast to conventional type I IFNs, IFNε is **constitutively expressed** at high levels by **epithelial cells** of the **FRT** (see **Figures 24** and **25**), in particular within the uterus, ovary, and cervix and vagina of both mice and human (283). Comparatively lower expression of *Ifnε* has been observed within the brain, heart, lung, adrenal glands and heart of adult mice, but could not be detected in thymus, spleen, testis, liver, and kidney (202). According to Hardy M.P., *et. al.,* (2004), *Ifnε* transcript was just detectable at all stages of mouse embryonic development from E14 (more specifically in the developing brain, liver, lung, kidney, large intestine, and thymus). Interestingly, *Ifnε* was also present in the placentas of gestating mice at various stages of pregnancy.

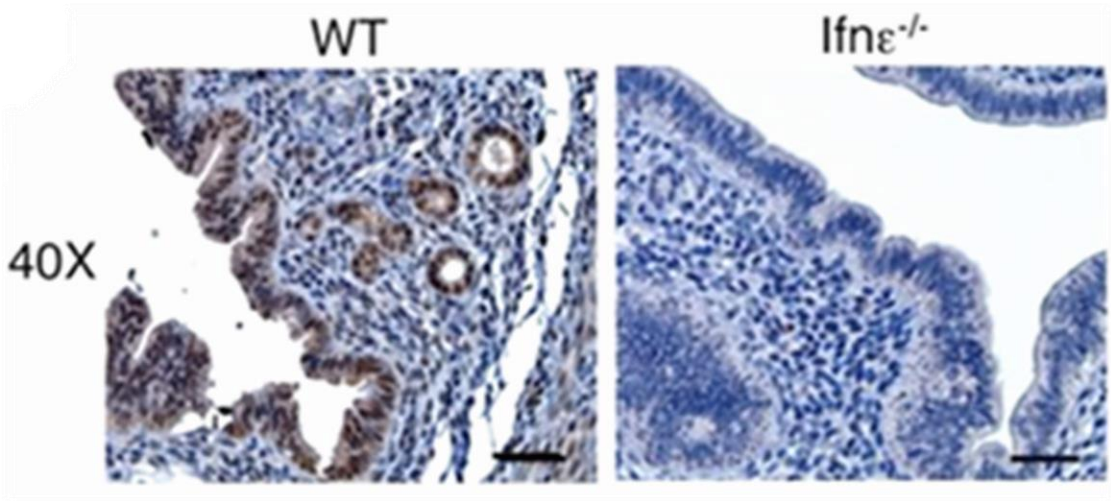

Figure 24. IFNε Protein Localisation in Epithelial Cells of Mouse Endometrium
Immunohistochemical analysis of IFNε protein of endometrial tissue from wild-type (WT) C57BL/6 mice. Scale bar is equivalent to 50µm. Adapted from (285).

The Hardy M.P., *et al.,* (2004) study also suggested that apart from *Ifnε,* other type I IFN members such as *Ifnα* and *Ifnβ* where not constitutively expressed in the mouse FRT. In conjunction, a recent comprehensive study by our laboratory analysed type I (ε, β, α4, α2, α1), type II (IFNγ) and type III (λ1, λ2, λ3) IFN mRNA in vaginal, cervical, and endometrial human tissues (obtained from healthy women, clear from infections, non-pregnant, and with regular menstrual cycles) (286). This is the first study to show that IFNε was the only highly expressed interferon member in human FRT, eluding to its distinguished roles within the FRT physiology.

Additionally, Bourke *et. al.,* (2018) demonstrated that in the lower human FRT (vagina and ectocervix), IFNε expression was localized to the basal layer of squamous epithelium (286). Whereas in the endometrial epithelium (upper FRT), constitutive expression of IFNε was detected primarily with in the glands and lumen and to a lesser degree in the stroma (286).

1.4.2.2 Hormonal regulation of IFNε independent to PRR signalling

IFNε expression is uniquely regulated by hormonal induction, independent of PRR signalling. Lack of conventional PRR pathway regulation of *Ifnε* gene expression is consistent with the absence of corresponding response elements associated with these pathways (IRFs, NF-κB, STAT, ISRE), in the Ifnε proximal promoter compared to other type I IFN genes (283). Hardy *et al.,* (2004), identified conserved motifs in the promoter of human and mice *Ifnε* genes by comparative analysis. Putative conserved transcription binding factor sequences included sites for STATs, IRFs, Ets (E-twenty-six), PRE (progesterone receptor response element) and CEBPh (CCAAT/ enhancing protein h (202).

Fung *et al.,* (2013), also confirmed that mouse *Ifnε* expression was upregulated following estrogen administration and varied according to the oestrous cycle, with the lowest levels associated with diestrus and highest levels at oestrus (**Figure 25.B**). During pregnancy, uterine *Ifnε* expression is dramatically down regulated from day 1.5 post coitus and lowest at day 4.5 (embryo implantation) and increases at E18.5 (285).

Subsequently, in the same study, human *Ifnε* expression fluctuated throughout the menstrual cycle within the FRT (**Figure 25.A**). High *IFNε* levels were observed in the proliferative phase of the endometrium, correlated with high oestrogen levels, followed by a 10-fold downregulation of *IFNε* in the secretory phase of the menstrual cycle (associated with high progesterone levels). Additionally, post-menopausal women have very low levels of *IFNε* in the FRT, which could be related to the depletion of reproductive hormones (283).

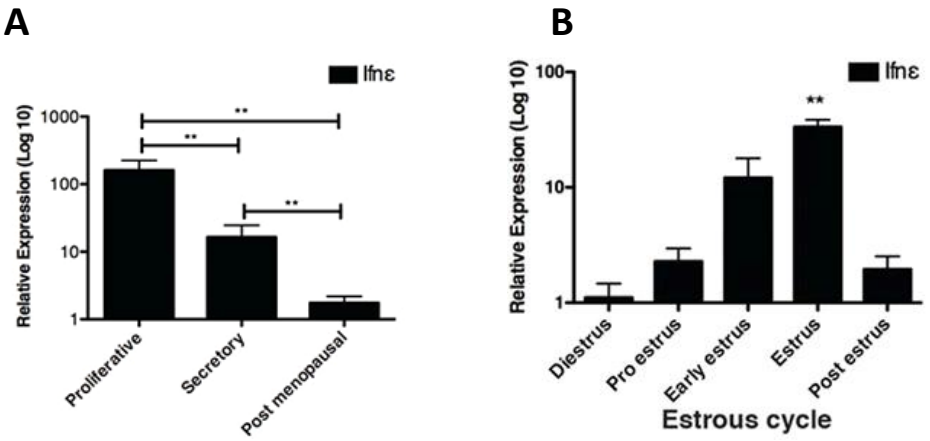

Figure 25. Human and Murine IFNε Cyclical Expression Patterns.
*A) Human IFNε mRNA levels in the endometrium, peak during the proliferative phase of the menstrual cycle. B) Similarly, murine IFNε mRNA expression is highest in the oestrus (high progesterone levels) cycle. mRNA normalised 18S ribosomal RNA, (data presented as mean ± SEM; *p<0.05; **p<0.01; ***p<0.001). Adapted from (193).*

In addition, further investigations within the human FRT revealed that the cyclical changes in expression of IFNε occurred only within the endometrial epithelium and were not observed in the lower FRT, vaginal or cervical epithelium (286). This suggests that constitutive expression of IFNε in the FRT is hormonally regulated exclusively within the endometrium. Further observations negatively correlated IFNε with progesterone receptor (PR) levels (both protein and transcript), eluding to PR associated repression of IFNε expression in the endometrium. Furthermore *in vitro* overexpression of PRs resulted in significant reductions of IFNε expression levels. Thus, corroborating that PR is a negatively regulator of IFNε in the FRT (286).

1.4.2.3 Anti-viral and Anti-bacterial properties of IFNε

Importantly, *Ifnε* exhibits an essential prophylactic role in the FRT, against sexually transmitted infections. Fung *et. al.,* (2013) demonstrated that *Ifnε* deficient mice presented increased susceptibility to vaginal infection by Herpes Simplex Virus 2 and *Chlamydia muridarum* (283). Furthermore Bourke *et al.,* (2018) determined a positive correlation between *IFNε* innate immunity ISGs (*MXA, CXCL10, OAS2*) expressed in the FRT, in line with our previous study which showed that *IFNε*$^{-/-}$ mice had reduced ISG expression in the FRT (285, 286). Concurrently, *in vitro* stimulation with r-IFNε induced the expression of innate immune genes (286). Other evidence has suggested that IFNε upregulation to semen exposure examined in ectocervix of seronegative female sex workers (highly exposed to HIV-1), is part of an immunoregulatory mechanism, associated with protection from HIV-1 infection (287, 288). Collectively, these results demonstrate the essential roles of constitutive IFNε in maintenance of basal IFN mediated immunity in the FRT. Importantly, the fluctuating levels of IFNε expression in could explain STI susceptibility according to the menstrual cycle phase.

1.4.2.4 Anti-tumour activities of IFNε

According to ground-breaking studies conducted by our group, there is evidence to suggest that the proliferation rate of primary uterine epithelial cells isolated from IFNε$^{-/-}$ mice, is significantly higher compared to the equivalent wild type as illustrated in **Figure 26** (Bourke NM and Mangan NE, unpublished). This could suggest that IFNε has a potentially important intrinsic anti-proliferative roles within the FRT.

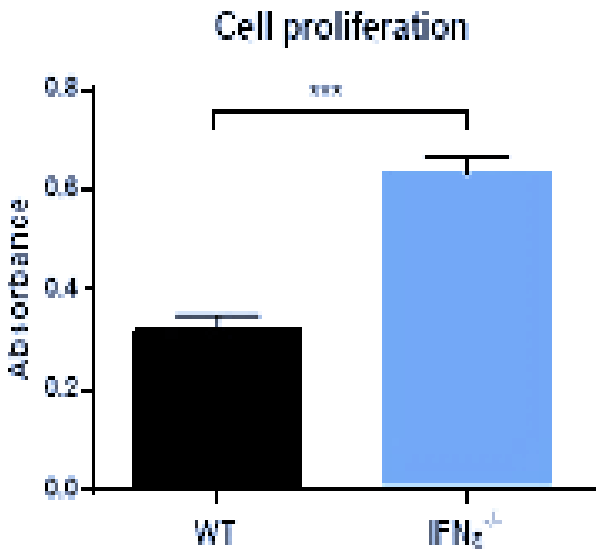

Figure 26. Proliferation of IFNε$^{-/-}$ Mice.
Uterine epithelial cells from IFNε$^{-/-}$ mice exhibit significantly higher proliferation compared to wild type equivalents. Adapted from (Bourke NM and Mangan NE, unpublished).

In addition, preliminary analysis of ovarian cancer samples, indicated that levels were significantly reduced in all samples relative to expression of IFNε in healthy controls. Next Generation Sequencing datasets of IFNε were carried out by our lab in collaboration with Prof David Bowtell, on fallopian epithelial cells from women with HGSC. The distinction in IFNε expression between the two groups was striking: IFNε expression was high and constitutive in 6 of the 7 healthy controls whereas 102 of the 112 HGSC patients (or 91%) display decreased IFNε levels. This is consistent with the hypothesis that IFNε has anti-tumour activity and its suppression favours tumour development (Marks *et al.,* unpublished).

1.4.3 Therapeutic interventions of IFNε in uterine cancer

Based on the aforementioned data and signalling through IFNARs, we propose that IFNε exhibits anti-tumour effects, similar to other type I IFNs and that its unique properties render it particularly pertinent to FRT tumours. As discussed previously current type I IFN therapies have been extremely successful in eliminating a broad range of malignancies. However due to detrimental side effects and systemic toxicity observed in patients, they are unfavourable long-term cancer treatments. Whereas IFNε is constitutive expressed within the FRT suggesting that it may be well tolerated within this organ and may direct an organ-specific type I IFN response. The potential of IFNε in therapeutic development of uterine cancer requires further investigation.

1.5 Project Rationale, Hypothesis and Aims

Oncogenesis is a multistage process associated with cellular transformation, proliferation, invasion and metastasis. These processes under normal physiological conditions are tightly regulated, by cytokine cellular communication and are essential for maintaining homeostasis. The understanding of dysregulated cellular machinery is key to deciphering cancer pathogenesis. This thesis will examine two such pathways. Firstly, the **pro-tumourigenic Nodal** /TGF-β signalling and will attempt to shed some light as to how tumours utilize this pathway to facilitate oncogenic development (**Chapter 2** and **Chapter 3**). Secondly, we will investigate dysregulated **anti-tumourigenic** cytokines that have been implicated in tumourigenesis. As such, we will also examine the anti-cancer properties exhibited by the novel type I IFN **IFNε** (**Chapter 4**).

Nodal has been well characterized as an embryonic morphogen (63, 138). It is expressed in a highly restricted pattern, during embryogenesis and plays essential roles in early embryonic development. Although Nodal is rarely expressed in adult cells (except in regenerative tissues), substantial evidence suggests that it **re-emerges** during **carcinogenesis** (151, 289). Furthermore, Nodal expression is strongly correlated with tumour cell aggressiveness (151, 153, 160, 180, 290). It is suggested that Nodal promotes proliferation, EMT (Epithelial-mesenchymal transition), migration, invasion, angiogenesis, plasticity and stem cell properties of cancer cells (66, 160, 163, 168, 169, 171, 173, 188, 291). However, the precise mechanisms have not been fully clarified.

TGF-β proteins have been shown to play essential roles in tissue remodelling events across the cycling endometrium and during pregnancy. Expression of Nodal signalling components including signalling receptors (Alk4 and ActRIIA/B), Smads (downstream signalling molecules), Lefty (antagonist) as well as other TGF-β members have been detected in the **human endometrium** (292-295). Nevertheless, expression **of Nodal** as

well as co-receptor **Cripto** has not been investigated in this highly dynamic tissue. In non-embryonic tissues, Nodal signalling has been demonstrated to exhibit essential roles within regenerative adult tissues, including the placenta and mammary gland; as well as maintaining plasticity of human adult stem cells (149-151, 186). Furthermore, dysregulated Nodal signalling has been associated with tumour progression reported in various cancers. However, **Nodal signalling** components have not been examined in **human endometrial cancer**.

We thus ***hypothesised*** *that Nodal is expressed in normal human endometrium and that it could play a role in the progression of endometrial cancer*. To test these hypotheses, this study **aims** to identify the expression patterns of Nodal's signalling components in human cycling endometrium and endometrial cancer tissues, as described in **Chapter 2**.

We were the first group to propose that Nodal plays an important role in tissue remodelling events that occur across the **menstrual cycle** and more specifically during the **proliferative phase** (refer to **Chapter 2**) (296). This was also the first study to suggest that **dysregulated** Nodal and Cripto expression is correlated with the degree of **endometrial cancer aggressiveness** (296). Following observations of Nodal and Cripto re-activation in endometrial cancer we ***hypothesised*** *that dysregulated Nodal signalling is associated with cancer pathogenesis and progression.*

The **overall aim** to address this hypothesis, was to examine the effects of Nodal signalling blockade on cancer cell phenotype (refer to **Chapter 3**). The **specific aims** were:

i To develop a Nodal specific functional bioassay.
ii To employ anti-Cripto monoclonal antibodies to block Nodal signalling.
iii To examine the effects of Nodal blockade on cancer cell proliferation.

iv To evaluate cancer cell migration potential upon Nodal signalling blockade.

v To characterize downstream Smad signalling of cancer cells treated with anti-Cripto monoclonal antibody.

The female reproductive tract (FRT) epithelium is hormonally controlled, to constantly undergo remodelling processes for successful fertilization and pregnancy. Subsequently, it is also equipped with a specialized immune system for adequate protection against infections, as well as tolerance of the implanted embryo. Therefore, homeostatic mechanisms governed by cytokines are detrimental to the FRT physiology. **IFNε** is emerging as an essential **FRT cytokine**.

Our lab has also demonstrated that in contrast to conventional type I interferons, IFNε is constitutively expressed by epithelial cells of the FRT in both mice and human, and is hormonally regulated, exclusively within the endometrium (286). In addition, IFNε exhibits prophylactic roles within the FRT, against sexually transmitted infections (HSV-2, *Chlamydia muridarum*) (6). Furthermore, the constitutive expression of IFNε contributes to the maintenance of basal IFN mediated immunity.

Preliminary studies conducted in our group demonstrated that loss of IFNε increased proliferation propensity of mouse uterine epithelial cells, compared to homologous wild type controls. This suggests that IFNε has potentially important intrinsic anti-tumourigenic roles, and that its suppression may favour pathogenic tumour development. However, the direct **anti-cancer properties** exhibited by **IFNε** have not yet been investigated in **FRT cancer** with the exception of ovarian cancer. Also, the precise mechanisms by which IFNε may regulate such cellular processes, have not been fully elucidated.

*We **hypothesised** that IFNε displays intrinsic anti-cancer properties in the FRT*. This study **aimed** to primarily investigate the **anti-tumourigenic** effects of **IFNε** on **FRT** epithelial **cancer** cell lines, described in **Chapter 4**.

The specific **aims** of this study were:

i To identify FRT cancer cell lines responsive to IFN stimulation.

ii To characterize IFNε mediated IRG regulation of FRT cancer cell lines.

iii To examine the modulation of anti-apoptotic and pro-apoptotic genes by IFNε.

iv To assess the effects of IFNε on FRT cancer cell proliferation.

v To investigate the effects of IFNε on FRT cancer cell apoptosis.

1.6 References

1. Rothschild BM, Tanke DH, Helbling M, 2nd, Martin LD. Epidemiologic study of tumors in dinosaurs. Die Naturwissenschaften. 2003;90(11):495-500.

2. B. FG. A brief history of cancer: Age-old milestones underlying our current knowledge database. International Journal of Cancer. 2015;136(9):2022-36.

3. Hippocrates Aphorism 165-6 (Aphorisms of hippocrates from the Latin version of Verhoofd with literal translation). Available from: http://archive.org/stream/AphorismsOfHippocratesFromTheLatinVersionOfVerhoofd/Aphorisms_of_Hippocrates_from_the_Latin_version_of_Verhoofd_djvu.txt

4. Hippocrates Aphorism 131-38. (Aphorisms of hippocrates from the Latin version of Verhoofd with literal translation). Available from: http://archive.org/stream/AphorismsOfHippocratesFromTheLatinVersionOfVerhoofd/Aphorisms_of_Hippocrates_from_the_Latin_version_of_Verhoofd_djvu.txt

5. Australian Institute of H, Welfare. Cancer in Australia: Actual incidence data from 1982 to 2013 and mortality data from 1982 to 2014 with projections to 2017. Asia-Pacific Journal of Clinical Oncology. 2017.

6. Hanahan D, Weinberg RA. The Hallmarks of Cancer. Cell. 2000;100(1):57-70.

7. Hanahan D, Weinberg Robert A. Hallmarks of Cancer: The Next Generation. Cell. 2011;144(5):646-74.

8. Ferlay J, Soerjomataram I, Dikshit R, Eser S, Mathers C, Rebelo M, et al. Cancer incidence and mortality worldwide: Sources, methods and major patterns in GLOBOCAN 2012. International Journal of Cancer. 2015;136(5): E359-E86.

9. Welfare. AIoHa. Cancer in Australia 2017. Cancer series 101 2017.

10. Wira CR, Fahey JV, Sentman CL, Pioli PA, Shen L. Innate and adaptive immunity in female genital tract: cellular responses and interactions. Immunological reviews. 2005;206(1):306-35.

11. Iijima N, Thompson JM, Iwasaki A. Dendritic cells and macrophages in the genitourinary tract. Mucosal Immunol. 2008;1(6):451-9.

12. Salamonsen LA, Nancarrow CD. 10 - Cell Biology of the Oviduct and Endometrium A2 - Findlay, J.K. Molecular Biology of the Female Reproductive System. San Diego: Academic Press; 1994. p. 289-328.

13. Buffet NC, Djakoure C, Maitre SC, Bouchard P. Regulation of the Human Menstrual Cycle. Frontiers in Neuroendocrinology. 1998;19(3):151-86.

14. Gargett CE, Chan RW, Schwab KE. Endometrial stem cells. Current opinion in obstetrics & gynecology. 2007;19(4):377-83.

15. Available from: http://micro2tele.com/2013/01/20/histoquarterly-cervix.

16. Available from: www.memorangapp.com/flashcards/127450/10-19+Female+ Reproductive +Histology/.

17. Pearson Education I. 2011 [menstrual cycle]. Available from: http: //droualb. faculty.mjc.edu/Course%20Materials/Physiology%20101/Chapter%20Notes /Fall%202007/chapter_22%20Fall%202007.htm.

18. Al M. Mescher Al: Junqueira' Basic Histology: Text and Atlas: TheMcGraw-Hill Companies, Inc.; 12th Edition: Available from: http://www.accessmedicine. com.

19. Jabbour HN, Kelly RW, Fraser HM, Critchley HOD. Endocrine Regulation of Menstruation. Endocrine Reviews. 2006;27(1):17-46.

20. Aitken RJ, Baker MA, Doncel GF, Matzuk MM, Mauck CK, Harper MJK. As the world grows: contraception in the 21st century. The Journal of Clinical Investigation. 2008;118(4):1330-43.

21. Ferenczy A, Bertrand G, Gelfand MM. Proliferation kinetics of human endometrium during the normal menstrual cycle. American journal of obstetrics and gynecology. 1979;133(8):859-67.

22. Monteleone P, Mascagni G, Giannini A, Genazzani AR, Simoncini T. Symptoms of menopause - global prevalence, physiology and implications. Nature reviews Endocrinology. 2018;14(4):199-215.

23. Australian Institute of H, Welfare. Australian Cancer Incidence and Mortality (ACIM) books: Uterine cancer. 2017.

24. Okuda T, Sekizawa A, Purwosunu Y, Nagatsuka M, Morioka M, Hayashi M, et al. Genetics of endometrial cancers. Obstetrics and gynecology international. 2010; 2010:984013.

25. Goodman MT, Hankin JH, Wilkens LR, Lyu L-C, McDuffie K, Liu LQ, et al. Diet, Body Size, Physical Activity, and the Risk of Endometrial Cancer. Cancer Research. 1997;57(22):5077-85.

26. Bansal N, Yendluri V, Wenham RM. The molecular biology of endometrial cancers and the implications for pathogenesis, classification, and targeted therapies. Cancer Control. 2009;16(1):8-13.

27. Haidopoulos D, Simou M, Akrivos N, Rodolakis A, Vlachos G, Fotiou S, et al. Risk factors in women 40 years of age and younger with endometrial carcinoma. Acta Obstetricia et Gynecologica Scandinavica. 2010;89(10):1326-30.

28. Burke WM, Orr J, Leitao M, Salom E, Gehrig P, Olawaiye AB, et al. Endometrial cancer: A review and current management strategies: Part II. Gynecologic Oncology. 2014;134(2):393-402.

29. Burke WM, Orr J, Leitao M, Salom E, Gehrig P, Olawaiye AB, et al. Endometrial cancer: A review and current management strategies: Part I. Gynecologic Oncology. 2014;134(2):385-92.

30. Amant F, Moerman P, Neven P, Timmerman D, Van Limbergen E, Vergote I. Endometrial cancer. The Lancet. 2005;366(9484):491-505.

31. Goodman MT, Hankin JH, Wilkens LR, Lyu LC, McDuffie K, Liu LQ, et al. Diet, body size, physical activity, and the risk of endometrial cancer. Cancer Res. 1997;57(22):5077-85.

32. Bokhman JV. Two pathogenetic types of endometrial carcinoma. Gynecologic Oncology. 1983;15(1):10-7.

33. Lax SF, Kurman RJ. A dualistic model for endometrial carcinogenesis based on immunohistochemical and molecular genetic analyses. Verhandlungen der Deutschen Gesellschaft fur Pathologie. 1997; 81:228-32.

34. Doll A, Abal M, Rigau M, Monge M, Gonzalez M, Demajo S, et al. Novel molecular profiles of endometrial cancer—new light through old windows. The Journal of Steroid Biochemistry and Molecular Biology. 2008;108(3–5):221-9.

35. Creasman WT, Odicino F, Maisonneuve P, Quinn MA, Beller U, Benedet JL, et al. Carcinoma of the Corpus Uteri. International Journal of Gynecology & Obstetrics. 2006;95, Supplement 1(0):S105-S43.

36. Di Cristofano A, Ellenson LH. Endometrial Carcinoma. Annual Review of Pathology: Mechanisms of Disease. 2007;2(1):57-85.

37. Registries AIoHaWaAAoC. Cancer in Australia: an overview, 2012 Canberra: : AIHW; (2012) [Available from: www.aihw.gov.au.

38. Murali R, Soslow RA, Weigelt B. Classification of endometrial carcinoma: more than two types. The Lancet Oncology. 2014;15(7):e268-78.

39. Di Cristofano A, Ellenson LH. Endometrial carcinoma. Annual review of pathology. 2007; 2:57-85.

40. Sorosky JI. Endometrial cancer. Obstetrics and gynecology. 2008;111(2 Pt 1):436-47.

41. Pecorelli S, Zigliani L, Odicino F. Revised FIGO staging for carcinoma of the cervix. International Journal of Gynecology & Obstetrics. 2009;105(2):107-8.

42. Available from: http://www.cancerresearchuk.org/about-cancer/type/womb-cancer/treatment/stages-of-womb-cancer.

43. Bakkum-Gamez JN, Gonzalez-Bosquet J, Laack NN, Mariani A, Dowdy SC. Current Issues in the Management of Endometrial Cancer. Mayo Clinic Proceedings. 2008;83(1):97-112.

44. Sorosky JI. Endometrial cancer. Obstetrics and gynecology. 2012;120(2 Pt 1):383-97.

45. Salvesen HB, Haldorsen IS, Trovik J. Markers for individualised therapy in endometrial carcinoma. The Lancet Oncology. 2012;13(8):e353-e61.

46. Shi Y, Massague J. Mechanisms of TGF-beta signaling from cell membrane to the nucleus. Cell. 2003;113(6):685-700.

47. Frolik CA, Dart LL, Meyers CA, Smith DM, Sporn MB. Purification and initial characterization of a type beta transforming growth factor from human placenta. Proceedings of the National Academy of Sciences. 1983;80(12):3676-80.

48. Hinck AP. Structural studies of the TGF-βs and their receptors – insights into evolution of the TGF-β superfamily. FEBS Letters. 2012;586(14):1860-70.

49. Derynck R, Zhang Y, Feng XH. Smads: transcriptional activators of TGF-beta responses. Cell. 1998;95(6):737-40.

50. Massague J. TGF-beta signal transduction. Annual review of biochemistry. 1998; 67:753-91.

51. Allendorph GP, Isaacs MJ, Kawakami Y, Izpisua Belmonte JC, Choe S. BMP-3 and BMP-6 Structures Illuminate the Nature of Binding Specificity with Receptors. Biochemistry. 2007;46(43):12238-47.

52. Gray AM, Mason AJ. Requirement for activin A and transforming growth factor--beta 1 pro-regions in homodimer assembly. Science. 1990;247(4948):1328-30.

53. Gray PC, Greenwald J, Blount AL, Kunitake KS, Donaldson CJ, Choe S, et al. Identification of a binding site on the type II activin receptor for activin and inhibin. The Journal of biological chemistry. 2000;275(5):3206-12.

54. Harrison CA, Gray PC, Koerber SC, Fischer W, Vale W. Identification of a functional binding site for activin on the type I receptor ALK4. The Journal of biological chemistry. 2003;278(23):21129-35.

55. Hart PJ, Deep S, Taylor AB, Shu Z, Hinck CS, Hinck AP. Crystal structure of the human TbetaR2 ectodomain--TGF-beta3 complex. Nature structural biology. 2002;9(3):203-8.

56. Vitt UA, Mazerbourg S, Klein C, Hsueh AJW. Bone Morphogenetic Protein Receptor Type II Is a Receptor for Growth Differentiation Factor-9. Biology of Reproduction. 2002;67(2):473-80.

57. Kitisin K, Saha T, Blake T, Golestaneh N, Deng M, Kim C, et al. TGF-β Signaling in Development. Science's STKE. 2007;2007(399):1-5.

58. Kirkbride KC, Ray BN, Blobe GC. Cell-surface co-receptors: emerging roles in signaling and human disease. Trends in biochemical sciences. 2005;30(11):611-21.

59. Lewis KA, Gray PC, Blount AL, MacConell LA, Wiater E, Bilezikjian LM, et al. Betaglycan binds inhibin and can mediate functional antagonism of activin signalling. Nature. 2000;404(6776):411-4.

60. Wakefield LM, Hill CS. Beyond TGFbeta: roles of other TGFbeta superfamily members in cancer. Nat Rev Cancer. 2013;13(5):328-41.

61. Heldin CH, Miyazono K, ten Dijke P. TGF-beta signalling from cell membrane to nucleus through SMAD proteins. Nature. 1997;390(6659):465-71.

62. Conlon FL, Barth KS, Robertson EJ. A novel retrovirally induced embryonic lethal mutation in the mouse: assessment of the developmental fate of embryonic stem cells homozygous for the 413.d proviral integration. Development. 1991;111(4):969-81.

63. Zhou X, Sasaki H, Lowe L, Hogan BL, Kuehn MR. Nodal is a novel TGF-beta-like gene expressed in the mouse node during gastrulation. Nature. 1993;361(6412):543-7.

64. NCBI. National Center for Biotechnology Information, U.S. National Library of Medicine; Available from: www.ncbi.nlm.nih.gov /genome /gdv/ browser/ ? context =gene&acc=4838.

65. Schier AF. Nodal signaling in vertebrate development. Annual review of cell and developmental biology. 2003; 19:589-621.

66. Topczewska JM, Postovit LM, Margaryan NV, Sam A, Hess AR, Wheaton WW, et al. Embryonic and tumorigenic pathways converge via Nodal signaling: role in melanoma aggressiveness. Nat Med. 2006;12(8):925-32.

67. Beck S, Le Good JA, Guzman M, Ben Haim N, Roy K, Beermann F, et al. Extraembryonic proteases regulate Nodal signalling during gastrulation. Nature cell biology. 2002;4(12):981-5.

68. Constam DB. Riding shotgun: a dual role for the epidermal growth factor-Cripto/FRL-1/Cryptic protein Cripto in Nodal trafficking. Traffic (Copenhagen, Denmark). 2009;10(7):783-91.

69. Blanchet MH, Le Good JA, Mesnard D, Oorschot V, Baflast S, Minchiotti G, et al. Cripto recruits Furin and PACE4 and controls Nodal trafficking during proteolytic maturation. Embo j. 2008;27(19):2580-91.

70. Yan YT, Gritsman K, Ding J, Burdine RD, Corrales JD, Price SM, et al. Conserved requirement for EGF-CFC genes in vertebrate left-right axis formation. Genes & development. 1999;13(19):2527-37.

71. Germain S, Howell M, Esslemont GM, Hill CS. Homeodomain and winged-helix transcription factors recruit activated Smads to distinct promoter elements via a common Smad interaction motif. Genes & development. 2000;14(4):435-51.

72. Chen C, Shen MM. Two modes by which Lefty proteins inhibit nodal signaling. Current biology: CB. 2004;14(7):618-24.

73. Cheng SK, Olale F, Brivanlou AH, Schier AF. Lefty blocks a subset of TGFbeta signals by antagonizing EGF-CFC coreceptors. PLoS biology. 2004;2(2):E30.

74. Tabibzadeh S, Hemmati-Brivanlou A. Lefty at the crossroads of "stemness" and differentiative events. Stem cells (Dayton, Ohio). 2006;24(9):1998-2006.

75. Piccolo S, Agius E, Leyns L, Bhattacharyya S, Grunz H, Bouwmeester T, et al. The head inducer Cerberus is a multifunctional antagonist of Nodal, BMP and Wnt signals. Nature. 1999;397(6721):707-10.

76. Harms PW, Chang C. Tomoregulin-1 (TMEFF1) inhibits nodal signaling through direct binding to the nodal coreceptor Cripto. Genes & development. 2003;17(21):2624-9.

77. Haffner C, Frauli M, Topp S, Irmler M, Hofmann K, Regula JT, et al. Nicalin and its binding partner Nomo are novel Nodal signaling antagonists. Embo j. 2004;23(15):3041-50.

78. Meno C, Gritsman K, Ohishi S, Ohfuji Y, Heckscher E, Mochida K, et al. Mouse Lefty2 and zebrafish antivin are feedback inhibitors of nodal signaling during vertebrate gastrulation. Molecular cell. 1999;4(3):287-98.

79. Gritsman K, Zhang J, Cheng S, Heckscher E, Talbot WS, Schier AF. The EGF-CFC protein one-eyed pinhead is essential for nodal signaling. Cell. 1999;97(1):121-32.

80. Ciccodicola A, Dono R, Obici S, Simeone A, Zollo M, Persico MG. Molecular characterization of a gene of the 'EGF family' expressed in undifferentiated human NTERA2 teratocarcinoma cells. Embo j. 1989;8(7):1987-91.

81. Minchiotti G, Manco G, Parisi S, Lago CT, Rosa F, Persico MG. Structure-function analysis of the EGF-CFC family member Cripto identifies residues essential for nodal signalling. Development. 2001;128(22):4501-10.

82. Watanabe K, Hamada S, Bianco C, Mancino M, Nagaoka T, Gonzales M, et al. Requirement of glycosylphosphatidylinositol anchor of Cripto-1 for trans activity as a Nodal co-receptor. The Journal of biological chemistry. 2007;282(49):35772-86.

83. Yan YT, Liu JJ, Luo Y, E C, Haltiwanger RS, Abate-Shen C, et al. Dual roles of Cripto as a ligand and coreceptor in the nodal signaling pathway. Mol Cell Biol. 2002;22(13):4439-49.

84. Blanchet MH, Le Good JA, Oorschot V, Baflast S, Minchiotti G, Klumperman J, et al. Cripto localizes Nodal at the limiting membrane of early endosomes. Science signaling. 2008;1(45):ra13.

85. Reissmann E, Jornvall H, Blokzijl A, Andersson O, Chang C, Minchiotti G, et al. The orphan receptor ALK7 and the Activin receptor ALK4 mediate signaling by Nodal proteins during vertebrate development. Genes & development. 2001;15(15):2010-22.

86. Yeo C, Whitman M. Nodal signals to Smads through Cripto-dependent and Cripto-independent mechanisms. Molecular cell. 2001;7(5):949-57.

87. Bianco C, Strizzi L, Rehman A, Normanno N, Wechselberger C, Sun Y, et al. A Nodal- and ALK4-independent signaling pathway activated by Cripto-1 through Glypican-1 and c-Src. Cancer Res. 2003;63(6):1192-7.

88. Shani G, Fischer WH, Justice NJ, Kelber JA, Vale W, Gray PC. GRP78 and Cripto form a complex at the cell surface and collaborate to inhibit transforming growth factor beta signaling and enhance cell growth. Mol Cell Biol. 2008;28(2):666-77.

89. Gray PC, Vale W. Cripto/GRP78 modulation of the TGF-beta pathway in development and oncogenesis. FEBS Lett. 2012;586(14):1836-45.

90. Bianco C, Rangel MC, Castro NP, Nagaoka T, Rollman K, Gonzales M, et al. Role of Cripto-1 in stem cell maintenance and malignant progression. Am J Pathol. 2010;177(2):532-40.

91. Shen MM, Schier AF. The EGF-CFC gene family in vertebrate development. Trends in genetics: TIG. 2000;16(7):303-9.

92. Saloman DS, Bianco C, Ebert AD, Khan NI, De Santis M, Normanno N, et al. The EGF-CFC family: novel epidermal growth factor-related proteins in development and cancer. Endocr Relat Cancer. 2000;7(4):199-226.

93. Conlon FL, Lyons KM, Takaesu N, Barth KS, Kispert A, Herrmann B, et al. A primary requirement for nodal in the formation and maintenance of the primitive streak in the mouse. Development. 1994;120(7):1919-28.

94. Gu Z, Nomura M, Simpson BB, Lei H, Feijen A, van den Eijnden-van Raaij J, et al. The type I activin receptor ActRIB is required for egg cylinder organization and gastrulation in the mouse. Genes & development. 1998;12(6):844-57.

95. Song J, Oh SP, Schrewe H, Nomura M, Lei H, Okano M, et al. The type II activin receptors are essential for egg cylinder growth, gastrulation, and rostral head development in mice. Developmental biology. 1999;213(1):157-69.

96. Xu C, Liguori G, Persico MG, Adamson ED. Abrogation of the Cripto gene in mouse leads to failure of postgastrulation morphogenesis and lack of differentiation of cardiomyocytes. Development. 1999;126(3):483-94.

97. Ding J, Yang L, Yan YT, Chen A, Desai N, Wynshaw-Boris A, et al. Cripto is required for correct orientation of the anterior-posterior axis in the mouse embryo. Nature. 1998;395(6703):702-7.

98. Fuxe J, Vincent T, Garcia de Herreros A. Transcriptional crosstalk between TGF-beta and stem cell pathways in tumor cell invasion: role of EMT promoting Smad complexes. Cell cycle (Georgetown, Tex). 2010;9(12):2363-74.

99. Minchiotti G, Parisi S, Liguori GL, D'Andrea D, Persico MG. Role of the EGF-CFC gene cripto in cell differentiation and embryo development. Gene. 2002;287(1-2):33-7.

100. Klauzinska M, Bertolette D, Tippireddy S, Strizzi L, Gray PC, Gonzales M, et al. Cripto-1: an extracellular protein - connecting the sequestered biological dots. Connect Tissue Res. 2015;56(5):364-80.

101. Ciardiello F, Dono R, Kim N, Persico MG, Salomon DS. Expression of cripto, a novel gene of the epidermal growth factor gene family, leads to in vitro transformation of a normal mouse mammary epithelial cell line. Cancer Res. 1991;51(3):1051-4.

102. Brandt R, Normanno N, Gullick WJ, Lin JH, Harkins R, Schneider D, et al. Identification and biological characterization of an epidermal growth factor-related protein: cripto-1. The Journal of biological chemistry. 1994;269(25):17320-8.

103. Niemeyer CC, Persico MG, Adamson ED. Cripto: roles in mammary cell growth, survival, differentiation and transformation. Cell Death Differ. 1998;5(5):440-9.

104. Sun Y, Strizzi L, Raafat A, Hirota M, Bianco C, Feigenbaum L, et al. Overexpression of human Cripto-1 in transgenic mice delays mammary gland development and differentiation and induces mammary tumorigenesis. Am J Pathol. 2005;167(2):585-97.

105. Wechselberger C, Strizzi L, Kenney N, Hirota M, Sun Y, Ebert A, et al. Human Cripto-1 overexpression in the mouse mammary gland results in the development of hyperplasia and adenocarcinoma. Oncogene. 2005;24(25):4094-105.

106. Ciardiello F, Tortora G, Bianco C, Selvam MP, Basolo F, Fontanini G, et al. Inhibition of CRIPTO expression and tumorigenicity in human colon cancer cells by antisense RNA and oligodeoxynucleotides. Oncogene. 1994;9(1):291-8.

107. Adkins HB, Bianco C, Schiffer SG, Rayhorn P, Zafari M, Cheung AE, et al. Antibody blockade of the Cripto CFC domain suppresses tumor cell growth in vivo. J Clin Invest. 2003;112(4):575-87.

108. Xing PX, Hu XF, Pietersz GA, Hosick HL, McKenzie IF. Cripto: a novel target for antibody-based cancer immunotherapy. Cancer Res. 2004;64(11):4018-23.

109. Ebert AD, Wechselberger C, Nees M, Clair T, Schaller G, Martinez-Lacaci I, et al. Cripto-1-induced increase in vimentin expression is associated with enhanced migration of human Caski cervical carcinoma cells. Exp Cell Res. 2000;257(1):223-9.

110. Wechselberger C, Ebert AD, Bianco C, Khan NI, Sun Y, Wallace-Jones B, et al. Cripto-1 enhances migration and branching morphogenesis of mouse mammary epithelial cells. Exp Cell Res. 2001;266(1):95-105.

111. Normanno N, De Luca A, Bianco C, Maiello MR, Carriero MV, Rehman A, et al. Cripto-1 overexpression leads to enhanced invasiveness and resistance to anoikis in human MCF-7 breast cancer cells. J Cell Physiol. 2004;198(1):31-9.

112. Strizzi L, Bianco C, Normanno N, Seno M, Wechselberger C, Wallace-Jones B, et al. Epithelial mesenchymal transition is a characteristic of hyperplasias and tumors in mammary gland from MMTV-Cripto-1 transgenic mice. J Cell Physiol. 2004;201(2):266-76.

113. Bianco C, Strizzi L, Ebert A, Chang C, Rehman A, Normanno N, et al. Role of human cripto-1 in tumor angiogenesis. J Natl Cancer Inst. 2005;97(2):132-41.

114. Gray PC, Harrison CA, Vale W. Cripto forms a complex with activin and type II activin receptors and can block activin signaling. Proc Natl Acad Sci U S A. 2003;100(9):5193-8.

115. Kelber JA, Panopoulos AD, Shani G, Booker EC, Belmonte JC, Vale WW, et al. Blockade of Cripto binding to cell surface GRP78 inhibits oncogenic Cripto signaling via MAPK/PI3K and Smad2/3 pathways. Oncogene. 2009;28(24):2324-36.

116. Bianco C, Strizzi L, Normanno N, Khan N, Salomon DS. Cripto-1: an oncofetal gene with many faces. Current topics in developmental biology. 2005; 67:85-133.

117. Strizzi L, Bianco C, Normanno N, Salomon D. Cripto-1: a multifunctional modulator during embryogenesis and oncogenesis. Oncogene. 2005;24(37):5731-41.

118. Bianco C, Strizzi L, Mancino M, Rehman A, Hamada S, Watanabe K, et al. Identification of cripto-1 as a novel serologic marker for breast and colon cancer. Clinical cancer research: an official journal of the American Association for Cancer Research. 2006;12(17):5158-64.

119. Gong YP, Yarrow PM, Carmalt HL, Kwun SY, Kennedy CW, Lin BP, et al. Overexpression of Cripto and its prognostic significance in breast cancer: a study with long-term survival. European journal of surgical oncology: the journal of the European Society of Surgical Oncology and the British Association of Surgical Oncology. 2007;33(4):438-43.

120. Miyoshi N, Ishii H, Mimori K, Sekimoto M, Doki Y, Mori M. TDGF1 is a novel predictive marker for metachronous metastasis of colorectal cancer. International journal of oncology. 2010;36(3):563-8.

121. Xu CH, Chi CZ, Zhang Q, Wang YC, Wang W, Yuan Q, et al. Diagnostic and prognostic value of serum Cripto-1 in patients with non-small cell lung cancer. The clinical respiratory journal. 2018.

122. Mahmoudian RA, Abbaszadegan MR, Forghanifard MM, Moghbeli M, Moghbeli F, Chamani J, et al. Biological and Clinicopathological Significance of Cripto-1 Expression in the Progression of Human ESCC. Reports of biochemistry & molecular biology. 2017;5(2):83-90.

123. Xu QQ, Ren CC, Yang L, Ban ZY, Liu L, Lu JH, et al. [Prognostic significance of Cripto-1 in cervical squamous carcinoma]. Zhonghua bing li xue za zhi = Chinese journal of pathology. 2017;46(5):338-9.

124. Karkampouna S, van der Helm D, Gray PC, Chen L, Klima I, Grosjean J, et al. CRIPTO promotes an aggressive tumour phenotype and resistance to treatment in hepatocellular carcinoma. The Journal of pathology. 2018;245(3):297-310.

125. Tang WWC, Kobayashi T, Irie N, Dietmann S, Surani MA. Specification and epigenetic programming of the human germ line. Nature Reviews Genetics. 2016; 17:585.

126. Rossant J, Tam PP. Blastocyst lineage formation, early embryonic asymmetries and axis patterning in the mouse. Development. 2009;136(5):701-13.

127. Skreb N, Solter D, Damjanov I. Developmental biology of the murine egg cylinder. Int J Dev Biol. 1991;35(3):161-76.

128. Piliszek A, Grabarek JB, Frankenberg SR, Plusa B. Cell fate in animal and human blastocysts and the determination of viability. MHR: Basic science of reproductive medicine. 2016;22(10):681-90.

129. Rossant J, Tam PPL. Blastocyst lineage formation, early embryonic asymmetries and axis patterning in the mouse. Development. 2009;136(5):701-13.

130. Heemskerk I, Warmflash A. Pluripotent stem cells as a model for embryonic patterning: From signaling dynamics to spatial organization in a dish. Developmental Dynamics. 2016;245(10):976-90.

131. Pispa J, Thesleff I. Mechanisms of ectodermal organogenesis. Developmental biology. 2003;262(2):195-205.

132. Tirosh-Finkel L, Elhanany H, Rinon A, Tzahor E. Mesoderm progenitor cells of common origin contribute to the head musculature and the cardiac outflow tract. Development. 2006;133(10):1943-53.

133. Tam PPL, Kanai-Azuma M, Kanai Y. Early endoderm development in vertebrates: lineage differentiation and morphogenetic function. Current Opinion in Genetics & Development. 2003;13(4):393-400.

134. Mesnard D, Guzman-Ayala M, Constam DB. Nodal specifies embryonic visceral endoderm and sustains pluripotent cells in the epiblast before overt axial patterning. Development. 2006;133(13):2497-505.

135. Camus A, Perea-Gomez A, Moreau A, Collignon J. Absence of Nodal signaling promotes precocious neural differentiation in the mouse embryo. Developmental biology. 2006;295(2):743-55.

136. Vallier L, Reynolds D, Pedersen RA. Nodal inhibits differentiation of human embryonic stem cells along the neuroectodermal default pathway. Developmental biology. 2004;275(2):403-21.

137. Agius E, Oelgeschlager M, Wessely O, Kemp C, De Robertis EM. Endodermal Nodal-related signals and mesoderm induction in Xenopus. Development. 2000;127(6):1173-83.

138. Shen MM. Nodal signaling: developmental roles and regulation. Development. 2007;134(6):1023-34.

139. Ben-Haim N, Lu C, Guzman-Ayala M, Pescatore L, Mesnard D, Bischofberger M, et al. The nodal precursor acting via activin receptors induces mesoderm by maintaining a source of its convertases and BMP4. Dev Cell. 2006;11(3):313-23.

140. Morkel M, Huelsken J, Wakamiya M, Ding J, van de Wetering M, Clevers H, et al. Beta-catenin regulates Cripto- and Wnt3-dependent gene expression programs in mouse axis and mesoderm formation. Development. 2003;130(25):6283-94.

141. Stainier DY. A glimpse into the molecular entrails of endoderm formation. Genes & development. 2002;16(8):893-907.

142. Vincent SD, Dunn NR, Hayashi S, Norris DP, Robertson EJ. Cell fate decisions within the mouse organizer are governed by graded Nodal signals. Genes & development. 2003;17(13):1646-62.

143. Rossant J, Tam PP. Emerging asymmetry and embryonic patterning in early mouse development. Dev Cell. 2004;7(2):155-64.

144. Perea-Gomez A, Vella FD, Shawlot W, Oulad-Abdelghani M, Chazaud C, Meno C, et al. Nodal antagonists in the anterior visceral endoderm prevent the formation of multiple primitive streaks. Dev Cell. 2002;3(5):745-56.

145. Schier AF, Neuhauss SC, Helde KA, Talbot WS, Driever W. The one-eyed pinhead gene functions in mesoderm and endoderm formation in zebrafish and interacts with no tail. Development. 1997;124(2):327-42.

146. Chu J, Ding J, Jeays-Ward K, Price SM, Placzek M, Shen MM. Non-cell-autonomous role for Cripto in axial midline formation during vertebrate embryogenesis. Development. 2005;132(24):5539-51.

147. Shiratori H, Hamada H. The left-right axis in the mouse: from origin to morphology. Development. 2006;133(11):2095-104.

148. Collignon J, Varlet I, Robertson EJ. Relationship between asymmetric nodal expression and the direction of embryonic turning. Nature. 1996;381(6578):155-8.

149. Ma GT, Soloveva V, Tzeng SJ, Lowe LA, Pfendler KC, Iannaccone PM, et al. Nodal regulates trophoblast differentiation and placental development. Developmental biology. 2001;236(1):124-35.

150. Park CB, DeMayo FJ, Lydon JP, Dufort D. NODAL in the uterus is necessary for proper placental development and maintenance of pregnancy. Biol Reprod. 2012;86(6):194.

151. Kenney NJ, Adkins HB, Sanicola M. Nodal and Cripto-1: embryonic pattern formation genes involved in mammary gland development and tumorigenesis. Journal of mammary gland biology and neoplasia. 2004;9(2):133-44.

152. Bianco C, Adkins HB, Wechselberger C, Seno M, Normanno N, De Luca A, et al. Cripto-1 activates nodal- and ALK4-dependent and -independent signaling pathways in mammary epithelial Cells. Mol Cell Biol. 2002;22(8):2586-97.

153. Quail DF, Siegers GM, Jewer M, Postovit L-M. Nodal signalling in embryogenesis and tumourigenesis. The International Journal of Biochemistry & Cell Biology. 2013;45(4):885-98.

154. Brisken C, Park S, Vass T, Lydon JP, O'Malley BW, Weinberg RA. A paracrine role for the epithelial progesterone receptor in mammary gland development. Proc Natl Acad Sci U S A. 1998;95(9):5076-81.

155. Watson CJ, Khaled WT. Mammary development in the embryo and adult: a journey of morphogenesis and commitment. Development. 2008;135(6):995-1003.

156. Herrera MB, Bruno S, Buttiglieri S, Tetta C, Gatti S, Deregibus MC, et al. Isolation and characterization of a stem cell population from adult human liver. Stem cells (Dayton, Ohio). 2006;24(12):2840-50.

157. Zhao F, Huang F, Tang M, Li X, Zhang N, Amfilochiadis A, et al. Nodal induces apoptosis through activation of the ALK7 signaling pathway in pancreatic INS-1 beta-cells. American journal of physiology Endocrinology and metabolism. 2012;303(1): E132-43.

158. Lee JT, Herlyn M. Embryogenesis meets tumorigenesis. Nature Medicine. 2006; 12:882.

159. Kulesa PM, Kasemeier-Kulesa JC, Teddy JM, Margaryan NV, Seftor EA, Seftor RE, et al. Reprogramming metastatic melanoma cells to assume a neural crest cell-like phenotype in an embryonic microenvironment. Proc Natl Acad Sci U S A. 2006;103(10):3752-7.

160. Postovit LM, Seftor EA, Seftor RE, Hendrix MJ. Influence of the microenvironment on melanoma cell fate determination and phenotype. Cancer Res. 2006;66(16):7833-6.

161. Strizzi L, Postovit LM, Margaryan NV, Seftor EA, Abbott DE, Seftor RE, et al. Emerging roles of nodal and Cripto-1: from embryogenesis to breast cancer progression. Breast disease. 2008; 29:91-103.

162. Postovit LM, Seftor EA, Seftor RE, Hendrix MJ. A three-dimensional model to study the epigenetic effects induced by the microenvironment of human embryonic stem cells. Stem cells (Dayton, Ohio). 2006;24(3):501-5.

163. Postovit L-M, Margaryan NV, Seftor EA, Kirschmann DA, Lipavsky A, Wheaton WW, et al. Human embryonic stem cell microenvironment suppresses the tumorigenic phenotype of aggressive cancer cells. Proceedings of the National Academy of Sciences. 2008;105(11):4329-34.

164. Lynne-Marie P, V. MN, A. SE, C. HMJ. Role of nodal signaling and the microenvironment underlying melanoma plasticity. Pigment Cell & Melanoma Research. 2008;21(3):348-57.

165. Yu L, Harms PW, Pouryazdanparast P, Kim DS, Ma L, Fullen DR. Expression of the embryonic morphogen Nodal in cutaneous melanocytic lesions. Mod Pathol. 2010;23(9):1209-14.

166. Hooijkaas AI, Gadiot J, van Boven H, Blank C. Expression of the embryological morphogen Nodal in stage III/IV melanoma. Melanoma research. 2011;21(6):491-501.

167. Hardy KM, Kirschmann DA, Seftor EA, Margaryan NV, Postovit LM, Strizzi L, et al. Regulation of the embryonic morphogen Nodal by Notch4 facilitates manifestation of the aggressive melanoma phenotype. Cancer Res. 2010;70(24):10340-50.

168. McAllister JC, Zhan Q, Weishaupt C, Hsu MY, Murphy GF. The embryonic morphogen, Nodal, is associated with channel-like structures in human malignant melanoma xenografts. Journal of cutaneous pathology. 2010;37 Suppl 1:19-25.

169. Kirsammer G, Strizzi L, Margaryan NV, Gilgur A, Hyser M, Atkinson J, et al. Nodal signaling promotes a tumorigenic phenotype in human breast cancer. Seminars in Cancer Biology. 2014; 29:40-50.

170. Aykul S, Ni W, Mutatu W, Martinez-Hackert E. Human Cerberus prevents nodal-receptor binding, inhibits nodal signaling, and suppresses nodal-mediated phenotypes. PLoS One. 2015;10(1):e0114954.

171. Quail DF, Walsh LA, Zhang G, Findlay SD, Moreno J, Fung L, et al. Embryonic protein nodal promotes breast cancer vascularization. Cancer Res. 2012;72(15):3851-63.

172. Meyer MJ, Fleming JM, Ali MA, Pesesky MW, Ginsburg E, Vonderhaar BK. Dynamic regulation of CD24 and the invasive, CD44posCD24neg phenotype in breast cancer cell lines. Breast Cancer Res. 2009;11(6): R82.

173. Gong W, Sun B, Sun H, Zhao X, Zhang D, Liu T, et al. Nodal signaling activates the Smad2/3 pathway to regulate stem cell-like properties in breast cancer cells. American journal of cancer research. 2017;7(3):503-17.

174. Strizzi L, Hardy KM, Margaryan NV, Hillman DW, Seftor EA, Chen B, et al. Potential for the embryonic morphogen Nodal as a prognostic and predictive biomarker in breast cancer. Breast Cancer Res. 2012;14(3):R75.

175. Lee CC, Jan HJ, Lai JH, Ma HI, Hueng DY, Lee YC, et al. Nodal promotes growth and invasion in human gliomas. Oncogene. 2010;29(21):3110-23.

176. Hueng DY, Lin GJ, Huang SH, Liu LW, Ju DT, Chen YW, et al. Inhibition of Nodal suppresses angiogenesis and growth of human gliomas. Journal of neuro-oncology. 2011;104(1):21-31.

177. Sun G, Shi L, Li M, Jiang N, Fu L, Guo J. Lefty inhibits glioma growth by suppressing Nodal-activated Smad and ERK1/2 pathways. J Neurol Sci. 2014;347(1-2):137-42.

178. Sun J, Liu SZ, Lin Y, Cao XP, Liu JM. TGF-beta promotes glioma cell growth via activating Nodal expression through Smad and ERK1/2 pathways. Biochem Biophys Res Commun. 2014;443(3):1066-72.

179. Nana AW, Yang PM, Lin HY. Overview of Transforming Growth Factor beta Superfamily Involvement in Glioblastoma Initiation and Progression. Asian Pacific journal of cancer prevention: APJCP. 2015;16(16):6813-23.

180. Oliveira-Nunes MC, Assad Kahn S, de Oliveira Barbeitas AL, TC ES, Dubois LG, Ventura Matioszek GM, et al. The availability of the embryonic TGF-beta protein Nodal is dynamically regulated during glioblastoma multiforme tumorigenesis. Cancer Cell Int. 2016; 16:46.

181. Cavallari C, Fonsato V, Herrera MB, Bruno S, Tetta C, Camussi G. Role of Lefty in the anti tumor activity of human adult liver stem cells. Oncogene. 2013;32(7):819-26.

182. Sun C, Sun L, Jiang K, Gao DM, Kang XN, Wang C, et al. NANOG promotes liver cancer cell invasion by inducing epithelial-mesenchymal transition through NODAL/SMAD3 signaling pathway. Int J Biochem Cell Biol. 2013;45(6):1099-108.

183. Lawrence MG, Margaryan NV, Loessner D, Collins A, Kerr KM, Turner M, et al. Reactivation of Embryonic Nodal Signaling is Associated with Tumor Progression and Promotes the Growth of Prostate Cancer Cells. The Prostate. 2011;71(11):1198-209.

184. Spiller CM, Gillis AJ, Burnet G, Stoop H, Koopman P, Bowles J, et al. Cripto: Expression, epigenetic regulation and potential diagnostic use in testicular germ cell tumors. Mol Oncol. 2016;10(4):526-37.

185. Spiller C, Burnet G, Bowles J. Regulation of fetal male germ cell development by members of the TGFbeta superfamily. Stem Cell Res. 2017; 24:174-80.

186. Lonardo E, Hermann PC, Mueller MT, Huber S, Balic A, Miranda-Lorenzo I, et al. Nodal/Activin signaling drives self-renewal and tumorigenicity of pancreatic cancer stem cells and provides a target for combined drug therapy. Cell Stem Cell. 2011;9(5):433-46.

187. Lonardo E, Frias-Aldeguer J, Hermann PC, Heeschen C. Pancreatic stellate cells form a niche for cancer stem cells and promote their self-renewal and invasiveness. Cell cycle (Georgetown, Tex). 2012;11(7):1282-90.

188. Duan W, Li R, Ma J, Lei J, Xu Q, Jiang Z, et al. Overexpression of Nodal induces a metastatic phenotype in pancreatic cancer cells via the Smad2/3 pathway. Oncotarget. 2015;6(3):1490-506.

189. Kong B, Wang W, Esposito I, Friess H, Michalski CW, Kleeff J. Increased expression of Nodal correlates with reduced patient survival in pancreatic cancer. Pancreatology: official journal of the International Association of Pancreatology (IAP). 2015;15(2):156-61.

190. Isaacs A, Lindenmann J. Virus interference. I. The interferon. Proceedings of the Royal Society of London Series B, Biological sciences. 1957;147(927):258-67.

191. Pestka S, Krause CD, Walter MR. Interferons, interferon-like cytokines, and their receptors. Immunological reviews. 2004; 202:8-32.

192. de Weerd NA, Samarajiwa SA, Hertzog PJ. Type I interferon receptors: biochemistry and biological functions. The Journal of biological chemistry. 2007;282(28):20053-7.

193. Schroder K, Hertzog PJ, Ravasi T, Hume DA. Interferon-gamma: an overview of signals, mechanisms and functions. Journal of leukocyte biology. 2004;75(2):163-89.

194. Kotenko SV, Gallagher G, Baurin VV, Lewis-Antes A, Shen M, Shah NK, et al. IFN-lambdas mediate antiviral protection through a distinct class II cytokine receptor complex. Nature immunology. 2003;4(1):69-77.

195. Hoffmann H-H, Schneider WM, Rice CM. Interferons and viruses: an evolutionary arms race of molecular interactions. Trends in Immunology. 2015;36(3):124-38.

196. Trent JM, Olson S, Lawn RM. Chromosomal localization of human leukocyte, fibroblast, and immune interferon genes by means of in situ hybridization. Proceedings of the National Academy of Sciences. 1982;79(24):7809-13.

197. Weissmann C, Weber H. The Interferon Genes. In: Cohn WE, Moldave K, editors. Progress in Nucleic Acid Research and Molecular Biology. 33: Academic Press; 1986. p. 251-300.

198. Díaz MO, Pomykala HM, Bohlander SK, Maltepe E, Malik K, Brownstein B, et al. Structure of the Human Type-I Interferon Gene Cluster Determined from a YAC Clone Contig. Genomics. 1994;22(3):540-52.

199. Hertzog PJ, Hwang SY, Kola I. Role of interferons in the regulation of cell proliferation, differentiation, and development. Molecular reproduction and development. 1994;39(2):226-32.

200. Dandoy F, Kelley KA, DeMaeyer-Guignard J, DeMaeyer E, Pitha PM. Linkage analysis of the murine interferon-alpha locus on chromosome 4. The Journal of Experimental Medicine. 1984;160(1):294-302.

201. van der Korput JA, Hilkens J, Kroezen V, Zwarthoff EC, Trapman J. Mouse interferon alpha and beta genes are linked at the centromere proximal region of chromosome 4. The Journal of general virology. 1985;66 (Pt 3):493-502.

202. Hardy MP, Owczarek CM, Jermiin LS, Ejdebäck M, Hertzog PJ. Characterization of the type I interferon locus and identification of novel genes. Genomics. 2004;84(2):331-45.

203. Domanski P, Witte M, Kellum M, Rubinstein M, Hackett R, Pitha P, et al. Cloning and expression of a long form of the beta subunit of the interferon alpha beta receptor that is required for signaling. The Journal of biological chemistry. 1995;270(37):21606-11.

204. de Weerd NA, Nguyen T. The interferons and their receptors—distribution and regulation. Immunology And Cell Biology. 2012; 90:483.

205. Sen GC. Viruses and Interferons. Annual Review of Microbiology. 2001;55(1):255-81.

206. Gessani S, Belardelli F. IFN-γ Expression in Macrophages and Its Possible Biological Significance. Cytokine & Growth Factor Reviews. 1998;9(2):117-23.

207. Yoshimoto T, Takeda K, Tanaka T, Ohkusu K, Kashiwamura S-i, Okamura H, et al. IL-12 Up-Regulates IL-18 Receptor Expression on T Cells, Th1 Cells, and B Cells: Synergism with IL-18 for IFN-γ Production. The Journal of Immunology. 1998;161(7):3400-7.

208. Frucht DM, Fukao T, Bogdan C, Schindler H, O'Shea JJ, Koyasu S. IFN-γ production by antigen-presenting cells: mechanisms emerge. Trends in Immunology. 2001;22(10):556-60.

209. Erika A. Bach, Aguet M, Schreiber RD. THE IFNγ RECEPTOR: A Paradigm for Cytokine Receptor Signaling. Annual Review of Immunology. 1997;15(1):563-91.

210. Schroder K, Hertzog PJ, Ravasi T, Hume DA. Interferon-γ: an overview of signals, mechanisms and functions. Journal of leukocyte biology. 2004;75(2):163-89.

211. Fox BA, Sheppard PO, O'Hara PJ. The role of genomic data in the discovery, annotation and evolutionary interpretation of the interferon-lambda family. PLoS One. 2009;4(3): e4933.

212. Sheppard P, Kindsvogel W, Xu W, Henderson K, Schlutsmeyer S, Whitmore TE, et al. IL-28, IL-29 and their class II cytokine receptor IL-28R. Nature immunology. 2003;4(1):63-8.

213. Wack A, Terczyńska-Dyla E, Hartmann R. Guarding the frontiers: the biology of type III interferons. Nature immunology. 2015; 16:802.

214. Sommereyns C, Paul S, Staeheli P, Michiels T. IFN-lambda (IFN-lambda) is expressed in a tissue-dependent fashion and primarily acts on epithelial cells in vivo. PLoS pathogens. 2008;4(3):e1000017.

215. Pott J, Mahlakoiv T, Mordstein M, Duerr CU, Michiels T, Stockinger S, et al. IFN-lambda determines the intestinal epithelial antiviral host defense. Proc Natl Acad Sci U S A. 2011;108(19):7944-9.

216. Liu Y-J. IPC: Professional Type 1 Interferon-Producing Cells and Plasmacytoid Dendritic Cell Precursors. Annual Review of Immunology. 2005;23(1):275-306.

217. Ivashkiv LB, Donlin LT. Regulation of type I interferon responses. Nat Rev Immunol. 2014;14(1):36-49.

218. Takeuchi O, Akira S. Pattern recognition receptors and inflammation. Cell. 2010;140(6):805-20.

219. McNab F, Mayer-Barber K, Sher A, Wack A, O'Garra A. Type I interferons in infectious disease. Nat Rev Immunol. 2015;15(2):87-103.

220. Lutfalla G, Holland SJ, Cinato E, Monneron D, Reboul J, Rogers NC, et al. Mutant U5A cells are complemented by an interferon-alpha beta receptor subunit generated by alternative processing of a new member of a cytokine receptor gene cluster. Embo j. 1995;14(20):5100-8.

221. Hardy MP, Owczarek CM, Trajanovska S, Liu X, Kola I, Hertzog PJ. The soluble murine type I interferon receptor Ifnar-2 is present in serum, is independently regulated, and has both agonistic and antagonistic properties. Blood. 2001;97(2):473-82.

222. Gazziola C, Cordani N, Carta S, De Lorenzo E, Colombatti A, Perris R. The relative endogenous expression levels of the IFNAR2 isoforms influence the cytostatic and pro-apoptotic effect of IFNalpha on pleomorphic sarcoma cells. International journal of oncology. 2005;26(1):129-40.

223. Cohen B, Novick D, Barak S, Rubinstein M. Ligand-induced association of the type I interferon receptor components. Molecular and Cellular Biology. 1995;15(8):4208-14.

224. Platanias LC, Fish EN. Signaling pathways activated by interferons. Exp Hematol. 1999; 27:1583-92.

225. Darnell JE, Jr., Kerr IM, Stark GR. Jak-STAT pathways and transcriptional activation in response to IFNs and other extracellular signaling proteins. Science. 1994;264(5164):1415-21.

226. Schindler C, Levy DE, Decker T. JAK-STAT Signaling: From Interferons to Cytokines. Journal of Biological Chemistry. 2007;282(28):20059-63.

227. Stark GR, Kerr IM, Williams BR, Silverman RH, Schreiber RD. How cells respond to interferons. Annual review of biochemistry. 1998; 67:227-64.

228. Wagner TC, Velichko S, Chesney SK, Biroc S, Harde D, Vogel D, et al. Interferon receptor expression regulates the antiproliferative effects of interferons on cancer cells and solid tumors. Int J Cancer. 2004;111(1):32-42.

229. Rusinova I, Forster S, Yu S, Kannan A, Masse M, Cumming H, et al. Interferome v2.0: an updated database of annotated interferon-regulated genes. Nucleic acids research. 2013;41(Database issue): D1040-6.

230. Hall JC, Rosen A. Type I interferons: crucial participants in disease amplification in autoimmunity. Nature reviews Rheumatology. 2010;6(1):40-9.

231. Porritt RA, Hertzog PJ. Dynamic control of type I IFN signalling by an integrated network of negative regulators. Trends Immunol. 2015;36(3):150-60.

232. Kirkwood JM, Ibrahim JG, Sondak VK, Richards J, Flaherty LE, Ernstoff MS, et al. High- and low-dose interferon alfa-2b in high-risk melanoma: first analysis of intergroup trial E1690/S9111/C9190. Journal of clinical oncology: official journal of the American Society of Clinical Oncology. 2000;18(12):2444-58.

233. Neuwirt H, Puhr M, Santer FR, Susani M, Doppler W, Marcias G, et al. Suppressor of Cytokine Signaling (SOCS)-1 Is Expressed in Human Prostate Cancer and Exerts Growth-Inhibitory Function through Down-Regulation of Cyclins and Cyclin-Dependent Kinases. The American Journal of Pathology. 2009;174(5):1921-30.

234. Parker BS, Rautela J, Hertzog PJ. Antitumour actions of interferons: implications for cancer therapy. Nat Rev Cancer. 2016;16(3):131-44.

235. Platanias LC. Mechanisms of type-I- and type-II-interferon-mediated signalling. Nature Reviews Immunology. 2005; 5:375.

236. Zhou Z, Hamming OJ, Ank N, Paludan SR, Nielsen AL, Hartmann R. Type III interferon (IFN) induces a type I IFN-like response in a restricted subset of cells through signaling pathways involving both the Jak-STAT pathway and the mitogen-activated protein kinases. J Virol. 2007;81(14):7749-58.

237. Grumbach IM, Mayer IA, Uddin S, Lekmine F, Majchrzak B, Yamauchi H, et al. Engagement of the CrkL adaptor in interferon alpha signalling in BCR-ABL-expressing cells. British journal of haematology. 2001;112(2):327-36.

238. Gresser I. The antitumor effects of interferon: A personal history. Biochimie. 2007;89(6–7):723-8.

239. Bekisz J, Sato Y, Johnson C, Husain SR, Puri RK, Zoon KC. Immunomodulatory Effects of Interferons in Malignancies. Journal of Interferon & Cytokine Research. 2013;33(4):154-61.

240. Borden EC, Sen GC, Uze G, Silverman RH, Ransohoff RM, Foster GR, et al. Interferons at age 50: past, current and future impact on biomedicine. Nat Rev Drug Discov. 2007;6(12):975-90.

241. Chatterjee D, Savarese TM. Posttranscriptional regulation of c-myc proto-oncogene expression and growth inhibition by recombinant human interferon-beta ser17 in a human colon carcinoma cell line. Cancer Chemother Pharmacol. 1992; 30:12-20.

242. Gierek D, Baczynska D, Ugorski M, Bazer F, Kurpisz M, Bednarski T, et al. Differential effect of IFN-tau on proliferation and distribution of lymphocyte subsets in one-way mixed lymphocyte reaction in cows and heifers. Journal of reproductive immunology. 2006;71(2):126-31.

243. Pokrovskaja K, Panaretakis T, Grander D. Alternative signaling pathways regulating type I interferon-induced apoptosis. J Interferon Cytokine Res. 2005;25(12):799-810.

244. Johns TG, Mackay IR, Callister KA, Hertzog PJ, Devenish RJ, Linnane AW. Antiproliferative potencies of interferons on melanoma cell lines and xenografts: higher efficacy of interferon beta. J Natl Cancer Inst. 1992;84(15):1185-90.

245. Falk LA, Vogel SN. Differential production of IFN-alpha//beta by CSF-1- and GM-CSF-derived macrophages. Journal of leukocyte biology. 1990; 48:43-9.

246. Hamilton JA, Whitty GA, Kola I, Hertzog PJ. Endogenous IFN-alpha beta suppresses colony-stimulating factor (CSF)-1-stimulated macrophage DNA synthesis and mediates inhibitory effects of lipopolysaccharide and TNF-alpha. J Immunol. 1996; 156:2553-7.

247. Hwang SY, Hertzog PJ, Holland KA, Sumarsono SH, Tymms MJ, Hamilton JA. A null mutation in the gene encoding a type I interferon receptor component eliminates antiproliferative and antiviral responses to interferons alpha and beta and alters macrophage responses. Proc Natl Acad Sci USA. 1995; 92:11284-8.

248. Raveh T, Hovanessian AG, Meurs EF, Sonenberg N, Kimchi A. Double-stranded RNA-dependent protein kinase mediates c-Myc suppression induced by type I interferons. The Journal of biological chemistry. 1996; 271:25479-84.

249. Hu X, Bies J, Wolff L. Interferon beta increases c-Myc proteolysis in mouse monocyte//macrophage leukemia cells. Leuk Res. 2005; 29:1307-14.

250. Einat M, Resnitzky D, Kimchi A. Close link between reduction of c-myc expression by interferon and G0/G1 arrest. Nature. 1985;313(6003):597-600.

251. Elmore S. Apoptosis: a review of programmed cell death. Toxicologic pathology. 2007;35(4):495-516.

252. Chawla-Sarkar M, Lindner DJ, Liu YF, Williams BR, Sen GC, Silverman RH. Apoptosis and interferons: role of interferon-stimulated genes as mediators of apoptosis. Apoptosis. 2003; 8:237-49.

253. Yen J-H, Ganea D. Interferon β induces mature dendritic cell apoptosis through caspase-11/caspase-3 activation2009 2009-08-13 00:00:00. 1344-54 p.

254. Thyrell L, Erickson S, Zhivotovsky B, Pokrovskaja K, Sangfelt O, Castro J, et al. Mechanisms of Interferon-alpha induced apoptosis in malignant cells. Oncogene. 2002;21(8):1251-62.

255. Chen Q, Gong B, Mahmoud-Ahmed AS, Zhou A, Hsi ED, Hussein M, et al. Apo2L/TRAIL and Bcl-2–related proteins regulate type I interferon–induced apoptosis in multiple myeloma2001 2001-10-01 00:00:00. 2183-92 p.

256. Oshima K, Yanase N, Ibukiyama C, Yamashina A, Kayagaki N, Yagita H. Involvement of TRAIL//TRAIL-R interaction in IFN-alpha-induced apoptosis of Daudi B lymphoma cells. Cytokine. 2001; 14:193-201.

257. Clemens MJ. Interferons and apoptosis. J Interferon Cytokine Res. 2003; 23:277-92.

258. Zhou A, Paranjape J, Brown TL, Nie H, Naik S, Dong B. Interferon action and apoptosis are defective in mice devoid of 2[prime]5[prime]-oligoadenylate-dependent RNase L. EMBO J. 1997;16:6355-63.

259. Sanceau J, Hiscott J, Delattre O, Wietzerbin J. IFN-beta induces serine phosphorylation of Stat-1 in Ewing's sarcoma cells and mediated apoptosis via induction of IRF-1 and activation of caspase-7. Oncogene. 2000; 19:3372-83.

260. Toomey NL, Deyev VV, Wood C, Boise LH, Scott D, Liu LH. Induction of a TRAIL-mediated suicide program by interferon alpha in primary effusion lymphoma. Oncogene. 2001; 20:7029-40.

261. Noppert SJ, Fitzgerald KA, Hertzog PJ. The role of type I interferons in TLR responses. Immunol Cell Biol. 2007;85(6):446-57.

262. Bekisz J, Sato Y, Johnson C, Husain SR, Puri RK, Zoon KC. Immunomodulatory effects of interferons in malignancies. J Interferon Cytokine Res. 2013;33(4):154-61.

263. Gidlund M, Orn A, Wigzell H, Senik A, Gresser I. Enhanced NK cell activity in mice injected with interferon and interferon inducers. Nature. 1978;273(5665):759-61.

264. Hervas-Stubbs S, Perez-Gracia JL, Rouzaut A, Sanmamed MF, Le Bon A, Melero I. Direct effects of type I interferons on cells of the immune system. Clinical cancer research: an official journal of the American Association for Cancer Research. 2011;17(9):2619-27.

265. Tough DF. Modulation of T-cell function by type I interferon. Immunol Cell Biol. 2012;90(5):492-7.

266. Bidwell BN, Slaney CY, Withana NP, Forster S, Cao Y, Loi S, et al. Silencing of Irf7 pathways in breast cancer cells promotes bone metastasis through immune escape. Nat Med. 2012.

267. Roffi L, Mels GC, Antonelli G, Bellati G, Panizzuti F, Piperno A, et al. Breakthrough during recombinant interferon alfa therapy in patients with chronic hepatitis C virus infection: Prevalence, etiology, and management. Hepatology. 1995;21(3):645-9.

268. Mazzella G, Saracco G, Festi D, Rosina F, Marchetto S, Jaboli F, et al. Long-term results with interferon therapy in chronic type B hepatitis: a prospective randomized trial. The American journal of gastroenterology. 1999;94(8):2246-50.

269. Vezali E, Aghemo A, Colombo M. Interferon in the treatment of chronic hepatitis C: a drug caught between past and future. Expert Opinion on Biological Therapy. 2011;11(3):301-13.

270. Marrie RA, Rudick RA. Drug Insight: interferon treatment in multiple sclerosis. Nature Clinical Practice Neurology. 2006; 2:34+.

271. Zhornitsky S, Greenfield J, Koch MW, Patten SB, Harris C, Wall W, et al. Long-term persistence with injectable therapy in relapsing-remitting multiple sclerosis: an 18-year observational cohort study. PLoS One. 2015;10(4):e0123824.

272. Clerico M, Contessa G, Durelli L. Interferon-beta1a for the treatment of multiple sclerosis. Expert Opin Biol Ther. 2007;7(4):535-42.

273. Quesada JR, Reuben J, Manning JT, Hersh EM, Gutterman JU. Alpha interferon for induction of remission in hairy-cell leukemia. The New England journal of medicine. 1984;310(1):15-8.

274. Talpaz M, Kantarjian H, McCredie K, Keating M, Trujillo J, Gutterman J. Clinical investigation of human alpha interferon in chronic myelogenous leukemia1987 1987-05-01 00:00:00. 1280-8 p.

275. Quesada JR, Alexanian R, Hawkins M, Barlogie B, Borden E, Itri L, et al. Treatment of multiple myeloma with recombinant alpha-interferon. Blood. 1986;67(2):275-8.

276. Mitsuyasu RT. Interferon alpha in the treatment of AIDS-related Kaposi's sarcoma. British journal of haematology. 1991;79 Suppl 1:69-73.

277. Kirkwood JM, Harris JE, Vera R, Sandler S, Fischer DS, Khandekar J, et al. A randomized study of low and high doses of leukocyte alpha-interferon in metastatic renal cell carcinoma: the American Cancer Society collaborative trial. Cancer Res. 1985;45(2):863-71.

278. Fuchs SY. Hope and fear for interferon: the receptor-centric outlook on the future of interferon therapy. J Interferon Cytokine Res. 2013;33(4):211-25.

279. Rizza P, Moretti F, Belardelli F. Recent advances on the immunomodulatory effects of IFN-alpha: implications for cancer immunotherapy and autoimmunity. Autoimmunity. 2010;43(3):204-9.

280. Colman H, Berkey BA, Maor MH, Groves MD, Schultz CJ, Vermeulen S, et al. Phase II Radiation Therapy Oncology Group trial of conventional radiation therapy followed by treatment with recombinant interferon-beta for supratentorial glioblastoma: results of RTOG 9710. International journal of radiation oncology, biology, physics. 2006;66(3):818-24.

281. Repetto L, Giannessi PG, Campora E, Pronzato P, Vigani A, Naso C, et al. Tamoxifen and interferon-beta for the treatment of metastatic breast cancer. Breast Cancer Res Treat. 1996;39(2):235-8.

282. Recchia F, Sica G, Candeloro G, Necozione S, Bisegna R, Bratta M, et al. Beta-interferon, retinoids and tamoxifen in metastatic breast cancer: long-term follow-up of a phase II study. Oncology reports. 2009;21(4):1011-6.

283. Fung KY, Mangan NE, Cumming H, Horvat JC, Mayall JR, Stifter SA, et al. Interferon-ε Protects the Female Reproductive Tract from Viral and Bacterial Infection. Science. 2013;339(6123):1088-92.

284. Stifter SA, Matthews AY, Mangan NE, Fung KY, Drew A, Tate MD, et al. Defining the distinct, intrinsic properties of the novel type I interferon, epsilon. Journal of Biological Chemistry. 2017.

285. Fung KY, Mangan NE, Cumming H, Horvat JC, Mayall JR, Stifter SA, et al. Interferon-epsilon protects the female reproductive tract from viral and bacterial infection. Science. 2013;339(6123):1088-92.

286. Bourke NM, Achilles SL, Huang SU, Cumming HE, Papageorgiou I, Gearing LJ, Thakore S, Mangan NE, Mesiano S, Hertzog PJ. Human IFNε: Spaciotemporal expression, hormone regulation and innate immunity in the female reproductive tract. bioRxiv. October 16, 2018.

287. Sharkey DJ, Macpherson AM, Tremellen KP, Robertson SA. Seminal plasma differentially regulates inflammatory cytokine gene expression in human cervical and vaginal epithelial cells. Molecular human reproduction. 2007;13(7):491-501.

288. Abdulhaqq SA, Zorrilla C, Kang G, Yin X, Tamayo V, Seaton KE, et al. HIV-1-negative female sex workers sustain high cervical IFNvarepsilon, low immune activation, and low expression of HIV-1-required host genes. Mucosal Immunol. 2016;9(4):1027-38.

289. Kalyan A, Carneiro BA, Chandra S, Kaplan J, Chae YK, Matsangou M, et al. Nodal Signaling as a Developmental Therapeutics Target in Oncology. Mol Cancer Ther. 2017;16(5):787-92.

290. Li P, Sun D, Li X, He Y, Li W, Zhao J, et al. Elevated expression of Nodal and YAP1 is associated with poor prognosis of gastric adenocarcinoma. Journal of cancer research and clinical oncology. 2016;142(8):1765-73.

291. Bodenstine TM, Chandler GS, Seftor RE, Seftor EA, Hendrix MJ. Plasticity underlies tumor progression: role of Nodal signaling. Cancer metastasis reviews. 2016;35(1):21-39.

292. Polli V, Bulletti C, Galassi A, Borini A, Ciotti PM, Seracchioli R, et al. Transforming growth factor-beta 1 in the human endometrium. Gynecological endocrinology: the official journal of the International Society of Gynecological Endocrinology. 1996;10(5):297-302.

293. Robertson SA, Mau VJ, Hudson SN, Tremellen KP. Cytokine-leukocyte networks and the establishment of pregnancy. Am J Reprod Immunol. 1997;37(6):438-42.

294. Jones RL, Salamonsen LA, Findlay JK. Activin A promotes human endometrial stromal cell decidualization in vitro. The Journal of clinical endocrinology and metabolism. 2002;87(8):4001-4.

295. Jones RL, Stoikos C, Findlay JK, Salamonsen LA. TGF-β superfamily expression and actions in the endometrium and placenta. Reproduction. 2006;132(2):217-32.

296. Papageorgiou I, Nicholls PK, Wang F, Lackmann M, Makanji Y, Salamonsen LA, et al. Expression of nodal signalling components in cycling human endometrium and in endometrial cancer. Reprod Biol Endocrinol. 2009; 7:122.

Chapter 2

Expression of Nodal Signalling Components in Cycling Human Endometrium and in Endometrial Cancer

Irene Papageorgiou, Peter K Nicholls, Fang Wang, Martin Lackmann, Yogeshwar Makanji, Lois A Salamonsen, David M Robertson and Craig A Harrison

Reproductive Biology and Endocrinology
(2009) 7: 122

"Everything you can imagine is real."

-Pablo Picasso

Chapter 2

Reproductive Biology and Endocrinology

BioMed Central

Open Access

Research

Expression of nodal signalling components in cycling human endometrium and in endometrial cancer

Irene Papageorgiou[1,2], Peter K Nicholls[1,3], Fang Wang[1], Martin Lackmann[3], Yogeshwar Makanji[1,2], Lois A Salamonsen[1], David M Robertson[1] and Craig A Harrison*[1]

Address: [1]Prince Henry's Institute of Medical Research, 246 Clayton Road, Clayton, Vic 3168, Australia, [2]Department of Obstetrics and Gynecology, Monash University, Clayton, Vic 3168, Australia and [3]Department of Biochemistry and Molecular Biology, Monash University, Clayton, Vic 3168, Australia

Email: Irene Papageorgiou - irene.papageorgiou@princehenrys.org; Peter K Nicholls - peter.nicholls@princehenrys.org; Fang Wang - frwang@msn.com; Martin Lackmann - martin.lackmann@med.monash.edu.au; Yogeshwar Makanji - yogeshwar.makanji@princehenrys.org; Lois A Salamonsen lois.salamonsen@princehenrys.org; David M Robertson -david.robertson@princehenrys.org; Craig A Harrison* - craig.harrison@princehenrys.org * Corresponding author

Published: 29 October 2009 Received: 14 August 2009 Accepted: 29 October 200 *Reproductive*

Biology and Endocrinology 2009, **7**:122 doi:10.1186/1477-7827-7-122
This article is available from: http://www.rbej.com/content/7/1/122

Abstract

Background: The human endometrium is unique in its capacity to remodel constantly throughout adult reproductive life. Although the processes of tissue damage and breakdown in the endometrium have been well studied, little is known of how endometrial regeneration is achieved after menstruation. Nodal, a member of the transforming growth factor-beta superfamily, regulates the processes of pattern formation and differentiation that occur during early embryo development.

Methods: In this study, the expression of Nodal, Cripto (co-receptor) and Lefty A (antagonist) was examined by RT-PCR and immunohistochemistry across the menstrual cycle and in endometrial carcinomas.

Results: Nodal and Cripto were found to be expressed at high levels in both stromal and epithelial cells during the proliferative phase of the menstrual cycle. Although immunoreactivity for both proteins in surface and glandular epithelium was maintained at relatively steady-state levels across the cycle, their expression was significantly decreased within the stromal compartment by the midsecretory phase. Lefty expression, as has previously been reported, was primarily restricted to glandular epithelium and surrounding stroma during the late secretory and menstrual phases. In line with recent studies that have shown that Nodal pathway activity is upregulated in many human cancers, we found that Nodal and Cripto immunoreactivity increased dramatically in the transition from histologic Grade 1 to histologic Grades 2 and 3 endometrial carcinomas. Strikingly, Lefty expression was low or absent in all cancer tissues.

Conclusion: The expression of Nodal in normal and malignant endometrial cells that lack Lefty strongly supports an important role for this embryonic morphogen in the tissue remodelling events that occur across the menstrual cycle and in tumourigenesis.

Background

Nodal, a member of the transforming growth factor-beta (TGF-β) superfamily, regulates the processes of pattern formation and differentiation that occur during early embryo development [1]. In particular, Nodal signalling is essential for mesoderm and endoderm induction, neural patterning and the specification of the primary body axes [1]. Nodal signals through activin type I (ALK4) and type II (ActRII or ActRIIB) serine-threonine kinase receptors [2]. However, unlike activin, Nodal lacks intrinsic affinity for ALK4 and ActRII/IIB, suggesting the requirement for a co-receptor to potentiate its actions [3]. Indeed, recent studies have shown that Nodal effects are dependent upon interactions with Cripto, a small cysteine-rich extracellular protein that is attached to the plasma membrane through a glycosyl phosphatidyl inositol linkage [1]. Cripto interacts with Nodal and ALK4, independently, and promotes the formation of a stable high affinity complex with activin type II receptors [4]. Phosphorylation of ALK4 within this complex initiates signaling via Smad2/ Smad3 signal transducers [3]. The TGF-β signaling antagonist, Lefty, blocks Nodal actions by competing for access to the ligand binding site of Cripto [5].

Consistent with its crucial developmental function, nodal is first expressed throughout the embryonic ectoderm shortly after implantation (5.25 days post-coitum). Expression continues during the initial stages of primitive streak formation and is then rapidly down regulated as the streak elongates. Subsequently, nodal expression is detected in a small subset of node progenitors, and following the formation of the morphologically distinct node becomes restricted to the edges of the notochordal plate [1,6,7]. Until recently, Nodal expression was widely thought to be embryonically restricted [8]. However, several studies have shown that Nodal and its signalling partners are expressed at defined stages in a variety of adult tissues, including the lactating mammary gland and regenerating islet cells in the pancreas [9,10]. In addition, there is increasing evidence that Nodal pathway activity is upregulated in many human cancers. Hendrix and colleagues [11,12] have shown that expression of Nodal in metastatic melanomas and breast carcinomas is correlated with cancer progression, whereas pathway inhibition decreases cell invasiveness, colony formation and tumourigenicity.

Components of the Nodal signalling pathway have also been detected in human endometrium. Lefty A, which was originally designated endometrial bleeding associated factor (ebaf), is highly expressed in endometrium during the late secretory and menstrual phases, but is significantly reduced in proliferative, early and mid-secretory endometria [13,14]. Lefty A stimulates the production of several matrix metalloproteinases and may be a key local regulator of focal extracellular matrix breakdown in the cycling human endometrium [15]. Furthermore, dysregulated endometrial expression of Lefty is associated with infertility [14], and in vivo gene transfer of Lefty leads to implantation failure in mice [16]. Curiously, given Lefty's welldocumented mechanism of action during vertebrate embryogenesis [5,17], the presence of Nodal and Cripto mRNA in human endometrium has only recently been established [18].

In the current study, RT-PCR and immunohistochemistry were utilised to examine the site- and menstrual cycle stage-specific expression of Nodal and Cripto in the human endometrium. As recent studies have suggested that increased Nodal signalling has a key role in melanoma cell plasticity and tumourigenicity, the expression profiles of Nodal, Cripto and Lefty were also examined in endometrial carcinomas. The expression of Nodal and Cripto in normal and malignant endometrial cells that lack Lefty strongly supports an important role for this embryonic morphogen in the endometrial remodelling events that occur across the menstrual cycle and in tumourigenesis.

Methods

Tissue Collection

Ethical approval was obtained from appropriate Institutional Ethics Committees for all tissue and sample collections. Written informed consent was obtained prior to tissue and sample collection from all subjects. Human endometrial biopsies were obtained from normal fertile women undergoing curettage following laparoscopic sterilization or assessment of tubal patency. Cycle stage was confirmed by histological dating, according to standard criteria [19]; thereafter samples were allocated to one of six groups: menstrual (days 1-4, n = 4), early proliferative (days 5-8, n = 4), mid proliferative (days 8-10, n = 4), late proliferative (days 11-13, n = 4), early secretory (days 1417, n = 4), mid secretory (days 18-24, n = 4) and late secretory (days 25-28, n = 4). Endometrial biopsies were divided in two: one portion was fixed in 10% buffered formalin overnight, then washed three times in Tris-buffered saline (TBS, pH 7.6) before routine histological processing to paraffin blocks. The remainder was placed into RNA Later solution (Ambion, Austin, TX) before snap-freezing and stored at -80°C for subsequent RNA extraction. No RNA was extracted from mid proliferative tissue samples. The collection, grading and preparation for immunohistochemistry of endometrial cancer biopsies has been described previously [20]. In the current study, Grade 1 (n = 4), Grade 2 (n = 4) and Grade 3 (n = 4) endometrial carcinomas were examined for the immunolocalisation of Nodal, Lefty and Cripto.

RNA extraction, Reverse Transcription and Quantitative real-time PCR

Total RNA was extracted from endometrial samples from each menstrual cycle phase (n = 4 per stage: menstrual, early and late proliferative, early, mid and late secretory) using a total RNA extraction kit (Qiagen; Hildens, Germany) as previously described [21]. Contaminating DNA was removed using a DNA free kit (Ambion, Austin, Texas) for 25 min at 37°C after which reverse transcription was performed with 500 ng total RNA/sample using SuperScript-III (Invitrogen, Carlsbad, California) following the manufacturer's instructions, before being snap frozen and stored at -80°C. Quantitative real-time PCR analysis was then performed using the Roche Lightcycler 380 (Roche, Basel Switzerland) with the FastStart DNA Master SYBR-Green I system (Roche), or the Corbett Rotor-Gene 2000 (Corbett Lifesciences, Sydney, Australia) using universal SYBR-Green (Invitrogen). Oligonucleotide primer sequences were obtained from published sources [22], or were designed using Primer3 software (see Table 1), and were ordered from Sigma Genosys (Castle Hill, Australia). Relative quantification of Nodal, Cripto and Lefty mRNA expression across the cycle was determined using the 2-ΔΔCT method [23] with β-actin as internal control. Full details of PCR amplification conditions are summarised in Table 1. After 38 cycles of PCR, a melting curve analysis was performed to monitor PCR product purity, and in initial experiments, the identity of the amplicons was confirmed by DNA sequencing.

Immunohistochemistry

Antibodies directed against Nodal (goat anti-mouse Nodal; R&D Systems, Minneapolis, MN), Lefty A (goat anti-human Lefty; Santa Cruz Biotechnology, Santa Cruz, CA) Cripto (produced by M. Lackmann), and the Cripto binding protein, glucose-regulated protein 78 (GRP78; goat anti-human GRP78; Santa Cruz Biotechnology) were used to localize the respective proteins to 5-μm sections of formalin-fixed paraffin-embedded endometrial tissue using standard immunohistochemical protocols. These antisera were selected because we showed that they were suitable for detecting human endometrial proteins or they had previously been used for Western blotting of human endometrial tissue [24,25]. Briefly, sections were dewaxed in histosol, dehydrated in ethanol, and washed in water. Antigen retrieval was achieved by microwaving the sections in 1 mM EDTA-NaOH (pH 8.0, Titriplex III; Merck, Darmstadt, Germany) for 10 min before allowing to cool and equilibrating in 0.1 M PBS, pH 7.4. The sections were blocked for 30 min in 10% normal serum, after which the primary antibody (4 μg/ml (Nodal); 1.7 μg/ml (Cripto): 1 μg/ml (Lefty); 0.25 μg/ml (GRP78)), was added and the sections incubated O/N at 4°C for Nodal and Cripto, or 1 h at room temperature for Lefty and GRP78. Following extensive washing in PBS, slides were incubated with secondary antibodies (1:200) for 30 min at room temperature (goat anti-mouse HRP (Dako, Victoria, Australia) for Cripto; donkey anti-sheep/goat HRP (Chemicon, Billerica, MA) for Nodal; biotinylated rabbit anti-goat for Lefty and GRP78 detection (Vector Laboratories; Burlingame, CA, USA). For Lefty and GRP78 detection, an additional 30 min room temperature incubation with Vectastain ABC amplification (Vector Laboratories, Burlingame, CA) was required. The reaction product was developed using 3,3' diaminobenzidine tetrahydrochloride (Dako). Sections were counterstained with a 1:10 dilution of Harris' hematoxylin (Sigma-Aldrich, St. Louis, MO), dehydrated in ethanol, cleared in histosol and mounted using DPX (Sigma-Aldrich). The control sections received preimmune IgG (mouse or goat; AbD Serotec, Oxford, UK) diluted appropriately, in place of the primary antibody.

The intensity of staining was scored for each tissue and each antibody on a scale of 0 (no staining) to 4 (maximal intense staining) in each of the cellular compartments; luminal epithelium (if available), glandular epithelium, stroma and vasculature. One whole section was evaluated per sample by two independent observers and agreed scores were recorded. Data for Nodal, Cripto and Lefty expression in glandular epithelium and stroma is shown. N = 4 tissues were assessed for each stage.

Detection of Nodal in human uterine fluid

The collection of human uterine lavages (uterine washings) has been described previously [26]. Lavage fluid from two normally cycling women and a woman

Table 1: Primer-specific conditions used for quantitative PCR analysis

Gene	Primer sequence (5'-3')	size (bp)	Mg^{2+}(mM)	Anneal temp (°C)	Ex'sion time (s)	Read temp (°C)[1]
Cripto	F AAGATGGCCCGCTTCTCTTACAGT R AAAGTGGTAGTACGTGCAGACGGT	511	2	64	20	88
Nodal	F AGACATCATCCGCAGCCTACA R GTCCATCTGAAACCGCTCTAAG	330	3	59.2	20	88
Lefty A	F GGGAATTGGGATACCTGGAT R CTAAATATGCACGGGCAAGG	206	3	62	25	80
β-Actin	F CGAGCGCGGCTACAGCTT R TCATACTCCTGCTTGCTGATCC	500	2	64	14	85

[1] The temperature (temp) at which the fluorescence of the PCR product was quantified during LightCycler analysis.

with endometrial cancer was concentrated 50-fold using Nanosep microconcentration devices with a 10 K cut-off (Pall Life Sciences, East Hills, NY). Reduced samples were analysed by SDS-PAGE and Western blotting. The mature and precursor forms of Nodal were identified using a rat monoclonal anti-Nodal antibody (R&D Systems, Minneapolis, MN).

Statistical analysis

To determine if there were significant differences in mRNA expression levels for Nodal, Lefty A and Cripto at the different stages of the menstrual cycle, data were subjected to analysis of variance with Tukey's post hoc test. A value of $P < 0.05$ was considered statistically significant.

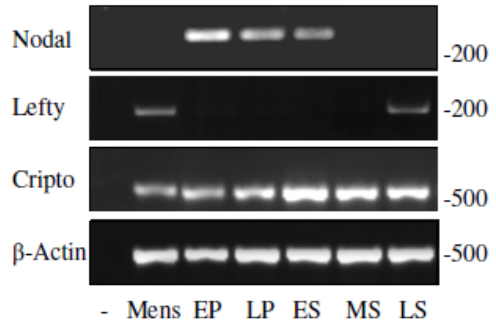

Figure 1
Representative products from PCR reactions to amplify Nodal, Lefty and Cripto in endometrial samples collected at all stages of the menstrual cycle (n = 4/stage). A band corresponding to 330 bp was detected for Nodal, 206 bp for Lefty, and 511 bp for Cripto. PCR for β-actin (500 bp) on the same samples was performed to assess RNA loading. Mens = menstrual phase, EP = early proliferative, LP = late proliferative, ES = early secretory, MS = mid secretory, LS = late secretory.

Results

Changes in gene expression of Nodal, Lefty and Cripto in the endometrium across the menstrual cycle

Nodal, Lefty and Cripto mRNAs were expressed in nonpregnant endometrial samples, with cyclical variations evident (Fig. 1). Nodal mRNA expression was highest during the proliferative and early secretory phases before declining rapidly during the mid-secretory phase. This supports an earlier study, which showed Nodal mRNA was absent in mid-late secretory endometrium [27]. In contrast, Lefty mRNA expression was barely detectable during the proliferative and early secretory phases, but increased markedly during the late secretory phase and was maintained throughout menses. Cripto mRNA wasexpressed across the menstrual cycle, peaking during the secretory phase.

To further investigate these cyclic variations, mRNA expression was quantitated using real-time PCR. The relative concentration of each PCR product was determined using the 2-ΔΔCT method with β-actin mRNA expression as the internal control. Although this method does not allow for absolute quantitation of mRNA transcripts, the relative expression levels of individual genes can be compared between the different phases of the menstrual cycle. Nodal mRNA was significantly elevated ($P < 0.05$) during the early secretory phase of the menstrual cycle when compared with expression levels during the mid/late secretory and menstrual phases (Fig. 2A). Indeed, a 48fold increase in Nodal mRNA expression was observed between the menstrual and early secretory phases. Strikingly, mRNA expression for the Nodal antagonist, Lefty, was nearly undetectable during the peak of Nodal expression, but rose dramatically (155-fold: $P < 0.05$) in the late secretory phase (Fig. 2B). Cripto mRNA expression increased marginally across the cycle, such that levels present in the late secretory phase were significantly (Fig. 2C; $P < 0.05$) higher than those observed during the menstrual and proliferative phases.

Immunolocalization of Nodal, Lefty and Cripto in the endometrium throughout the menstrual cycle

Immunostaining of Nodal during the early proliferative phase of the menstrual cycle showed strong staining of stromal and epithelial cells (both glandular and luminal) (Fig. 3B). This pattern of staining was maintained across the proliferative phase (Fig. 3C), however, Nodal immunoreactivity was significantly decreased within the stromal compartment by the early secretory phase (Fig. 3D) and this was maintained through the late secretory and menstrual phases (Fig. 3E-F). In contrast, Nodal staining in both surface and glandular epithelium was sustained at relatively steady-state levels across the menstrual cycle (Fig. 3I). Additional staining was observed for Nodal in endothelial cells of spiral arterioles (Fig. 3G). The precipitous decrease in the stromal localization of Nodal during the secretory phase mirrors the decrease observed in Nodal mRNA at this time. Therefore, it is likely that stromal cells account for the majority of Nodal expression within the endometrium, although the possibility remains that other endometrial cells secrete Nodal into the stromal compartment.

Lefty A immunoreactivity within human endometrium has previously been shown to be restricted to glandular epithelium and surrounding stroma during the late secretory and menstrual phases [13] and our results support these findings (Fig. 3J and data not shown). Interestingly, within the glands Lefty expression was highly polarized

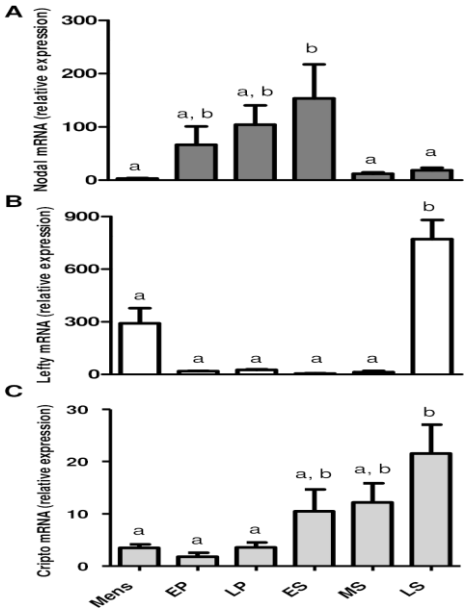

Figure 2

Quantitation of Nodal, Lefty and Cripto mRNA expression patterns across the menstrual cycle by RT-PCR (normalized for β-actin mRNA expression). Histograms illustrating fluctuations in mRNA expression (mean values ± SEM) for Nodal, Lefty and Cripto across the menstrual cycle (Mens = menstrual phase, EP = early proliferative, LP = late proliferative, ES = early secretory, MS = mid secretory, LS = late secretory; *n* = 4 for each stage). Significantly elevated expression of Nodal mRNA was detected in the early secretory phase compared with the menstrual or mid/late secretory phases, while Lefty and Cripto mRNAs were significantly elevated in the late secretory phase only. Different letters indicate significant differences, $P < 0.05$.

with prominent apical and basal staining. Localized staining within the stroma was also evident with highest levels of Lefty expression observed in cells surrounding spiral arterioles (data not shown).

As expected, Cripto has a similar pattern of expression as its ligand, Nodal. During the proliferative phase, Cripto was strongly expressed in the stroma and the glandular and luminal epithelia (Fig. 4A &4B). Stromal Cripto staining decreased during the secretory phases (Fig. 4C &4D) and only low level staining was observed in the stromal compartment by the menstrual phase (Fig. 4E &4H). In contrast, Cripto immunoreactivity within the glandular and luminal epithelium increased across the cycle (Fig. 4I). Additional immunostaining was detected in endothelial cells of spiral arterioles (Fig. 4F). The recently identified Cripto binding protein, GRP78, has a similar expression pattern within the endometrium. GRP78 is strongly expressed in glandular and luminal epithelial cells and weakly expressed throughout the stroma (Fig. 4J). Together, Cripto and GRP78 are thought to form a complex at the cell surface and collaborate to mediate TGF-β superfamily signalling [28,29].

Immunolocalization of Nodal, Cripto and Lefty in endometrial carcinomas

A recent study [12] showed that Nodal expression is positively associated with melanoma tumour progression: there is more Nodal protein in metastases than in primary tumours and none at all in normal skin. This study implicated Nodal as a diagnostic marker of disease progression and a target for the treatment of aggressive cancers such as melanomas [12]. Given that the components of the Nodal signaling pathway are present within the endometrium, we next assessed their expression patterns during the progression of endometrial cancer. Using immunohistochemistry, we found that Nodal expression in Grade 1 endometrial carcinomas is similar to that observed in the normal mid-proliferative endometrium (Fig.5A) prominent staining in the glandular epithelial tumour cells and moderate staining in the stroma. In Grade 2 and Grade 3 endometrial carcinomas, Nodal staining increased dramatically and was primarily localized to the tumour cells, although less prominent tumour stroma staining was also evident (Fig. 5B &5C).

As in the normal endometrium, Cripto co-localized with Nodal in the endometrial carcinomas (Fig. 5D-F). In Grade 1 carcinomas, moderate Cripto staining was observed in both the glandular epithelial tumour cells and the surrounding stroma (Fig. 5D). Cripto staining intensity increased in the transition from histologic Grade 1 to histologic Grades 2 and 3 carcinomas. Strikingly, the expression of the Nodal antagonist, Lefty A, was reduced in Grade 1 carcinomas (Fig. 5G) compared to late secretory endometrium (Fig. 3J). Moreover, Lefty expression was absent in Grade 2 and 3 carcinomas (Fig. 5H-I); suggesting that Nodal signalling in these tumours would be unregulated.

Nodal is secreted into the uterine lumen

As the majority of glandular derived products are secreted apically, we examined uterine lavages for the presence of Nodal. Western blot analysis of concentrated lavage fluid indicated that the 50 kDa Nodal precursor was present in samples from both normal cycling women and women with endometrial cancer (Fig. 6). The Nodal precursor has previously been shown to be the major secreted form of the protein [30].

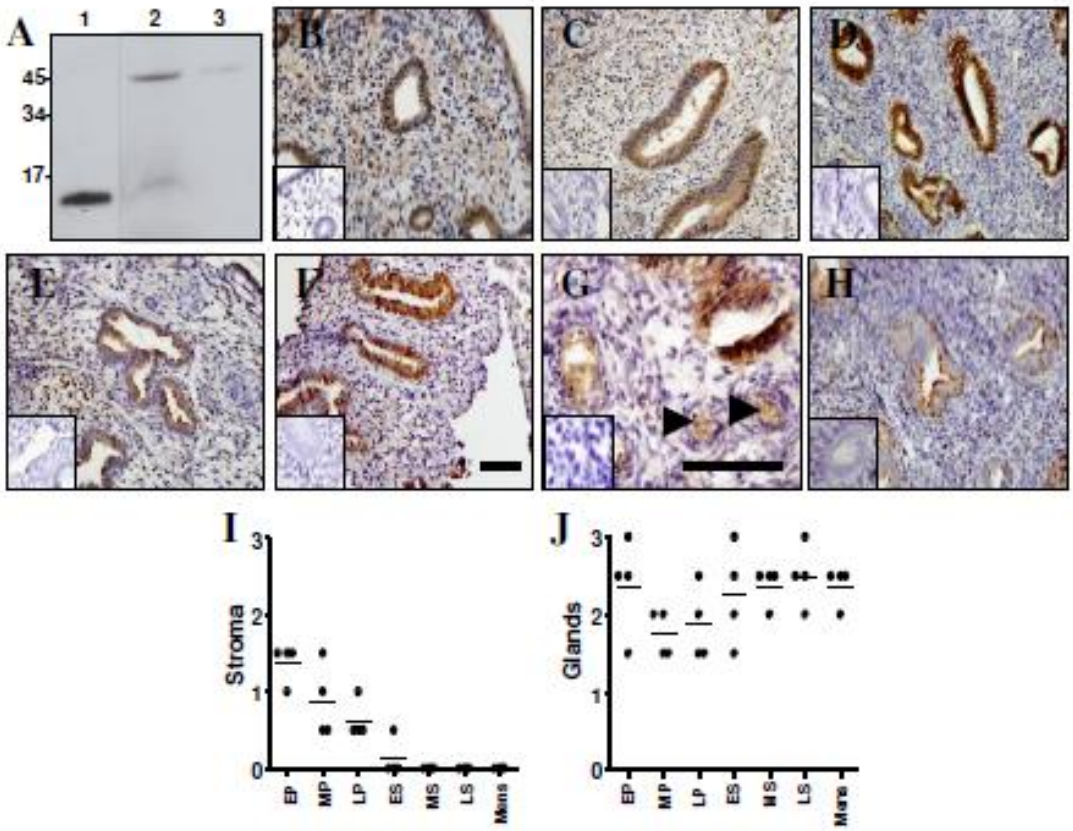

Figure 3

Immunohistochemical localization of Nodal in endometrium across the menstrual cycle. (A) Late secretory human endometrial tissue (*lanes 2 and 3*) was analysed by reducing SDS-PAGE and Western blot using a Nodal-specific antibody. A 13 kDa band representing mature Nodal monomer and a 40 kDa band representing Nodal precursor were detected in the absence of a blocking protein (*lane 2*). The inclusion of a blocking protein significantly reduced the intensity of the Nodal bands (*lane 3*). Recombinant Nodal (*lane 1*) was included as a positive control. The Nodal antibody was used to localize Nodal in early proliferative (B), late proliferative (C), early secretory (D & G), mid secretory (E) and menstrual phase (F) endometrium. Note the precipitous decrease in Nodal staining within the stromal compartment during the early/mid secretory phases. In menstrual tissue, Nodal expression coincided with the expression of its antagonist, Lefty (H). Negative controls for immunostaining by replacement of antisera with goat IgG at a matching concentration are shown in *insets*. *Arrowheads* (G) indicate specific Nodal staining in endothelial cells during the early secretory phase. *Bar*, 50 μm. Scale bar on (F) relates to panels (B-F & H), whereas scale bar on (G) relates to panel (G). Tissue sections were also scored according to Nodal staining intensity within endometrial stroma (I) and epithelial glands (J). Intensity of staining is shown as individual (filled circles) and mean scores (I & J).

indicated that the 50 kDa Nodal precursor was present in samples from both normal cycling women and women with endometrial cancer (Fig. 6). The Nodal precursor has previously been shown to be the major secreted form of the protein [30].

Discussion

The human endometrium is divided into two layers: the functionalis, which comprises the upper two-thirds, and the basalis, which remains during and following menstruation and is thought to be the origin of a new functionalis in the subsequent cycle [31]. The restructuring of the functional layer is critical to the development of a tissue ready for implantation or, in the

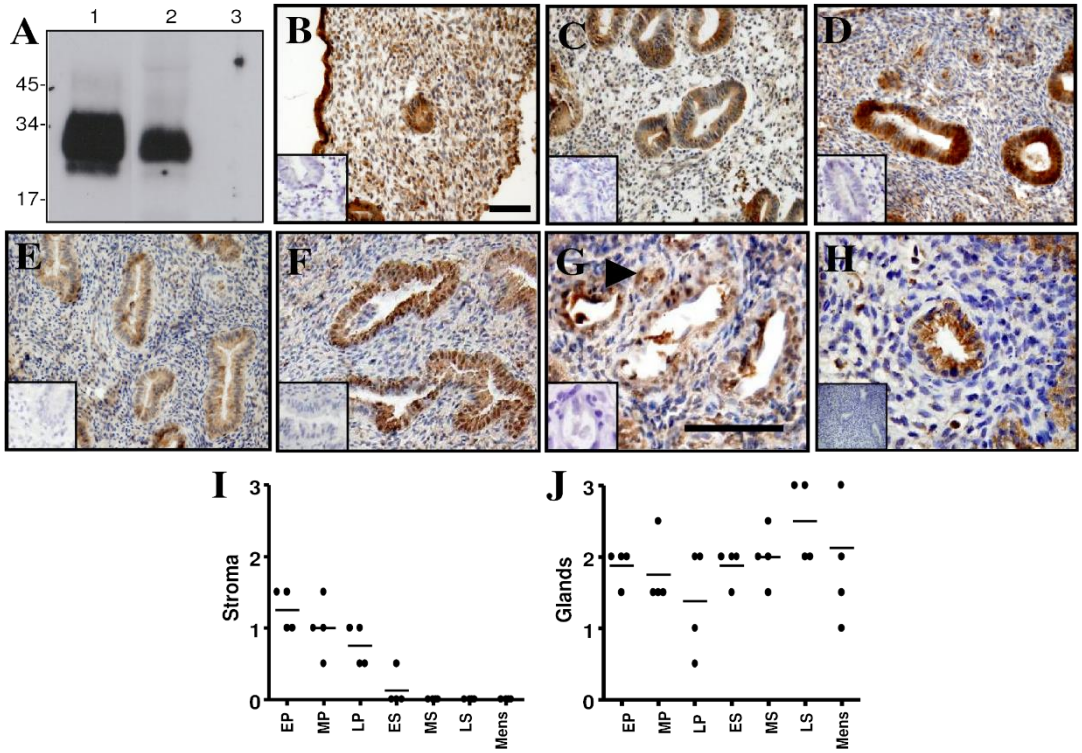

Figure 4

Immunohistochemical localization of Cripto in endometrium across the menstrual cycle. (A) Late secretory human endometrial tissue (*lanes 2 and 3*) was analysed by SDS-PAGE and Western blot using a Cripto-specific antibody. A 28 kDa band was detected in the absence (*lane 2*) but not the presence (*lane 3*) of a blocking protein. Recombinant Cripto (*lane 1*) was included as a positive control. The Cripto monoclonal antibody was used to localize Cripto in early proliferative (B), mid proliferative (C), early secretory (D), mid secretory (E & G) and menstrual phase (F) endometrium. Immunostaining for GRP78 in mid secretory endometrium (H) indicated that its expression coincided with that of its binding partner, Cripto. Negative controls for immunostaining by replacement of antisera with goat IgG at a matching concentration are shown in *insets*. *Arrowhead* (G) indicates specific Cripto staining in endothelial cells during the mid secretory phase. *Bar*, 50 μm. Scale bar on (B) relates to panels (B-F), whereas scale bar on (G) relates to panel (G & H). Tissue sections were also scored according to Cripto staining intensity within endometrial stroma (I) and epithelial glands (J). Intensity of staining is shown as individual (filled circles) and mean scores (H & I).

absence of a conceptus, for menstruation [32]. Endometrial repair and regeneration involves re-epithelialization (which occurs very rapidly even while menstruation is still in progress), angiogenesis and vessel remodeling, stromal and glandular epithelial cell proliferation, and extracellular matrix (ECM) deposition ([33]. Adult stem/progenitor cells likely underpin most aspects of this endometrial regeneration [31], however, the molecular and cellular mechanisms that mediate the regeneration process are still not well understood.

Given their established roles in wound healing, cell growth, ECM production and the maintenance of stem cell pluripotency [34-36], members of the TGF-β superfamily that signal via Smad2/3 (e.g. TGF-β1, TGF-β2, TGFβ3, activin A, activin B and Nodal)

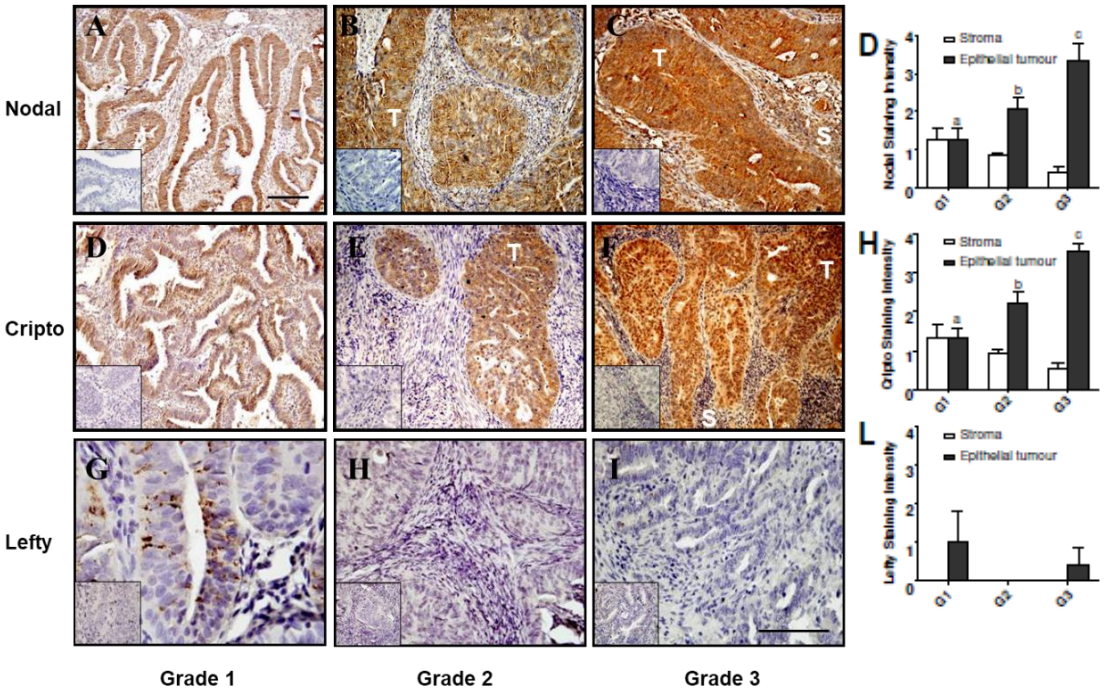

Figure 5

Representative histochemical localization of Nodal (A-C), Cripto (E-G) and Lefty (I-K) in endometrial carcinomas of Grade 1 (A, E, I), Grade 2 (B, F, J) and Grade 3 (C, G, K). Tumour-associated (*T*) Nodal and Cripto staining increased in intensity with increasing tumour grade, whereas stromal (*S*) staining remains relatively unchanged. Negative controls for immunostaining by replacement of antisera with goat IgG at a matching concentration are shown in *insets*. *Bar*, 50 μm. Scale bar on (A) relates to panels (A-C & E-G), whereas scale bar on (K) relates to panels (I-K). Tissue sections were also scored according to Nodal (D), Cripto (H) and Lefty (L) staining intensity within endometrial stroma and tumour epithelial cells. Intensity of staining is shown as mean ± SD.

are likely to be important mediators of endometrial repair and regeneration. Indeed, endometrial repair is retarded in the absence of activin A [37]. In this study, we showed that Nodal, as well as its co-receptor, Cripto, are co-expressed in human endometrial tissue throughout the menstrual cycle. Immunohistochemistry localized Nodal and Cripto primarily to stromal and epithelial cells, although moderate staining was also observed in endothelial cells associated with spiral arterioles. Nodal protein levels were maintained in the glandular and luminal epithelium at relatively steady-state levels across the cycle, however, stromal localization was primarily restricted to the proliferative and early secretory phases. Cripto displayed a similar spatiotemporal localization to Nodal within the endometrium, although the amount of Cripto detected in glandular epithelium increased significantly during the late secretory phase of the cycle.

To be responsive to Nodal, a cell must express activin type I and type II receptors, in addition to Cripto. Jones et al. [21] have shown that endometrial stromal cells express each of the activin receptor subtypes (ALK4, ActRII and ActRIIB) with highest expression during the early secretory phase. Potential functions of the Nodal signalling pathway within the endometrial stromal compartment can be extrapolated from its roles in embryogenesis [1]. In early development, Nodal acts as a graded morphogen, instructing stem cells to adopt specific cell fates concurrent with proliferation and migration [8]. Similar actions during the proliferative phase of the menstrual cycle would ensure Nodal plays a key role in endometrial restoration.

Interestingly, activin receptors are not present in either surface or glandular epithelium at any stage of the cycle [21], suggesting that Nodal expressed in these cells cannot

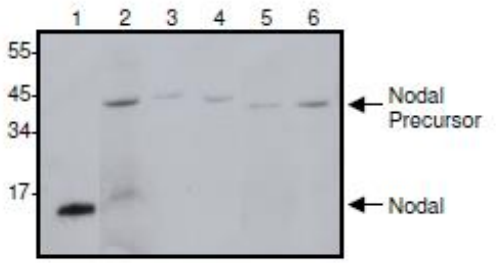

Figure 6
Nodal Expression in uterine lavages. Concentrated uterine lavage fluid from normal cycling women (*lanes 3 and* 4) or a woman with endometrial cancer (*lane* 5) was analysed by SDS-PAGE and Western blot using a Nodal-specific antibody. Recombinant Nodal (*lane 1*) and late secretory endometrial tissue (*lane 2*) were included as positive controls for the mature and precursor forms of Nodal, respectively. The size of molecular weight markers is indicated.

be functioning in a paracrine/autocrine manner. Indeed, as the majority of glandular derived products are secreted apically, it seemed likely that the endometrium must secrete Nodal into the uterine cavity. In support, we identified Nodal precursor in the uterine lavage fluid of both normal cycling women and women with endometrial carcinoma. Roles for endometrially derived Nodal could be similar to those proposed for activins, i.e. embryogenesis [38], steroidogenesis [39] and trophoblast differentiation [40]. In contrast to Nodal, Cripto within the epithelial compartment may be functional due to its ability to directly activate mitogen-activated protein kinase (MAPK) and phosphatidylinositol 3-kinase (PI3K)/Akt pathways via c-Src [9,41]. These actions of Cripto have led to its designation as a tumour growth factor and may be particularly relevant in endometrial carcinomas.

During embryogenesis, members of the Lefty subclass of TGF-β proteins act as extracellular antagonists of the Nodal signalling pathway [17]. Lefty blocks the formation of the Nodal receptor complex by binding to Nodal directly [17] or by interacting with Cripto [5]. Lefty expression is absolutely dependent upon Nodal function and within the embryo and developing tissues, such as the pancreas [10], the juxtaposition of these two factors limits their respective range of influence. It is interesting, therefore, that Nodal and Lefty have spatially and temporally distinct patterns of expression within the endometrium. The lack of Lefty expression in the proliferative phase of the menstrual cycle would ensure that the morphogenic actions of Nodal were not restricted at this time. In contrast, co-localization of Nodal, Cripto and Lefty within glandular and luminal epithelial cells during the late secretory and menstrual phases suggests that, at these times, Nodal signalling requires strict control. Indeed, the recently identified role for Lefty as a key local regulator of focal ECM breakdown in the cycling human endometrium [15] may derive from its ability to antagonise Nodal signalling.

Finally, recent studies have shown that expression of Nodal in metastatic melanomas and breast carcinomas is correlated with cancer progression, whereas pathway inhibition decreases cell invasiveness, colony formation and tumourigenicity [11,12]. These findings are consistent with the upregulation of Cripto that is observed in many epithelial cancers [41,42], and with the ability of Cripto to initiate several aspects of tumour progression, including increased proliferation, migration, invasion, angiogenesis, and epithelial-to-mesenchymal transition [29]. In the current study, we showed that Nodal and Cripto are expressed in normal endometrium and that their expression is dramatically upregulated in endometrial carcinomas.

Conclusion

The expression of Nodal in normal and malignant endometrial cells that lack Lefty strongly supports an important role for this embryonic morphogen in the tissue remodelling events that occur across the menstrual cycle and in tumourigenesis. In addition, these findings identify Nodal and Cripto as diagnostic markers of endometrial cancer progression and, potentially, as molecular targets for the treatment of these aggressive tumours.

List of abbreviations

TGFβ: transforming growth factor-beta; ALK4: activin type I receptor; ActRII: activin type II receptor; GRP78: glucoseregulated protein 78; ECM: extracellular matrix.

Competing interests

The authors declare that they have no competing interests.

Authors' contributions

IP participated in the immunohistochemistry and PCR studies and helped draft the manuscript. PN participated in the immunohistochemistry studies. FW participated in the PCR studies. ML produced the Cripto monoclonal antibodies. YM helped draft the manuscript and performed the statistical analysis. LS provided endometrial tissues and intellectual input. DR participated in the studies design. CH conceived of the study, and participated in its design and coordination and helped to draft the manuscript. All authors read and approved the final manuscript.

Acknowledgements

The authors would like to thank Dr Eva Dimitriadis, Dr Natalie Hannan and Dr Premila Paiva for assistance with immunohistochemistry; Professor Tony Burgess, Assoc. Professor Ed Nice and Dr Jenny Catimel for providing

References

1. Shen MM: **Nodal signaling: developmental roles and regulation.** *Development* 2007, **134(6):**1023-1034.
2. Harrison CA, Gray PC, Koerber SC, Fischer W, Vale W: **Identification of a functional binding site for activin on the type I receptor ALK4.** *J Biol Chem* 2003, **278(23):**21129-21135.
3. Kelber JA, Shani G, Booker EC, Vale WW, Gray PC: **Cripto is a noncompetitive activin antagonist that forms analogous signaling complexes with activin and nodal.** *J Biol Chem* 2008, **283(8):**4490-4500.
4. Gray PC, Harrison CA, Vale W: **Cripto forms a complex with activin and type II activin receptors and can block activin signaling.** *Proc Natl Acad Sci USA* 2003, **100(9):**5193-5198.
5. Cheng SK, Olale F, Brivanlou AH, Schier AF: **Lefty blocks a subset of TGFbeta signals by antagonizing EGF-CFC coreceptors.** *PLoS Biol* 2004, **2(2):**E30.
6. Brennan J, Lu CC, Norris DP, Rodriguez TA, Beddington RS, Robertson EJ: **Nodal signalling in the epiblast patterns the early mouse embryo.** *Nature* 2001, **411(6840):**965-969.
7. Schier AF, Shen MM: **Nodal signalling in vertebrate development.** *Nature* 2000, **403(6768):**385-389.
8. Kenney NJ, Adkins HB, Sanicola M: **Nodal and Cripto-1: embryonic pattern formation genes involved in mammary gland development and tumorigenesis.** *J Mammary Gland Biol Neoplasia* 2004, **9(2):**133-144.
9. Bianco C, Adkins HB, Wechselberger C, Seno M, Normanno N, De Luca A, Sun Y, Khan N, Kenney N, Ebert A, Williams KP, Sanicola M, Salomon DS: **Cripto-1 activates nodal- and ALK4-dependent and -independent signaling pathways in mammary epithelial Cells.** *Mol Cell Biol* 2002, **22(8):**2586-2597.
10. Zhang YQ, Sterling L, Stotland A, Hua H, Kritzik M, Sarvetnick N: **Nodal and lefty signaling regulates the growth of pancreatic cells.** *Dev Dyn* 2008, **237(5):**1255-1267.
11. Postovit LM, Margaryan NV, Seftor EA, Hendrix MJ: **Role of nodal signaling and the microenvironment underlying melanoma plasticity.** *Pigment Cell Melanoma Res* 2008, **21(3):**348-357.
12. Topczewska JM, Postovit LM, Margaryan NV, Sam A, Hess AR, Wheaton WW, Nickoloff BJ, Topczewski J, Hendrix MJ: **Embryonic and tumorigenic pathways converge via Nodal signaling: role in melanoma aggressiveness.** *Nat Med* 2006, **12(8):**925-932.
13. Tabibzadeh S, Lessey B, Satyaswaroop PG: **Temporal and site-specific expression of transforming growth factor-beta4 in human endometrium.** *Mol Hum Reprod* 1998, **4(6):**595-602.
14. Tabibzadeh S, Mason JM, Shea W, Cai Y, Murray MJ, Lessey B: **Dysregulated expression of ebaf, a novel molecular defect in the endometria of patients with infertility.** *J Clin Endocrinol Metab* 2000, **85(7):**2526-2536.
15. Cornet PB, Galant C, Eeckhout Y, Courtoy PJ, Marbaix E, Henriet P: **Regulation of matrix metalloproteinase-9/gelatinase B expression and activation by ovarian steroids and LEFTY-A/ endometrial bleeding-associated factor in the human endometrium.** *J Clin Endocrinol Metab* 2005, **90(2):**1001-1011.
16. Tang M, Taylor HS, Tabibzadeh S: **In vivo gene transfer of lefty leads to implantation failure in mice.** *Hum Reprod* 2005, **20(7):**1772-1778.
17. Chen C, Shen MM: **Two modes by which Lefty proteins inhibit nodal signaling.** *Curr Biol* 2004, **14(7):**618-624.
18. Torres PB, Florio P, Galleri L, Reis FM, Borges LE, Petraglia F: **Activin A, activin receptor type II, nodal, and cripto mRNA are expressed by eutopic and ectopic endometrium in women with ovarian endometriosis.** *Reprod Sci* 2009, **16(8):**727-733.
19. Noyes RW, Hertig AT, Rock J: **Dating the endometrial biopsy.** *Fertil Steril* 1950, **1:**3-25.
20. Paiva P, Van Damme MP, Tellbach M, Jones RL, Jobling T, Salamonsen LA: **Expression patterns of hyaluronan, hyaluronan synthases and hyaluronidases indicate a role for hyaluronan in the progression of endometrial cancer.** *Gynecol Oncol* 2005, **98(2):**193-202.
21. Jones RL, Salamonsen LA, Zhao YC, Ethier JF, Drummond AE, Findlay JK: **Expression of activin receptors, follistatin and betaglycan by human endometrial stromal cells; consistent with a role for activins during decidualization.** *Mol Hum Reprod* 2002, **8(4):**363-374.
22. Besser D: **Expression of nodal, lefty-a, and lefty-B in undifferentiated human embryonic stem cells requires activation of Smad2/3.** *J Biol Chem* 2004, **279(43):**45076-45084.
23. Livak KJ, Schmittgen TD: **Analysis of relative gene expression data using real-time quantitative PCR and the 2(-Delta Delta C(T)) Method.** *Methods* 2001, **25(4):**402-408.
24. Lachance C, Bailey JL, Leclerc P: **Expression of Hsp60 and Grp78 in the human endometrium and oviduct, and their effect on sperm functions.** *Hum Reprod* 2007, **22(10):**2606-2614.
25. Tang M, Mikhailik A, Pauli I, Giudice LC, Fazelabas AT, Tulac S, Carson DD, Kaufman DG, Barbier C, Creemers JW, Tabibzadeh S: **Decidual differentiation of stromal cells promotes Proprotein Convertase 5/6 expression and lefty processing.** *Endocrinology* 2005, **146(12):**5313-5320.
26. Hannan NJ, Stoikos CJ, Stephens AN, Salamonsen LA: **Depletion of high-abundance serum proteins from human uterine lavages enhances detection of lower-abundance proteins.** *J Proteome Res* 2009, **8(2):**1099-1103.
27. Stoikos CJ, Harrison CA, Salamonsen LA, Dimitriadis E: **A distinct cohort of the TGFbeta superfamily members expressed in human endometrium regulate decidualization.** *Hum Reprod* 2008, **23(6):**1447-1456.
28. Kelber JA, Panopoulos AD, Shani G, Booker EC, Belmonte JC, Vale WW, Gray PC: **Blockade of Cripto binding to cell surface GRP78 inhibits oncogenic Cripto signaling via MAPK/PI3K and Smad2/3 pathways.** *Oncogene* 2009, **28(24):**2324-2336.
29. Shani G, Fischer WH, Justice NJ, Kelber JA, Vale W, Gray PC: **GRP78 and Cripto form a complex at the cell surface and collaborate to inhibit transforming**

growth factor beta signaling and enhance cell growth. *Mol Cell Biol* 2008, **28(2):**666-677.
30. Constam DB, Robertson EJ: **Regulation of bone morphogenetic protein activity by pro domains and proprotein convertases.** *J Cell Biol* 1999, **144(1):**139-149.
31. Gargett CE, Chan RW, Schwab KE: **Hormone and growth factor signaling in endometrial renewal: role of stem/progenitor cells.** *Mol Cell Endocrinol* 2008, **288(1-2):**22-29.
32. Maruyama T, Yoshimura Y: **Molecular and cellular mechanisms for differentiation and regeneration of the uterine endometrium.** *Endocr J* 2008, **55(5):**795-810.
33. Salamonsen LA: **Tissue injury and repair in the female human reproductive tract.** *Reproduction* 2003, **125(3):**301-311.
34. Derynck R, Akhurst RJ, Balmain A: **TGF-beta signaling in tumor suppression and cancer progression.** *Nat Genet* 2001, **29(2):**117-129.
35. Gordon KJ, Blobe GC: **Role of transforming growth factor-beta superfamily signaling pathways in human disease.** *Biochim Biophys Acta* 2008, **1782(4):**197-228.
36. Young GD, Murphy-Ullrich JE: **Molecular interactions that confer latency to transforming growth factor-beta.** *J Biol Chem* 2004, **279(36):**38032-38039.
37. Kaitu'u-Lino TJ, Phillips DJ, Morison NB, Salamonsen LA: **A new role for activin in endometrial repair after menses.** *Endocrinology* 2009, **150(4):**1904-1911.
38. He ZY, Liu HC, Mele CA, Barmat L, Veeck LL, Davis O, Rosenwaks Z: **Expression of inhibin/activin subunits and their receptors and binding proteins in human preimplantation embryos.** *J Assist Reprod Genet* 1999, **16(2):**73-80.
39. Ni X, Luo S, Minegishi T, Peng C: **Activin A in JEG-3 cells: potential role as an autocrine regulator of steroidogenesis in humans.** *Biol Reprod* 2000, **62(5):**1224-1230.
40. Caniggia I, Lye SJ, Cross JC: **Activin is a local regulator of human cytotrophoblast cell differentiation.** *Endocrinology* 1997, **138(9):**3976-3986.
41. Strizzi L, Bianco C, Normanno N, Salomon D: **Cripto-1: a multifunctional modulator during embryogenesis and oncogenesis.** *Oncogene* 2005, **24(37):**5731-5741.
42. Ayhan A, Tuncer ZS, Ruacan S, Yasui W, Tahara E: **Abnormal expression of cripto and p53 protein in endometrial carcinoma and its precursor lesions.** *Eur J Gynaecol Oncol* 1998, **19(3):**316-318.

Chapter 3

Monoclonal Antibody Treatment Targeting Nodal Signalling Reverses Cancer Cell Tumourigenesis

"True knowledge exists in knowing that you know nothing"

-Socrates

Chapter 3

3.1 Declaration

In the case of Chapter 3, my contribution to the work involved the following:

Thesis Chapter	Publication Title	Status	Nature and % of student contribution	Co-author name(s) Nature and % of Co-author's contribution*	Co-author(s), Monash student
3	*Monoclonal Antibody Treatment Targeting Nodal Signalling Reverses Cancer Cell Tumourigenesis*	*Prepared for submission*	Involved in project conception, design, performed experiments, as well as data analysis and prepared the manuscript. **93%**	1) Martin Lackmann: provided the Cripto monoclonal antibodies. **2%** 2) David M. Robertson involved in the project design and intellectual input. **1%** 3) Craig A. Harrison: involved in project conception, provided intellectual input. **4%**	**No**

Student signature: [redacted] **Date:** 23/08/2018

The undersigned hereby certify that the above declaration correctly reflects the nature and extent of the student's and co-authors' contributions to this work. In instances where I am not the responsible author I have consulted with the responsible author to agree on the respective contributions of the authors.

Main Supervisor signature: [redacted] **Date:** 23/08/2018

Monoclonal Antibody Treatment Targeting Nodal Signalling Reverses Cancer Cell Tumourigenesis – Manuscript

Irene Papageorgiou, *[1 2] Martin Lackmann,[3] Craig A. Harrison,[4] David M. Robertson,[5]

1. Centre for Innate Immunity and Infectious Diseases, Hudson Institute of Medical Research, Clayton, 3168, Victoria, Australia;

2. Department of Molecular and Translational Science, Monash University, Clayton, Victoria, 3168, Australia;

3. Cancer Program, Monash Biomedicine Discovery Institute and Department of Biochemistry and Molecular Biology, Monash University, Clayton, Victoria 3800, Australia;

4. Monash Biomedicine Discovery Institute and Department of Physiology, Monash University, Clayton, Victoria 3800, Australia;

5. Centre for Endocrinology and Metabolism, Hudson Institute of Medical Research, Clayton, Victoria, Australia;

* To whom correspondence should be addressed

Postal: Centre for Innate Immunity and Infectious Diseases, Hudson Institute of Medical Research, 27-31 Wright Street, Clayton, VIC 3168, Australia

Email: irene.papageorgiou@hudson.org.au

Abstract

Background: Nodal, a member of the TGF-β superfamily, plays essential roles in early embryonic development. In concert with its co-receptor Cripto, Nodal signals via the Smad 2/3 pathway. Although Nodal and Cripto are rarely expressed in most normal adult tissues (with the exception of reproductive tissues), previous studies implicate re-emerge in tumourigenesis. It is thus hypothesised that dysregulated Nodal signalling is associated with the pathogenesis of cancer. This study aims to evaluate the effects of Nodal signalling blockade in cancer cells using anti-Cripto MAbs.

Methods and Results: Assessment of anti-Cripto MAbs to specifically block Nodal signalling was validated in a Nodal-responsive luciferase bio-functional assay. This assay identified 6E10 and 3D1 as potent inhibitors of Nodal signalling. The *in vitro* biological effects of 6E10 on cancer cell growth and migration were also investigated by performing CyQuant proliferation assays, and wound healing assays, in NTERA 2-D1 (testicular teratocarcinoma), PC-3 and LNCaP (both prostate cancer) cancer cells. Interestingly, 6E10 significantly suppressed cancer cell growth and migration of *NODAL*$^{+}$*/CRIPTO*$^{+}$ expressing NTERA 2-D1, LNCaP and PC-3 cells. Finally, we monitored the effects of 6E10 on down-stream Nodal cascade, Smad 2/3 phosphorylation by Western blot of NTERA 2-D1 cells. We observed that 6E10 Mab effectively obliterated Smad 2/3 phosphorylation of testicular teratocarcinoma, NTERA 2-D1 cells.

Conclusions: 6E10 Cripto monoclonal antibody effectively blocks Nodal signalling and suppresses cancer cell growth and migration. Our findings suggest that dysregulated Nodal signalling is implicated in the development and progression of cancer and involves transduction of the Smad 2/3 TGF-β axis. Subsequently Nodal may be a promising target for therapeutic interventions in metastatic malignancy.

Introduction

It has become apparent that critical proteins known to play important roles in embryonic development are also associated with tumourigenesis and cancer progression. Hence it could be considered that oncogenic progression recapitulates embryogenesis in a dysregulated manner (1, 2). Embryonic morphogen Nodal belongs to the TGF-β (transforming growth factor-beta) superfamily. It is expressed in a highly restricted pattern during embryogenesis and exhibits essential functions in early embryonic development (3, 4). Although Nodal is rarely expressed in adult cells (except for regenerative tissues or embryonic stem cells) aberrant re-activation of Nodal has been extensively documented to accompany tumourigenesis (5-7).

Essential for Nodal signalling is co-receptor Cripto, a GPI (glycosylphosphatidylinositol)-linked membrane protein (8). Cripto or TDGF-1 (teratoma-derived growth factor 1), is a member of the EGF-CFC family of growth factors and is also an essential regulator of embryonic development (9, 10). Cripto expression, similarly to Nodal, is also restricted to embryogenic tissue, or regenerative adult tissue (9). The re-emergence of Cripto in normal adult cells accompanies pathological malignancy.

Nodal signals via the canonical TGF-β pathway, by interaction with hetero-multimeric complexes formed with co-receptor Cripto (EGF-like domain), activin type I (ALK4) and type II (ActRIIA/ActRIIB) serine-threonine kinase receptors (11). Phosphorylation of ALK4 within this complex, initiates signalling via Smad 2/3 signal transducers, triggering association with Smad4 and translocation to the nucleus (12, 13). Within the nucleus the active Smad complexes interact with Fox H1 (or mixer transcription factors) and the transcriptional co-activator complex mediator, leading to transcriptional activation of target genes (11, 14). Nodal signalling antagonist, Lefty blocks Nodal/TGF-β signalling by competing for access to the ligand binding site of Cripto (15, 16). Whereas TGF-β

antagonist, Cerberus binds directly to Nodal and prevents downstream signalling (17, 18).

Cripto mediated Nodal signalling is tightly regulated during embryogenesis to orchestrate pleotropic fundamental cellular processes including differentiation, proliferation, remodelling, self-renewal, plasticity, pluripotency, epithelial-to-mesenchymal transition, wound repair, migration, invasion, angiogenesis, morphogenesis, and organogenesis (3, 4, 9, 10, 19-24). Although expression and signalling of both Nodal and Cripto ceases in non-embryonic or non-regenerative adult cells, a growing body of evidence suggests that aberrant re-emergence of these morphogens coincides with cancer development and progression. Upregulation of either Nodal or Cripto has been reported in a different cancer types, such as: melanoma, colon, brain, breast, lung, hepatic, pancreatic, prostate, testicular, oesophageal, oral squamous cell carcinoma (5, 25-37).

We previously described the cyclical expression of Cripto and Nodal within normal human endometrial tissue coinciding with remodelling events of menstrual cycle, especially during the proliferative phase (38). More importantly, immunohistochemical studies of human endometrial cancer tissues revealed co-localisation of Nodal and Cripto in glands, stroma and to a greater extent in epithelial tumour cells. It was clearly observed that Nodal and Cripto staining intensities increased dramatically in the transition from Grade 1 to Grades 2 and 3 within the epithelial tumour, with absence or low expression of TGF-β antagonist Lefty, in line with former studies of melanoma progression (7). These results further suggest that dysregulated Nodal signalling may facilitate endometrial cancer pathogenesis and aggressiveness (7).

Even though, dysregulated Nodal signalling has become increasingly important in oncogenic processes, the specific underlying molecular mechanisms have not been fully

investigated. To shed some light in this area a panel of anti-Cripto MAbs were utilized to specifically block Nodal signalling by binding to Cripto co-receptor. Functional characterization of the MAb panel identified 3D1 and 6E10 as neutralising antibodies, using a Nodal bio-functional assay. We further employed 6E10 MAb to examine the effects of Nodal signalling blockade on cancer cell behaviour. Strikingly, 6E10 treatment significantly suppressed cell proliferation and migration of highly aggressive cancer cell line models, dependent upon the *PC-3*-expression status. More importantly we report that *in vitro* blockade of Nodal signalling, by 6E10 antibody treatment obliterated Smad 2/3 phosphorylation levels. We thus postulated that the anti-tumour properties exhibited by 6E10 anti-Cripto MAb, are mediated via the Smad 2/3 TGF-β axis pathway blockade.

Methods

Tissue Culture

All cells in tissue culture were propagated in complete media (Gibco, Life Technologies) as denoted below in table 1 specific for each cell line, under a sterile environment and incubated at 37°C at 5% $C0_2$ (for general tissue culture procedures refer to Appendix C, p263-264). HEK 293 CHO-Cripto, MCF-7, C8161, MUM-2C cell lines were generously provided by Associate Professor Martin Lackmann, (Cancer Program, Monash Biomedicine Discovery Institute and Department of Biochemistry and Molecular Biology, Monash University, Clayton, Victoria, Australia). NTERA 2-D1 testicular teratocarcinoma cells were kindly provide by Mrs Janelle Ryan, (Sex Determination and Gonadal Development Research Group, Hudson Institute for Medical Research). LNCaP, PC-3, DU 145, prostate cancer cells generously supplied by Dr Birunthi Niranjan, (Prostate Cancer Research Group, Monash Institute of Medical Research Clayton, Victoria). HEK 293, LIM 1215, LIM 1863, SW 480 colon cancer cells were a kind gift from Dr

Francesca Walker (Professor Antony Burgess Epithelial Cancer laboratory, Ludwig Institute for Cancer Research, Royal Melbourne Hospital, Parkville, Victoria, Australia). Finally, KGN and COV 434 ovarian granulosa cells were supplied by PHI (Prince Henry's Institute of Medical Research, Clayton, Vic, Australia). CHO-Cripto where generated by our collaborator Associate Professor Martin Lackmann by cloning of Cripto cDNA into expression vector pEF-BOS and incorporation of in frame IL3 signal and FLAG tag sequences to facilitate in subsequent secretion, and purification of recombinant Cripto. The mammalian expression system of CHO-K1 cells, deficient in dehydrofolate reductase (DHFR) gene, was utilized. The cDNA was subsequently inserted into CHO-K1 cell expression vector containing DHFR gene. Stable CHO-Cripto transfected cells were propagated in the presence of methotrexate, allowing for selection of cells containing high copy numbers of the transfected vector containing both Cripto and DHFR cDNA (Sigma Aldrich, MERK). Mycoplasma testing of all cell lines was frequently performed by the Laboratory and Technical Services at PHI or Hudson Institute for Medical Research using MycoAlert PLUS Mycoplasma Detection Kit (Lonza).

Table 1. Cell Line Subcultivation Properties

Cell line name	***Cell type***	***Complete media***	***References***
HEK 293 (ATCC® CRL-1573™)	Human embryonic kidney cells; immortalized by adenovirus type 5	MEM, 10 % FCS, 1 % P/S	(39)
CHO-Cripto	The CHO-K1 (Chinese hamster ovary); cell line cloned to stably express Cripto	DMEM, 10 % FCS, 10^{-8} methotrexate, 1 % P/S	(40, 41)

NTERA2-D1 (ATCC® CRL-1973™)	Human secondary testicular teratocarcinoma; (pluripotent embryonal carcinoma); derived from lung	DMEM/F12, 10 % FCS, 1 % P/S	(42, 43)
KGN	Human ovarian granulosa tumour	DMEM/F12, 10 % FCS, 1 % P/S	(44)
COV 434	Human ovarian granulosa primary tumour	DMEM/F12, 10 % FCS, 1 % P/S	(45)
MCF-7 (ATCC® HTB-22™)	Human breast adenocarcinoma; derived from pleural effusion	DMEM/F12, 10 % FCS, 1 % P/S	(46)
LNCaP (ATCC® CRL-1740™)	Human secondary prostate carcinoma; derived from left supraclavicular lymph node	DMEM/F12, 10 % FCS, 1 % P/S	(47)
PC-3 (ATCC® CRL-1435™)	Human secondary prostate grade IV adenocarcinoma; derived from bone	DMEM/F12, 10 % FCS, 1 % P/S	(48)
DU 145 (ATCC® HTB-81™)	Human secondary prostate carcinoma; derived from brain lesion	DMEM/F12, 10 % FCS, 1 % P/S	(49)
C8161	Cutaneous melanoma; derived from abdominal wall	RPMI 1640, 25 mM Hepes, 10 % FCS, 1 % P/S	(50)
MUM-2C	Human uveal melanoma; derived from liver	RPMI 1640, 25 mM Hepes, 10 % FCS, 1 % P/S	(51)

LIM 1215	Secondary human colon carcinoma; derived from omentum	RPMI 1640, 25 mM Hepes, 10 % FCS, 1 mg/ml hydrocortisone, 0.01 mg/ml thyoglycerol, 0.025 U/ml insulin, 1% P/S	(52)
LIM 1863	Human colon carcinoma; derived from ileocecal valve	RPMI 1640, 25mM Hepes, 10% FCS, 1 mg/ml hydrocortisone, 0.01 mg/ml thyoglycerol, 0.025 U/ml insulin, 1% P/S	(53)
SW 480 (ATCC® CCL-227™)	Human primary colorectal adenocarcinoma	RPMI 1640, 25mM Hepes, 10% FCS, 1 mg/ml hydrocortisone, 0.01 mg/ml thyoglycerol, 0.025 U/ml insulin, 1% P/S	(54)

Nodal Signalling Pathway Inhibitors, Anti-Cripto MAbs and Other Reagents

To examine the *in vitro* effects of Nodal blockade, a panel of anti-Cripto MAbs generated and supplied by our collaborator Associate Professor Martin Lackmann, was employed in functional cell assays. Recombinant Cripto protein purified (by SE-HPLC) from CHO-Cripto transfected cells was used for the immunization of mice. Spleen cells of Balb/C mice mounting an immune response against r-Cripto, were used to generate antibody producing hybridoma cells. Binding of anti-Cripto MAbs, 6E10, 4G4, 3D1, 1C3 was analysed by: ELISA, Biacore, Western Blot and Immunohistochemistry (41). In the

current study we used these MAbs [7.4 mg/ml 6E10, 6.9 mg/ml 4G4, 1.12 mg/ml 3D1, 2.2 mg/ml 1C3)] to examine effects on cancer cell biology. All anti-Cripto MAbs were stored in PBS solution and the vehicle control used for functional assays was PBS equivalent to the highest MAb dosage concentration. In addition, SB-431542 (100 mM in DMSO) was used as pharmacological TGF-β type I receptor (ALK4, ALK5, ALK7) kinase activity inhibitor, (TOCRIS Bioscience) and compared to vehicle control of DMSO at equivalent concentration.

Cripto Protein Detection by Western Blot Analysis

Protein Extraction

Protein extractions of whole cell lysates and conditioned media derived from NTERA 2-D1, CHO-Cripto, MUM-2C, C8161 cells were subjected to Immunoprecipitation (IP) and Western blot analysis. Conditioned media was collected from cells cultured in reduced serum media, with OPTI-MEM (Gibco, Life Technologies). Cells were lysed on ice in RIPA buffer (50 mM Tris-HCL pH 7.4, 1% NP-40, 0.25% sodium-deoxycholate, 150 nM NaCL) containing 1 x protease inhibitor cocktail (Roche Applied Science). Following homogenisation with a 23G needle syringe the samples were centrifuged at 13,000 x g for 15 mins at 4°C, the pellet was discarded, and the extracted protein supernatant was collected.

Immunoprecipitation

6E10 (74 µg/ml) monoclonal antibody was added to extracted protein samples for 24 hrs, with rotation at 4°C. 10 µl of protein G sepharose slurry (50%) (GE Healthcare) was added to the protein preparations and incubated for 24 hrs with rotation at 4°C. Samples were then centrifuged at 11,000 x g for 5 mins, at 4°C and the supernatant was

discarded. The samples were boiled in 2 x SDS-PAGE loading buffer (4% SDS, 10% β-mercaptoethanol, 20% glycerol, 0.004% bromophenol blue, 0.125 M Tris-HCL) at 95°C for 5 mins and the eluted protein was collected by centrifugation at 11,000 x g, 5 mins at room temperature. The remaining G-Sepharose beads were further heated at at 95°C with deionized H_20 for 5 mins followed by centrifugation (at 11,000 x g for 5 mins). The supernatant protein was then centrifuged and combined with the eluted protein sample.

Western Blotting

30 µl of protein extract was denatured at 95°C for 5 mins with 1% DTT (Sigma Aldrich, Merk) and electrophoresed on 12% SDS/polyacrylamide gels (refer to Appendix A, p 258-260). Recombinant Cripto protein purified by SE-HPLC from stable CHO-Cripto transfected cells, was concurrently run as internal positive Cripto standard (generated and supplied by our collaborator Associate Professor Martin Lackmann). Protein was then electroblotted onto PVDF membrane (Immobilin-P, Millipore) and blocked with 5% BSA in TTBS (Tris-buffered saline containing 0.05% Tween-20) for 1 hr. The membranes were incubated overnight at 4°C with 4G4 anti-human Cripto MAb (3.45 µg/ml) in 1% BSA/TTBS. Following washing, the membranes were then probed with 1:2000 diluted anti-Mouse IgG, peroxidase-linked species-specific whole antibody (from sheep), (GE Healthcare Life Sciences) for 1 hr at room temperature. After three washes, the membranes were developed using the ECL Western blotting detection reagents and analysis system according to the manufacturer's instructions (Amersham Biosciences). The membranes were then exposed to HyperfilmTM ECL film (GE Healthcare Life Sciences) and developed using AGFA CP1000 automated developer.

Detection of Cripto and Nodal mRNA Expression in Cancer Cell Line Panel

mRNA Extraction

Total RNA was extracted from cultured cells using the RNeasy Mini Kit (Qiagen) according to the manufacturer's instructions. Cells were lysed in 600 µl of β-mercaptoethanol / buffer RLT and homogenized by syringing up and down through a 25-gauge needle. 600 µl of 70% ethanol was added to the lysate, thoroughly mixed, and transferred to a RNeasy spin column. The sample was centrifuged for 15 secs at 8,000 x g (Microfuge) and the flow through discarded. The column was washed with 700 µl buffer RW1 and centrifuged for 15 secs at 8,000 x g (Microfuge) and the flow through discarded. The column was washed with 500 µl of buffer RPE, centrifuged for 15 secs at 8,000 x g (Microfuge) and the flow through was discarded. An additional 500 µl of buffer RPE was added, centrifuged for 2 mins at 8,000 x g (Microfuge) and the flow through was discarded. The column was then transferred to a fresh 2 ml collection tube and centrifuged for 1 min, at 8,000 x g (Microfuge). RNA was eluted by addition of 30 µl RNase-free water to the column and centrifugation for 1 min at 8,000 x g (Microfuge). The total RNA extracts were snap frozen and stored at -80^{o}C.

DNase Treatment

Extracted RNA was subjected to DNAse treatment using Ambion DNA-free Kit, DNase treatment (Applied Biosystems) following to the manufacturer's directions. 3 µl of 10 x DNase buffer as well as 1 µl of DNase were added to 30 µl of RNA, mixed and incubated for 30 mins at 37°C. 5 µl of Slurry was incorporated to the RNA sample and incubated at room temperature for 2 mins and centrifuged for 1 min, at 8,000 x g (Microfuge). The supernatant containing DNase treated RNA was collected.

RNA Quantification

RNA yield and quality assessments were carried out using the ultraviolet spectrophotometer (BioPhotometer, Eppendorf). 100 µl of diluted RNA (1:100 dilution ratio in RNase-free water, Qiagen) were added into a plastic cuvette and measured the absorbance. Absorbance reading of >1.82 was considered to indicate a pure sample of total RNA. Alternatively, the NanoDrop, ND-1000 spectrophotometer (Analytical Technologies) was also use for RNA quantification. The instrument was washed with deionised Milli-Q water and calibrated using 1µl of RNase-free water (Qiagen). Concentration and purity of RNA were determined by loading 1µl of sample and measuring absorbance of 260 nm/280 nm and 260 nm/230 nm. Absorbance ratios close to 2 for 260 nm /280 nm and between 2.0-2.2 for 260 nm/230 nm, were considered as acceptable RNA quality for cDNA synthesis.

cDNA Synthesis

First strand DNA was generated from 500 ng RNA using SuperScript™ II Reverse Transcriptase (Invitrogen Life Technologies, Thermo Fisher Scientific) as per manufacturer's recommendations. In brief, 500 ng mRNA were combined with 1 µl (250 ng/µl) random primers, 1 µl (10 mM) dNTP mix and total reaction volume was adjusted to 13 µl with Nuclease-Free Water (Ambion). The reaction was heated to 65°C for 5 mins, chilled on ice and briefly centrifuged (Microfuge) prior to addition of 1 µl (5x) first strand buffer, 1 µl (0.1M) DTT, 1 µl (40 units/µl) RNase out, 1 µL (200 units) SuperScript™ II RT Superscript. The mixture was subsequently incubated at 25°C, 5 mins and 50°C, 60 mins followed by inactivation at 70°C, 15 mins. Finally, single stranded cDNA was chilled on ice for 2 mins and stored at -20°C.

PCR

To monitor *NODAL* and *CRIPTO* (*TDGF-1*), mRNA expression in cancer cells, Platinum® Taq DNA Polymerase kit (Invitrogen Life Technologies, Thermo Fisher Scientific) was utilized in PCR amplification, and *B-ACTIN* was included as a housekeeping gene. For each reaction, 2 µl of cDNA was combined with 5 µl (10x) PCR buffer, 1.5 µl (50 mM) $MgCl_2$, 1 µl (10 mM) dNTP Mix, 1 µl of each forward and reverse 1 µl (10 mM) primer, 0.4 µl (5 U/µl) Platinum® Taq DNA Polymerase and the final volume was adjusted to 50 µl with Nuclease-Free Water (Ambion). PCR was then performed using MyCycler Thermal Cycler (Bio-Rad) according to cycle reaction parameters denoted in table 2 below for each gene. PCR products were visualized by agarose gel electrophoresis (see Appendix B, p 261-262). Human *B-ACTIN* primers were generously provided by Dr Mark McCabe, whereas *NODAL* and *CRIPTO* primers were designed using primer-BLAST/NCBI software (see table 3 below for primer sequences).

qRT-PCR

Quantitative PCR was also performed as described previously using universal SYBR-Green (Invitrogen, Life Technologies, Thermo Fisher Scientific) and the Corbett Rotor-Gene 2000 (Corbett Lifesciences) (38). Oligonucleotide primer sequences are denoted below in table 3. Relative mRNA levels of *NODAL* and *CRIPTO* expressed endogenously in human cancer cells were determined using the $2^{-\Delta\Delta CT}$ method normalized to corresponding housekeeping *B-ACTIN* and expressed relative to a quality control standard. The quality control standard was generated from NTERA 2-D1 cDNA diluted appropriately and used in each experiment as internal control. The identity of the amplicons was confirmed by DNA sequencing.

Table 2. PCR Cycling Parameters

		CRIPTO (TDGF-1)	***NODAL***	***B-ACTIN***	
Stage 1 x 1 cycle	Step 1	94°C, 2 mins	94°C, 2 mins	94°C, 2 mins	
Stage 2 x 38 cycles	Step 1	94°C, 30 secs	94°C, 30 secs	94°C, 30 secs	*primer denaturation*
	Step 2	64°C, 30 secs	59.2°C, 30 secs	64°C, 30 secs	*primer annealing*
	Step 3	72°C, 1 min	72°C, 1 min	72°C, 1 min	*primer extension*
Stage 3 x 2 cycles	Step 1	72°C, 10 mins	72°C, 10 mins	72°C, 10 mins	*final primer extension*
	Step 2	20°C, hold	20°C, hold	20°C, hold	

Table 3. Primer sequences

Human Gene Name	**Primer**	**Primer Sequence (5'-3')**	**Product size (bp)**
CRIPTO (TDGF-1)	F	AAGATGGCCCGCTTCTCTTACAGT	511
	R	AAAGTGGTAGTACGTGCAGACGGT	
NODAL	F	AGACATCATCCGCAGCCTACA	250
	R	GTCCATCTGAAACCGCTCTAAG	
B-ACTIN	F	CGAGCGCGGCTACAGCTT	506
	R	TCATACTCCTGCTTGCTGATCC	

Luciferase Assay

To assess the biological effects of anti-Cripto MAbs, we developed a Nodal bioassay. NTERA 2-D1 cells were seeded in a 48 well plate at a density of $1x10^5$ cells/well in 350 µl of complete medium (as denoted in table 1, without antibiotics) and incubated for 24 hr, at 37 °C and 5 % CO_2. The cells were then transfected with Nodal-responsive luciferase constructs A3-lux and FAST2 (FoxH1) using Lipofectamine TM 2000 (Invitrogen, LifeTechnologies, Thermo Fisher Scientific). DNA mix (A3-lux, FAST2/FoxH1, CMV-β-galactosidase) /Lipofectamine complex [500 ng/ 1.25 µl] was incubated with OPTI-MEM and added directly to the cells. A3-lux contains three tandem copies of Nodal/activin responsive element from the *Xenopus Mix2* promoter, linked to a luciferase reporter gene (55, 56). At 24 hrs post-transfection the cells were stimulated with human recombinant Nodal (R&D Systems) or human recombinant activin A (R&D Systems) with or without increasing doses of anti-Cripto MAb. Cells were further incubated in solubilization buffer (1% Triton X-100, 25 mM glycylglycine pH 7.8, 15 mM MgSO4, 4 mM EGTA, 1 mM DTT) for 20 mins on ice. Luciferase reporter activity was then measured immediately after the addition of D-luciferin (Invitrogen, Thermo Fisher Scientific), by a single injectable tube luminometer (Lumat LB 9501, Bethold). Calculation of the luciferase response was determined as a measure of relative fold stimulation normalized to control.

Proliferation Assay

Cell proliferation was monitored using CyQUANT® Cell Proliferation Assay Kit (Invitrogen, Molecular Probes, Thermo Fisher Scientific). This highly sensitive assay is based on dye fluorescence enhancement, upon binding to nucleic acids allowing for cell density measurements (57). Cells were serum starved for 16 hrs, prior to seeding in 96

well microplates at a cell density of 500 cells/well in 100 µl of complete media. 1 x 10^6 cells were frozen at -80°C, to generate a reference standard curve for converting sample fluorescence values into cell numbers. After 24 hrs, cells were either treated with anti-Cripto MAbs or left untreated with subsequent treatment doses supplemented every 2 days and proliferation was monitored over 8 days. Fluorescence intensity at excitation of 480 nm and emission of 520 nm was recorded by Wallac Victor2 1420 Multilabel Counter Microplate Reader (Perkin Elmer, Life Sciences). A standard curve was derived using MultiCalc software (Perkin Elmer, Life Sciences) and relative cell numbers were thus deduced.

Migration Assay

Cell migration was assessed by performing wound healing assays (58). Cells were plated in a 48 well plate in complete media and allowed to reach confluency. They were then serum starved for 24 hrs (in media containing 1% FCS). The cell monolayer was scraped with a p20 pipet tip, in a straight line to create a wounded gap. Following removal of cell debris by consecutive gentle washes with PBS (Gibco) fresh serum starving media (1% FCS) was added to the cells, with or without anti-Cripto MAb. Cells were monitored until the wounded gap was healed over 96 hrs dependent upon the cell line as specified. Images were taken using OLYMPUS inverted microscope (OLYMPUS CORPORATION) with 10 x magnification objective at various time points of wound healing. Cellular migration was quantified using analySIS LS professional software (OLYMPUS CORPORATION).

Smad Phosphorylation Assay

Smad phosphorylation assays were performed to assess the effects of 6E10 MAb on down-stream Nodal mediated signal transduction. NTERA 2-D1 cells were seeded at a density of $2.5x10^5$ cells per well in a 12 well plate and incubated for 4 hrs, at 37 °C and 5 % CO_2. The cells were then serum starved (in media containing 1% FCS), for 16 hrs prior to 6E10 anti-Cripto MAb treatment for 30 mins and compared to untreated control vehicle. Cells were lysed in 50 µl RIPA buffer (50 mM Tris-HCL pH 7.4, 1% NP-40, 0.25% sodium-deoxycholate, 150 nM NaCL) containing 1 mM EDTA, 1% SDS, 1 mM PMSF, 1 x protease and phosphatase inhibitor cocktail (Roche Applied Science), on ice for 30 mins. Lysates were centrifuged (13,000 x g, 10 mins, 4°C) and reduced in 4 x LDS sample buffer (Invitrogen, LifeTechnologies, Thermo Fisher Scientific), with 5% β-mercaptoethanol (BioRad). Proteins were separated in 10% SDS-PAGE, analysed by Western blotting (BIO-RAD), transferred onto ECL Hybond-C Super membrane (GE Healthcare) and blocked in 5% BSA TTBS. The membrane was probed with anti-Phospho-Smad2 (Cell Signaling Technologies) antibody diluted 1:2000 in 1% BSA/TTBS at 4°C, overnight. Following washing, the membrane was then probed with goat anti-rabbit IgG, HRP-linked antibody (Cell Signaling Technologies) diluted 1:2000 in 1 % BSA/TTBS at 4°C, 2 hrs. The membrane was washed, developed and signal was detected using ChemiDoc™ MP System and Image Lab™ software (BIO-RAD) for Image analysis. Subsequently the membrane was stripped by incubation in boiled water for 10 mins and immunoblotted again to detect total Smad2 by probing with Smad2 antibodies [Cell Signaling Technologies (1:2000 dilution in 1% BSA/TTBS)].

Statistical Analysis

Statistical analysis was performed using GraphPad Prism (GraphPad Software 7.0). Assessment of statistical significance between groups was carried out using one-way ANOVA, with Tukey's multiple comparisons test. Alternatively, multiple groups were compared using uncorrected Fisher's LSD comparisons test with two-way repeated measures ANOVA as specified. Results with P values < 0.05 were considered statistically significant.

Results

Characterisation of Anti-Cripto Monoclonal Antibodies

To study the effects of Nodal blockade, anti-Cripto MAbs were employed. A panel of Anti-Cripto MAbs generated from hybridoma spleen cells of mice (Balb/C) immunised with recombinant Cripto (resembling native protein), was provided by Associate Professor Martin Lackmann. Binding studies were conducted by L. Kravets and M. Lackmann, to assess recognition specificity of 4G4, 6E10, 3D1 and 1C3 antibodies to Cripto protein, as summarized in supplementary Figure 1 (41). Biacore analysis revealed that 4G4 and 3D1 antibodies were highly responsive in binding monomeric and denatured Cripto protein with decreased sensitivity to dimeric Cripto protein. 6E10 and 1C3 exhibited diminished reactivity to denatured Cripto Biacore sensor, whereas for the corresponding native monomer, both antibodies were weakly effective. In turn binding to dimeric native Cripto was of low effectiveness for 6E10 and it diminished for 1C3. As demonstrated by L. Kravets and M Lackmann (41), both 4G4 and 6E10 antibodies effectively detected purified Cripto standard by Western blotting, whereas 3D1 and 1C3 failed to do so. In addition, detection of denatured or native Cripto protein by 4G4 in

Western blot analysis of NTERA 2-D1 cell total cell lysates and condition media was observed. 4G4 and 6E10 MAbs were also efficient in IPs of native Cripto expressed in NTERA 2-D1 cells.

Furthermore, 4G4, 6E10 and 3D1 antibodies recognized cell-associated Cripto in FACS analysis studies of NTERA 2-D1 cells (refer to supplementary Figure 1). This response was ablated in NTERA 2-D1 cells treated with retinoic acid (for 7 days), which has been previously shown to induce cell differentiation and abrogation of Cripto expression (59). Subsequently, 4G4 and 3D1 MAbs detected Cripto expression in MEFs (mouse embryonic fibroblast) cells as well and HC-11 (mouse mammary epithelial) cells using immunofluorescence (41). In addition, 4G4 MAb also detected Cripto in immunohistochemical studies of pregnant and lactating mouse mammary epithelial cell tissues, confirming previous reports of its roles in mediating developmental and lactational processes within human and mouse mammary ducts (60). Finally, preliminary immunohistochemical analysis of human colon and breast carcinoma patient specimens using 4G4 MAb revealed overexpression of Cripto in tumour cells. However, staining of Cripto protein from homologous normal human colon and breast tissue indicated low expression or absence of Cripto protein (41). These findings have also been confirmed in subsequent studies clearly linking overexpression of Cripto in human breast and colon tissue compared to non-cancerous adjacent tissue, implicating Cripto in oncogenesis (61, 62).

Nodal and Cripto mRNA Expression of Human Cancer Cell Lines

RT-PCR and qRT-PCR analyses of various cancer cell lines revealed expression of both *NODAL* and *CRIPTO* (*TDGF-1*) mRNA (or *NODAL*$^{+}$*/CRIPTO*$^{+}$ phenotype) (Figures 1 and 2)

in the highly aggressive NTERA 2-D1 (testicular teratocarcinoma cells); PC-3, LNCaP, DU 145 (prostate cancer cells); and LIM 1215, LIM 1863, SW 480 (colon cancer cells); whereas KGN (ovarian cancer cells) and C8161 (melanoma cells) expressed *CRIPTO* but not *NODAL* mRNA (*NODAL*$^{-}$*/CRIPTO*$^{+}$). High expression (or overexpressing) levels of *CRIPTO* transcript were detected in CHO-Cripto (Cripto - transfected-CHO cells), NTERA 2-D1 and LNCaP. Moderate *CRIPTO* expression levels were seen in KGN, DU 145, LIM 1215, LIM 1863, and cells. Whereas C8161, PC-3, and SW 480 cells expressed low levels of *CRIPTO* mRNA. In addition, *NODAL* mRNA was expressed at high, moderate, and low levels in NTERA-2D1, LNCaP, DU 145, LIM 1215, LIM 1863, SW 480; CHO-Cripto; PC-3; respectfully. Both *NODAL* and *CRIPTO* transcripts (*NODAL*$^{-}$*/CRIPTO*$^{-}$) remained undetected in HEK 293 (embryonic kidney cells), MCF-7 (breast cancer cells) COV 434 (ovarian cancer cells) and MUM-2C (melanoma cells).

Detection of Cripto Protein in NTERA 2-D1 Cells

To confirm endogenous expression of Cripto within NTERA 2-D1 testicular teratocarcinoma cells as previously suggested, (59) total cell lysates and conditioned medial were analysed by Western blot, as seen in Figure 3. 4G4 MAb detected a 26 kDa Cripto protein in: in transfected CHO-Cripto cells (overexpressing Cripto), and in NTERA 2-D1 coinciding with 3 ng recombinant standard band. Cripto protein is observed in both cell lysates and in conditioned media, confirming the presence of transmembrane and secreted Cripto. In addition, 6E10 MAb was effective in immunoprecipitating Cripto from CHO-Cripto and NTERA 2-D1 conditioned media, accompanied by a slight enhancement of protein signal detection (Figure 3), validating M Lackmann's immunoblot studies. However, Cripto protein was not detected in C8161 and MUM-2C cells. Although C8161 cells expressed *CRIPTO* mRNA, protein expression was not detected by Western blotting.

Therefore, due to reduced sensitivity of protein detection by immunoblotting, endogenous *CRIPTO* and *NODAL* expression levels within the cancer cell line panel were deduced by the highly sensitive qRT-PCR method as described above (Figures 1,2).

Anti-Cripto MAb Inhibits Nodal Induced Luciferase Activity

We established a Nodal dependent Smad 2/3 functional assay using the NTERA 2-D1 cellular model. TGF-β ligand activin A, which shares receptors (ALK4 and ActRII) with Nodal, induced a dose dependent luciferase response curve in NTERA 2-D1 cells transfected with Smad 2/3 responsive A3-luciferase reporter as demonstrated in Figure 4. Thus, serving as a positive control for this bio-functional assay, and indicating that both activin type I and type II receptors (also essential for Nodal signalling) are active within this cellular system. Treatment of NTERA 2-D1 cells with human recombinant Nodal, also induced luciferase activity in a dose dependent manner, although less potent than activin.

We then utilized this Nodal responsive functional system to assess the effects of anti-Cripto MAbs. It is evident in Figure 5B, that activin A induced luciferase activity was not affected with anti-Cripto MAb antibody treatment. This is expected as activin A does not utilize Cripto as a co-receptor (63). In contrast 6E10 and 3D1 MAbs significantly decreased Nodal-induced luciferase activity, in a dose dependent manner, compared to both PBS vehicle and 1C3 anti-Cripto MAb (non-neutralising) control responses, as illustrated in Figure 5A. Therefore, both 6E10 and 3D1 anti-Cripto antibodies ablate Nodal signalling.

Anti-Cripto MAbs Suppress Cancer Cell Growth

Next, we examined the effects of anti-Cripto MAbs on cancer cell growth by performing CyQuant proliferation assays over 8 days with antibody treatment every 2 days. Strikingly, both 6E10 and 3D1 neutralising antibodies completely suppressed NTERA 2-D1 cell proliferation compared to the control (vehicle containing PBS) and 1C3 MAb non-neutralising control (Figure 6.B). Additional proliferation assays were extended to include cancer cells expressing different levels of Nodal and Cripto (according to Figure 2). Proliferation of highly aggressive cell lines with *NODAL*$^{+}$*/CRIPTO*$^{+}$ phenotype, NTERA 2-D1 (testicular teratocarcinoma) and LNCaP (prostate cancer); expressing high levels of Cripto and Nodal, was completely obliterated with 125 μg/ml (high dose) of 6E10 treatment (see Figure 7). A significant reduction in proliferation of 57% was also observed in metastatic prostate *NODAL*$^{+}$*/CRIPTO*$^{+}$ Du 145 cancer cells, expressing moderate/high levels of Cripto and Nodal, treated with 6E10 (high dose) as compared to control (PBS). Interestingly cell lines with undetected Nodal expression and low to moderate levels of Cripto, exhibited a decrease in cellular proliferation of 58%, 50% for C8161 (melanoma), KGN (granulosa ovarian cancer) respectively (*NODAL*$^{-}$*/CRIPTO*$^{+}$), compared to homologous control cells. This could be attributed to Cripto mediated pro-tumourigenic effects independent of Nodal signalling (64). Whereas treatment of 6E10 (125 μg/ml) resulted in a 30% reduction of cell proliferation in PC-3 (prostate cancer, expressing low levels of Nodal and Cripto) compared to control. This data suggests that both 6E10 and 3D1 neutralising antibodies display anti-proliferative actions reflecting cellular expression levels of *CRIPTO* and *NODAL.*

6E10 Anti-Cripto MAb Represses Cancer Cell Migration

The effects of Nodal blockade on cancer cell migration were also examined, by performing *in vitro* wound healing assays. Figure 8 illustrates untreated (control UT) testicular teratocarcinoma NTERA 2-D1, cellular migration within the wounded-scratched area at different time points, with complete wound healing of 100%, occurring at 48 hrs. To eliminate buffering effects of 6E10 MAb and SB-431542 treatments, PBS and DMSO vehicle controls were also respectfully included, which did not affect cell migration (as seen in Figure 9). Whereas treatment with 6E10 (50 μg/ml) for 48 hrs significantly reduced NTERA 2-D1 cellular migration by 62% and followed a dose dependent pattern (see Figure 9). In comparison, we observed a 50% reduction of NTERA 2-D1 cellular migration with 10 μM SB-431542 treatment (TGF-β receptor type I, kinase inhibitor). We also observed that non-neutralising anti-Cripto MAb control 1C3, did not affect migration of NTERA 2-D1.

In contrast, untreated LNCaP cells monitored over 96 hrs, did not reach complete wound closure (as demonstrated in Figure 10). However, LNCaP cell motility was greatly reduced by 47% with 6E10 (50 μg/ml) MAb treatment compared to untreated control. 6E10 exhibited a dose dependent reduction of cell migration (as seen in Figure 11), whereas treatment with (10 μM) SB-431542 suppressed migration by 39%. Neither vehicle controls affected LNCaP cellular migration rates.

Finally, we examined the motility of PC-3 cells expressing lower levels of *CRIPTO* and *NODAL* compared to NTERA 2-D1 and LNCaP (see Figure 12). We observed a significate reduction in PC-3 cell motility of 25%, 17%, upon treatment with of (50 μg/ml) 6E10 MAb, (10 μM) SB-431542 respectively compared to untreated controls (see Figure 13). These results suggest that 6E10 MAb presents anti-migratory properties according to

expression status of *CRIPTO* and *NODAL,* complementary to the anti-proliferative effects.

6E10 Anti-Cripto MAb Suppresses Smad 2/3 Phosphorylation

Finally, we assessed the effects of neutralising 6E10 MAb on down-stream Nodal mediated signalling by Western blot analysis of Smad 2/3 phosphorylation levels as seen in Figure 14. In this *in vitro* study, the NTERA 2-D1 cellular model was employed as it expresses high endogenous levels of Nodal and co-receptor Cripto, as well as other essential molecular components of Nodal/Smad 2/3 signalling. Treatment of NTERA 2-D1 with 6E10 MAb for 30 mins abrogated Smad 2/3 phosphorylation levels compared to control (containing PBS vehicle). Endogenous total-Smad 2 protein levels were comparable among 6E10 treated and control NTERA 2-D1 samples. Hence, this data suggests that *in vitro* blockade of Nodal signalling, via 6E10 MAb treatment significantly suppresses Smad 2/3 phosphorylation levels.

Discussion

One of the countless difficulties in treating cancer is the insufficient knowledge of the precise molecular mechanisms acquired by oncogenic transformation to favour malignancy, thereby escaping cellular homeostatic controls. A key morphogenic pathway consistently reported to pathologically re-emerge and drive carcinogenesis is the Nodal /TGF-β cascade.

We previously observed that high grade human endometrial cancer tissues correlated with upregulation of both signalling ligands Nodal and Cripto accompanied by the absence of TGF-β antagonist, Lefty. This observation implicates un-inhibited reactivation of Nodal signalling transduction in the development and progression of endometrial cancer (38). Cumulative evidence further suggests that increased Nodal or co-receptor Cripto expression coincides with clinicopathological features, as well as reduced patient survival rates in human malignancies involving melanoma, colon, brain, breast, lung, hepatic, pancreatic, prostate, oesophageal, oral squamous (26, 28-30, 34, 36, 37, 62). These findings substantiate the use of both Nodal and Cripto as potential prognostic cancer biomarkers. Given the oncogenic properties associated with re-activation of Nodal, the current study intends to further delineate the underlying molecular TGF-β mechanisms involved. Specific anti-Cripto MAbs where therefore characterized and employed to examine the *in vitro* anti-tumourigenic properties, of Nodal signalling blockade.

Anti-Cripto MAbs were developed and screened in binding studies by the late Associate Professor Martin Lackmann (Supplementary Figure 1). The antibodies were reactive within the EGF or CFC Cripto structural domain, and towards the native and denatured protein. Preliminary studies showed that both 4G4 and 3D1 antibodies detected native and denatured Cripto protein via FACS analysis of cells as well as immunohistochemistry of fixed or frozen tissue sections and immunoblotting of cell lysates. In addition, the late Associate Professor Martin Lackmann identified 6E10 as a conformational-specific anti-Cripto MAb as it reacted only with native Cripto protein in FACS analysis and immunoprecipitation.

The biological effects of the MAbs were ascertained utilizing cancer cell lines expressing various levels of *NODAL* and *CRIPTO* genes (refer to Figures 1 and 2). Expression of both *NODAL* and *CRIPTO* genes (*NODAL*$^{+}$*/CRIPTO*$^{+}$) where detected in highly aggressive cancer

cells: NTERA-2D1 (testicular teratocarcinoma cells); PC-3, LNCaP, DU 145 (prostate cancer cells); and LIM 1215, LIM 1863, SW 480 (colon cancer cells). *CRIPTO* only expressing cells (*NODAL*$^{-}$*/CRIPTO*$^{+}$) included: KGN (ovarian cancer cells) and C8161 (melanoma cells), with undetected *NODAL* gene expression. In addition, Western blot analysis confirmed over-expression of Cripto protein in NTERA 2-D1 cells, (see Figure 3) as previously documented (59).

NTERA 2-D1 (testicular teratocarcinoma) cells over-expressing both *NODAL* and *CRIPTO* co-receptor, (*NODAL*$^{+}$*/CRIPTO*$^{+}$), were used to develop a Nodal dependent Smad 2/3 bio-functional luciferase assay to examine the effects of anti-Cripto monoclonal antibodies. Subsequently NTERA 2-D1 cells were responsive to Nodal dependent Smad 2/3 signalling [as all essential signalling components are present, including signalling receptors (65)]. More importantly, 3D1 and 6E10 MAbs significantly reduced Nodal mediated luciferase activity in a dose dependent manner, compared to both vehicle and 1C3 controls (figure 5A). We have thus identified 3D1 and 6E10 anti-Cripto MAbs as potent neutralising antibodies that exhibit specificity in blocking Nodal-mediated Smad 2/3 signalling, without affecting activities of other TGF-β ligands including activin A [which shares Nodal's receptors complex, (see figure 5B)].

Abrogated cell survival is a key feature of pathogenic cellular transformation and elucidating in detail the underlying molecular mechanisms is of vital importance in cancer biology (66). Consequently, the effects of Nodal pathway blockade on cellular proliferation were further examined. MAb treatment of highly aggressive NTERA 2-D1 (testicular teratocarcinoma) cells profoundly suppressed proliferation with both neutralising antibodies 3D1 and 6E10. Furthermore, 6E10 anti-proliferative effects observed in LNCaP, Du 145, PC-3 (metastatic prostate); cancer cells; were dependent upon expression status of Cripto and Nodal. These results complement previous findings showing growth suppression of Du 145 and PC-3 cells upon anti-Cripto antibody

treatment (67), whereas overexpression of Nodal in LNCaP cells enhanced cancer growth (35).

In addition, it has been previously demonstrated that Cripto can signal independent of the Nodal/Smad cascade, to facilitate tumourigenic events. Cripto can antagonistically interact with cytostatic TGF-β ligands, such as TGF-β1 and activin A/B to attenuate downstream signalling and promote anti-apoptotic or pro-cell survival mechanisms, favouring oncogenesis (68). Cripto can alternatively facilitate lipid raft signalling via binding to Glypican-1, triggering c-src/ MAPK (mitogen activated protein kinase) and PI3K/Akt, (phosphatidylinositol 3-kinase) pathways associated with pro-proliferative, pro-survival and pro-migratory cellular activities (1). Alternatively, c-src/ MAPK and PI3K/Akt pathways can also be activated by Cripto's interactions with GRP78 (69). Based on this evidence we speculate that the observed 6E10 anti-proliferative effects of *NODAL*$^{-}$*/CRIPTO*$^{+}$ C8161 (melanoma), and KGN (granulosa ovarian), cancer cells demonstrated in the current study, are likely to be mediated by Cripto alternative signalling, independent of Nodal/Smad cascade. However, this remains to be further validated.

Another vital characteristic of cancer cell progression is the ability to migrate from the primary tumourigenic site and metastasize into neighbouring sites and distant tissues. This complex mechanism is acquired by cancer cells, rendering treatment challenging. We subsequently report in this study, *in vitro* anti-migratory effects exhibited by 6E10 MAb treatment concurrent to its anti-proliferative properties, reflecting cellular expression status of *NODAL/CRIPTO*, TGF-β ligands. Strikingly, 6E10 MAb treatment of highly metastatic NTERA 2-D1 (testicular) and LNCaP, PC-3 (both prostate); cancer cell lines, significantly suppressed cellular migration in a dose dependent manner. 6E10 displayed a greater efficiency in reducing migration of *NODAL*$^{+}$*/CRIPTO*$^{+}$ overexpressing NTERA 2-D1 and LNCaP, cells compared to low *NODAL*$^{+}$*/CRIPTO*$^{+}$ expressing PC-3 cells,

in accordance to the observed anti-proliferative effects. Subsequently 6E10 MAb treatment of NTERA 2-D1 abrogated Smad 2/3 phosphorylation levels, implicating involvement of Smad 2/3 activation pathway, in Nodal-mediated signalling activities.
Due to correlations between dysregulated Nodal signalling and oncogenesis involving a growing list of different cancer types, this pathway has received rising interests in targeted therapy. Studies of Nodal-knockout using a melanoma mouse model, were accompanied with reduction in tumour cell growth (7). Concurrently, Nodal antagonism by Cerberus (TGF-β pathway inhibitor) treatment of human breast cancer cells, significantly reduced proliferation, and migration of Nodal-expressing cells (18). In addition, lentiviral knockdown of Nodal in pancreatic cells was associated with reduced tumourigenicity *in vitro* (70).

Furthermore, anti-Cripto MAbs have been used to target Nodal's actions, in both *in vivo* and *in vitro* cancer models with promising anti-tumour effects (67, 71-74). Kelly, *et al.,* (2011), developed an immunoconjugate cytotoxic antibody consisting of anti-Cripto MAb linked by maytansinoid derivative, (DM4). The authors suggested that internalization of this compound by Cripto-expressing tumour cells, triggered release of DM4 upon cell division, leading to cell death (71). Unfortunately, phase I clinical trials of BIIB015 were withdrawn due to insufficient efficacy (75).

Recently, anti-Nodal MAbs designed to block Nodal/Cripto signalling via the Smad 2/3 pathway, reduced vascularization of melanoma and breast cancers (76, 77). However, this antibody cannot target alternative Nodal-independent pathways, such as soluble Cripto paracrine signalling. We postulate that 6E10 and 3D1 anti-Cripto MAbs presented in the current study, could also potentially target the alternative non-canonical Cripto-Smad 2/3 independent signalling mechanisms, however this should be further explored in subsequent future studies. Therefore, we propose that 6E10 MAb treatment would be pharmacologically advantageous compared to the currently developed anti-Nodal

antibodies described by Focà A, *et. al.,* (2015) in anti-cancer immunotherapy applications.

Conclusions

Our findings support the hypothesis, that re-activation of embryogenic Nodal is a key driver of cancer development and progression. The current study further confirms the regulatory roles of Nodal in cancer cell growth and migration, mediated by the Smad 2/3 signalling axis. Interestingly, 6E10 and 3D1 have been identified as neutralising anti-Cripto monoclonal antibodies that specifically block Nodal signalling. Importantly 6E10 MAb treatment greatly suppresses cancer cell proliferation and migration. Furthermore, Nodal blockade by conformational-specific 6E10 anti-Cripto MAb treatment, abolished down-stream TGF-β/Smad 2/3 phosphorylation levels of NTERA 2-D1 cells, mediating the observed regulatory cellular responses. The significance of this study complements previous findings, suggesting that both TGF-β ligands Nodal and co-receptor Cripto could serve as potential prognostic biomarkers of cancer progression. Subsequently, 6E10 monoclonal antibody could be utilized as a potential therapeutic agent of targeted Nodal signalling in oncology.

Competing Interests

The authors declare no competing interests.

Authors' Contributions

Conception and design: M.Lackmann and C. Harrison.

Development and methodology: I. Papageorgiou, M.Lackmann.

Data acquisition: I. Papageorgiou.

Data analysis and interpretation: I. Papageorgiou.

Writing, review and editing of manuscript: I. Papageorgiou.

Study supervision: C.A. Harrison and D.M. Robertson.

Acknowledgements

The authors would like to acknowledge co-author and collaborator Professor Martin Lackmann (3 November 1956 to 22 May 2014), for his invaluable contributions towards this work. Professor Martin Lackmann is sadly missed, and we dedicate this manuscript in his memory. We are thankful to Dr Michael Christie, Jenny Catimel, Professor Ed Nice, and Dr Kaye Wycherley for supplying us with the Cripto MAbs. We are especially grateful to Professor Tony Burgess for his intellectual input in this project. We greatly appreciate Mrs Janelle Ryan, Dr Birunthi Niranj and Dr Francesca Walker for kindly providing us with tissue culture cell lines. Additionally, we thank Dr Mark McCabe for generously providing human β-actin primers. We further acknowledge Dr Maree Bilandzic and Dr Mai Sarraj for their technical assistance in wound healing assays and quantification protocols. We finally owe our gratitude to Dr Helen Cumming for critically reading this manuscript.

List of Abbreviations

ALK4, Activin type I receptor; ActRII, Activin type II receptor; ActRIIB, Activin type II receptor; ANOVA, Analysis of variance; bp, Base pairs; CMV, Cytomegalovirus; DHFR, Dihydrofolate reductase; DMSO, Dimethyl sulfoxide; ELISA, Enzyme-linked immunosorbent assay; EGF-CFC, Epidermal growth factor-Cripto-FRL1-Cryptic; FAST2, Forkhead activin signal transducer 2; GRP78, Glucose-regulated protein 78; GPI, Glycosylphosphatidylinositol; FoxH1, Homolog of Xenopus forkhead activin signal transducer-1; mRNA, Messenger RNA; MAPK, Mitogen activated protein kinase; MAb, Monoclonal antibody; PI3K/Akt, phosphatidylinositol-3-kinase/protein kinase B; qRT-PCR, quantitative polymerase chain reaction; R-Cripto, Recombinant-Cripto; Smad, Small mothers against decapentaplegic; TDGF-1,Teratoma-derived growth factor 1; TGF-β, Transforming growth factor-beta; WB, Western blot;

Grant Support

Supported by NHRMC (Aust) Program Grant # 241000

References

1. Bianco C, Strizzi L, Normanno N, Khan N, Salomon DS. Cripto-1: an oncofetal gene with many faces. Current topics in developmental biology. 2005; 67:85-133.

2. Strizzi L, Bianco C, Normanno N, Salomon D. Cripto-1: a multifunctional modulator during embryogenesis and oncogenesis. Oncogene. 2005; 24(37): 5731 -41.

3. Schier AF. Nodal signaling in vertebrate development. Annual review of cell and developmental biology. 2003; 19:589-621.

4. Shen MM. Nodal signaling: developmental roles and regulation. Development. 2007;134(6):1023-34.

5. Quail DF, Siegers GM, Jewer M, Postovit L-M. Nodal signalling in embryogenesis and tumourigenesis. The International Journal of Biochemistry & Cell Biology. 2013;45(4):885-98.

6. Strizzi L, Hardy KM, Margaryan NV, Hillman DW, Seftor EA, Chen B, et al. Potential for the embryonic morphogen Nodal as a prognostic and predictive biomarker in breast cancer. Breast Cancer Res. 2012;14(3): R75.

7. Topczewska JM, Postovit LM, Margaryan NV, Sam A, Hess AR, Wheaton WW, et al. Embryonic and tumorigenic pathways converge via Nodal signaling: role in melanoma aggressiveness. Nat Med. 2006;12(8):925-32.

8. Watanabe K, Hamada S, Bianco C, Mancino M, Nagaoka T, Gonzales M, et al. Requirement of glycosylphosphatidylinositol anchor of Cripto-1 for trans activity as a Nodal co-receptor. The Journal of biological chemistry. 2007;282(49):35772-86.

9. Ding J, Yang L, Yan YT, Chen A, Desai N, Wynshaw-Boris A, et al. Cripto is required for correct orientation of the anterior-posterior axis in the mouse embryo. Nature. 1998;395(6703):702-7.

10. Minchiotti G, Parisi S, Liguori GL, D'Andrea D, Persico MG. Role of the EGF-CFC gene cripto in cell differentiation and embryo development. Gene. 2002;287(1-2):33-7.

11. Shi Y, Massague J. Mechanisms of TGF-beta signaling from cell membrane to the nucleus. Cell. 2003;113(6):685-700.

12. Derynck R, Zhang Y, Feng XH. Smads: transcriptional activators of TGF-beta responses. Cell. 1998;95(6):737-40.

13. Heldin CH, Miyazono K, ten Dijke P. TGF-beta signalling from cell membrane to nucleus through SMAD proteins. Nature. 1997;390(6659):465-71.

14. Massague J. TGF-beta signal transduction. Annual review of biochemistry. 1998; 67:753-91.

15. Chen C, Shen MM. Two modes by which Lefty proteins inhibit nodal signaling. Current biology: CB. 2004;14(7):618-24.

16. Cheng SK, Olale F, Brivanlou AH, Schier AF. Lefty blocks a subset of TGFbeta signals by antagonizing EGF-CFC coreceptors. PLoS biology. 2004;2(2): E30.

17. Aykul S, Martinez-Hackert E. New Ligand Binding Function of Human Cerberus and Role of Proteolytic Processing in Regulating Ligand-Receptor Interactions and Antagonist Activity. J Mol Biol. 2016;428(3):590-602.

18. Aykul S, Ni W, Mutatu W, Martinez-Hackert E. Human Cerberus prevents nodal-receptor binding, inhibits nodal signaling, and suppresses nodal-mediated phenotypes. PLoS One. 2015;10(1): e0114954.

19. Brons IG, Smithers LE, Trotter MW, Rugg-Gunn P, Sun B, Chuva de Sousa Lopes SM, et al. Derivation of pluripotent epiblast stem cells from mammalian embryos. Nature. 2007;448(7150):191-5.

20. Fiorenzano A, Pascale E, D'Aniello C, Acampora D, Bassalert C, Russo F, et al. Cripto is essential to capture mouse epiblast stem cell and human embryonic stem cell pluripotency. Nature Communications. 2016; 7:12589.

21. Kruithof-de Julio M, Alvarez MJ, Galli A, Chu J, Price SM, Califano A, et al. Regulation of extra-embryonic endoderm stem cell differentiation by Nodal and Cripto signaling. Development. 2011;138(18):3885-95.

22. Loh YH, Wu Q, Chew JL, Vega VB, Zhang W, Chen X, et al. The Oct4 and Nanog transcription network regulates pluripotency in mouse embryonic stem cells. Nature genetics. 2006;38(4):431-40.

23. Schier AF, Shen MM. Nodal signalling in vertebrate development. Nature. 2000;403(6768):385-9.

24. Vallier L, Reynolds D, Pedersen RA. Nodal inhibits differentiation of human embryonic stem cells along the neuroectodermal default pathway. Developmental biology. 2004;275(2):403-21.

25. Castro NP, Fedorova-Abrams ND, Merchant AS, Rangel MC, Nagaoka T, Karasawa H, et al. Cripto-1 as a novel therapeutic target for triple negative breast cancer. Oncotarget. 2015;6(14):11910-29.

26. Liu Q, Cui X, Yu X, Bian B-S-J, Qian F, Hu X-g, et al. Cripto-1 acts as a functional marker of cancer stem-like cells and predicts prognosis of the patients in esophageal squamous cell carcinoma. Molecular Cancer. 2017;16(1):81.

27. Mancino M, Strizzi L, Wechselberger C, Watanabe K, Gonzales M, Hamada S, et al. Regulation of human Cripto-1 gene expression by TGF-beta1 and BMP-4 in embryonal and colon cancer cells. J Cell Physiol. 2008;215(1):192-203.

28. Pilgaard L, Mortensen JH, Henriksen M, Olesen P, Sorensen P, Laursen R, et al. Cripto-1 expression in glioblastoma multiforme. Brain pathology (Zurich, Switzerland). 2014;24(4):360-70.

29. Wang J-h, Wei W, Xu J, Guo Z-x, Xiao C-z, Zhang Y-f, et al. Elevated expression of Cripto-1 correlates with poor prognosis in hepatocellular carcinoma. Oncotarget. 2015;6(33):35116-28.

30. Xu CH, Cao L, Wei Y, Yu LK. Serum cripto-1 as a clinical marker for lung cancer. The International journal of biological markers. 2015;30(4): e369-73.

31. Li P, Sun D, Li X, He Y, Li W, Zhao J, et al. Elevated expression of Nodal and YAP1 is associated with poor prognosis of gastric adenocarcinoma. Journal of cancer research and clinical oncology. 2016;142(8):1765-73.

32. Oliveira-Nunes MC, Assad Kahn S, de Oliveira Barbeitas AL, TC ES, Dubois LG, Ventura Matioszek GM, et al. The availability of the embryonic TGF-beta protein Nodal is dynamically regulated during glioblastoma multiforme tumorigenesis. Cancer Cell Int. 2016; 16:46.

33. Strizzi L, Postovit L-M, Margaryan NV, Lipavsky A, Gadiot J, Blank C, et al. Nodal as a biomarker for melanoma progression and a new therapeutic target for clinical intervention. Expert review of dermatology. 2009;4(1):67-78.

34. Kong B, Wang W, Esposito I, Friess H, Michalski CW, Kleeff J. Increased expression of Nodal correlates with reduced patient survival in pancreatic cancer. Pancreatology: official journal of the International Association of Pancreatology (IAP). 2015;15(2):156-61.

35. Lawrence MG, Margaryan NV, Loessner D, Collins A, Kerr KM, Turner M, et al. Reactivation of Embryonic Nodal Signaling is Associated with Tumor Progression and Promotes the Growth of Prostate Cancer Cells. The Prostate. 2011;71(11):1198-209.

36. Strizzi L, Margaryan NV, Gerami P, Haghighat Z, Harms PW, Madonna G, et al. Translational significance of Nodal, Cripto-1 and Notch4 in adult nevi. Oncology Letters. 2016;12(2):1349-54.

37. Yoon HJ, Hong JS, Shin WJ, Lee YJ, Hong KO, Lee JI, et al. The role of Cripto-1 in the tumorigenesis and progression of oral squamous cell carcinoma. Oral oncology. 2011;47(11):1023-31.

38. Papageorgiou I, Nicholls PK, Wang F, Lackmann M, Makanji Y, Salamonsen LA, et al. Expression of nodal signalling components in cycling human endometrium and in endometrial cancer. Reprod Biol Endocrinol. 2009; 7:122.

39. Graham FL, Smiley J, Russell WC, Nairn R. Characteristics of a human cell line transformed by DNA from human adenovirus type 5. The Journal of general virology. 1977;36(1):59-74.

40. Puck TT, Cieciura SJ, Robinson A. Genetics of somatic mammalian cells. III. Long-term cultivation of euploid cells from human and animal subjects. J Exp Med. 1958;108(6):945-56.

41. L. Kravets, C. Mc Faralane, E. Stanley, J. Visvader, G. Linderman, A. Scott, R. Harvey. M. Ernest, A.W.Burgess, M Lackmann. Production and Characterisation of Monoclonal Antibodies against Human Cripto-1. Unpublished Work.

42. Andrews PW. Human teratocarcinomas. Biochimica et Biophysica Acta (BBA) - Reviews on Cancer. 1988;948(1):17-36.

43. Andrews PW, Damjanov I, Simon D, Banting GS, Carlin C, Dracopoli NC, et al. Pluripotent embryonal carcinoma clones derived from the human teratocarcinoma cell line Tera-2. Differentiation in vivo and in vitro. Lab Invest. 1984;50(2):147-62.

44. Nishi Y, Yanase T, Mu Y-M, Oba K, Ichino I, Saito M, et al. Establishment and Characterization of a Steroidogenic Human Granulosa-Like Tumor Cell Line, KGN, That Expresses Functional Follicle-Stimulating Hormone Receptor. Endocrinology. 2001;142(1):437-45.

45. van den Berg-Bakker CAM, Hagemeijer A, Franken-Postma EM, Smit VTHBM, Kuppen PJK, Claasen HHVR, et al. Establishment and characterization of 7 ovarian carcinoma cell lines and one granulosa tumor cell line: Growth features and cytogenetics. International Journal of Cancer. 1993;53(4):613-20.

46. Soule HD, Vazquez J, Long A, Albert S, Brennan M. A Human Cell Line From a Pleural Effusion Derived From a Breast Carcinoma2. JNCI: Journal of the National Cancer Institute. 1973;51(5):1409-16.

47. Horoszewicz JS, Leong SS, Chu TM, Wajsman ZL, Friedman M, Papsidero L, et al. The LNCaP cell line--a new model for studies on human prostatic carcinoma. Progress in clinical and biological research. 1980; 37:115-32.

48. Kaighn ME, Narayan KS, Ohnuki Y, Lechner JF, Jones LW. Establishment and characterization of a human prostatic carcinoma cell line (PC-3). Investigative urology. 1979;17(1):16-23.

49. Stone KR, Mickey DD, Wunderli H, Mickey GH, Paulson DF. Isolation of a human prostate carcinoma cell line (DU 145). International Journal of Cancer. 1978;21(3):274-81.

50. Bregman MD, Meyskens FL. Difluoromethylornithine enhances inhibition of melanoma cell growth in soft agar by dexamethasone, clone a interferon and retinoic acid. International Journal of Cancer. 1986;37(1):101-7.

51. Seftor EA, Meltzer PS, Kirschmann DA, Pe'er J, Maniotis AJ, Trent JM, et al. Molecular determinants of human uveal melanoma invasion and metastasis. Clinical & Experimental Metastasis. 2002;19(3):233-46.

52. Whitehead RH, Macrae FA, St. John DJB, Ma J. A Colon Cancer Cell Line (LIM1215) Derived From a Patient With Inherited Nonpolyposis Colorectal Cancer2. JNCI: Journal of the National Cancer Institute. 1985;74(4):759-65.

53. Whitehead RH, Jones JK, Gabriel A, Lukies RE. A New Colon Carcinoma Cell Line (LIM1863) That Grows as Organoids with Spontaneous Differentiation into Crypt-like Structures in Vitro. Cancer Research. 1987;47(10):2683-9.

54. Leibovitz A, Stinson JC, McCombs WB, McCoy CE, Mazur KC, Mabry ND. Classification of Human Colorectal Adenocarcinoma Cell Lines. Cancer Research. 1976;36(12):4562-9.

55. Gray PC, Harrison CA, Vale W. Cripto forms a complex with activin and type II activin receptors and can block activin signaling. Proc Natl Acad Sci U S A. 2003;100(9):5193-8.

56. Liu F, Pouponnot C, Massague J. Dual role of the Smad4/DPC4 tumor suppressor in TGFbeta-inducible transcriptional complexes. Genes & development. 1997;11(23):3157-67.

57. Jones LJ, Gray M, Yue ST, Haugland RP, Singer VL. Sensitive determination of cell number using the CyQUANT® cell proliferation assay. Journal of Immunological Methods. 2001;254(1):85-98.

58. Lampugnani MG. Cell Migration into a Wounded Area In Vitro. In: Dejana E, Corada M, editors. Adhesion Protein Protocols. Totowa, NJ: Humana Press; 1999. p. 177-82.

59. Ciccodicola A, Dono R, Obici S, Simeone A, Zollo M, Persico MG. Molecular characterization of a gene of the 'EGF family' expressed in undifferentiated human NTERA2 teratocarcinoma cells. Embo j. 1989;8(7):1987-91.

60. Salomon DS, Bianco C, De Santis M. Cripto: a novel epidermal growth factor (EGF)-related peptide in mammary gland development and neoplasia. BioEssays: news and reviews in molecular, cellular and developmental biology. 1999;21(1):61-70.

61. Dublin E, Bobrow L, Barnes D, Gullick W. Amphiregulin and cripto overexpression in breast-cancer - relationship with prognosis and clinical and molecular-variables. International journal of oncology. 1995;7(3):617-22.

62. Bianco C, Strizzi L, Mancino M, Rehman A, Hamada S, Watanabe K, et al. Identification of cripto-1 as a novel serologic marker for breast and colon cancer. Clinical cancer research: an official journal of the American Association for Cancer Research. 2006;12(17):5158-64.

63. Gray PC, Vale W. Cripto/GRP78 modulation of the TGF-beta pathway in development and oncogenesis. FEBS Lett. 2012;586(14):1836-45.

64. Shani G, Fischer WH, Justice NJ, Kelber JA, Vale W, Gray PC. GRP78 and Cripto form a complex at the cell surface and collaborate to inhibit transforming growth factor beta signaling and enhance cell growth. Mol Cell Biol. 2008;28(2):666-77.

65. Available from: www.proteinatlas.org.

66. Hanahan D, Weinberg RA. The Hallmarks of Cancer. Cell. 2000;100(1):57-70.

67. Xing PX, Hu XF, Pietersz GA, Hosick HL, McKenzie IF. Cripto: a novel target for antibody-based cancer immunotherapy. Cancer Res. 2004;64(11):4018-23.

68. Klauzinska M, Castro NP, Rangel MC, Spike BT, Gray PC, Bertolette D, et al. The multifaceted role of the embryonic gene Cripto-1 in cancer, stem cells and epithelial-mesenchymal transition. Semin Cancer Biol. 2014; 29:51-8.

69. Kelber JA, Panopoulos AD, Shani G, Booker EC, Belmonte JC, Vale WW, et al. Blockade of Cripto binding to cell surface GRP78 inhibits oncogenic Cripto signaling via MAPK/PI3K and Smad2/3 pathways. Oncogene. 2009;28(24):2324-36.

70. Lonardo E, Hermann PC, Mueller MT, Huber S, Balic A, Miranda-Lorenzo I, et al. Nodal/Activin signaling drives self-renewal and tumorigenicity of pancreatic cancer stem cells and provides a target for combined drug therapy. Cell Stem Cell. 2011;9(5):433-46.

71. Kelly RK, Olson DL, Sun Y, Wen D, Wortham KA, Antognetti G, et al. An antibody-cytotoxic conjugate, BIIB015, is a new targeted therapy for Cripto positive tumours. Eur J Cancer. 2011;47(11):1736-46.

72. Bianco C, Salomon DS. Targeting the embryonic gene Cripto-1 in cancer and beyond. Expert Opin Ther Pat. 2010;20(12):1739-49.

73. Hu XF, Li J, Yang E, Vandervalk S, Xing PX. Anti-Cripto Mab inhibit tumour growth and overcome MDR in a human leukaemia MDR cell line by inhibition of Akt and activation of JNK/SAPK and bad death pathways. British journal of cancer. 2007;96(6):918-27.

74. Adkins HB, Bianco C, Schiffer SG, Rayhorn P, Zafari M, Cheung AE, et al. Antibody blockade of the Cripto CFC domain suppresses tumor cell growth in vivo. J Clin Invest. 2003;112(4):575-87.

75. Kalim M, Chen J, Wang S, Lin C, Ullah S, Liang K, et al. Intracellular trafficking of new anticancer therapeutics: antibody-drug conjugates. Drug design, development and therapy. 2017; 11:2265-76.

76. Strizzi L, Sandomenico A, Margaryan NV, Foca A, Sanguigno L, Bodenstine TM, et al. Effects of a novel Nodal-targeting monoclonal antibody in melanoma. Oncotarget. 2015;6(33):34071-86.

77. Focà A, Sanguigno L, Focà G, Strizzi L, Iannitti R, Palumbo R, et al. New Anti-Nodal Monoclonal Antibodies Targeting the Nodal Pre-Helix Loop Involved in Cripto-1 Binding. International Journal of Molecular Sciences. 2015;16(9):21342.

Figures

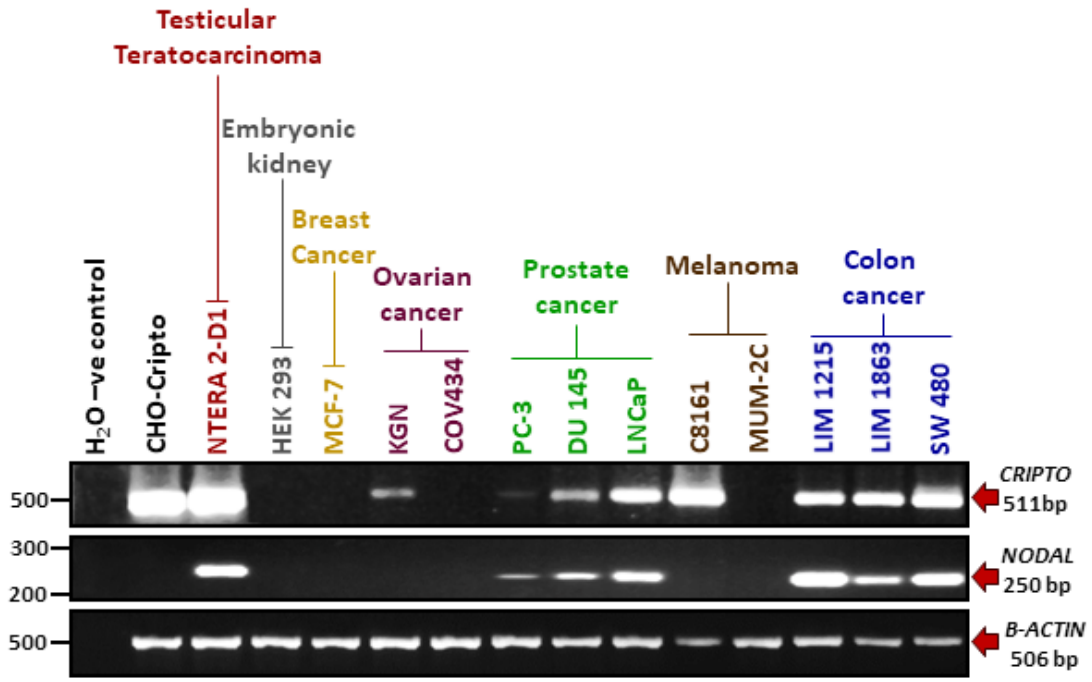

Figure 1. Nodal and Cripto mRNA Expression of Human Cancer Cell Line Panel.
cDNA was generated by reverse transcription of RNA (500 ng) extracted from the following human cell lines: CHO-Cripto (Cripto-stably transfected in CHO cells); NTERA 2-D1 testicular teratocarcinoma; HEK 293, embryonic kidney; MCF-7 breast cancer; KGN, COV 434, ovarian granulosa cancer; PC-3, LNCaP, DU 145, prostate cancer; C8161, MUM-2C, melanoma; LIM 1215, LIM 1863, SW 480 colon cancer. Expression of NODAL (250 bp), CRIPTO (511bp) and housekeeping B-ACTIN (506 bp) mRNA, was monitored by PCR. A negative PCR control containing nuclease-Free H_20 (no cDNA) was also included. Data is representative of four independent biological experiments.

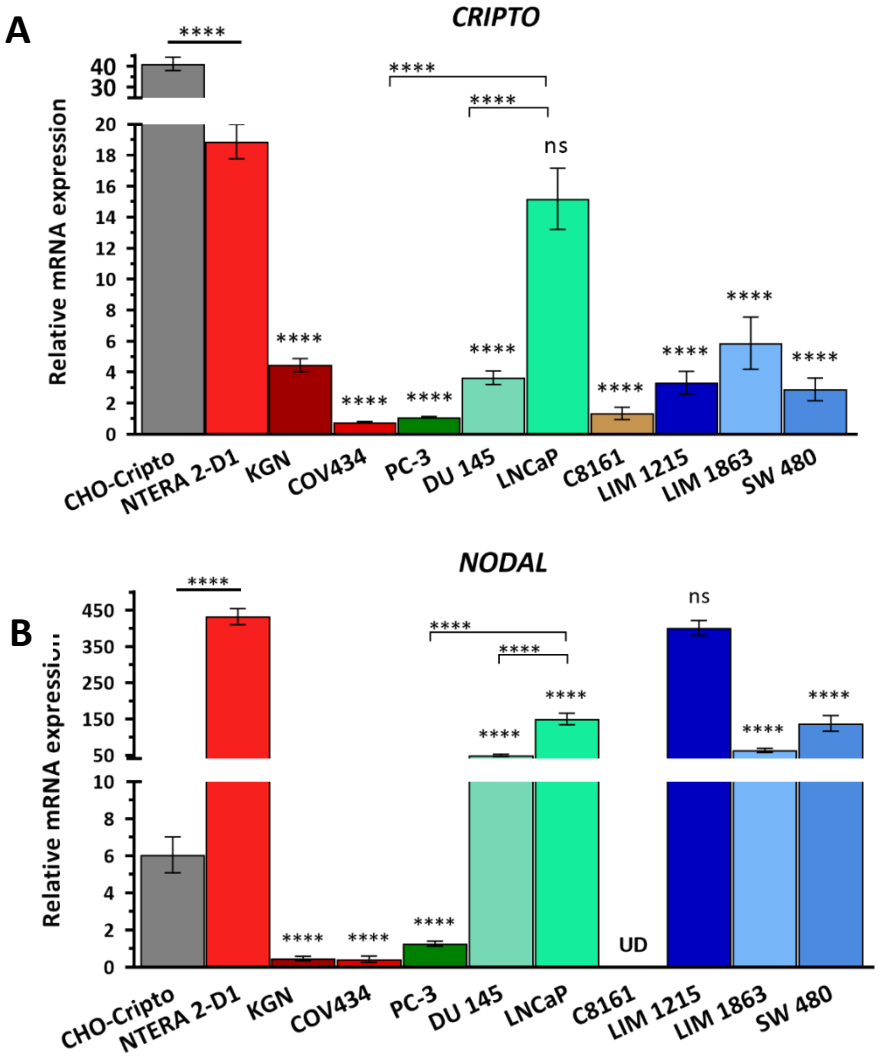

Figure 2. Endogenous CRIPTO/NODAL mRNA Expression in Human Cancer Cells.
Graphical representation of endogenous CRIPTO (A) and NODAL (B) transcripts, quantified by qRT-PCR in the following human cancer cell lines: CHO-Cripto (Cripto transfected-CHO); NTERA 2-D1 (testicular teratocarcinoma); KGN, COV 434, (ovarian granulosa); PC-3, LNCaP, DU 145 (prostate); C8161(melanoma); LIM 1215, LIM 1863, SW 480 (colon). Histograms showing relative mRNA expression, are deduced using the $2^{-\Delta\Delta CT}$ *method, normalized to corresponding housekeeping B-ACTIN and expressed relative to a quality control standard. The quality control standard was generated from NTERA 2-D1 cDNA. NODAL could not be detected in C8161 cells (UD: undetected). Data is presented as mean ± SEM, from three independent biological experiments, performed in technical triplicates. Statistical analysis was performed using one-way ANOVA with Tukey's multiple comparisons, (*P<0.05, **P<0.01, ***P<0.001, ****P<0.0001). UD, undetermined.*

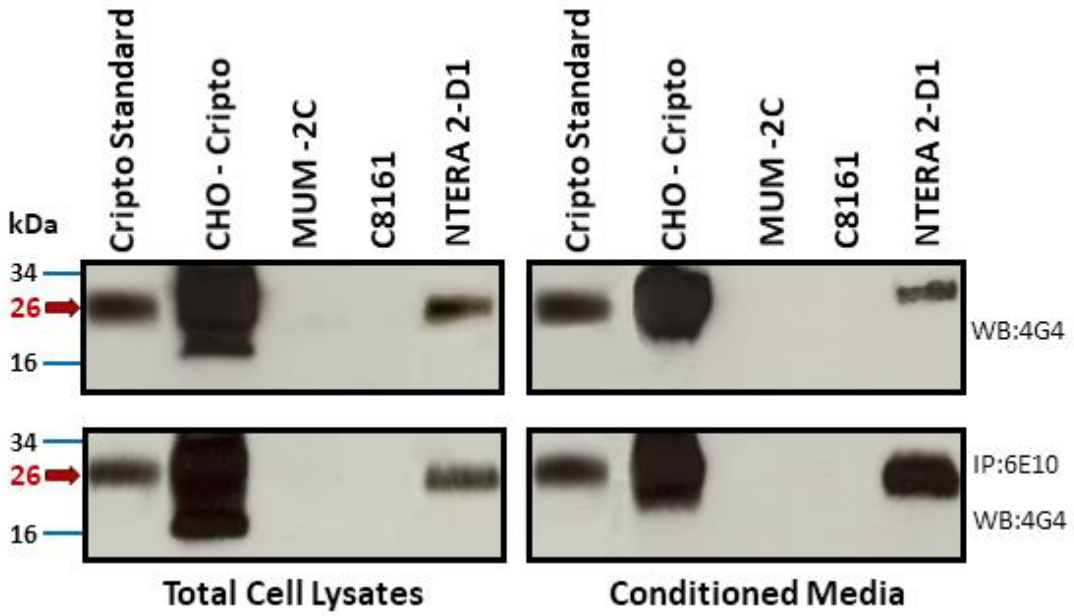

Figure 3. Detection of Cripto Protein in NTERA 2-D1 Testicular Teratocarcinoma Cells. *Representative immunoblot analysis of total cell lysates (left panel) or conditioned media (right panel) derived from CHO-Cripto (Cripto -stably transfected- CHO cells); MUM-2C, C8161, melanomas; and NTERA 2-D1, testicular teratocarcinoma. 3 ng of recombinant Cripto standard was included as a positive control. Samples were probed with 4G4 anti-Cripto MAb (3.45 µg/ml) and secondary anti-Mouse IgG-HRP (1:2000 dilution). A slight improvement in Cripto detection sensitivity was obtained by using 6E10 Cripto MAb for immunoprecipitation (bottom- left and right panels). Data is representative of three independent biological experiments.*

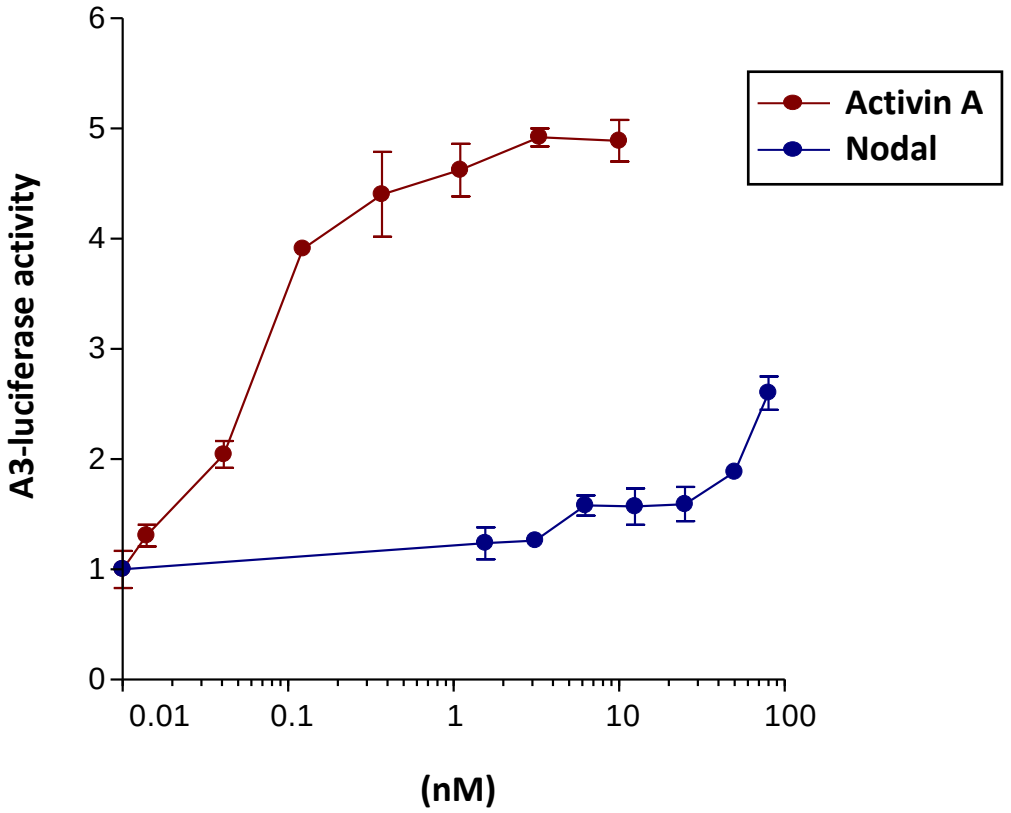

Figure 4. Development of Nodal Dependant Functional Bioassay.
NTERA 2-D1 cells were transfected with Nodal/Smad 2/3 responsive A3-luciferase reporter and stimulated with increasing doses human recombinant, Nodal (depicted in blue), or activin A (depicted in red). Luciferase activity was determined as fold induction relative to control. Data is representative of mean ± SEM, from four independent biological experiments, performed in technical duplicates.

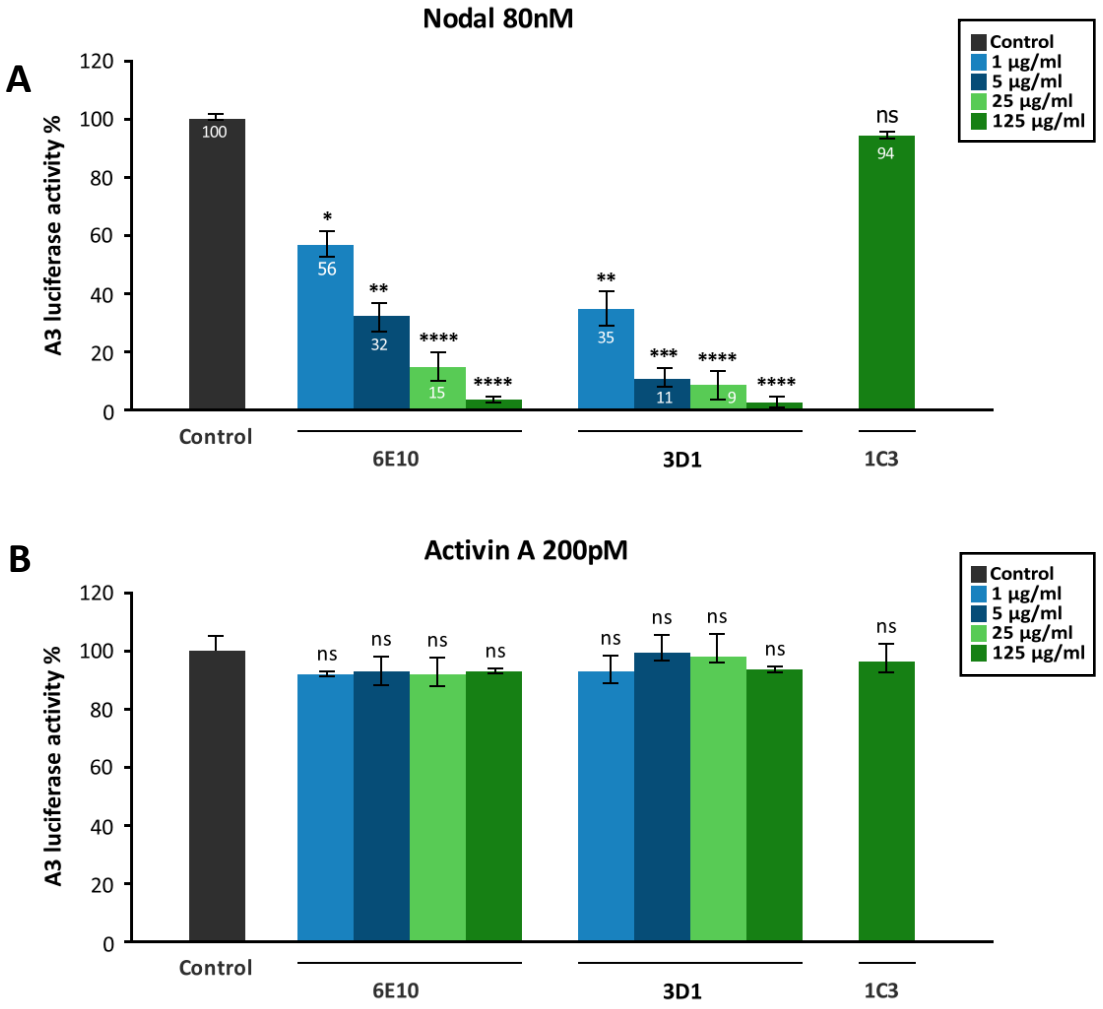

Figure 5. Anti-Cripto MAb Inhibition of Nodal-Induced Luciferase Activity.
*NTERA 2-D1 cells transfected with Nodal induced Smad 2/3 responsive A3- luciferase reporter, were stimulated with recombinant human, Nodal (80 nM), or Activin A (200 pm) with or without increasing doses of 6E10, and 3D1. 1C3 (125 µg/ml) was identified as a non-neutralising anti-Cripto MAb control. Luciferase activity was determined as fold induction % relative to control (PBS vehicle control). Data is representative of mean ± SEM, from four independent biological experiments, performed in technical duplicates. Statistical analysis was performed using one-way ANOVA, with Tukey's multiple comparisons test, (*P<0.05, **P<0.01, ***P<0.001, ****P<0.0001).*

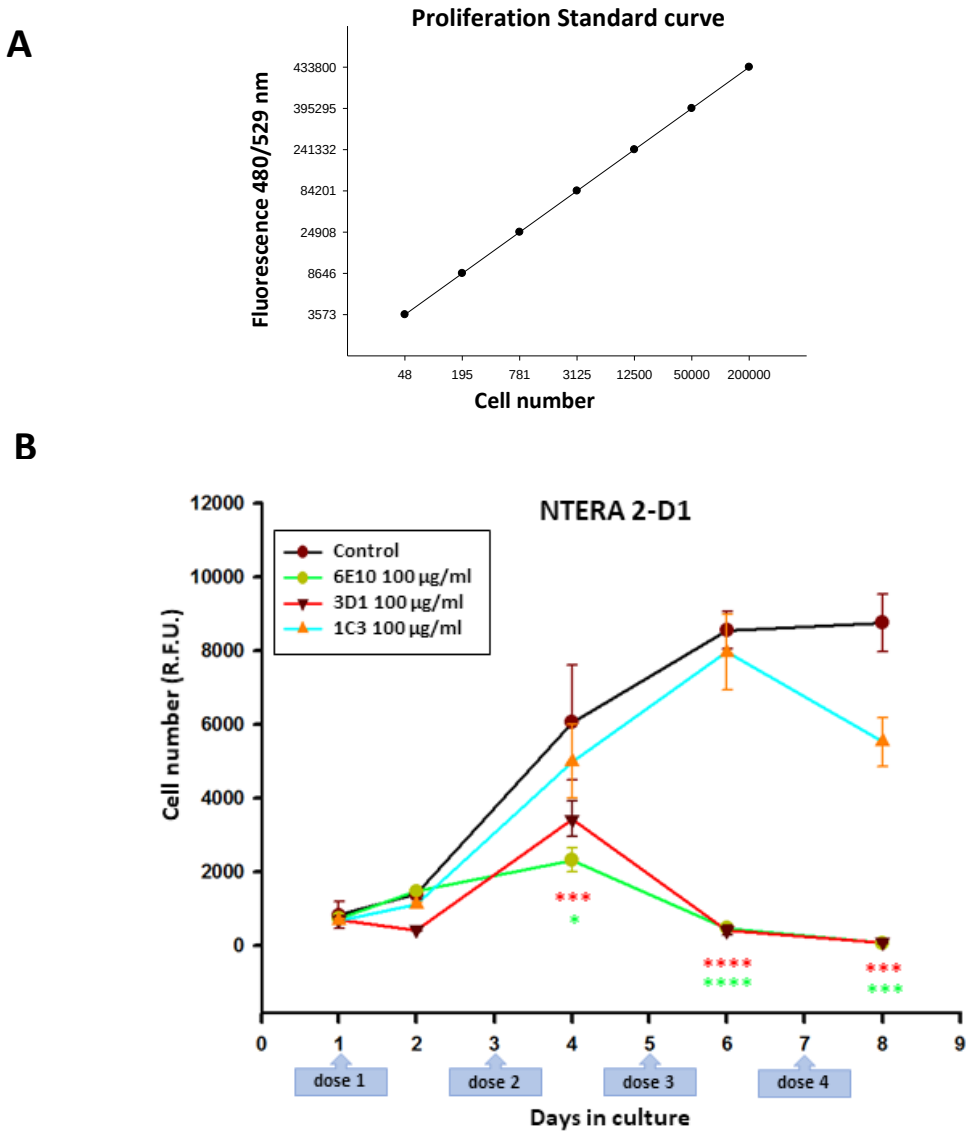

Figure 6. Anti-Proliferative Effects of Cripto MAbs in NTERA 2-D1 cells.

*A) Representative CyQUANT® cell proliferation assay standard curve deduced by measuring fluorescence (480/520mn) of 1x10^6 NTERA 2-D1 cells (serially diluted). Relative cell number was determined using MultiCalc software. B) Graphical representation of NTERA 2-D1 CyQUANT® assay monitored over 8 days in culture upon treatment with 100 µg/ml of: 6E10, 3D1, and 1C3 (non-neutralising control) MAbs or vehicle control (containing PBS). Supplementary MAb treatment every 2 days (indicated in blue boxed arrows). Cell number R.F.U. (relative fluorescence units) was derived by MultiCalc software according to the standard curve. Data is representative of mean ± SEM, from four independent biological experiments, performed in technical triplicates. Statistical analysis was performed using one-way ANOVA, with Tukey's multiple comparisons test, (*P<0.05, **P<0.01, ***P<0.001, ****P<0.0001).*

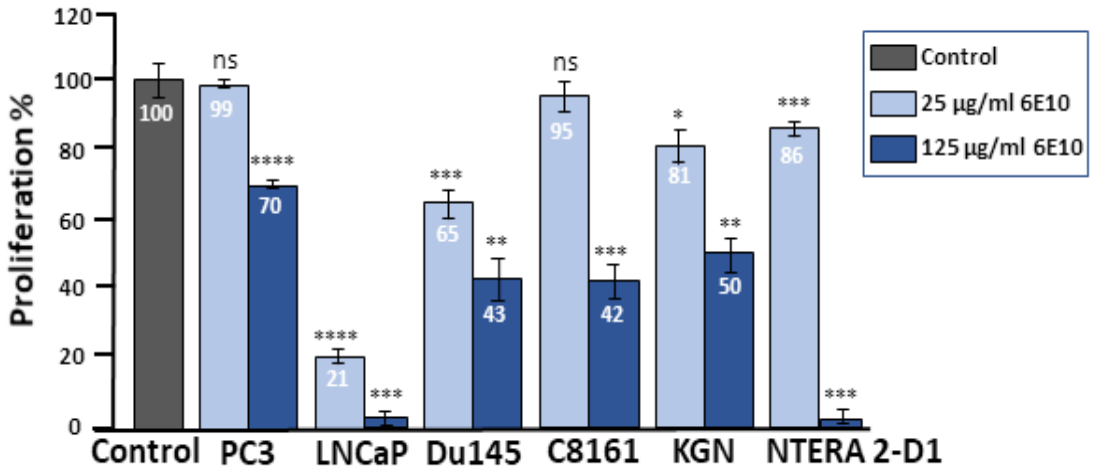

Figure 7. Anti-Proliferative Effects of 6E10 Cripto MAb in cancer cells

*Graphical representation of CyQUANT® proliferation of the following cancer cells: PC-3, LNCaP, DU 145 (prostate); C8161 (melanoma); KGN (ovarian); NTERA 2-D1 (testicular teratocarcinoma), monitored over 8 days in culture. Cells were treated with 6E10 (25 µg/ml, 125 µg/ml) or vehicle control (containing PBS) and proliferation % is expressed relative to control. Non-neutralising 1C3 control did not alter cellular proliferation (data not shown). Data is representative of mean ± SEM, from three independent biological experiments, performed in technical triplicates. Statistical analysis was performed using one-way ANOVA, with Tukey's multiple comparisons test, (*P<0.05, **P<0.01, ***P<0.001, ****P<0.0001).*

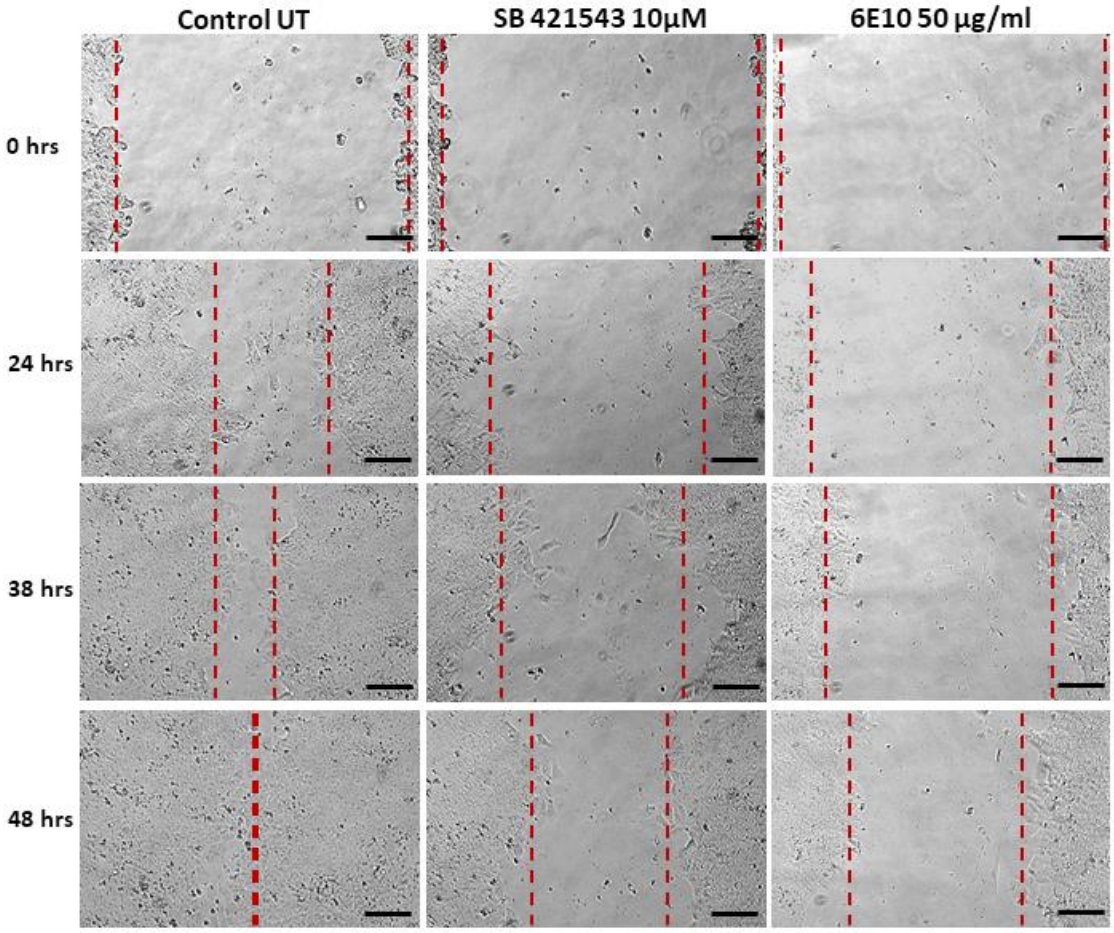

Figure 8. The Effects of 6E10 MAb on NTERA 2-D1 Cell Migration.
In vitro wound-healing, scratch assay of NTERA 2-D1 cells monitored until gap closure. NTERA 2-D1 teratocarcinoma cells, were treated with 10 µM, SB-431542 (TGF-β receptor type I, kinase inhibitor) or 6E10 (50 µg/ml) or untreated (UT) control. Photomicrographs were obtained at 0 hrs, 24 hrs, 38 hrs, 48 hrs, using an OLYMPUS inverted microscope with a 10x objective. Representative images from four independent biological experiments, performed in technical duplicates. Scale bar is equivalent to 25µm.

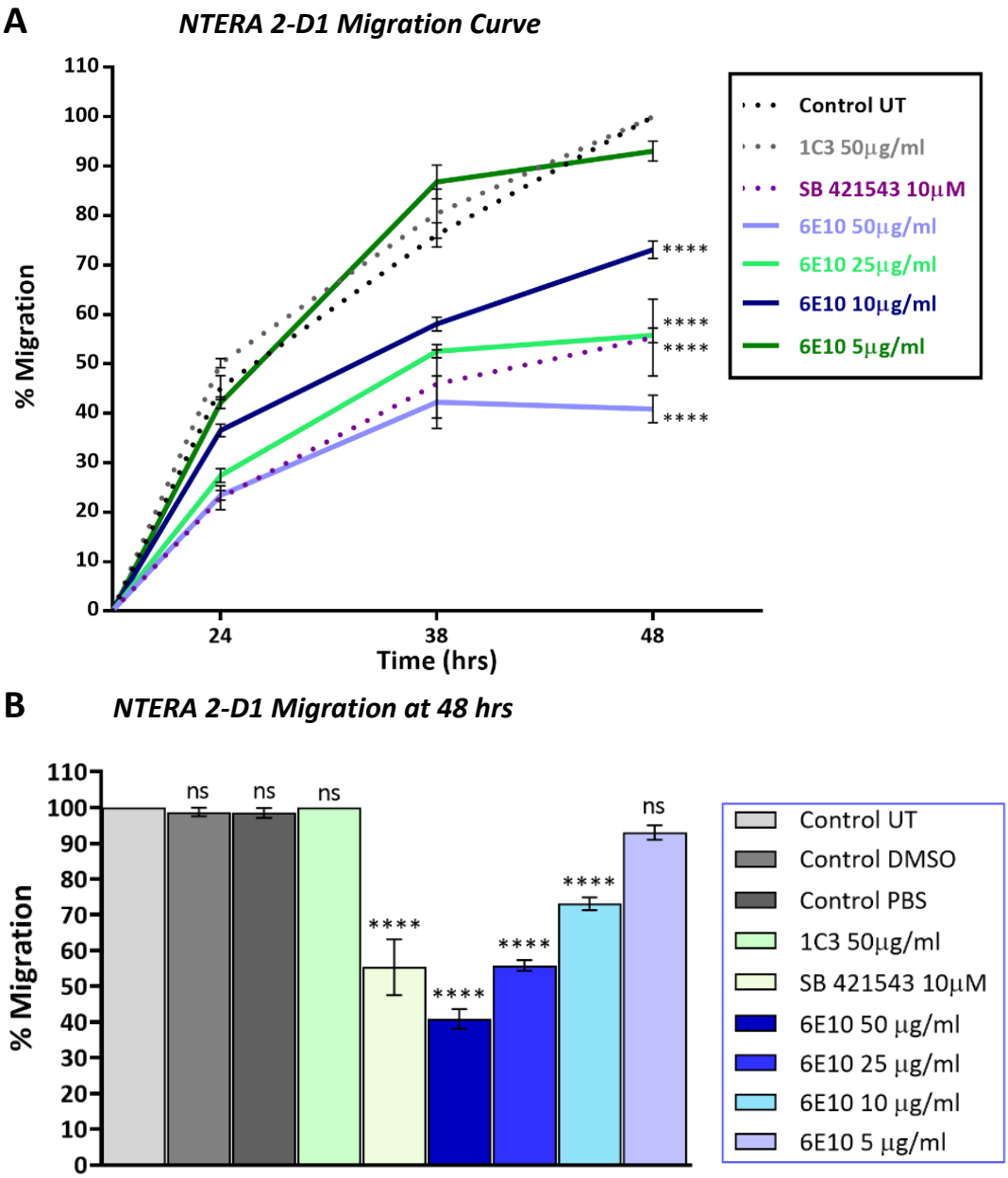

Figure 9. 6E10 MAb Suppression of NTERA 2-D1 Cellular Motility.

Figure 9. 6E10 MAb Suppression of NTERA 2-D1 Cellular Motility.
A) Graphical representation of NTERA 2-D1 cell migration curve, as determined by wound healing-scratch assay, upon anti-Cripto MAb treatment over a 48-hr time course. % Migration is expressed relative to untreated (UT) control. Statistical analysis was performed using one-way ANOVA, with Tukey's multiple comparisons test.
*B) Wound healing quantification at 48 hrs. Statistical analysis was performed using two-way Repeated measures ANOVA, with Uncorrected Fisher's LSD comparisons test, (*P<0.05, **P<0.01, ***P<0.001, ****P<0.0001). The denoted statistical significance is relative to the control UT. Cells were treated with: SB-431542 [(10 µM) TGF-β receptor type I, kinase inhibitor], 6E10 (5-50 µg/ml) and compared to controls: 1C3 [(50 µg/ml), non-neutralising MAb control] untreated (control UT), control PBS (Cripto MAb vehicle control), and control DMSO (SB-431542 vehicle control). Images were acquired using OLYMPUS inverted microscope, with a 10x objective, and cellular migration was quantified using analySIS LS professional software. Data is representative of mean ± SEM, from four independent biological experiments, performed in technical duplicates. Indicated significance relative to untreated control (*P<0.05, **P<0.01, ***P<0.001, ****P<0.0001).*

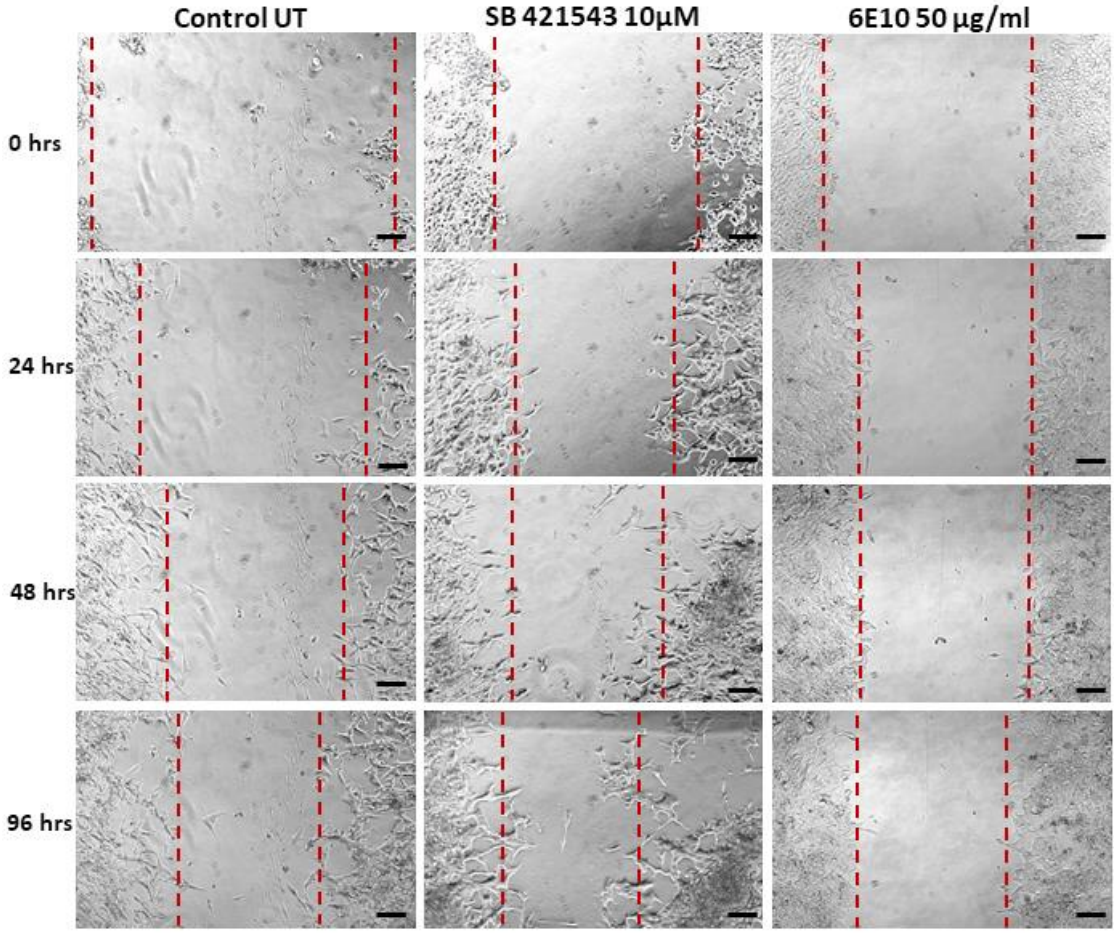

Figure 10. Effects of 6E10 MAb on LNCaP Cancer Cell Migration.
In vitro wound-healing, scratch assay of LNCaP (metastatic prostate cancer) cells monitored until partial gap closure. Cells were treated with 10 µM, SB-431542 (TGF-β receptor type I, kinase inhibitor) or 6E10 (50 µg/ml) or untreated control (UT). Photomicrographs were obtained at 0 hrs, 24 hrs, 48 hrs, 96 hrs using an OLYMPUS inverted microscope with a 10x objective. Representative images from three independent biological experiments, performed in technical duplicates. Scale bar is equivalent to 25 µm.

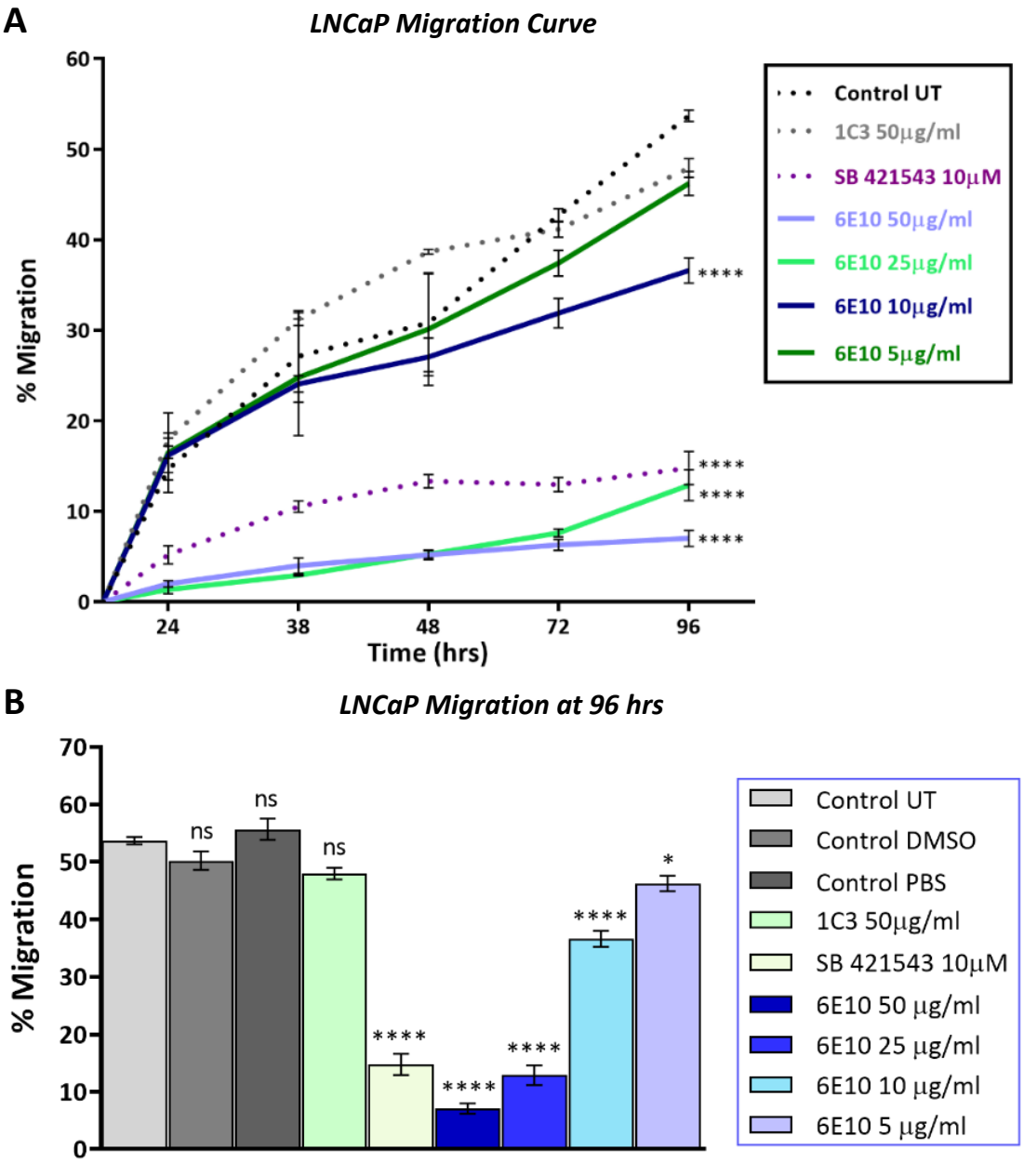

Figure 11. 6E10 MAb Suppression of LNCaP Cellular Motility Quantification.

Figure 11. 6E10 MAb Suppression of LNCaP Cellular Motility Quantification.
A) Graphical representation of LNCaP migration curve determined by wound healing-scratch assay, upon anti-Cripto MAb treatment over a 96-hr time course. % Migration is expressed relative to untreated control (Control UT).
*B) Wound healing quantification at 96 hrs. Statistical analysis was performed two-way Repeated measures ANOVA, with Uncorrected Fisher's LSD comparisons test. Cells were treated with: SB-431542 [(10 µM) TGF-β receptor type I, kinase inhibitor], 1C3[(50 µg/ml), non-neutralising MAb control], 6E10 (5-50 µg/ml) and compared to controls: untreated (control UT), control PBS (Cripto MAb vehicle control), and control DMSO (SB-431542 vehicle control). Images were acquired using OLYMPUS inverted microscope with a 10x objective and cellular migration was quantified using analySIS LS professional software. Data is representative of mean ± SEM, from four independent biological experiments, performed in technical duplicates. Indicated significance relative to untreated control (*P<0.05, **P<0.01, ***P<0.001, ****P<0.0001).*

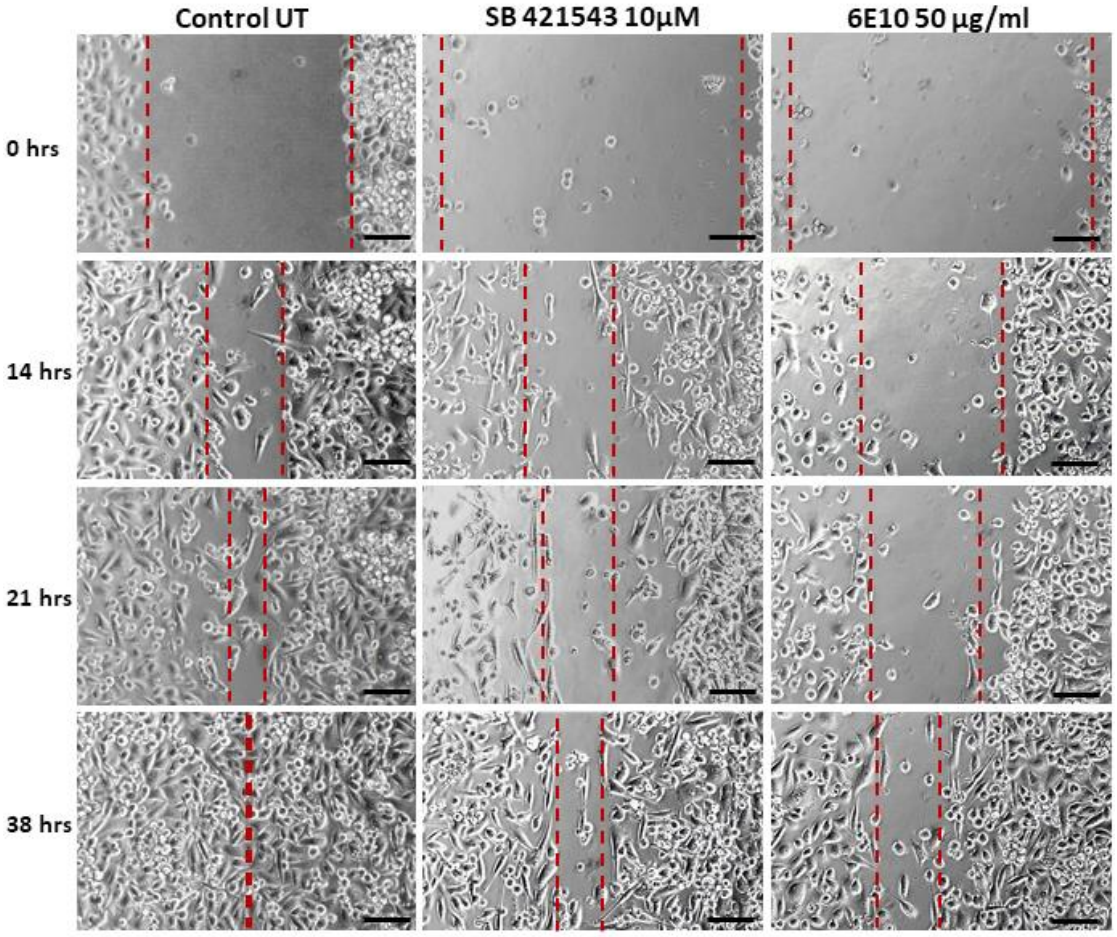

Figure 12. Effects of 6E10 MAb on PC-3 Cancer Cell Migration.
In vitro wound-healing, scratch assay of PC-3 (prostate cancer) cells monitored until gap closure was reached. Prostate cancer cells were treated with 10 µM, SB-431542 (TGF-β receptor type I, kinase inhibitor) or 6E10 (50 µg/ml) or untreated control (UT). Photomicrographs were obtained at 0 hrs, 14 hrs, 21 hrs, 38 hrs using an OLYMPUS inverted microscope with a 10x objective. Representative images from three independent biological experiments, performed in technical duplicates. Scale bar is equivalent to 25µm.

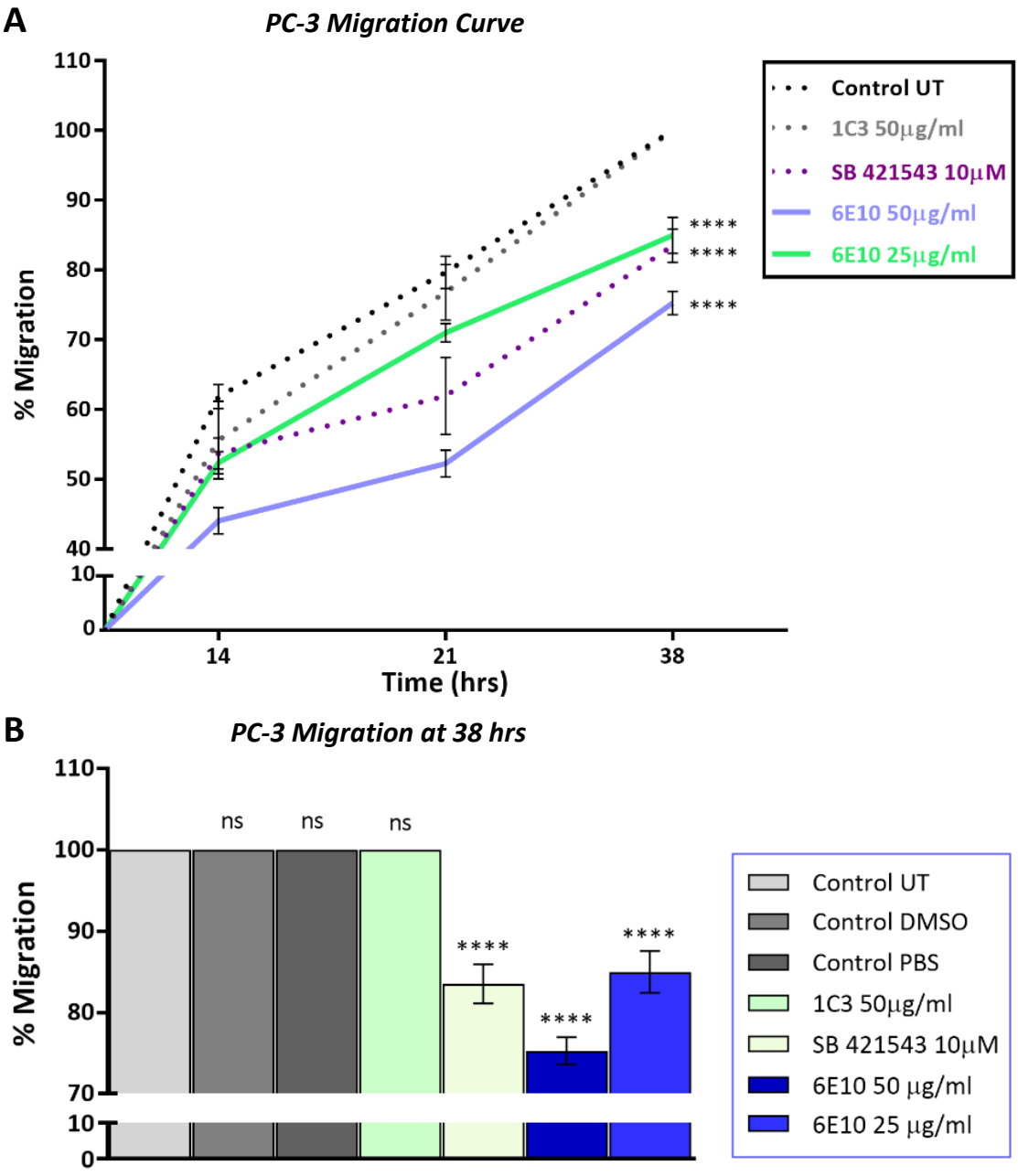

Figure 13. 6E10 MAb Suppression of PC-3 Cellular Motility Quantification.

Figure 13. 6E10 MAb Suppression of PC-3 Cellular Motility Quantification.

A) Graphical representation of PC-3 cellular migration curve determined by wound healing-scratch assay, upon Cripto MAb treatment over a 38-hr time course. % Migration is expressed relative to untreated control (Control UT). Statistical analysis was performed using one-way ANOVA, with Tukey's multiple comparisons test.

*B) Wound healing quantification at 38 hrs. Statistical analysis was performed using two-way Repeated measures ANOVA, with Uncorrected Fisher's LSD comparisons test. Cells were treated with: SB-431542 [(10 µM) TGF-β receptor type I, kinase inhibitor], 1C3[(50 µg/ml), non-neutralising MAb control], 6E10 (25-50 µg/ml) and compared to controls: untreated (control UT), control PBS (Cripto MAb vehicle control), control DMSO (SB-431542 vehicle control). Images were acquired using OLYMPUS inverted microscope with a 10x objective and cellular migration was quantified by gap closure measurements using analySIS LS professional software. Data is representative of mean ± SEM, from four independent biological experiments, performed in technical duplicates. Indicated significance relative to untreated control (*P<0.05, **P<0.01, ***P<0.001, ****P<0.0001).*

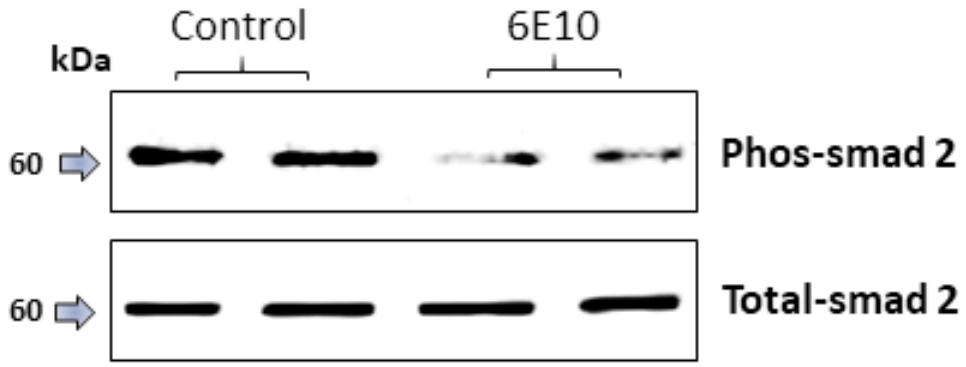

Figure 14. 6E10 Cripto MAb Supresses Smad 2/3 Phosphorylation.
Phosphorylation of Smad 2/3 was monitored by western blotting. Cell lysates derived from testicular teratocarcinoma NTERA 2-D1 cells, treated with 6E10 (100 µg/ml), or control (containing PBS as vehicle control) for 30 mins, were subjected to 10 % SDS-PAGE run in duplicate lanes. Immunobloting was performed with anti-Phospho Smad 2/3 or anti-Smad2 (1:2000 in 1% BSA/TTBS) and secondary probing with anti-rabbit IgG, HRP-linked antibody (1:2000 in 1% BSA/TTBS). Enhanced chemiluminescence was detected with ChemiDoc™ MP System and Image was acquired using Image Lab™ software. Data is representative of three independent biological experiments.

Supplementary Figure 1

	Anti-Cripto MAbs			
Cripto Detection Technique	***4G4***	***3D1***	***6E10***	***1C3***
WB	+	+	-	-
IP	+	-	+	-
Biacore *monomer*	+ moderate	+ very high	+ moderate	+ very weak
Biacore *denatured*	+ moderate	+ high	+ moderate	-
Biacore *dimer*	-	+ moderate	-	-
FACS	+	+	+	n/e
IHC	+	+	n/e	n/e
IF	+	n/e	n/e	n/e

Supplementary Figure 1. Characterisation Summary of Cripto Monoclonal Antibodies.

Supplementary Figure 1. Characterisation Summary of Cripto Monoclonal Antibodies. *Anti-Cripto MAbs generated from hybridoma spleen cells of mice (Balb/C) immunised with recombinant Cripto, where provided by Associate Professor Martin Lackmann. The ability of 4G4, 6E10, 3D1 and 1C3 antibodies to bind to Cripto protein was characterised by Associate Professor Martin Lackmann and results are summarised in this table (L. Kravets et al., unpublished work). Positive binding to Cripto protein is represented by the **+** sign, whereas negative binding is represented by the **–** sign. Detection of denatured (26kDa) or native Cripto protein was conducted by Western blot and immunoprecipitation of NTERA 2-D1 total cell lysates and condition media. MAbs were screened by Biacore for detection of monomeric, dimeric and denatured, Cripto protein respectfully. The effectiveness of anti-Cripto MAbs to recognise endogenous Cripto protein was assessed by FACS analysis of NTERA 2-D1 cells. 4G4 and 3D1 antibodies were utilised in immunofluorescence staining of MEFs (mouse embryonic fibroblasts) as well as HC-11 (mouse mammary epithelial) cells. 4G4 MAbs detected Cripto protein in immunohistochemical studies of pregnant and lactating mouse mammary epithelial cell tissues, as well as in human colon cancer tissues and breast cancer tissues. Data summary compiled with the permission of the late Associate Professor Martin Lackmann (41). WB, Western blot; IP, Immunoprecipitation; IHC, Immunohistochemistry; IF, Immunofluorescence; n/e, not examined.*

Chapter 4

The Anti-Tumourigenic roles of Interferon Epsilon in Endometrial Cancer

"Others have seen what is and asked why. I have seen what could be and asked why not".

-Pablo Picasso

Chapter 4

4.1 Declaration

In the case of Chapter 4, my contribution to the work involved the following:

Thesis Chapter	Publication Title	Status	Nature and % of student contribution	Co-author name(s) Nature and % of Co-author's contribution*	Co-author(s), Monash student
4	*The Anti-Tumourigenic roles of Interferon Epsilon in Endometrial Cancer*	*Prepared for submission*	Involved in project conception, design, performed experiments, as well as data analysis and prepared the manuscript. **80%**	1) Antony Y. Matthews (**0.5%**), 2) San Lim (**0.5%**) and 3) Nicole A deWeerd (**1%**): involved in the preparation of r-hIFNε and r-mIFNε 4) Nollaig Bourke (**9%**) and 5) Paul J Hertzog (**9%**): involved in the project design and conception, provided intellectual input and manuscript revision.	**No**

Student signature: [redacted] **Date:** 23/08/2018

The undersigned hereby certify that the above declaration correctly reflects the nature and extent of the student's and co-authors' contributions to this work. In instances where I am not the responsible author I have consulted with the responsible author to agree on the respective contributions of the authors.

Main Supervisor signature: [redacted] **Date:** 23/08/2018

The Anti-Tumourigenic roles of Interferon Epsilon in Endometrial Cancer - Manuscript

Irene Papageorgiou [1,2*], Antony Y. Matthews [1,2], San Lim [1,2], Nicole A deWeerd [1,2], Nollaig Bourke [1,3*], Paul J Hertzog [1,2*]

1. Centre for Innate Immunity and Infectious Diseases, Hudson Institute of Medical Research, Clayton, Victoria, Australia;

2. Department of Molecular and Translational Sciences, Monash University, Clayton, Victoria, Australia;

3. Department of Medical Gerontology, School of Medicine, Trinity Translational Medicine Institute, Trinity College Dublin, Ireland;

IP: irene.papageorgiou@hudson.org.au

AYM: antony.matthews@hudson.org.au

SL: san.lim@hudson.org.au

NAD: Nicole.deweerd@hudson.edu

NB: nbourke@tcd.ie

PJH: paul.hertzog@hudson.org.au

* These authors contributed equally to this work. To whom correspondence should be addressed.

Postal: Centre for Innate Immunity and Infectious Diseases, Hudson Institute of Medical Research, 27-31 Wright Street, Clayton, VIC 3168, Australia

Abstract

Background: Type I interferons (IFNs) are a family of cytokines displaying key regulatory roles in immunity and cancer. The discovery of Interferon Epsilon (IFNε) revealed a unique type I IFN with constitutive expression within the mouse female reproductive tract (FRT), associated with regulation of mucosal immunity against infections with viral and bacterial STIs. Further evidence suggested that IFNε may have anti-proliferative functions within the mouse uterine epithelium, properties yet to be investigate in human FRT cancer. We thus hypothesised that IFNε displays intrinsic anti-tumourigenic properties in the human FRT. This study aimed to investigate the *in vitro* effects of IFNε on FRT epithelial cancer cells.

Methods and Results: Induction of interferon-regulated gene mRNA was quantified by qRT-PCR in FRT cancer cells (vaginal, cervical, and endometrial) stimulated with recombinant IFNε. IFNε down-regulated anti-apoptotic genes and up-regulated pro-apoptotic genes in all cell types examined. Interestingly, IFNε significantly suppressed cellular proliferation of both lower FRT epithelium VK2 (vaginal) and Ect1 (ectocervical); as well as high grade endometrial cancer cells RL95-2 and AN3CA, monitored in real-time using xCELLigence assays. The effect of IFNε treatment on apoptosis was further assessed using FACS analysis with Annexin-V and PI staining, TUNEL staining and Caspase - 3/7 assays. Our results demonstrate that IFNε induces apoptosis upon 72 hrs of treatment associated with increased Caspase 3/7 activity. Furthermore, IFNε increases the percentage of TUNEL-positive apoptotic cells accompanied by DNA fragmentation by 96 hrs of stimulation.

Conclusions: Our findings suggest that IFNε treatment dramatically suppresses epithelial cancer cell proliferation and induces apoptosis. This study characterises the anti-tumourigenic properties IFNε and supports its potential use as a novel therapeutic agent in vaginal, cervical and endometrial cancers.

Introduction

Gynaecological cancers of the upper and lower female reproductive tract (FRT) are an important cause of morbidity and mortality worldwide [1]. FRT cancers include the most common ovarian, cervical, uterine (endometrial); as well as the rare vulva, vaginal, fallopian tube, placenta; and comprise the third most common diagnosed female malignancy [2]. In 2017, it was estimated that 1,769 deaths occurred from gynaecological cancer within Australia [2]. There is currently no early detection test and available therapies are limited to drastic hysterectomy in combination with chemotherapy and radiotherapy. Although the 5-year survival rate is 69% when gynaecological cancer is diagnosed at an early stage, survival rate is poor with high grade diagnosis or recurrent disease. In addition, the Fertility ramifications of woman undergoing current treatments are grave [2]. Thus, highlighting the importance of new diagnostic techniques as well as development of fertility sparing and improved therapeutic options for gynaecological cancer.

Endometrial cancer is the most common invasive gynaecological malignancy in the developed world with 320,000 new cases diagnosed in 2012 [1]. Type I endometrial cancer, also known as endometroid, is the most common type, occurring in 70-85% of cases and generally afflicts younger women (pre/peri-menopausal) [3]. Type I endometroid cancers of early stage or low grade (grade I), usually have a favourable prognosis compared to highly aggressive grade II or grade III tumours with poorer clinical outcomes and associated deaths [2]. There is currently no early detection test for endometrial cancer and diagnosis is often carried out by histopathological examination of endometrial biopsies [4]. Extensive surgery may be required for advanced FIGO stage disease and high-grade subtypes including hysterectomy and salpingo-opherectomy, in conjunction with radiation therapy and/or chemotherapy are to date the current treatment options [5-7]. Additionally, young women diagnosed with endometrial

cancer, will suffer grave ramifications to their fertility. It is thus evident that development of new diagnostic and treatment options are of vital importance.

Cervical carcinogenesis has been largely attributed to persistent sexually transmitted infections such as human papillomavirus (HPV) and *Chlamydia trachomatis* [8, 9]. Cervical cancer treatments consist of hysterectomy in conjunction with radiation therapy and/or chemotherapy in accordance with disease stage [11]. Utilization of cervical screening by Pap smear as well as administration of the HPV vaccine have contributed to reduced rates of cervical malignancies [10, 11]. HPV infection has also been associated with the pathogenesis of vaginal cancer [12]. For this rarer lower FRT malignancy there are no early diagnostic tests and prognosis is also dependent on disease stage. Disease management is challenging as therapeutic options are limited to surgery and radiotherapy [13, 14].

The cycling reproductive tract, particularly the endometrium, is unique in its capacity to undergo cellular remodelling events of proliferation and differentiation, in a tightly regulated manner under the hormonal control of estrogen and progesterone [15]. Innate and adaptive immune cells within the FRT are crucial in establishing homeostatic mechanisms including prophylaxis from sexually transmitted infection, fertilization, embryo implantation and pregnancy [16]. Modulation of such complex processes is essential for maintaining a healthy and fertile endometrium, coordinated by a large network of cytokine signalling with in the uterine microenvironment [17]. A cytokine that is emerging as a key regulator of cellular response within the FRT is interferon epsilon (IFNε).

IFNε was first discovered by our group [18] and belongs to the type I interferon (IFN) family of cytokines, which are well documented for their key regulatory roles in immunity and cancer [18, 19]. Our group found that in contrast to conventional type I IFNs, IFNε

is constitutively expressed at high levels by epithelial cells of the FRT in both mice and human and expression is uniquely regulated by hormones [20,21]. In these studies, IFNε-deficient mice presented increased susceptibility to vaginal infection by *Herpes Simplex Virus 2* and *Chlamydia muridarum* suggesting that IFNε exhibits essential prophylactic roles with in the FRT epithelium against sexually transmitted infections. However, unlike other type I IFN family members its expression is not affected by pathogen response [20]. IFNε has been characterized to mediate signal transduction via the canonical IFN type I signalling pathway [22-24]. Engagement of IFNε with IFN type I receptor, composed of the subunits IFNAR1 and IFNAR2, leads to activation of JAK/STAT pathway followed by induction of ISG (interferon stimulated gene) transcription to elicit biological functions [21,22,25].

Preliminary studies conducted in our lab suggested that loss of IFNε increased the proliferation propensity of primary mouse uterine epithelial cells compared to homologous wild type control cells [Bourke NM and Mangan NE, unpublished]. Subsequently, further evidence showed that IFNε was down regulated in fallopian tissues of HGSC (High Grade Serous Carcinoma) patients compared to healthy controls [*Marks et al.*, submitted]. This suggests that IFNε has potentially important intrinsic anti-proliferative roles within the FRT epithelium and that is suppression may favour tumour development. However, the direct anti-tumourigenic roles of IFNε have not yet been studied in FRT cells outside the ovary. Furthermore, the precise mechanisms by which IFNε may regulate such cellular processes have not been examined in detail.

Current type I IFN based therapies, using the classical type I IFNs IFNα and IFNβ, have been successful in eliminating a broad range of malignancies including leukemia, melanoma and breast cancer, however due to detrimental side effects and systemic toxicity observed in patients, they are unfavourable long-term cancer treatments [19, 27-29]. In contrast, the unique properties of IFNε render it particularly pertinent to endometrial cancer treatments as well as other FRT cancers, as IFNε is constitutively

expressed within the FRT suggesting that it may be well tolerated. The potential of IFNε in therapeutic development of FRT cancers would require further investigation. We hypothesised that IFNε displays key anti-tumourigenic roles within the FRT epithelium. This study aimed to investigate the *in vitro* effects of IFNε on FRT epithelial cancer cell lines and to examine the role of IFNε in endometrial, vaginal and cervical cancer cell development.

Methods

Cell Lines

Human epithelial cells of lower FRT origin: VK2 [vaginal (ATCC® CRL-2616™)], Ect1 [ectocervical (ATCC® CRL-2614™)] and End1 [endocervical (ATCC® CRL-2615™)] were kindly provided by Professor Gilda Tachedjian (Burnet Institute Melbourne). These cell lines were maintained in Keratynocyte-SFM (serum free medium), supplemented with 0.2ng/ml of human rEGF (recombinant epidermal growth factor), 20 µg/ml of rBPE (recombinant bovine pituitary extract), 1% Antibiotic-Antimycotic (Gibco, Life Technologies). Grade I- derived ECC-1 (ATCC® CRL-2923™) endometrial cancer cells were kindly provided by Dr Hong Nguyen (Hudson Institute of Medical Research) and propagated in DMEM F12 -(without phenol red) supplemented with 10% heat inactivated FCS (fetal calf serum) and 1% Antibiotic-Antimycotic (Gibco, Life Technologies). Grade II-derived endometrial carcinoma epithelial cells RL95-2 (ATCC® CRL-1671™), were generously supplied by Yao Wang (Professor Guiying Nie, Implantation and Placental Development laboratory, Hudson Institute for Medical Research) and were cultured in DMEM F12 supplemented with 10% heat inactivated FCS and 1% Antibiotic-Antimycotic (Gibco, Life Technologies). Grade III-derived endometrial carcinoma epithelial cells AN3CA (ATCC® HTB-111™), were generously provided by Dr Amy Winship (Professor Eva Dimitriadis, Embryo Implantation Laboratory Hudson

Institute for Medical Research), and propagated in MEM (Minimum Essential Medium) supplemented with 10% heat inactivated FCS and 1% Antibiotic-Antimycotic (Gibco, Life Technologies). All cells were maintained in a humidified incubator at 37°C, 5% CO_2 (for general tissue culture procedures refer to Appendix C, p263-264). Mycoplasma testing of all cell lines was performed by the Laboratory and Technical Services at Hudson Institute for Medical Research using MycoAlert PLUS Mycoplasma Detection Kit (Lonza). Authentication and identification of cell lines was performed by short tandem repeat profiling analysis carried out by the Medical Genomics facility at Monash Health Translational Precinct (see Appendix D and E, p265-278).

Recombinant IFNs and stimulations

Recombinant human and murine IFNε (r-hIFNε; r-mIFNε) utilized in interferon stimulations for *in vitro* assaying of FRT epithelial cancer cell lines, were both generated by our laboratory. Low endotoxin concentration was confirmed by ToxinSensor Endotoxin Assay (Genscript) as previously described [30]. Buffer control (B.control) treatments without recombinant hIFNε protein (20mM Phosphate Buffer pH 6, 150 mM NaCl, 0.8M L-Arginine) were also included in order to exclude buffer effects on cell assays. Additionally, recombinant human IFNβ (r-hIFNβ) Rebif® (Merk Serono) was also used as detailed in each study below.

IFN stimulations for gene induction analysis

FRT epithelial cancer cells were plated at a density of $1.5x10^5$ cells/well in a 12 well plate in 500 µl of complete medium. Lower FRT cancer cells VK2 (vaginal), Ect1 (ectocervical) and End1 (endocervical); as well as ECC-1 endometrial cancer cells, were stimulated with r-mIFNε (100 IU/ml) for 3 hrs; whereas, RL95-2 and AN3CA (endometrial cancer cells of upper FRT) were stimulated with r-mIFNε (1000 IU/ml) for 24 hrs, prior to mRNA extraction.

mRNA extraction

Total RNA was extracted using the RNeasy Mini Kit (Qiagen) according to the manufacturer's instructions. Cells were lysed in 350 µl of β-mercaptoethanol/buffer RLT and homogenized by syringing up and down through a 25-gauge needle (10 times). 350 µl of 70% ethanol was added to the lysate, thoroughly mixed, and transferred to a RNeasy spin column. The sample was centrifuged for 15 secs at 8000 x g and the flow through discarded. The column was washed with 700 µl buffer RW1 and centrifuged for 15 secs at 8000 x g and the flow through discarded. The column was washed with 500 µl of buffer RPE, centrifuged for 15 secs at 8000 x g and the flow through was discarded. An additional 500 µl of buffer RPE was added, centrifuged for 2 mins at 8000 x g and the flow through was discarded. The column was then transferred to a fresh 2 ml collection tube and centrifuged for 1 min, at 8000 x g. RNA was eluted by addition of 30 µl RNase-free water to the column and centrifugation for 1 min at 8000 x g. Eluted RNA was added back to the column and centrifuged for the second time at 8000 x g, 1 min to increase yield. The RNA was stored at -80°C. RNA yield and quality assessments were carried out using NanoDrop, ND-1000 spectrophotometer (Analytical Technologies).

DNase treatment of RNA sample

To remove genomic DNA, the RNA sample was treated with DNase. 500 ng of purified RNA was diluted in 7 µl of Nuclease-Free Water (Ambion) and 2 µl of 5 x MMLV buffer (Promega) together with 1 µl of RQ1 DNase (Promega) were added to each reaction sample. The sample was then incubated at 37°C for 30 mins. The reaction was ceased by addition of 1 µl DNase Stop solution (Promega) and incubation at 65°C for 15 mins. To remove condensation the sample was placed on ice for 2 mins and centrifuged for 1 min at 8000 x g.

cDNA synthesis

DNase treated RNA samples were equally divided between two tubes: reverse transcription positive reaction (RT+) and reverse transcription negative control reaction (RT-). The following reagents were added to each reaction: 1 µl (500 ng) of random hexamers (Promega), 2 µl of 10 mM dNTP (Bioline), 4 µl M-MLV 5 X Reaction Buffer, 7.5 µl Nuclease-Free Water (Ambion) and 0.5 µl of M-MLV Reverse Transcriptase (Promega) in the RT+ tube, or 0.5 µl Nuclease-Free Water (Ambion) in the RT- tube. The samples were incubated at 37°C for 1 hr, followed by enzyme inactivation at 70°C for 15 mins. The cDNA was stored at -20°C.

18s rRNA quality control PCR

18s ribosomal RNA (rRNA) PCR was performed on cDNA samples from both RT+ and RT- samples to determine cDNA quality and eliminate presence of genomic contamination. 1 µl of cDNA (both RT+ and RT-) was added to 12.5 µl of GoTaq Green Master Mix, 2 x (Promega), 1 µl of each forward and reverse 18s rRNA primers (10 µM) and the final reaction volume was adjusted to 25 µl with Nuclease-Free Water (Ambion). PCR was then performed using MyCycler Thermal Cycler (Bio-Rad) according to the cycle reaction parameters denoted in table 1. PCR products were visualized by electrophoresis on 1.5 % w/v agarose gel, run at 100 V for 30 mins.

Table 1. PCR Cycle Reaction Parameters.

Stage 1 x 1 cycle	Step 1	94°C, 2 mins	
Stage 2 x 35 cycles	Step 1	94°C, 30 secs	*primer denaturation*
	Step 2	55°C, 30 secs	*primer annealing*
	Step 3	72°C, 30 secs	*primer extension*
Stage 3 x 2 cycles	Step 1	72°C, 7 mins	*final primer extension*
	Step 2	20°C, hold	

Agarose gel electrophoresis

qRT-PCR samples were loaded on a 1.5 % w/v agarose (promega) gel/ 1 x TAE buffer [40 mM Tris-HCl (pH 8.0), 20 mM acetic acid, 1 mM EDTA (pH 8.0) in MQ water] containing 1:30 dilution of SYBR Safe DNA gel stain (Life Technologies) for visualization of bands. The gel was electrophoresed in 1 x TAE buffer at 100 V for 30 mins. Band size was determined according to 100 kb DNA ladder (NEB). Bands were visualized in a Safe Imager Blue Light Transilluminator (Invitrogen, LifeTechnologies, Thermo Fisher Scientific) and images acquired using Quantum ST4-100 camera (VILBER) and saved electronically via QUANTUM-capt image software.

qRT-PCR

Primers were designed to be intron-spanning, were possible, using primer-BLAST/NCBI software (refer to table 2 for primer sequences). 2 µl of cDNA [diluted 1:10 in Nuclease-Free Water (Ambion)] was aliquoted in triplicate into a 384 well plate (Applied Biosystems). To each reaction 0.2 µl of 10 µM forward primer, 0.2 µl of 10 µM reverse primer, 5 µl of SYBR Magic Master Mix (Invitrogen, LifeTechnologies, Thermo Fisher Scientific) and 2.6 µl of Nuclease-Free Water (Ambion) were added to a final reaction volume of 10 µl. Plates were sealed with MicroAmp optical adhesive film (Applied Biosystems), centrifuged at 800 x g for 3 mins (Heraeus Multifuge 3RS Plus centrifuge) and then subjected to PCR on a 7900HT Fast Real-Time PCR machine (Applied Biosystems) according to the thermal cycling profile parameters described in table 3. Ct (cycle threshold) values were analysed using SDS 2.4 software (Applied Biosystems) and expression levels of all genes were normalised against the corresponding expression of *18s* rRNA (housekeeping gene). Relative expression level was determined using $2^{-\Delta\Delta ct}$ method to determine fold induction of IFN stimulated samples relative to the unstimulated samples [31]. Alternatively, mRNA expression levels were deduced using the 2^{-CT} method and expressed as a ratio to 2^{-CT} 18s. Three independent biological experiments were performed in technical triplicates. Statistical analysis was performed using one-way ANOVA with Tukey's multiple comparisons or Dunnett's multiple comparisons test, (*P<0.05, **P<0.01, ***P<0.001, ****P<0.0001).

Table 2. Primer Sequences.

Human Gene Name	Primer	Primer Sequence (5'-3')
18s	F	GTAACCCGTTGAACCCCATT
	R	CCATCCAATCGGTAGTAGCG
MXA	F	GGTGGTGGTCCCCAGTAATG
	R	ACCACGTCCACAACCTTGTCT
CXCL10	F	TTCCTGCAAGCCATTTTGT
	R	TTCTTGATGGCCTTCGATTC
OAS2	F	GAAGCCCTACGAAGAATGTCAGA
	R	TCGGAGTTGCCTCTTAAGACTGT
ISG15	F	GCGAACTCATCTTTGCCAGT
	R	AGCATCTTCACCGTCAGGTC
IFNE	F	AGGACACACTCTGGCCATTC
	R	CTCCCAACCATCCAGAGAAA
IFNAR1	F	AGTGCCTCCACGCCTTTTTA
	R	GCTTGTACGCGGAGAAGGTA
IFNAR2	F	GCGAGAGCTGCAAAGATGTAA
	R	GGCATTCTGGCTCAAAAGCA
TAP1	F	CCTGTGGCACAAACTCGGG
	R	ATCTCCCCAAGAGAGGAGAGGA
BCL-2	F	AGGATAACGGAGGCTGGGATG
	R	TGATGCAAGCTCCCACCAG
CDC20	F	ATTCCCAGGTGTGCTCCATC
	R	GCCATGGTTGGGTACTTCCA
CASP1	F	GCCTGTTCCTGTGATGTGGA
	R	TTCACTTCCTGCCCACAGAC
ISG12A	F	ATCGCCTCGTCCTCCATA
	R	TGGCATGGTTCTCTTCTCT

Table 3. qRT-PCR Cycle Parameters.

Stage 1	50°C, 2 mins	*primer annealing*
Stage 2	95°C, 10 mins	*primer denaturation*
Stage 3 x 40 cycles	95°C, 15 secs	*primer denaturation*
	60°C, 1 min	*primer annealing*
Stage 4	95°C, 15 secs	*primer dissociation*
	60°C, 15 secs	
	95°C, 15 secs	

Cell Viability MTT assay

Cell viability was measured by colourimetric enzyme based MTT assay [32]. This technique relays on tetrazolium salt (MTT), which is reduced to a formazan product by mitochondrial enzyme succinate dehydrogenase reducing enzymes present only in metabolically active viable cells [32]. VK2 (vaginal) and Ect1 (ectocervical) epithelial cells were seeded in 96 well microplates at a cell density of $5x10^3$ cells/well and stimulated with r-hIFNε (1000-125 IU/ml), r-hIFNβ (1000 IU/ml), r-mIFNε, B.control (buffer control volume equivalent to the highest IFN treatment) including US control (unstimulated control cells) for 72 hrs. Cells were then incubated with 0.5 mg/ml of MTT reagent [3-(4, 5-Dimethylthiazol-2-yl)-2, 5-diphenyltetrazolium bromide (Sigma Aldrich)] for 3 hrs at 37°C. The supernatant was aspirated and MTT crystals were dissolved in DMSO (dimethyl sulfoxide). Absorbances were measured at 590 nm using a FluoStar OPTIMA plate reader (BMG Labtech).

Proliferation assay

Cellular proliferation was monitored in real-time using the xCELLigence system (Roche Applied Science, and ACEA Biosciences Inc.). Background measurements were taken from the wells by adding 50 µl complete growth medium to 96 well E-16 plates (containing gold microelectrodes located in their base) (ACEA Biosciences Inc.), used to calibrate the plates by the RTCA Software 1.2 (Roche Applied Science). Cells were then seeded (at cell densities of: $5x10^3$ cells/well for VK2 and Ect1; $2x10^4$cells/well for RL95-2; $1x10^4$ cells/well for AN3CA) in complete growth medium to a final volume of 100µl. RL95-2 and AN3CA cells were serum starved for 24 hrs (cell cycle synchronization) prior to seeding. Cells were incubated for 4 hrs, at 37°C and 5 % CO_2 prior to IFN treatment. VK2 and Ect1 cells were stimulated with r-hIFNβ, r-mIFNε, B.control (buffer control volume equivalent to 500 IU/ml) and r-hIFNε (125-500 IU/ml) or unstimulated; whereas RL95-2 and AN3CA cells were stimulated with r-hIFNβ, r-mIFNε, B.control (buffer control volume equivalent to 1000 IU/ml) and r-hIFNε (250-1000 IU/ml) or unstimulated. Impedance signals were recorded by the RTCA system every 15 mins up to the end of the experiment, over 90 hrs. Cell Index value at each time point is defined as well impedance containing cells minus background impedance (well containing medium only). Growth curve profiles were generated from mean cell index, normalized post treatment time, +/-SD recorded at 30 min intervals according to RTCA 1.2 software analysis. The cellular proliferation rates were then expressed as growth curve slope (1/ hrs) % relative to unstimulated control and doubling time, at 48 hr and 72 hr time points as deduced by the RTCA 1.2 software analysis. Three independent biological experiments were performed in technical quadruplicates. Statistical analysis was carried out using one-way ANOVA with Fisher's LSD multiple comparisons test, (*P<0.05, **P<0.01, ***P<0.001, ****P<0.0001).

Apoptosis assay: Annexin V staining/ FACS analysis

Ect1 cells were seeded in a 24 well plate at a density of $1x10^5$ cells/well in 1 ml of complete medium and incubated for 4 hrs, at 37°C and 5 % CO_2. Following adhesion to the well surface, cells were stimulated with 1000 IU/ml of r-hIFNε, r-mIFNε and r-hIFNβ for 72 hrs and compared to US control (unstimulated control). As a positive control of apoptosis, cells were also treated with 5 mM of H_20_2 for 4 hrs. To evaluate cellular apoptosis, V-FITC Annexin V Apoptosis Detection Kit II (BD Biosciences) was utilized according to the manufacturer's instructions. Following trypsinization, cells were harvested by centrifugation for 5 mins at 180 x g, 4°C and resuspended in 50 µl binding buffer (BD Biosciences). Cells were stained with 2.5 µl of both Annexin V-FITC and PI (propidium iodide) for 15 mins at room temperature in the dark. The stained cell suspension was subsequently supplemented with 50 µl of binding buffer (BD Biosciences) prior to analysis by FACSCanto II flow cytometer (BD Biosciences). Data from three independent biological experiments were performed in technical triplicates and quantified by FlowJo_10 software. Results were expresses as staining % for each phase of apoptosis identified as: necrosis (annexin V- $FITC^-/PI^+$), late apoptosis (annexin $V\text{-}FITC^+/PI^+$), early apoptosis (annexin $V\text{-}FITC^+/PI^-$) and live cells (annexin $V\text{-}FITC^-/PI^-$) [34, 35]. Statistical analysis was performed using one-way ANOVA, Holm-Sidak's multiple comparisons test, (*P<0.05, **P<0.01, ***P<0.001, ****P<0.0001).

Apoptosis assay: TUNEL staining

In vitro DNA fragmentation of epithelial cells was detected by TUNEL (terminal deoxynucleotidyl-transferase-mediated dUTP-biotin nick end-labeling) assay staining [36]. Ect1 cells were plated in a 96 well black-walled, clear bottom, imaging plate (Costar), at a density of $3x10^3$ cells/well in 100 µl of complete medium. Following adhesion to the well surface, cells were treated with 1000 IU/ml of r-hIFNε, r-mIFNε and

r-hIFNβ or untreated for 96 hrs. Cells were then fixed with 4% paraformaldehyde for 10 mins and permeabilized for 10 mins, at room temperature. The cells were washed twice with Nuclease-Free Water (Ambion), and finally stained using in situ cell apoptosis detection kit, Click-IT Plus TUNEL Assay (Molecular Probes, Life Technologies) according to the manufacturer's instructions. The cells were washed with 3 % BSA in PBS for 5 mins and stained with 0.5 μg/ml DAPI (Thermo Fisher Scientific) for 5 mins, protected from light. Each well was washed twice with PBS and cells were mounted with ibidi Mounting Medium for fluorescence imaging (DKSH). Cell Imaging was carried out by Cellomics Arrayscan VT1 high-throughput microscope (Thermo Fisher Scientific), located at the Peter MacCallum Cancer Centre, (Associate Professor Kaylene J. Simpson and Karla Cowdley, Victorian Centre for Functional Genomics, ACRF Translational RPPA platform, Victorian Comprehensive Cancer Centre). TUNEL-positive cells (green fluorescence) as well as DAPI staining (nuclear stain, blue fluorescence), were identified by Cellomics Scan software v7.6.2. (Cellomics, Thermo Fisher Scientific). Cell imaging of 49 fields per well was generated using a 10 x objective. Image acquisition and analysis were conducted with the Target Activation V3 Bioapplication by identification of nuclei in the DAPI channel, incorporation of cell segmentation, threshold, and quantitation of % TUNEL-positive cells in TUNEL-channel or % responders (TUNEL positive cells that corresponded to nuclei expressed as a percentage of total cell nuclei). Data is representative of mean ± SEM, from three independent biological experiments in technical triplicates. Statistical analysis was performed using performed one-way ANOVA, with Tukey's multiple comparisons test, (*P<0.05, **P<0.01, ***P<0.001, ****P<0.0001).

Apoptosis assay: Caspase activity assay

Ect1 cells were plated in a 96 well black-walled, clear bottom, imaging plate (Costar), at a density of $3x10^3$ cells/well in 100 µl of complete medium. Following adhesion to the well surface, cells were treated with 1000 IU/ml of r-hIFNε, r-mIFNε and r-hIFNβ or left untreated for 72 hrs. Active caspase-3/7 monitoring was performed using CellEvent Caspase-3/7 Green Detection Reagent (Life Technologies, Thermo Fisher Scientific) labelling assay according to the manufacturer's directions. Apoptotic cells encompassing active caspase-3/7, cleave the DEVD peptide, resulting in binding of the free dye to DNA accompanied by green fluorescence. Cell media was replaced with complete media containing 5 µM of CellEvent Caspase-3/7 Green Detection Reagent (Life Technologies, Thermo Fisher Scientific) and the plate was covered with foil and incubated for 30 mins, in the incubator at 37°C and 5 % CO_2. Cells were then fixed with 4% paraformaldehyde for 10 mins and subsequently permeabilized for 10 mins, at room temperature, light protected. The cells were washed twice with Nuclease-Free Water (Ambion), and counterstained with 0.5 µg/ml of DAPI (Thermo Fisher Scientific) for 5 mins, protected from light. Each well was washed twice with PBS and cells were mounted with Ibidi Mounting Medium for fluorescence imaging (DKSH). Cell Imaging was carried out by Cellomics Arrayscan VT1 high-throughput microscope (Thermo Fisher Scientific), located at the Peter McCallum Center, (Kaylen Simpson Karla Cowdley). Caspase-3/7 active-positive cells (green fluorescence) as well as DAPI staining (nuclear stain, blue fluorescence), were identified by Cellomics Scan software v7.6.2. (Cellomics, Thermo Fisher Scientific) from 49 fields per well, using a 10 x objective. Image acquisition and analysis were generated with the Target Activation V3 Bioapplication by identification of nuclei in the DAPI channel, incorporation of cell segmentation, threshold, and quantitation of % caspase-3/7 active positive in caspase-3/7-channel or % responders (caspase- 3/7 active positive cells that corresponded to nuclei expressed as a percentage of total cell nuclei). Set parameters exclude false positive fluorescence that does not correspond with nuclei objects. Data is representative of mean ± SEM, from three

independent biological experiments in technical triplicates. Statistical analysis was performed using one-way ANOVA, with Tukey's multiple comparisons test, (*P<0.05, **P<0.01, ***P<0.001, ****P<0.0001).

Results

IFNε Regulates Anti/Pro Apoptotic ISGs

To confirm expression of type I IFN receptors essential for type I interferon signalling endogenous mRNA expression levels of *IFNAR1*, *IFNAR2* and *IFNE* were measured by qRT-PCR (Figure 1). According to a previous study, IFNε expression was characterized with in the mouse FRT localized in vagina, cervix, uterus, and ovaries, whereas expression in human was only examined in the endometrium [20, 21]. For this reason, we selected a panel of human epithelial cancer cells lines of lower FRT origin: VK2 (vaginal), Ect1 (ectocervical), End1 (endocervical); as well as upper FRT origin: ECC-1 (grade I-derived), RL95-2 (grade II-derived), AN3CA (grade III-derived), endometrial cancer cells; for analysis. QRT-PCR analysis revealed that all six FRT cancer cell lines expressed both receptors *IFNAR1* and *IFNAR2*, with variable mRNA levels. Endogenous *IFNAR1* mRNA was detected in VK2, Ect1, RL95-2 and AN3CA at comparably high levels whereas End1 and ECC-1 had considerably lower expression levels. *IFNAR2* mRNA levels were strikingly high in the upper FRT endometrial cancer cells AN3CA (grade III -derived) and RL95 (grade II -derived) compared to cell lines originating from the lower FRT. Interestingly, *IFNE* transcript levels were extremely low in ECC-1 (grade I -derived), RL95-2 (grade II -derived), or undetectable in AN3CA (grade III -derived) endometrial cancer cells compared to VK2, Ect1 and End1 cells of lower FRT origin. Thus, in line with preliminary evidence indicative of down regulation of IFNε in fallopian tissues of HGSC

(High Grade Serous Carcinoma) patients, this observation may also implicate reduced IFNε expression to coincide with endometrial cancer progression.

Given that the FRT cell line panel contained type I IFN receptor components, we sought to examine cellular responsiveness to interferon stimulation by monitoring ISG induction using qRT-PCR. In these experiments, cells were stimulated with recombinant murine IFN (r-mIFNε), generated by our lab, and demonstrated to effectively induce ISGs specialized in HIV restriction factor activity as well as eliciting prophylaxis against HIV infection of human peripheral blood lymphocytes [26]. Such a cross-species reactivity is another unique feature of IFNε not exhibited by other type I IFN ligands, such as IFNα or IFNβ. As demonstrated by Fung K.Y., *et al*., 2013 it is anticipated that 3 hrs of interferon stimulation would suffice for adequate ISG induction to be monitored by qRT-PCR. In this study, VK2, Ect1, End1, RL95-2 and AN3CA cancer cells were responsive to IFNε and IFNβ stimulations (Figures 2-12). Significant upregulation of classical IRG mRNAs including *ISG15*, *MXA* (antiviral activity), *CXCL10* (chemokine) and *CAPS1* was observed in the lower FRT, VK2, Ect1 and End1 (Figures 2, 4, 5) cells upon 3 hrs of IFN stimulation (100 IU/ml); as well as in corresponding upper FRT, RL95-2 and AN3CA, endometrial cancer cells, (see figures 9,10) at 24 hrs of IFN stimulation (1000 IU/ml), in a cell dependent manner. As RL95-2 and AN3CA cells did not respond to 3 hrs of interferon stimulation, exhibiting no changes in classical ISGs *(ISG15*, *MXA*, *CXCL10, CAPS1)* analysed (data not shown), the appropriate stimulation time point selected for these cells was subsequently 24 hrs. Interferon treatment of ECC-1 cells for 3 hrs had a minimal effect on levels of *ISG15* or *MXA* transcripts compared to unstimulated control (Figure 8). Unexpectedly, both *OAS2* and *CXCL10* could not be detected, in either unstimulated control or IFN treated ECC-1 cells, and for these reasons, we did not perform further investigations utilizing this cellular system. Similarly, we were not able to detect *CXCL10* mRNA in RL95-2 and AN3CA endometrial cancer unstimulated control

or IFN stimulated cells. These results demonstrated that our chosen FRT cells lines are responsive to IFNε stimulation and that responses vary dependent on cell type.

Next, we investigated the regulation of IFNε on survival and apoptotic associated ISGs of FRT cells. Interestingly, IFNε treatment down regulated *BCL-2* and *CDC20* (pro-survival/anti-apoptotic IRGs) mRNA in VK2, End1, RL95-2, and AN3CA cells relative to unstimulated control cells (Figures 3, 7, 10, 12). In contrast, IFNε treatment lead to a significant upregulation of pro-apoptotic mediators *TAP1*, *OAS2*, *ISG12A* in VK2, Ect1 and End1, RL95-2, and AN3CA cancer cells (Figures 3, 5, 7, 10, 12). This suggests that IFNε may play important roles in suppressing expression of cell survival genes and concurrently enhance the expression of genes associated with pro-apoptotic mechanisms. This highlights the potential anti-tumourigenic properties of IFNε in FRT cancer epithelial cells by inducing the canonical IFN type I signalling pathway.

IFNε Suppresses FRT Cancer Cell Proliferation

MTT assays were used to examine the effects of IFNε on cell viability in VK2 and Ect1 cells. Both cell types displayed significant reductions in cell viability at 72 hrs post stimulation with IFNε and IFNβ (1000 IU/ml). Cell viability was reduced by 42% upon 1000 IU/ml of hIFNε treatment compared to a reduction of 46% and 32% with same concentration of r-mIFNε and r-hIFNβ, relative to unstimulated control Ect1 cells (Figure 13). More importantly, r-hIFNε stimulation reduced cell viability, in a dose dependent manner in both VK2 and Ect1.

To further ascertain whether IFNε treatment reduces cell viability by regulating proliferation, VK2, Ect1, RL95-2 and AN3CA cells were monitored in real-time using an xCELLigence analyser. Treatment of VK2 and Ect1 cells with IFNs significantly reduced

cell proliferation after 48 hrs and 72 hrs compared to unstimulated control cells (Figures 14, 15 ,16, 17). The most prominent IFN effects on VK2 and Ect1 cells, were obtained at 72 hr upon r-mIFNε, r-hIFNε and hIFNβ at a concentration of 500 IU/ml (Figures 14A and 16A). At 72 hrs of r-hIFNε treatment (500 IU/ml), cell proliferation (slope %) was reduced by 56% in VK2 (Figure 15B), and 58% in Ect1 (Figure 17B). Both VK2 and Ect1 cell lines (Figures 14, 15 ,16, 17) presented a dose dependent reduction in cell proliferation upon r-hIFNε 72 hr stimulations (500-125 IU/ml). Furthermore, these results also demonstrate that exogenous IFN treatment significantly increased doubling times of both vaginal and cervical cancer cells (VK2, Ect1) in a dose dependent manner (Figures 15D, 17D). These results suggest that IFNε may play a catalytic role in the regulation of epithelial cell proliferation, in accordance with other type I family members such as IFNβ.

Subsequently, IFN stimulation of endometrial cancer cells RL95 and AN3CA, greatly suppressed cell proliferation after 48 hrs and 72 hrs relative to unstimulated control cells. (Figures 18, 19, 20, 21). It was observed that in both RL95 and AN3CA cells at 72 hr treatments and at a concentration of 1000 IU/ml, r-hIFNε was the most effective in decreasing proliferation rates, followed by r-mIFNε and lastly hIFNβ causing less significant reductions (Figures 18, 19B, 20, 21B). At 72 hrs of r-hIFNε treatment (1000 IU/ml), cell proliferation (slope %) was decreased by 71% in RL95-2 (Figure 19B), and 45% in AN3CA (Figure 21B). Both RL95-2 and AN3CA cell lines displayed a dose dependent reduction in cell proliferation upon r-hIFNε 72 hr stimulations (1000-125 IU/ml). Whereas hIFNβ stimulation was less effective in reducing proliferation rates of endometrial cancer cells by 25% for RL95 (grade II-derived) and 31% for AN3CA (grade III-derived). In addition, these results also illustrate significant delays in doubling times of both RL95-2 and AN3CA cells, mediated by IFN treatment (Figures 19D, 21D). This data suggests, that IFNε may mediate endometrial cancer cell proliferation with greater efficiency than IFNβ.

IFNε Induces Cancer Cell Apoptosis

To further delineate the mechanisms mediating IFNε induced inhibition in cellular proliferation, the *in vitro* IFNε effects on apoptosis were investigated. Annexin V-FITC and PI staining of Ect1 cells was measured by FACS analysis upon 72 hrs of IFN treatment. Scatter plots (Figure 22) of Ect1 cells stimulated with r-hIFNε, r-mIFNε and r-hIFNβ (1000 IU/ml) for 72 hrs are indicative of an apoptotic phenotype. Representative side scatter (SSC) and forward scatter plots (FSC) further reveal that IFN treatment of Ect1 cells morphologically alters their size and granularity consistent with the state of apoptosis. Treatments of 1000 IU/ml with hIFNε, r-mIFNε and r-hIFNβ significantly enhanced the detection of early apoptotic (annexin V-FITC^{+}/PI^{-}) and late apoptotic (annexin V-FITC^{+}/PI^{+}) cell populations accompanied by reductions in unstained live cell populations (annexin V-FITC^{-}/PI $^{-}$) as compared to unstimulated controls (Figures 22 and 23). Importantly, neither IFN treatments altered the proportion of necrotic cells (annexin V- FITC $^{-}$/PI^{+}). Furthermore, r-hIFNε treatment lead to a 6% increase of both early apoptotic and late apoptotic cells as compared to unstimulated cells. These results suggest that IFNε significantly induces early and late apoptotic events without effecting necrosis, comparable to well characterized apoptotic events associated with IFNβ stimulation [37, 38].

To corroborate the direct pro-apoptotic effects of IFNε on epithelial cells, we utilized *in situ* TUNEL staining to examine DNA fragmentation occurring at the later stages of apoptosis. In these studies stimulations of Ect1 cells with 1000 IU/ml of r-hIFNε, r-mIFNε and r-hIFNβ for 96 hrs led to significant increase in the percentage of TUNEL positive cells by 4.2%, 2.2% and 2.2% respectively as quantified by cellomics system (Figures 24 and 25), accompanied by significant reductions in nuclear counts. These results suggest that IFNε is associated with DNA fragmentation observed in late apoptotic stages.

Finally, to validate the impact of IFNε treatment in early apoptotic events, active Caspase-3/7 was monitored using the CellEvent Detection system. 72 hr IFN stimulation of Ect1 at 1000 IU/ml, greatly enhanced active Caspase-3/7 by 15.5%, 42.5%, 27.5% with r-hIFNε, r-mIFNε and r-hIFNβ respectively (Figures 26, 27). This suggests that IFNε leads to activation of Caspase-3/7 indicative of early apoptotic events. Collectively the application of these three different apoptotic assays confirm the pro-apoptotic properties of IFNε. Thus, it has been clearly shown that recombinant IFNε induces early and late stages of apoptosis without affecting necrosis.

Discussion

Type I interferons exhibit pleotropic anti-tumour actions by employing extrinsic (activation of anti-tumour immune cells) and intrinsic mechanisms (regulation of cell proliferation and apoptosis) as reviewed by Parker *et al*., 2016 [19]. Studies to date have primarily been carried out to examine effects of classical type I IFNs such as IFNα and IFNβ. The anti-neoplastic properties exhibited by classical type I interferons IFNα/β have been applied to the development of a wide range of cancer therapies, however they were accompanied with severe side effects [19, 27-29].

Whereas IFNε is a unique type I interferon as it is constitutively expressed within the FRT suggesting that it may be well tolerated within this organ to direct an organ-specific type I IFN response. According to Hardy M.P., *et al.,* 2004, *Ifnε,* is the only type I IFN member found to be constitutively expressed within the mouse FRT (18). Concurrently, a recent comprehensive study by our laboratory investigated the expression of IFN mRNA in FRT human tissues obtained from healthy women, including type I (ε, β, α4, α2, α1), type II (IFNγ) and type III (λ1, λ2, λ3) [21]. This study further validated that IFNε was the only highly expressed interferon member in the human FRT, eluding to its distinguished roles

within the FRT physiology. Furthermore, the *in vitro* biological activities of murine IFNε where significantly reduced when directly compared to IFNα1 and IFNβ [30]. Thus, IFNε related activation of the interferon pathway within in the FRT epithelium, may provide increased tissue specificity and less likely side effects.

Type I IFNs also exert their anti-cancer potential via intrinsic mechanisms by regulating cell proliferation, differentiation, and apoptosis [37, 39, 40]. The current study focuses on the *in vitro* intrinsic anti-tumour properties of IFNε in FRT cancer epithelial cells. Recently, our group characterised IFNε, as "FRT-specific type I IFN" essential for protection against sexually transmitted infections [20]. It is novel within the type I IFN family for three major reasons: (i) it is constitutively expressed at high levels in the FRT, (ii) it is not upregulated in response to pathogens and (iii) it is hormonally regulated. Its expression fluctuates throughout the menstrual cycle with levels increasing prior to ovulation before dropping during the secretory phase. Additionally, post-menopausal women have very low levels of IFNε in the FRT, presumably due to a lack of hormones [20]. IFNε, similar to IFNα and IFNβ, signals through the type I IFN receptor (IFNARs) to regulate gene expression [20, 25].

To establish an appropriate cellular system for assessing the *in vitro* effects of IFNε, we utilized a panel of FRT cancer cells to initially examine endogenous expression of type I IFN receptors, essential for type I interferon signalling, *IFNAR1* and *IFNAR2* as well as *IFNE* ligand. We confirm that all six FRT cancer cell lines (VK2, Ect1, End1, ECC-1, RL95-2 and AN3CA) expressed both *IFNAR1* and *IFNAR2* signalling receptors.

Following validation of IFN type I receptor components present in these cells we examined responsiveness to recombinant interferon stimulation by monitoring ISG induction. It was observed that Vk2, Ect1, End1, RL95-2 and AN3CA cancer cells were responsive to both IFNε and IFNβ stimulation. Significant upregulation of classical ISGs

with antiviral activity (*MXA, ISG15* [41, 42]), chemokine function (*CXCL10* [43]) and pro-inflammatory (*CASP1* [44]) was observed in the lower FRT VK2, Ect1 and End1 cells; as well as in corresponding upper FRT RL95-2 and AN3CA endometrial cancer cells. The response profile displayed cell type specificity within the FRT cell line panel. The examined FRT cancer cells were sensitive to both IFNε and IFNβ stimuli, by mediating well known ISGs. Thus, corroborating that IFNε exerts its actions via the canonical IFN type I signalling pathway, as demonstrated clearly in a recent study conducted by our group [26]. Consequently, appropriate cellular models were established to further study underlying mechanisms by which IFNε exerts its biological actions. However lower FRT cells VK2, Ect1 and End1 were more sensitive to both IFNε and IFNβ stimulations and required lower dosage, compared to upper FRT RL95-2 and AN3CA endometrial cancer cells, which required a longer incubation period and higher dosage. This differential interferon activation could be dependent on the anatomical epithelial cell origin. It could be postulated that epithelial cells derived from the lower FRT are highly susceptible to infections requiring immediate activation of the immune system via type I IFN signalling compared to the relatively sterile upper FRT endometrial epithelium anatomy [45].

In addition, IFNε stimulation of FRT epithelial cells also regulated expression of survival and apoptotic IFN type I ISGs. Interestingly, IFNε treatment down regulated anti-apoptotic *BCL-2* (pro-survival), and *CDC20* (cell cycle check-point regulator) transcripts in VK2, End1, RL95-2, and AN3CA cells [46-48]. In contrast, IFNε treatment lead to a significant upregulation of pro-apoptotic transcript mediators *TAP1, OAS2, ISG12A* in VK2, Ect1 and End1, RL95-2, and AN3CA cancer cells [49-51]. Thus, this data highlights the propensity of IFNε to elicit anti-tumourigenic properties in endometrial and other FRT epithelial cancer cells by inducing IFN type I signalling and modulating ISGs with cell survival and apoptotic functions. Although we have examined a subset of ISGs regulated by IFNε, it is suggested that the type I IFN signalling cascade regulates the activity of hundreds of ISGs to collectively elicit pleotropic biological functions.

Aberrant proliferation is a fundamental trait associated with oncogenesis [52]. Thus, providing insights into molecular mechanisms that regulate such processes is important for cancer therapy. Having confirmed that IFNε regulates cell survival ISGs, we were also interested to determine if these effects were functionally translated *in vitro*. Therefore, FRT cells were further employed to examine the effects of IFNε on cellular growth. IFNε treatment significantly reduced both cell viability (MTT assay) and proliferation (xCELLigence assay) of VK2 and Ect1 epithelial cells. Analogous reductions in cellular growth were also observed upon treatment of these cells with IFNβ, also reported in previous *in vitro* studies using SKMel-28 (melanoma) cells [53], as well as HepG2 (hepatocellular carcinoma) cells [54]. These results suggest that IFNε regulates proliferation of lower FRT epithelium, similar to IFNβ. Furthermore, IFNε may play a key anti-proliferative role in the lower FRT epithelium and reactivation of interferon signalling may be of therapeutic importance for treatment of vaginal and cervical cancers.

Concomitantly, IFNε greatly reduced cellular growth of high grade endometrial cancer cells RL95 (grade II-derived) and AN3CA (grade III-derived). Whereas, hIFNβ was considerably less effective than IFNε in reducing proliferation rates of these endometrial cancer cell lines. According to Yi, B.R., *et al*., 2015, combination therapy employing stem cells expressing IFNβ with subsequent 5-fluorocytosine administration lead to reduced endometrial tumour growth (by 50-60%) of mouse model xenografts [55]. In this study neural stem cells genetically engineered to co-express IFNβ and cytosine deaminase (CD), were directly injected into the tumour followed by intraperitoneal administration of 5-fluorocytosine (non-toxic drug precursor) that is converted to cytotoxic 5-fluorouracil (acting as a DNA inhibitor) by CD. Our data identifies IFNε as an essential regulator of proliferation within the endometrial epithelium. However, as IFNε was demonstrated to elicit a greater reduction in endometrial cancer cell proliferation

compared IFNβ in the present study, we anticipate that it may also provide increased therapeutic benefits to combat endometrial cancer.

Apoptosis is a tightly regulated cellular death process, critical in embryonic development and maintenance of adult tissue homeostasis involving elimination of infected or genetically damaged cells [56, 57]. Evading apoptosis is a hallmark of cancer development [58]. Hence, understanding the molecular mechanisms that activate apoptotic processes could be beneficial in the development of potential anti-cancer therapies. Classical type I interferons such as IFNα and IFNβ, exhibit pro-apoptotic properties and have been successfully utilized in anti-cancer therapies [37, 38]. Indeed, we demonstrated that IFNε significantly induces early and late apoptotic events without effecting necrosis of Ect1 cells by FACS analysis of Annexin V-FITC and PI stained cells stimulated for 72 hrs. Induction of apoptosis was comparable amongst IFNε and IFNβ treatments. In addition, we demonstrated an increase in active Caspase-3/7 upon 72 hrs of IFN stimulation of Ect1 cells. This suggests that IFNε leads to activation of Caspase-3/7 essential in early apoptotic events. Further validation of the pro-apoptotic effects of IFNε were confirmed by an increase of TUNEL positive cells upon 96 hrs of stimulation of Ect1 cells. This evidence indicates that IFNε also induces late apoptotic events accompanied by DNA fragmentation. This is the first study to delineate cumulative evidence from three distinct methodologies, providing important insights into the mechanisms employed by IFNε to elicit pro-apoptotic activities in cancerous epithelial cells.

Conclusions

In conclusion, these results characterize IFNε as a key regulator of proliferation and apoptosis within the FRT epithelium. Exogenous IFNε stimulation of epithelial cancer

cells throughout the FRT could trigger type I interferon signalling and modulate classical ISGs accompanied by down regulation of anti-apoptotic ISGs and upregulation of pro-apoptotic ISGs. Functional assays of FRT cancer cells revealed significant reduction in proliferation and induction of apoptosis. Collectively, we have demonstrated that IFNε has potent intrinsic anti-tumour actions and therefore warrants further investigation into it potential as a novel FRT cancer therapeutic.

List of Abbreviations

BCL-2, B-cell lymphoma 2; CASP1,Caspase-1; CDC20, Cell-division cycle protein 20; CXCL10, Chemokine (C-X-C motif) ligand 10; DAPI, 4',6-diamidino-2-phenylindole; dUTP, 2'-Deoxyuridine 5'-Triphosphate; EU, Endotoxin units; FACS, Fluorescence activated cell sorting; FITC, Fluorescein isothiocyanate; FRT, Female reproductive tract; HSV, Herpes Simplex Virus; IFI27, Interferon alpha-inducible protein 27; IFN, Interferon; IFNAR, Interferon alpha receptor; IRG, Interferon regulated gene; ISG12, Interferon-stimulated gene 12a protein; ISG15, Interferon-stimulated gene 15; ISRE, Interferon stimulated response element; IU, International units; MTT, [3-(4, 5-Dimethylthiazol-2-yl)-2, 5-diphenyltetrazolium bromide; MXA, Myxovirus resistance protein 1; NK, Natural killer; OAS, Oligoadeylate synthetase; P, Propidium iodide; r-hIFNβ, Recombinant human interferon beta; r-hIFNε, Recombinant human interferon epsilon; r-mIFNε, Recombinant mouse interferon epsilon; rRNA, Ribosomal RNA; STAT, Signal transducer and activator of transcription; TAP1, Transporter associated with antigen processing 1; TUNEL, Terminal deoxynucleotidyl-transferase-mediated dUTP-biotin nick end-labeling;

Competing Interests

The authors declare no competing interests.

Authors' Contributions

Conception and design: Nollaig Bourke, Paul Hertzog

Development and methodology: Irene Papageorgiou, Nollaig Bourke

Provision of r-hIFNε r-mIFNε reagents: Antony Matthews, San Lim, Nicole A deWeerd and intellectual input

Data acquisition: Irene Papageorgiou

Data analysis and interpretation: Irene Papageorgiou, Nollaig Bourke

Writing, review and editing of manuscript: Irene Papageorgiou, Nollaig Bourke, Paul Hertzog

Study supervision: Nollaig Bourke, Paul Hertzog

Acknowledgements

The authors are grateful to Professor Gilda Tachedjian, Dr Hong Nguyen, Yao Wang, Professor Guiying Nie, Dr Amy Winship and Professor Eva Dimitriadis for supplying tissue culture cell lines. We thank Dr Eveline De Geus for kindly providing technical assistance with Annexin V staining / FACS analysis. Finally, we extend our gratitude to Karla Cowely, and Associate Professor Kayleen Simpson for their technical expertise in Cellomics high-throughput microscopy.

References

1. Ferlay, J., et al., Cancer incidence and mortality worldwide: Sources, methods and major patterns in GLOBOCAN 2012. International Journal of Cancer, 2015. 136(5): p. E359-E386.

2. Australian Institute of, H. and Welfare, Cancer in Australia: Actual incidence data from 1982 to 2013 and mortality data from 1982 to 2014 with projections to 2017. Asia-Pacific Journal of Clinical Oncology, 2017: p. n/a-n/a.

3. Di Cristofano, A. and L.H. Ellenson, Endometrial carcinoma. Annu Rev Pathol, 2007. 2: p. 57-85.

4. Shisler, R., et al., Life after endometrial cancer: A systematic review of patient-reported outcomes. Gynecol Oncol, 2017.

5. Pautier, P. and F. Pommeret, [Systemic therapy for advanced endometrial cancer]. Bull Cancer, 2017.

6. Salvesen, H.B., I.S. Haldorsen, and J. Trovik, Markers for individualised therapy in endometrial carcinoma. The Lancet Oncology, 2012. 13(8): p. e353-e361.

7. Sorosky, J.I., Endometrial cancer. Obstet Gynecol, 2012. 120(2 Pt 1): p. 383-97.

8. zur Hausen, H., Human papillomaviruses and their possible role in squamous cell carcinomas. Curr Top Microbiol Immunol, 1977. 78: p. 1-30.

9. Silva, J., F. Cerqueira, and R. Medeiros, Chlamydia trachomatis infection: implications for HPV status and cervical cancer. Archives of Gynecology and Obstetrics, 2014. 289(4): p. 715-723.

10. Brinkman, J.A., et al., The impact of anti HPV vaccination on cervical cancer incidence and HPV induced cervical lesions: consequences for clinical management. Eur J Gynaecol Oncol, 2005. 26(2): p. 129-42.

11. Zhang, L.F., et al., HPV6b virus like particles are potent immunogens without adjuvant in man. Vaccine, 2000. 18(11-12): p. 1051-8.

12. Okagaki, T., et al., Identification of human papillomavirus DNA in cervical and vaginal intraepithelial neoplasia with molecularly cloned virus-specific DNA probes. Int J Gynecol Pathol, 1983. 2(2): p. 153-9.

13. Tjalma, W.A.A., et al., The Role of Surgery in Invasive Squamous Carcinoma of the Vagina. Gynecologic Oncology, 2001. 81(3): p. 360-365.

14. Ali, M.M., et al., Radiation alone for carcinoma of the vagina: variation in response related to the location of the primary tumor. Cancer, 1996. 77(9): p. 1934-9.

15. Jabbour, H.N., et al., Endocrine Regulation of Menstruation. Endocrine Reviews, 2006. 27(1): p. 17-46.

16. Salamonsen, L.A., N.J. Hannan, and E. Dimitriadis, Cytokines and chemokines during human embryo implantation: roles in implantation and early placentation. Semin Reprod Med, 2007. 25(6): p. 437-44.

17. Salamonsen, L.A., et al., The Microenvironment of Human Implantation: Determinant of Reproductive Success. American Journal of Reproductive Immunology, 2016. 75(3): p. 218-225.

18. Hardy, M.P., et al., Characterization of the type I interferon locus and identification of novel genes. Genomics, 2004. 84(2): p. 331-345.

19. Parker, B.S., J. Rautela, and P.J. Hertzog, Antitumour actions of interferons: implications for cancer therapy. Nat Rev Cancer, 2016. 16(3): p. 131-44.

20. Fung, K.Y., et al., Interferon-epsilon protects the female reproductive tract from viral and bacterial infection. Science, 2013. 339(6123): p. 1088-92.

21. Bourke NM, Achilles SL, Huang SU, Cumming HE, Papageorgiou I, Gearing LJ, Thakore S, Mangan NE, Mesiano S, Hertzog PJ. Human IFNε: Spaciotemporal expression, hormone regulation and innate immunity in the female reproductive tract. bioRxiv. October 16, 2018.

22. Cohen, B., et al., Ligand-induced association of the type I interferon receptor components. Molecular and Cellular Biology, 1995. 15(8): p. 4208-14.

23. Platanias, L.C. and E.N. Fish, Signaling pathways activated by interferons. Exp. Hematol., 1999. 27: p. 1583-1592.

24. Peng, F.-W., et al., Purification of recombinant human interferon-ε and oligonucleotide microarray analysis of interferon-ε-regulated genes. Protein Expression and Purification, 2007. 53(2): p. 356-362.

25. de Weerd, N.A., S.A. Samarajiwa, and P.J. Hertzog, Type I interferon receptors: biochemistry and biological functions. J Biol Chem, 2007. 282(28): p. 20053-7.

26. Stifter, S.A., et al., Defining the distinct, intrinsic properties of the novel type I interferon, epsilon. Journal of Biological Chemistry, 2017.

27. Talpaz, M., et al., Clinical investigation of human alpha interferon in chronic myelogenous leukemia. Vol. 69. 1987. 1280-1288.

28. Ascierto, P.A., et al., Interferon alpha for the adjuvant treatment of melanoma: review of international literature and practical recommendations from an expert panel on the use of interferon. J Chemother, 2014. 26(4): p. 193-201.

29. Nicolini, A. and A. Carpi, Beta-interferon and interleukin-2 prolong more than three times the survival of 26 consecutive endocrine dependent breast cancer patients with distant metastases: an exploratory trial. Biomed Pharmacother, 2005. 59(5): p. 253-63.

30. Stifter, S.A., et al., Purification and biological characterization of soluble, recombinant mouse IFNβ expressed in insect cells. Protein Expression and Purification, 2014. 94: p. 7-14.

31. Livak, K.J. and T.D. Schmittgen, Analysis of Relative Gene Expression Data Using Real-Time Quantitative PCR and the 2−ΔΔCT Method. Methods, 2001. 25(4): p. 402-408.

32. Mosmann, T., Rapid colorimetric assay for cellular growth and survival: Application to proliferation and cytotoxicity assays. Journal of Immunological Methods, 1983. 65(1): p. 55-63.

33. Slater, T.F., B. Sawyer, and U. Sträuli, Studies on succinate-tetrazolium reductase systems: III. Points of coupling of four different tetrazolium salts III. Points of coupling of four different tetrazolium salts. Biochimica et Biophysica Acta, 1963. 77(Supplement C): p. 383-393.

34. Koopman, G., et al., Annexin V for flow cytometric detection of phosphatidylserine expression on B cells undergoing apoptosis. Blood, 1994. 84(5): p. 1415.

35. Vermes, I., et al., A novel assay for apoptosis Flow cytometric detection of phosphatidylserine expression on early apoptotic cells using fluorescein labelled Annexin V. Journal of Immunological Methods, 1995. 184(1): p. 39-51.

36. Gavrieli, Y., Y. Sherman, and S.A. Ben-Sasson, Identification of programmed cell death in situ via specific labeling of nuclear DNA fragmentation. J Cell Biol, 1992. 119(3): p. 493-501.

37. Chawla-Sarkar, M., et al., Apoptosis and interferons: role of interferon-stimulated genes as mediators of apoptosis. Apoptosis, 2003. 8: p. 237-249.

38. Clemens, M.J., Interferons and apoptosis. J Interferon Cytokine Res, 2003. 23: p. 277-292.

39. Chatterjee, D. and T.M. Savarese, Posttranscriptional regulation of c-myc proto-oncogene expression and growth inhibition by recombinant human interferon-beta ser17 in a human colon carcinoma cell line. Cancer Chemother Pharmacol, 1992. 30: p. 12-20.

40. Borden, E.C., et al., Interferons at age 50: past, current and future impact on biomedicine. Nat Rev Drug Discov, 2007. 6(12): p. 975-90.

41. Aebi, M., et al., cDNA structures and regulation of two interferon-induced human Mx proteins. Molecular and Cellular Biology, 1989. 9(11): p. 5062-5072.

42. Morales, D.J. and D.J. Lenschow, The Antiviral Activities of ISG15. Journal of Molecular Biology, 2013. 425(24): p. 4995-5008.

43. Loetscher, M., et al., Chemokine receptor specific for IP10 and mig: structure, function, and expression in activated T-lymphocytes. The Journal of Experimental Medicine, 1996. 184(3): p. 963.

44. Chowdhury, I., B. Tharakan, and G.K. Bhat, Caspases — An update. Comparative Biochemistry and Physiology Part B: Biochemistry and Molecular Biology, 2008. 151(1): p. 10-27.

45. Wira, C.R., M. Rodriguez-Garcia, and M.V. Patel, The role of sex hormones in immune protection of the female reproductive tract. Nat Rev Immunol, 2015. 15(4): p. 217-30.

46. Hardwick, J.M. and L. Soane, Multiple Functions of BCL-2 Family Proteins. Cold Spring Harbor perspectives in biology, 2013. 5(2): p. 10.1101 /cshperspect. a008722 a008722.

47. Vaux, D.L., S. Cory, and J.M. Adams, Bcl-2 gene promotes haemopoietic cell survival and cooperates with c-myc to immortalize pre-B cells. Nature, 1988. 335(6189): p. 440-2.

48. Weinstein, J., et al., A novel mammalian protein, p55CDC, present in dividing cells is associated with protein kinase activity and has homology to the Saccharomyces cerevisiae cell division cycle proteins Cdc20 and Cdc4. Mol Cell Biol, 1994. 14(5): p. 3350-63.

49. Grommé, M. and J. Neefjes, Antigen degradation or presentation by MHC class I molecules via classical and non-classical pathways. Molecular Immunology, 2002. 39(3): p. 181-202.

50. Zhou, A., et al., Interferon action and apoptosis are defective in mice devoid of 2[prime]5[prime]-oligoadenylate-dependent RNase L. EMBO J, 1997. 16: p. 6355-6363.

51. Rosebeck, S. and D.W. Leaman, Mitochondrial localization and pro-apoptotic effects of the interferon-inducible protein ISG12a. Apoptosis: An International Journal on Programmed Cell Death, 2008. 13(4): p. 562-72.

52. Hanahan, D. and R.A. Weinberg, The Hallmarks of Cancer. Cell, 2000. 100(1): p. 57-70.

53. Krasagakis, K., et al., Effects of Interferons on Cultured Human Melanocytes In Vitro: Interferon-Beta but Not -Alpha or -Gamma Inhibit Proliferation and All Interferons Significantly Modulate the Cell Phenotype. Journal of Investigative Dermatology, 1991. 97(2): p. 364-372.

54. Ethiraj, P., et al., Inhibitory effects of interferon-β on hepatocellular carcinoma HepG2 via Akt/STAT phosphorylation. Fundamental & Clinical Pharmacology, 2015. 29(3): p. 278-285.

55. Yi, B.R., S.U. Kim, and K.C. Choi, Additional effects of engineered stem cells expressing a therapeutic gene and interferon-beta in a xenograft mouse model of endometrial cancer. Int J Oncol, 2015. 47(1): p. 171-8.

56. Kerr, J.F., A.H. Wyllie, and A.R. Currie, Apoptosis: a basic biological phenomenon with wide-ranging implications in tissue kinetics. Br J Cancer, 1972. 26(4): p. 239-57.

57. Wyllie, A.H., J.F. Kerr, and A.R. Currie, Cell death: the significance of apoptosis. Int Rev Cytol, 1980. 68: p. 251-306.

58. Hanahan, D. and Robert A. Weinberg, Hallmarks of Cancer: The Next Generation. Cell, 2011. 144(5): p. 646-674

Figures

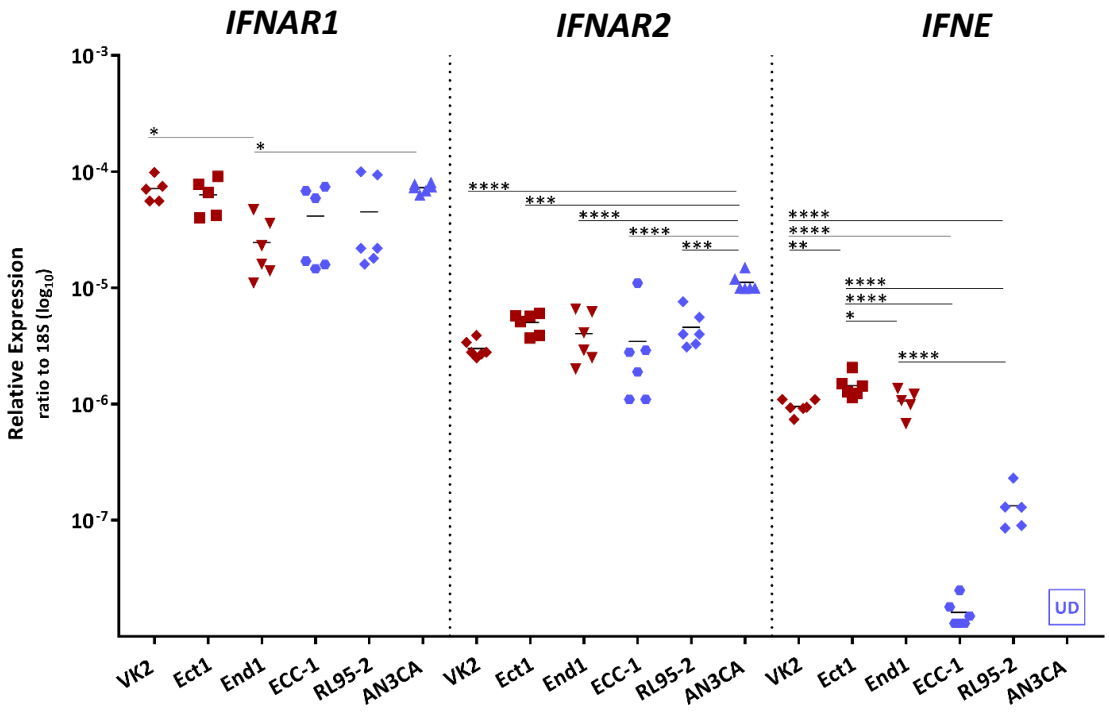

Figure 1. IFNAR1, IFNAR2, IFNε mRNA expression in human FRT cancer cells.
*Graphical representation of IFNAR1 (left side), IFNAR2 (middle) and IFNE (right side) transcripts expressed endogenously. Extracted mRNA from human cell lines: VK2 (vaginal), Ect1 (ectocervical), End1 (endocervical) of lower FRT origin; as well as ECC-1, RL95-2, AN3CA (endometrial cancer) of upper FRT origin, was quantified by qRT-PCR. Transcript expression levels were deduced using the 2^{-CT} method and expressed as a ratio to 2^{-CT} 18s. Data is representative of mean ± SEM, from three independent biological experiments, performed in technical triplicates. Statistical analysis was performed using one-way ANOVA with Tukey's multiple comparisons, (*P<0.05, **P<0.01, ***P<0.001, ****P<0.0001).*

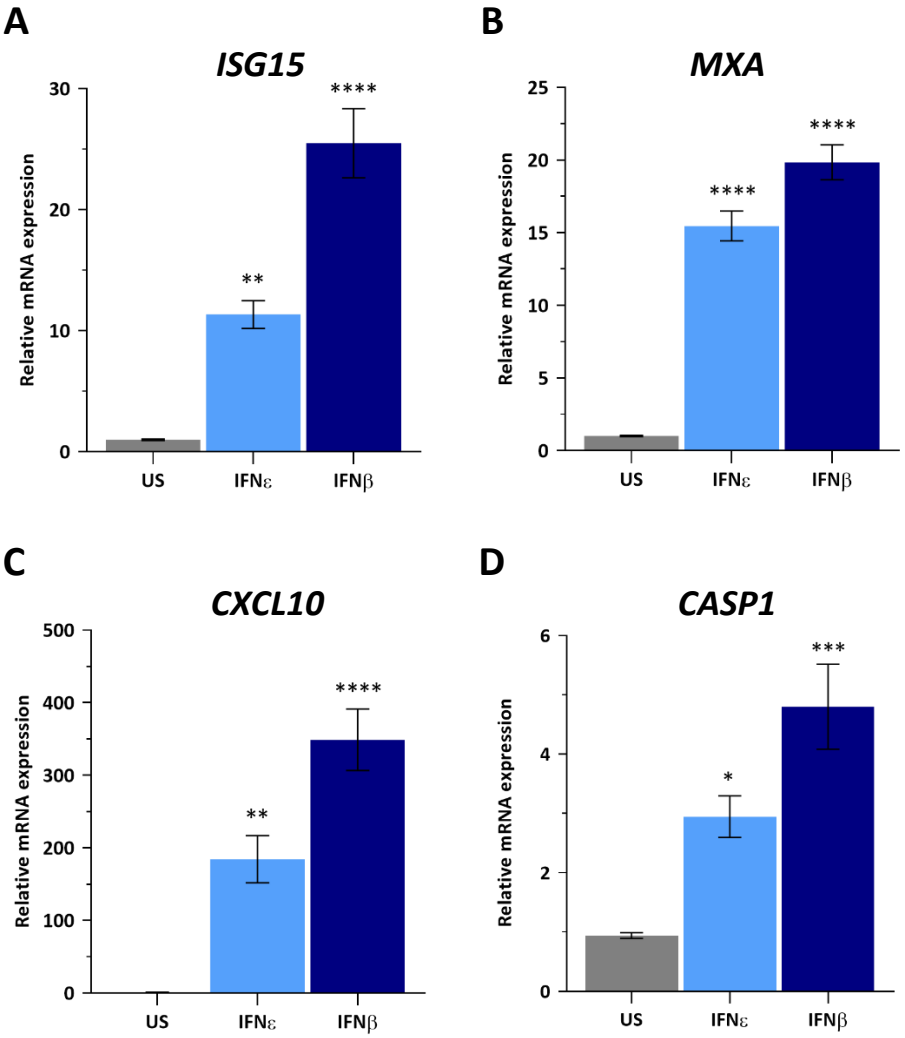

Figure 2. Induction of classical IRGs in human vaginal cancer cells (VK2).
*Graphs (A-D) illustrate responsiveness of VK2 cells to type I IFN stimulation. Cells were subjected to 3 hrs stimulation with 100 IU/ml of recombinant mIFNε or hIFNβ (Rebif®) and compared to US control (unstimulated control). Induction of ISG15(A), MXA(B), CXCL10(C) and CASP1(D) mRNA was quantified by qRT-PCR. Histograms showing relative mRNA expression or fold induction, are deduced using the $2^{-\Delta\Delta CT}$ method, normalized to corresponding endogenous 18s and expressed relative to unstimulated control. Data is representative of mean ± SEM, from three independent biological experiments, performed in technical triplicates. Statistical analysis was performed using one-way ANOVA with Dunnett's multiple comparisons test, (*P<0.05, **P<0.01, ***P<0.001, ****P<0.0001).*

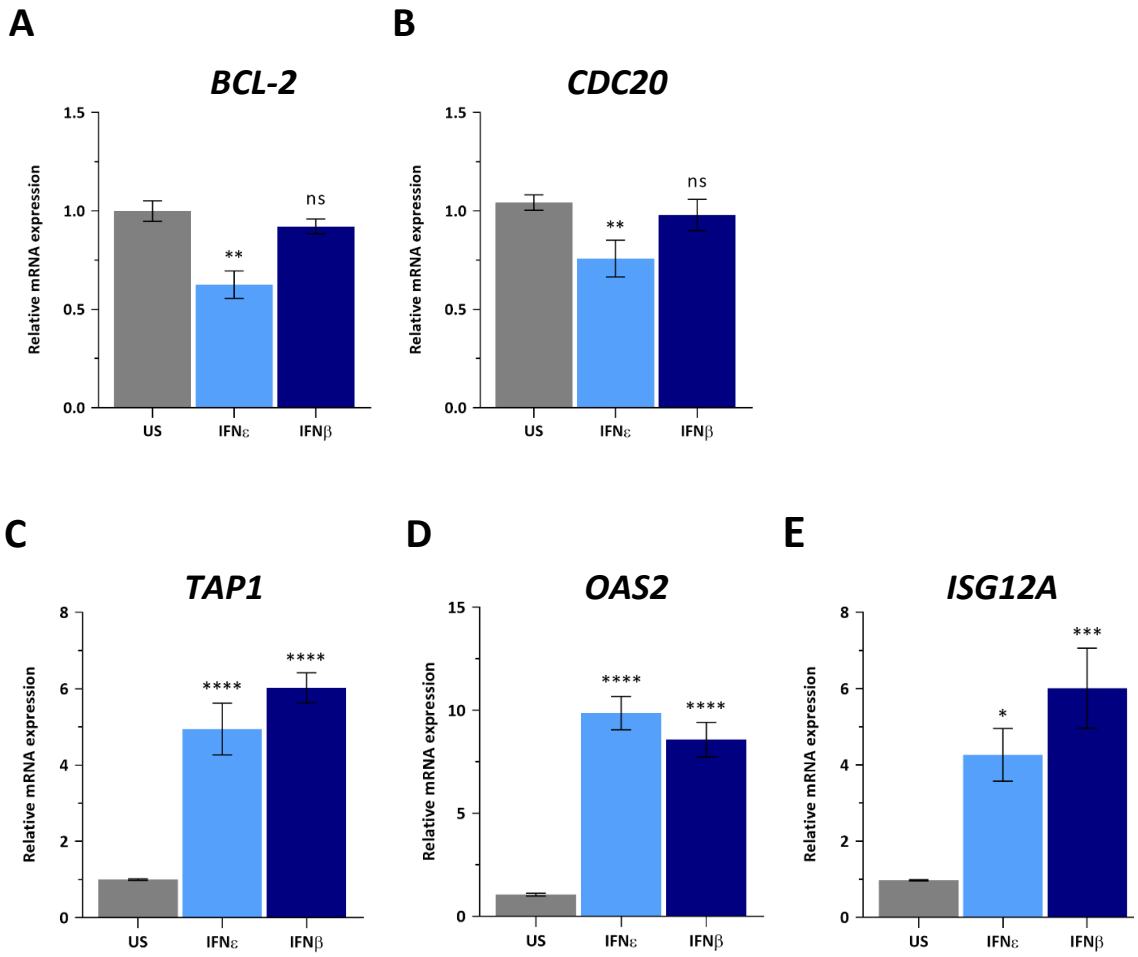

Figure 3. Regulation of cell survival and apoptotic ISGs in human vaginal cancer cells. *VK2 (human vaginal cancer) cells were subjected to 3 hrs stimulation with 100 IU/ml of recombinant mIFNε or hIFNβ (Rebif®) and compared to US control (unstimulated control). Expression of pro-survival: BCL-2(A), CDC20(B); and pro-apoptotic: TAP1(C), OAS2(D), ISG12A(E); mRNA, was quantified by qRT-PCR. Histograms showing relative mRNA expression or fold induction, are deduced using the $2^{-\Delta\Delta CT}$ method, normalized to corresponding endogenous 18s and expressed relative to unstimulated control. Data is representative of mean ± SEM, from three independent biological experiments, performed in technical triplicates. Statistical analysis was performed using one-way ANOVA with Dunnett's multiple comparisons test, (*P<0.05, **P<0.01, ***P<0.001, ****P<0.0001).*

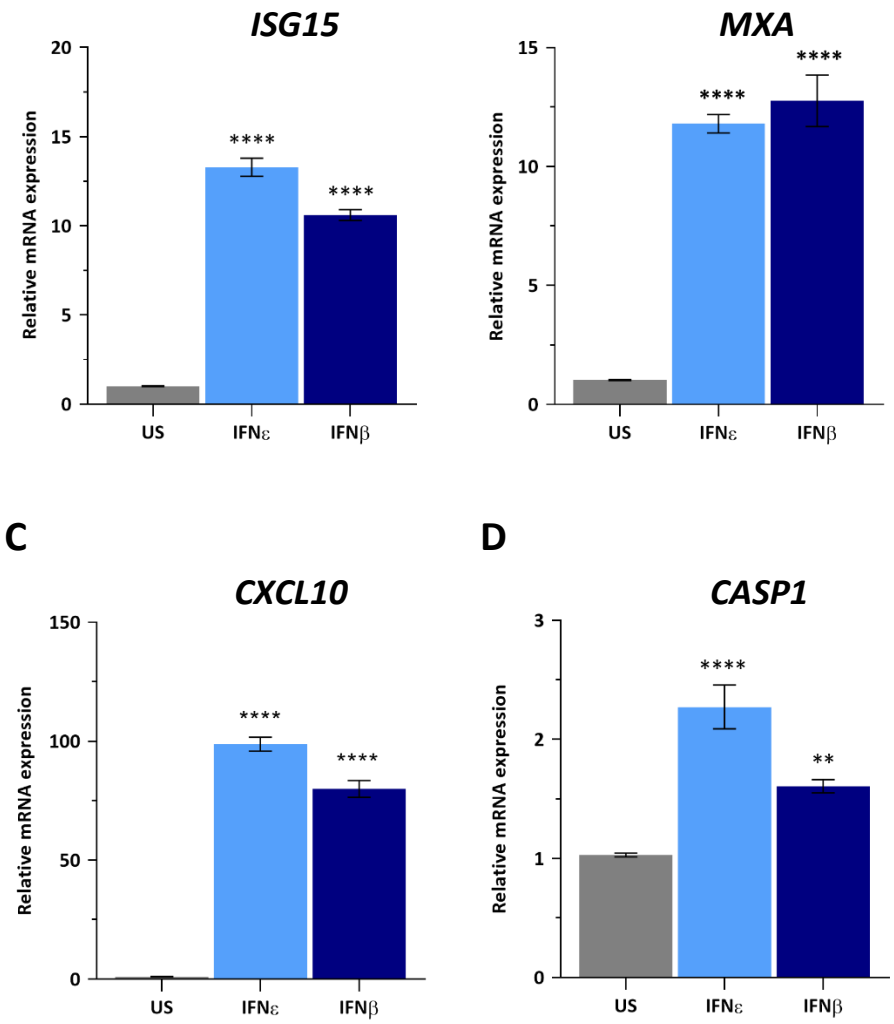

Figure 4. Induction of classical IRGs in human ectocervical cancer cells (Ect1).
*Graphs (A-D) illustrate responsiveness of Ect1 cells to type I IFN stimulation. These cells were subjected to 3 hrs stimulation with 100 IU/ml of recombinant mIFNε or hIFNβ (Rebif®) and compared to US control (unstimulated control). Expression of ISG15(A), MXA(B), CXCL10(C) and CASP1(D) mRNA was quantified by qRT-PCR. Histograms showing relative mRNA expression or fold induction, are deduced using the $2^{-\Delta\Delta CT}$ method, normalized to corresponding endogenous 18s and expressed relative to unstimulated control. Data is representative of mean ± SEM, from three independent biological experiments, performed in technical triplicates. Statistical analysis was performed using one-way ANOVA with Dunnett's multiple comparisons test, (*P<0.05, **P<0.01, ***P<0.001, ****P<0.0001).*

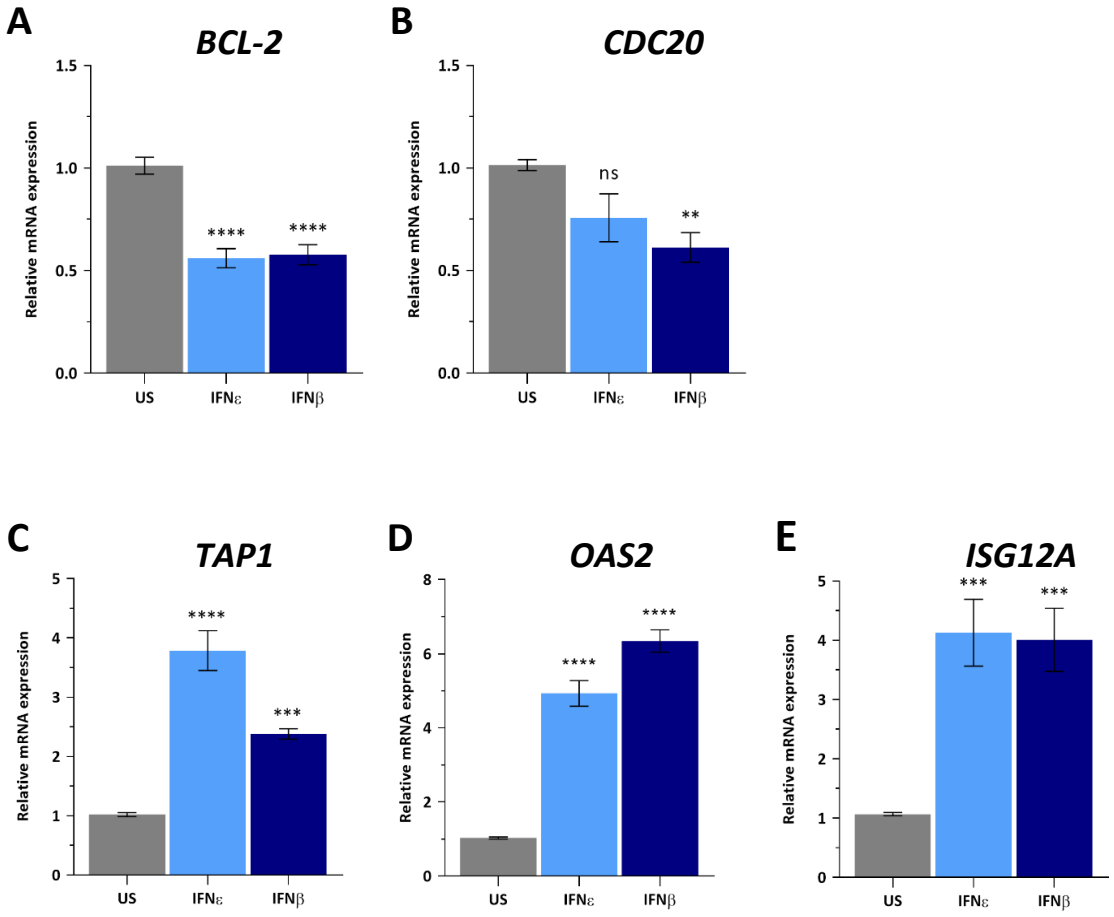

Figure 5. Regulation of cell survival and apoptotic ISGs in Ect1 cells.

*Ect1 (human ectocervical cancer) cells were subjected to 3 hrs stimulation with 100 IU/ml of recombinant mIFNε or hIFNβ (Rebif®) and compared to US control (unstimulated control). Expression of pro-survival: BCL-2(A), CDC20(B); and pro-apoptotic: TAP1(C), OAS2(D), ISG12A(E), mRNA, was quantified by qRT-PCR. Histograms showing relative mRNA expression or fold induction, are deduced using the $2^{-\Delta\Delta CT}$ method, normalized to corresponding endogenous 18s and expressed relative to unstimulated control. Data is representative of mean ± SEM, from three independent biological experiments, performed in technical triplicates. Statistical analysis was performed using one-way ANOVA with Dunnett's multiple comparisons test, (*P<0.05, **P<0.01, ***P<0.001, ****P<0.0001).*

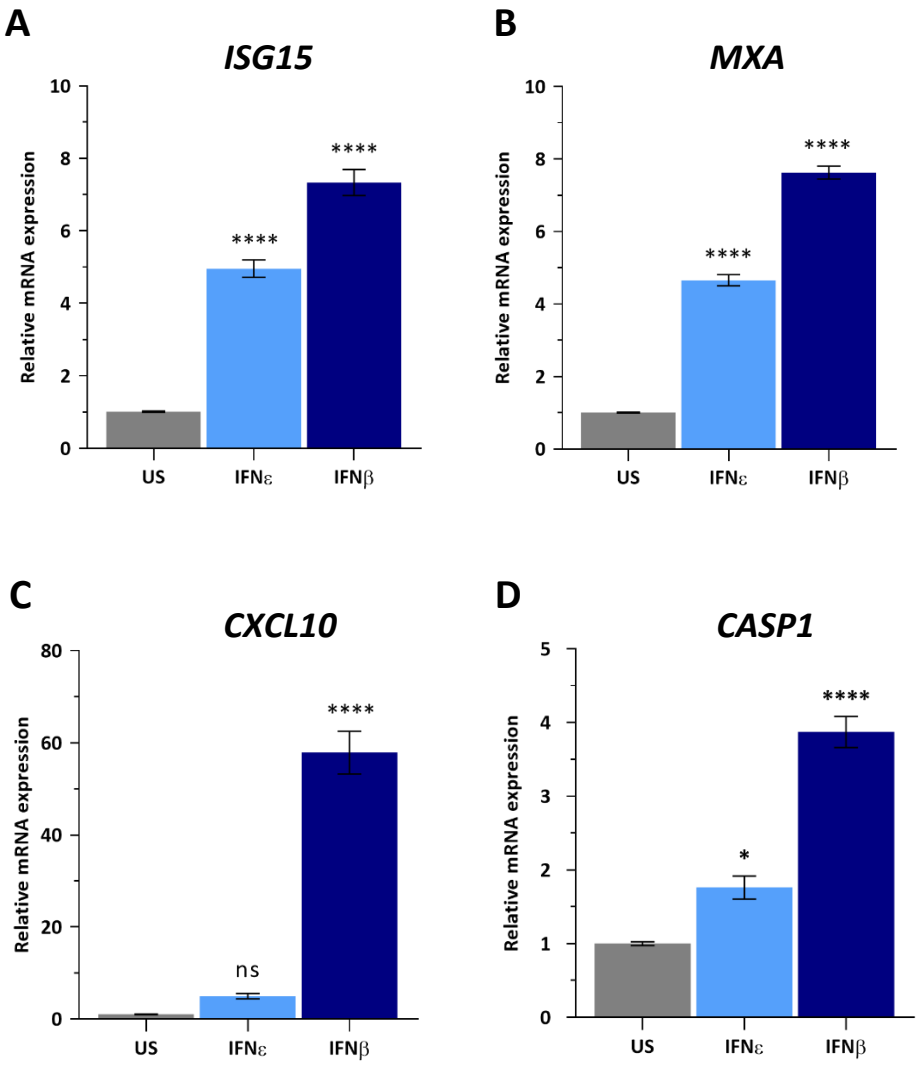

Figure 6. Induction of classical IRGs in human endocervical cancer cells (End1). *Graphs (A-D) illustrate responsiveness of End1 cells to type I IFN stimulation. These cells were subjected to 3 hrs stimulation with 100 IU/ml of recombinant mIFNε or hIFNβ (Rebif®) and compared to US control (unstimulated control). Expression of ISG15(A), MXA(B), CXCL10(C) and CASP1(D) mRNA was quantified by qRT-PCR. Histograms showing relative mRNA expression or fold induction, are deduced using the* $2^{-\Delta\Delta CT}$ *method, normalized to corresponding endogenous 18s and expressed relative to unstimulated control. Data is representative of mean ± SEM, from three independent biological experiments, performed in technical triplicates. Statistical analysis was performed using one-way ANOVA with Dunnett's multiple comparisons test, (*P<0.05, **P<0.01, ***P<0.001, ****P<0.0001).*

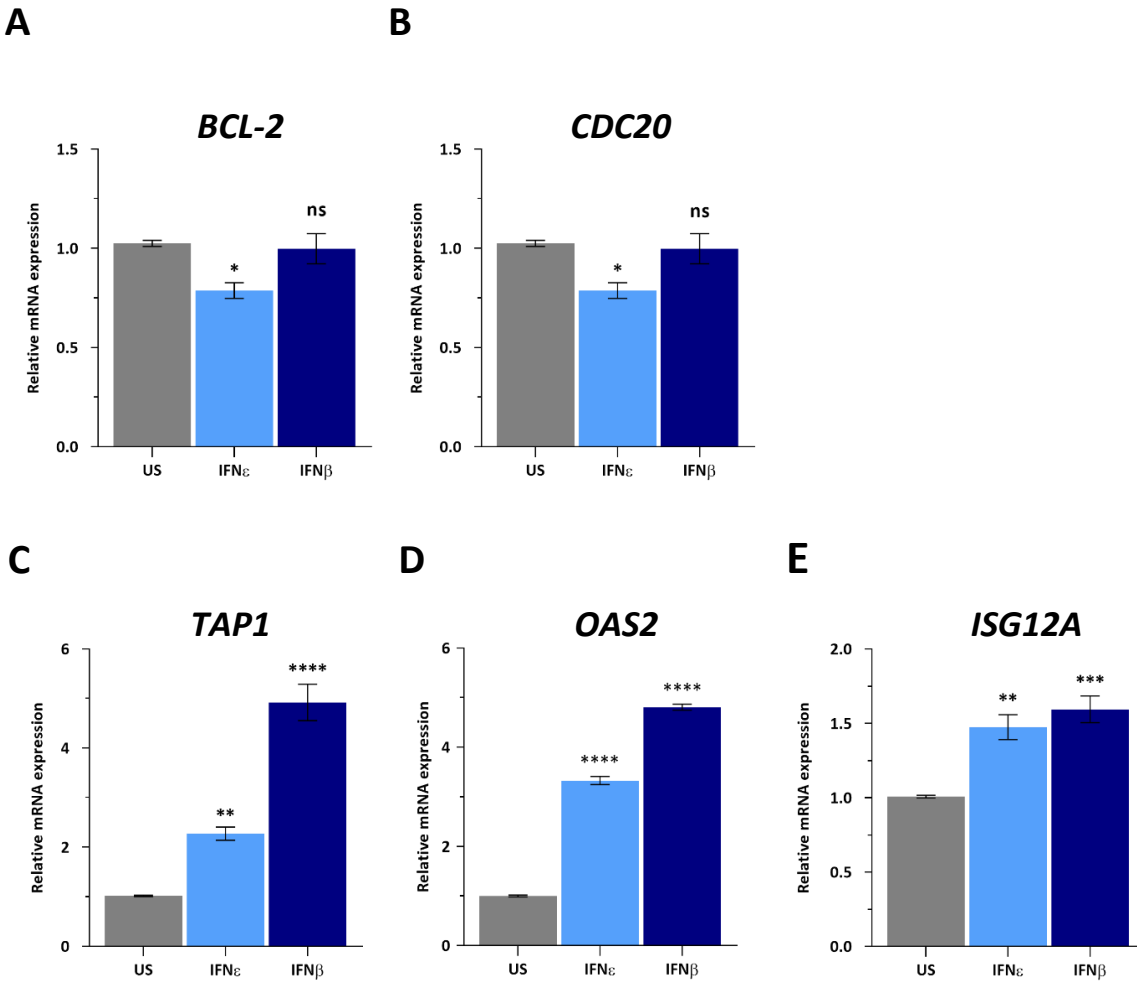

Figure 7. Regulation of cell survival and apoptotic ISGs in End1 cells.
*End1 (human endocervical cancer) cells were subjected to 3 hrs stimulation with 100 IU/ml of recombinant mIFNε or hIFNβ (Rebif®) and compared to US control (unstimulated control). Expression of pro-survival: BCL-2(A), CDC20(B); and anti-apoptotic: TAP1(C), OAS2(D), ISG12A(E), mRNA, was quantified by qRT-PCR. Histograms showing relative mRNA expression or fold induction, are deduced using the $2^{-\Delta\Delta CT}$ method, normalized to corresponding endogenous 18s and expressed relative to the unstimulated control. Data is representative of mean ± SEM, from three independent biological experiments, performed in technical triplicates. Statistical analysis was performed using one-way ANOVA with Dunnett's multiple comparisons test, (*P<0.05, **P<0.01, ***P<0.001, ****P<0.0001).*

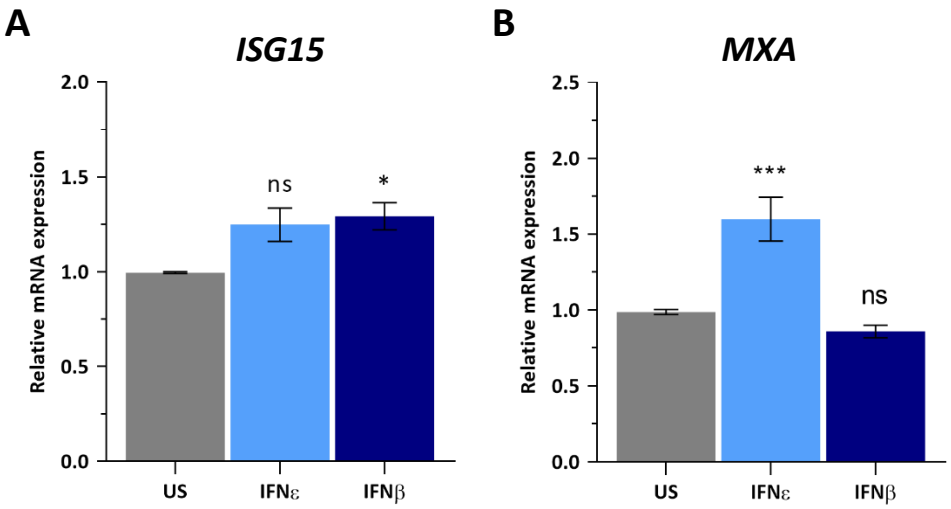

Figure 8. Induction of classical IRGs in human endometrial cancer cells (ECC-1). *ECC-1 cells were subjected to 3 hrs stimulation with 100 IU/ml of recombinant mIFNε or hIFNβ (Rebif®) and compared to US control (unstimulated control). Expression of ISG15(A) and MXA(B), mRNA was quantified by qRT-PCR. CXCL10 and OAS2 transcripts could not be detected. Histograms showing relative mRNA expression or fold induction, are deduced using the $2^{-\Delta\Delta CT}$ method, normalized to corresponding endogenous 18s and expressed relative to unstimulated control. Data is representative of mean ± SEM, from three independent biological experiments, performed in technical triplicates. Statistical analysis was performed using one-way ANOVA with Dunnett's multiple comparisons test, (*P<0.05, **P<0.01, ***P<0.001, ****P<0.0001).*

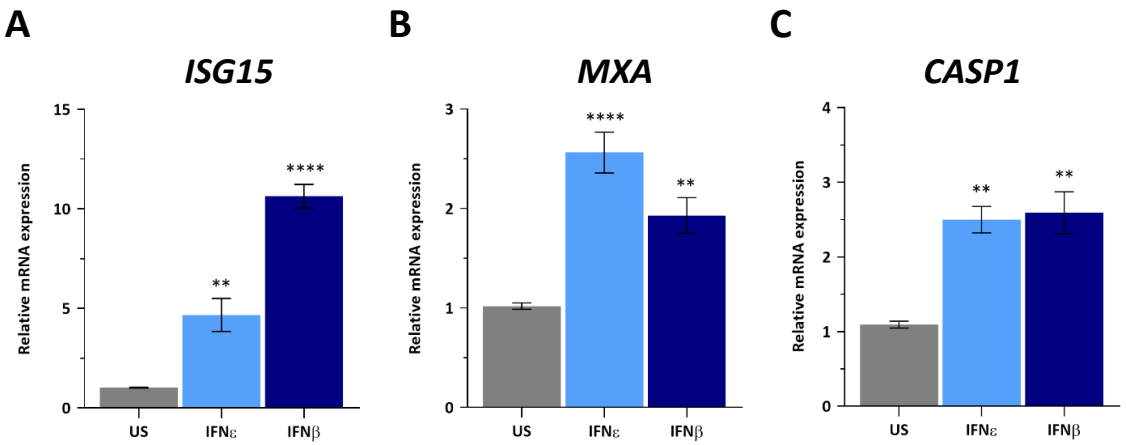

Figure 9. Induction of classical IRGs in human endometrial cancer cells (RL95-2).
*Graphs (A-C) illustrate responsiveness of RL95-2 cells to type I IFN stimulation. These cells were subjected to 24 hrs stimulation with 1000 IU/ml of recombinant mIFNε or hIFNβ (Rebif®) and compared to US control (unstimulated control). Expression of ISG15(A), MXA(B) and CASP1(C) mRNA was quantified by qRT-PCR. CXCL10 could not be detected. Histograms showing relative mRNA expression or fold induction, deduced using the $2^{-\Delta\Delta CT}$ method, normalized to corresponding endogenous 18s and expressed relative to unstimulated control. Data is representative of mean ± SEM, from three independent biological experiments, performed in technical triplicates. Statistical analysis was performed using one-way ANOVA with Dunnett's multiple comparisons test, (*P<0.05, **P<0.01, ***P<0.001, ****P<0.0001).*

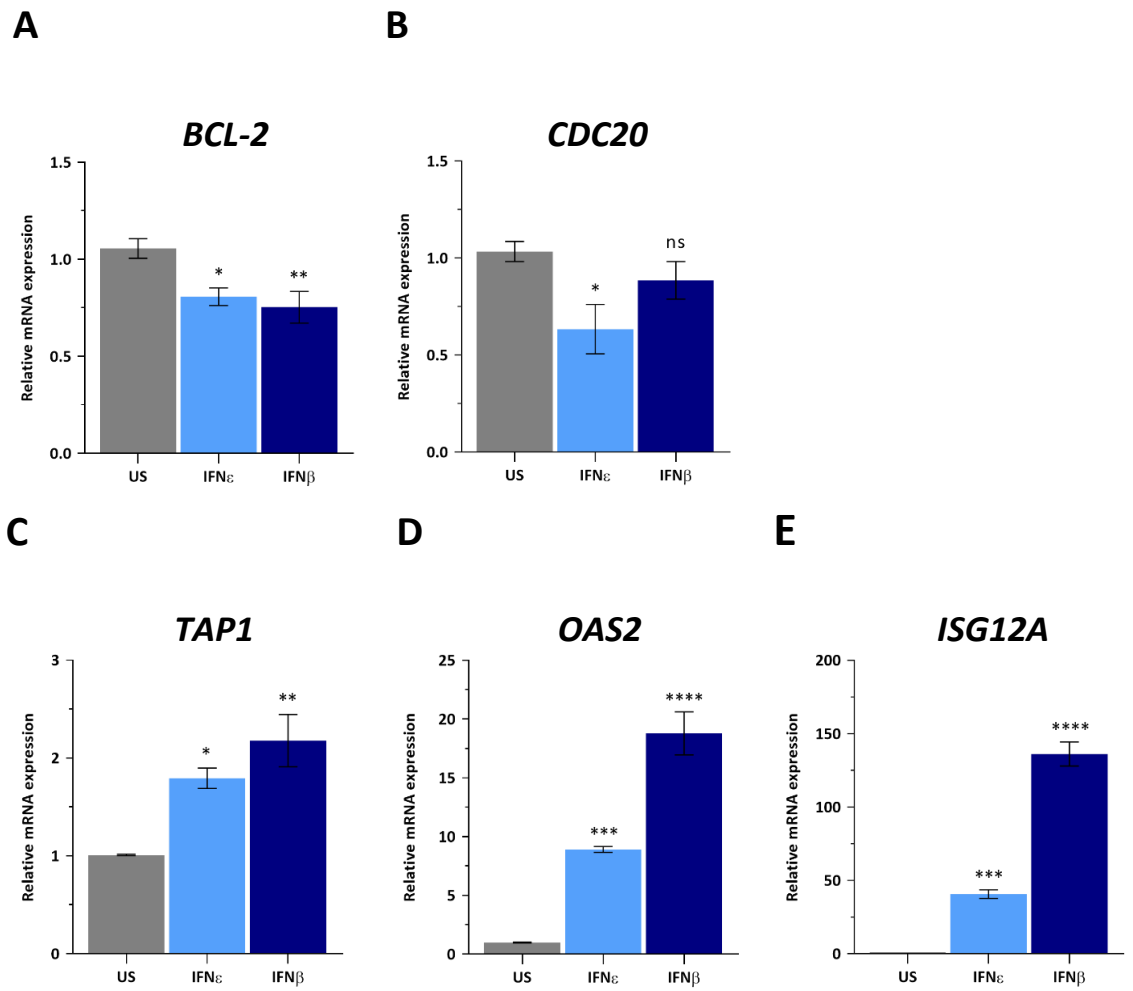

Figure 10. Regulation of cell survival and apoptotic ISGs in RL95-2 cells.
*RL95-2 (human endometrial cancer) cells were subjected to 24 hrs stimulation with 1000 IU/ml of recombinant mIFNε or hIFNβ (Rebif®) and compared to US control (unstimulated control). Expression of pro-survival: BCL-2(A), CDC20(B); and pro-apoptotic: TAP1(C), OAS2(D), ISG12A(E), mRNA, was quantified by qRT-PCR. Histograms showing relative mRNA expression or fold induction, are deduced using the $2^{-\Delta\Delta CT}$ method, normalized to corresponding endogenous 18s and expressed relative to unstimulated control. Data is representative of mean ± SEM, from three independent biological experiments, performed in technical triplicates. Statistical analysis was performed using one-way ANOVA with Dunnett's multiple comparisons test, (*P<0.05, **P<0.01, ***P<0.001, ****P<0.0001).*

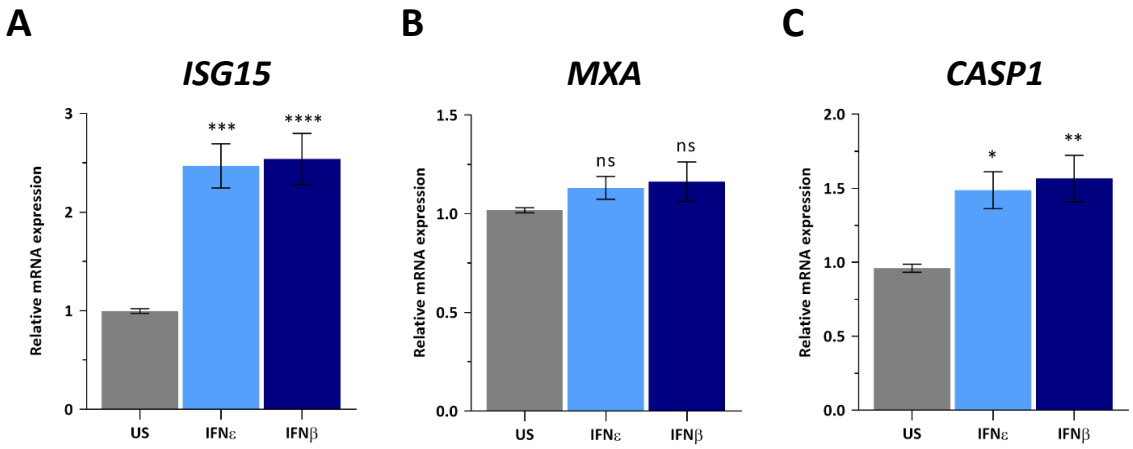

Figure 11. Induction of classical IRGs in human endometrial cancer cells (AN3CA). *Graphs (A-C) illustrate responsiveness of AN3CA cells to type I IFN stimulation. These cells were subjected to 24 hrs stimulation with 1000 IU/ml of recombinant mIFNε or hIFNβ (Rebif®) and compared to US control (unstimulated control). Expression of ISG15(A), MXA(B) and CASP1(C) mRNA was quantified by qRT-PCR. CXCL10 could not be detected. Histograms showing relative mRNA expression or fold induction, are deduced using $2^{-\Delta\Delta CT}$ method, normalized to corresponding endogenous 18s and expressed relative to unstimulated control. Data is representative of mean ± SEM, from three independent biological experiments, performed in technical triplicates. Statistical analysis was performed using one-way ANOVA with Dunnett's multiple comparisons test, (*P<0.05, **P<0.01, ***P<0.001, ****P<0.0001).*

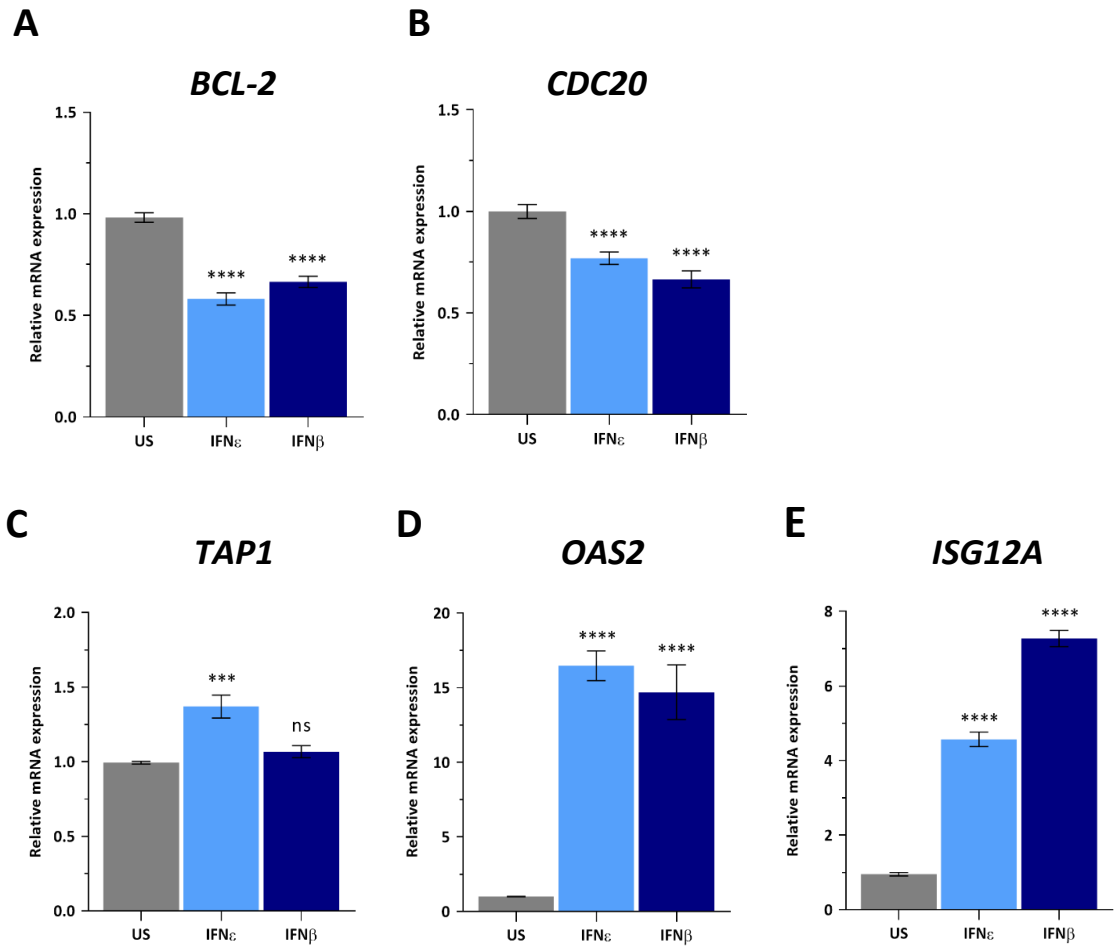

Figure 12. Regulation of cell survival and apoptotic ISGs in AN3CA cells.

*AN3CA (human endometrial cancer) cells were subjected to 24 hrs stimulation with 1000 IU/ml of recombinant mIFNε or hIFNβ (Rebif®) and compared to US control (unstimulated control). Expression of pro-survival: BCL-2(A), CDC20(B); and pro-apoptotic: TAP1(C), OAS2(D), ISG12A(E), mRNA, was quantified by qRT-PCR. Histograms showing relative mRNA expression or fold induction, are deduced using the $2^{-\Delta\Delta CT}$ method, normalized to corresponding endogenous 18s and expressed relative to unstimulated control. Data is representative of mean ± SEM, from three independent biological experiments, performed in technical triplicates. Statistical analysis was performed using one-way ANOVA with Dunnett's multiple comparisons test, (*P<0.05, **P<0.01, ***P<0.001, ****P<0.0001).*

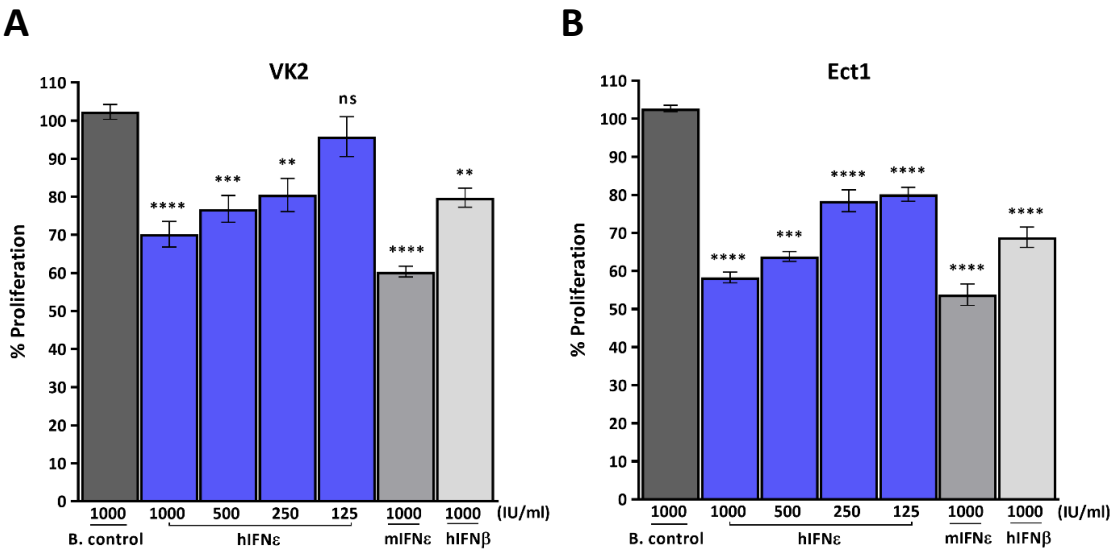

Figure 13. IFNe displays anti-proliferative properties in vitro.

*Cell viability of VK2 [vaginal (A)] and Ect1 [ectocervical (B)] lower FRT human epithelial cell lines was determined by MTT assay. Cells were treated for 72 hrs with recombinant hIFNε (125-1000 IU/ml); hIFNβ, mIFNε, B.control (buffer control) (1000 IU/ml) including US control (unstimulated control cells). Graphs represent % proliferation relative to US control absorbance (590nm, Fluorostar Optima plate reader). Data is representative of mean ± SEM, from three independent biological experiments, performed in technical quadruplicates. Statistical analysis was performed using one-way ANOVA with Tukey's multiple comparisons, (*P<0.05, **P<0.01, ***P<0.001, ****P<0.0001).*

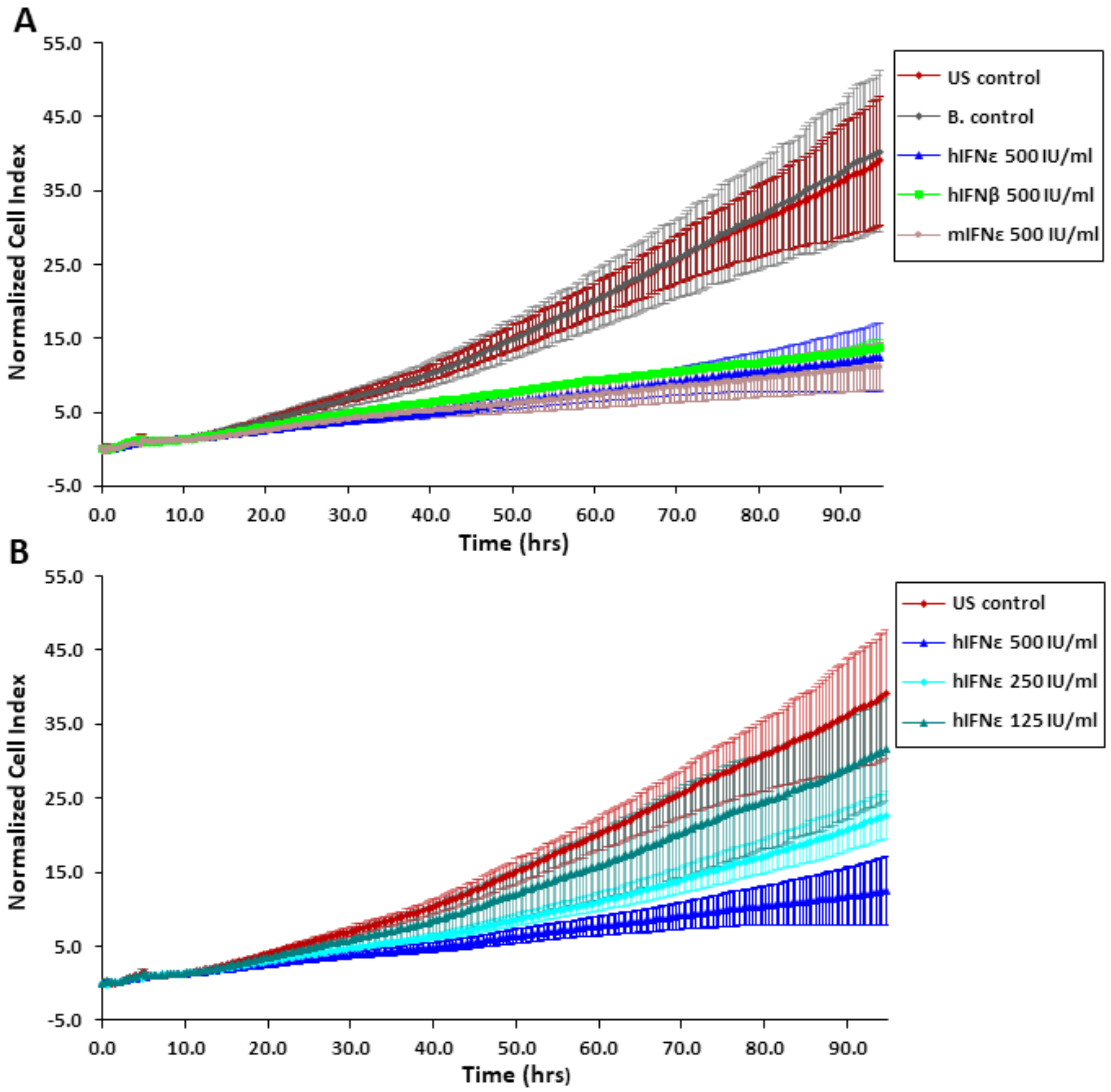

Figure 14. Anti-proliferative effects of type I interferons on lower FRT VK2 epithelial cells.

Graphical representation of mean cell index measurements in Real-Time by xCELLigence over a 90 hr time course. A) VK2 cell proliferation was inhibited with 500 IU/ml treatment of recombinant hIFNε, hIFNβ and mIFNε compared to B.control (buffer control) and US control (unstimulated control cells). B) demonstrates a dose dependent reduction of VK2 cell proliferation with hIFNε treatments of 125-500 IU/ml. Graphs represent the mean cell index +/-SD, measured at 30 min intervals normalized post treatment time as deduced from RTCA software. Data is representative of three independent biological experiments, performed in technical quadruplicates.

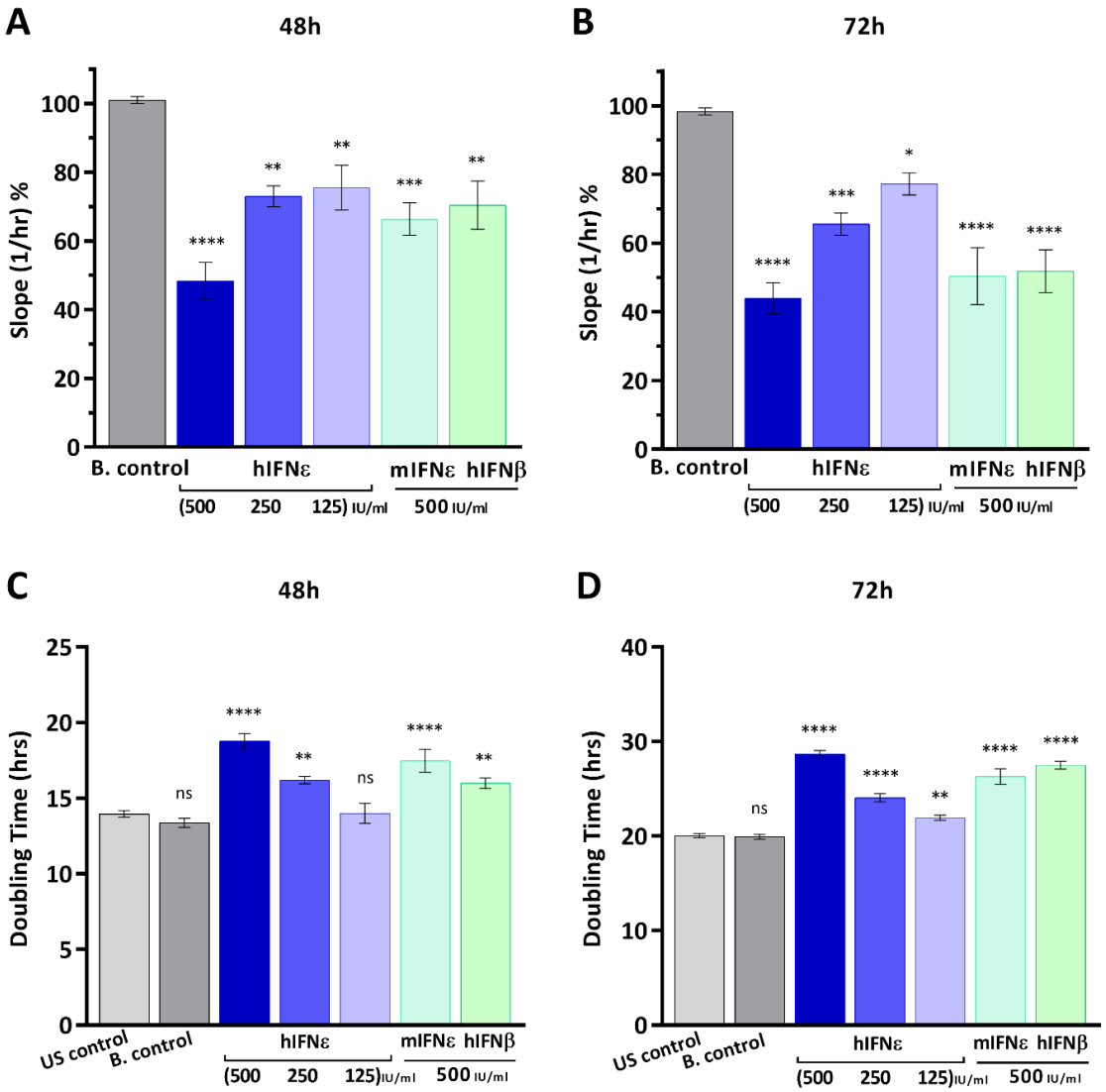

Figure 15. IFNε anti-proliferative effects on VK2 epithelial cells quantified.
*Graphs show data at 48 hrs (A, C) and 72 hrs (B, D) time point stimulations with recombinant hIFNε (125-500 IU/ml); hIFNβ, mIFNε, B.control (buffer control) (500 IU/ml) and US control (unstimulated control cells), by xCELLigence Real-Time measurements of VK2 (vaginal) cells. Data (A, B) show a dose dependent decrease in VK2 proliferation rates upon IFNε treatment expressed as slope (1/hrs) % relative to US control. Graphs (C, D) demonstrate doubling time increases in VK2 cells treated with type I IFNs. Data is representative of mean ± SEM, from three independent biological experiments, performed in technical quadruplicates. Statistical analysis was performed using one-way ANOVA with Fisher's LSD multiple comparisons test, (*P<0.05, **P<0.01, ***P<0.001, ****P<0.0001).*

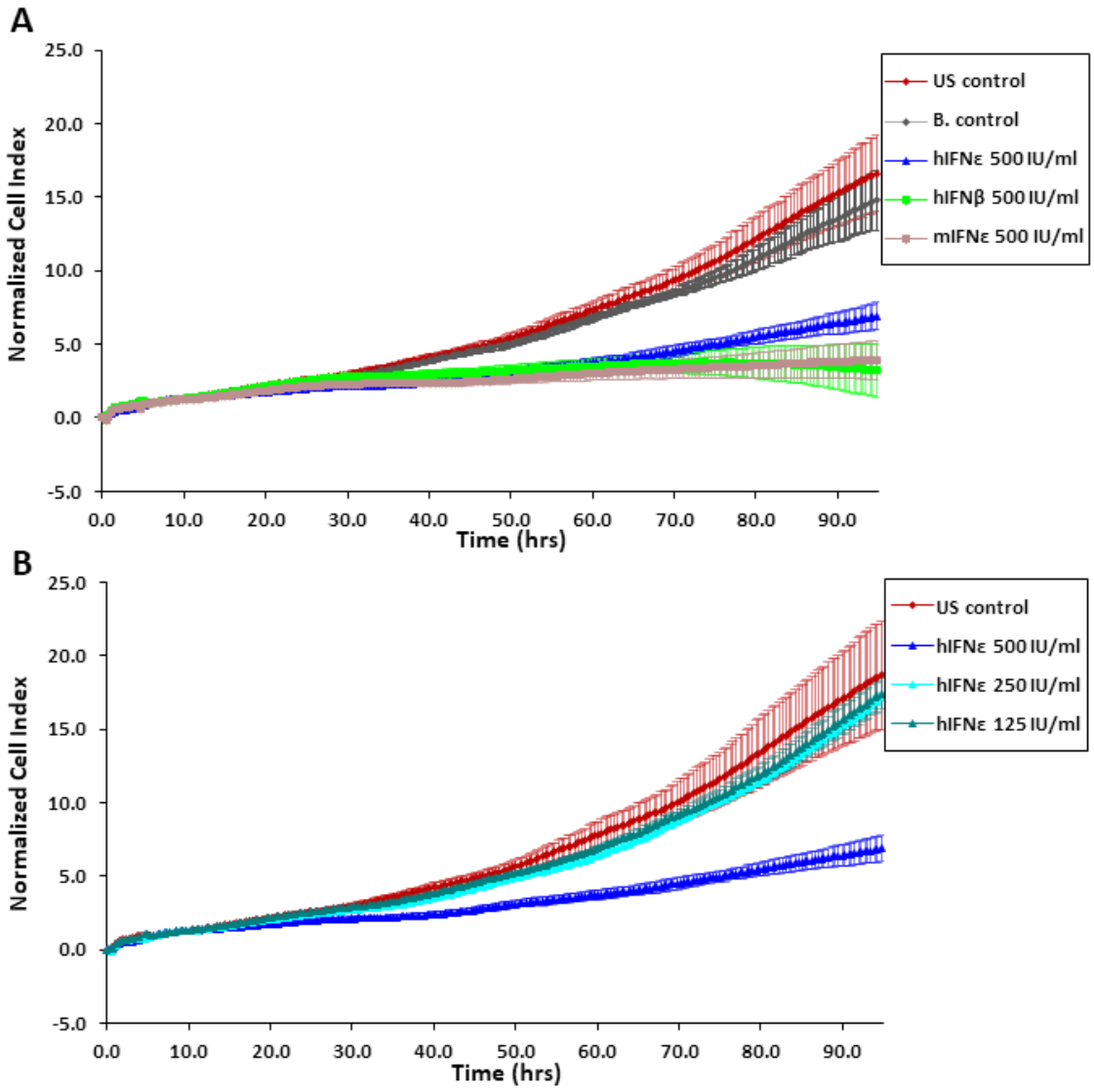

Figure 16. Antiproliferative effects of type I interferons on lower FRT Ect1 epithelial cells.

Graphical representation of mean cell index measurements in Real-Time by xCELLigence over a 90 hr time course. A) Ect1 (ectocervical) cell proliferation was inhibited with 500 IU/ml treatment of recombinant hIFNε, hIFNβ, mIFNε, B.control (buffer control) and US control (unstimulated control cells). B) demonstrates a dose dependent reduction of Ect1 cell proliferation with hIFNε treatments of 125-500 IU/ml. Graphs represent the mean cell index +/-SD, measured at 30 min intervals normalized post treatment time as deduced from RTCA software. Data is representative of three independent biological experiments, performed in technical quadruplicates.

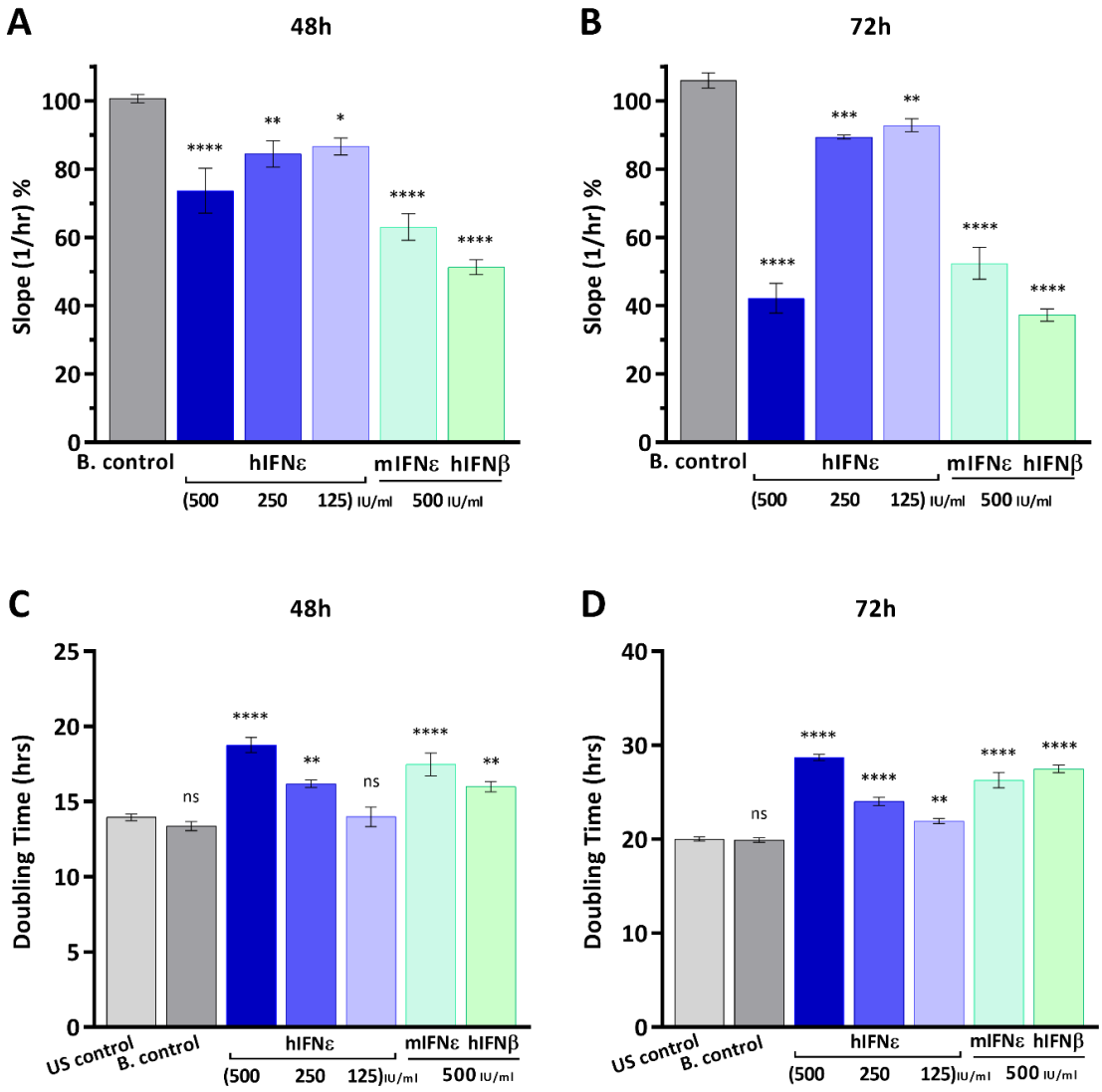

Figure 17. IFNε anti-proliferative effects on Ect1 epithelial cells quantified.
*Graphs show data at 48 hrs (A, C) and 72 hrs (B, D) time point stimulations with recombinant hIFNε (125-500 IU/ml); hIFNβ, mIFNε, B.control (buffer control) (500 IU/ml); and US control (unstimulated control cells), by xCELLigence Real-Time measurements of Ect1 (ectocervical) cells. Data (A, B) illustrate a dose dependent decrease in Ect1 proliferation rates upon IFNε treatment expressed as slope (1/hrs) % relative to US control. Graphs (C, D) demonstrate increases in doubling time of Ect1 cells treated with type I IFNs. Data is representative of mean ± SEM, from three independent biological experiments, performed in technical quadruplicates. Statistical analysis was performed using one-way ANOVA with Fisher's LSD multiple comparisons test, (*P<0.05, **P<0.01, ***P<0.001, ****P<0.0001).*

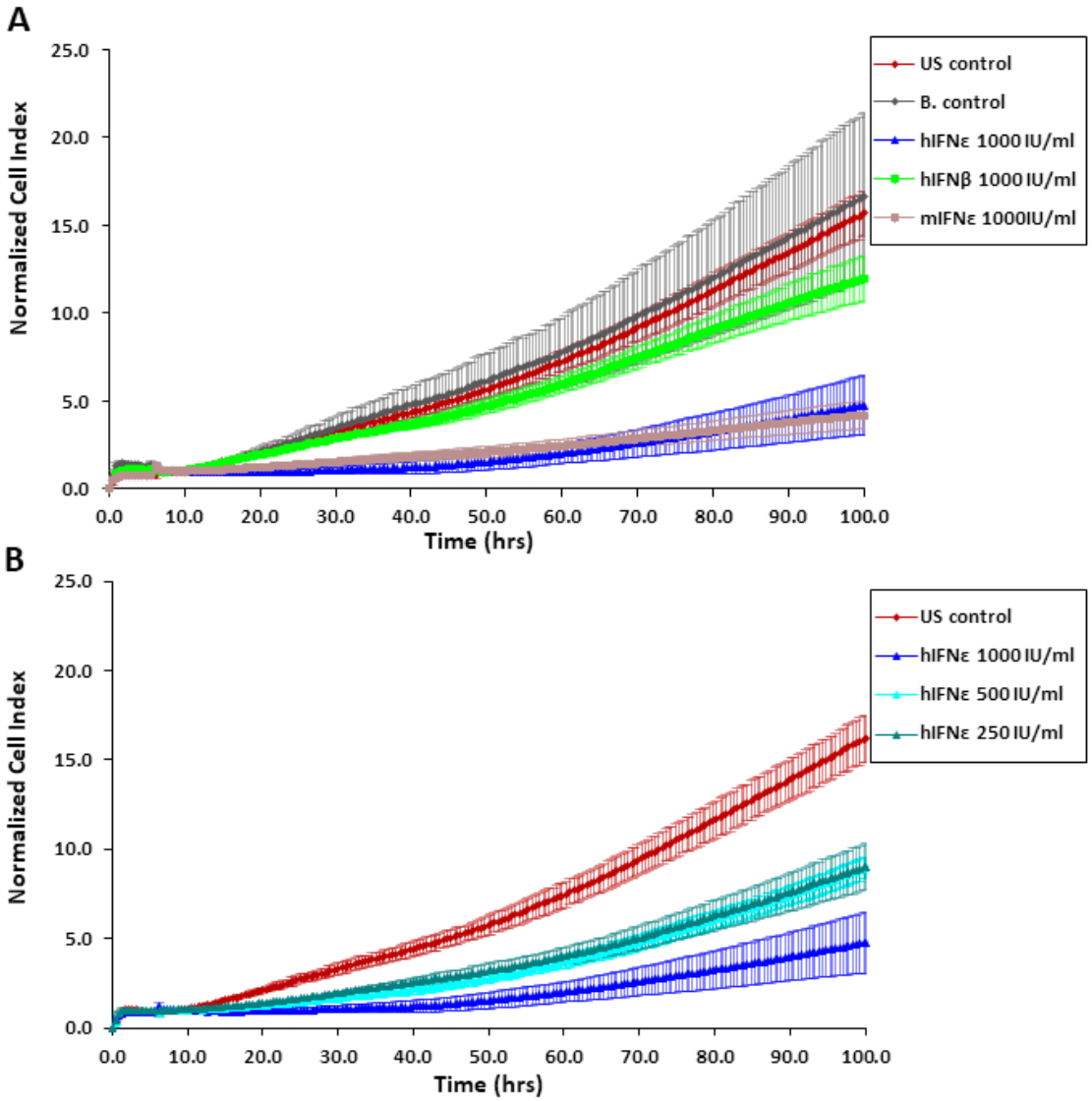

Figure 18. Antiproliferative effects of type I interferons on RL95-2 endometrial cancer cells.

Graphical representation of mean cell index measurements in Real-Time by xCELLigence over a 90 hr time course. A) RL95-2 cell proliferation was inhibited with 1000 IU/ml treatment of recombinant hIFNε, hIFNβ, mIFNε, B.control (buffer control) and US control (unstimulated control cells). Graph B demonstrates RL95-2 dose dependent reduction of cell proliferation with hIFNε treatments of 250-1000 IU/ml. Graphs represent the mean cell index +/-SD, measured at 30 min intervals normalized post treatment time as deduced from RTCA software. Data is representative of three independent biological experiments, performed in technical quadruplicates.

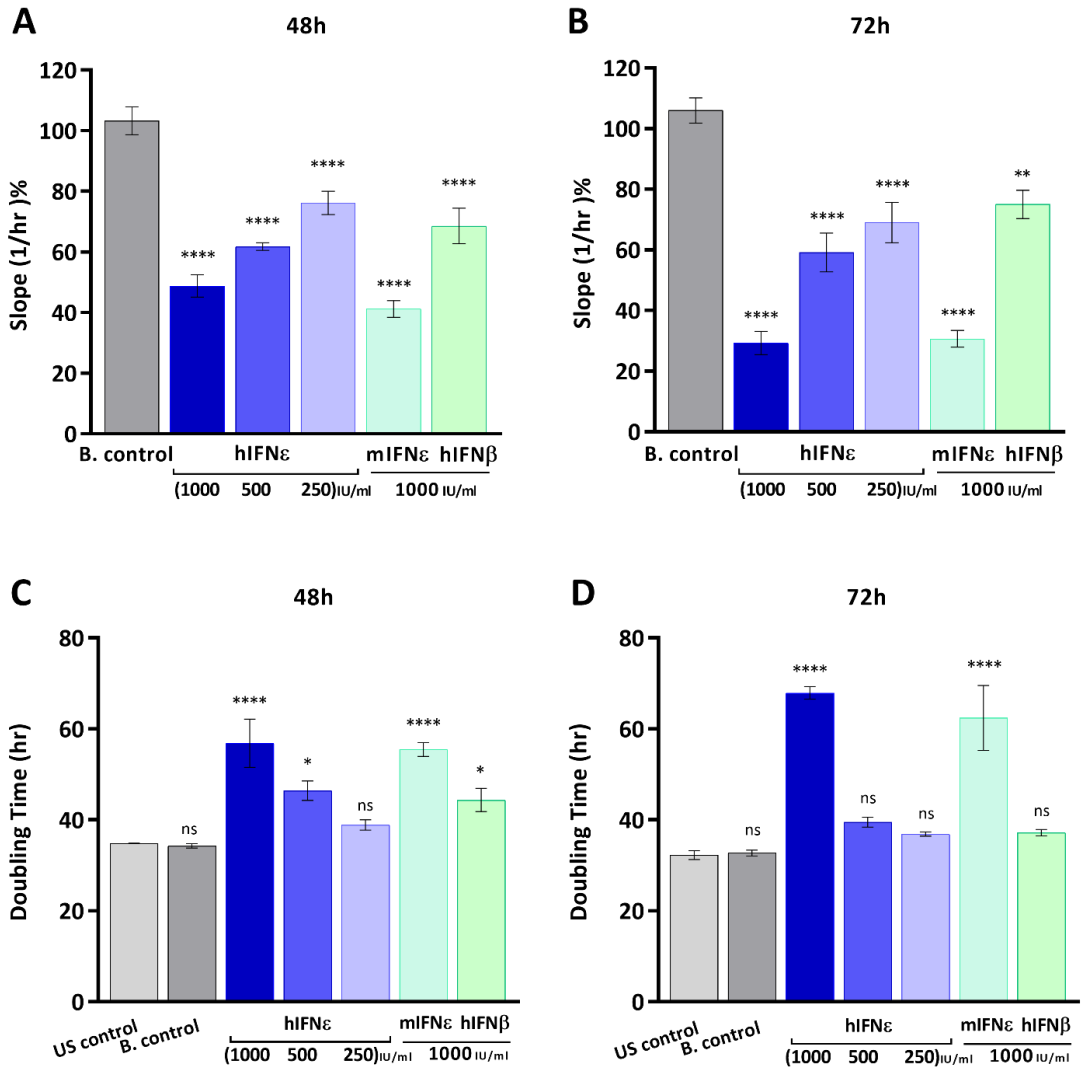

Figure 19. Quantification of IFNε's anti-proliferative effects on grade II derived endometrial cancer, RL95-2 cells.

*Graphs show data quantified at 48 hrs (A, C) and 72 hrs (B, D) time point stimulations with recombinant hIFNε (250-1000 IU/ml); hIFNβ, mIFNε, B.control (buffer control) (1000IU/ml); and US control (unstimulated control cells), by xCELLigence Real-Time measurements of RL95-2 endometrial cancer cells. Data (A, B) show a dose dependent decrease in RL95-2 cell proliferation upon IFNε treatment expressed as slope (1/hrs) % relative to US control. Graphs (C, D) demonstrate an increase in doubling time of RL95-2 cells treated with type I IFNs. Data is representative of mean ± SEM, from three independent biological experiments, performed in technical quadruplicates. Statistical analysis was performed using one-way ANOVA with Fisher's LSD multiple comparisons test, (*P<0.05, **P<0.01, ***P<0.001, ****P<0.0001).*

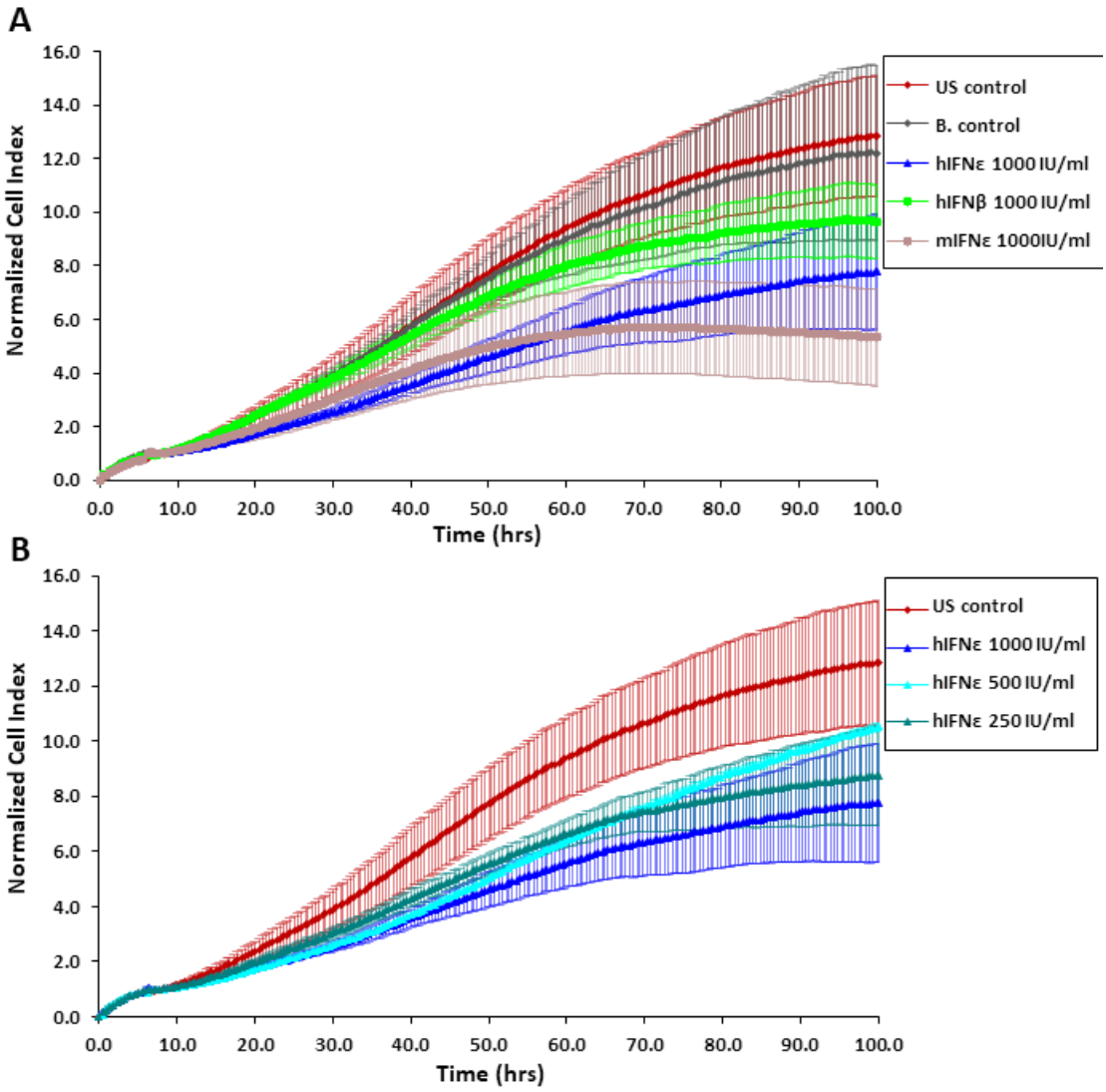

Figure 20. Anti-proliferative effects of type I interferons on AN3CA endometrial cancer cells.

Graphical representation of mean cell index measurements in Real-Time by xCELLigence over a 90 hr time course. A) AN3CA cell proliferation was inhibited with 1000IU/ml treatment of recombinant hIFNε, hIFNβ, mIFNε, B.control (buffer control) and US control (unstimulated control cells). Graph B demonstrates a dose dependent reduction of AN3CA cell proliferation with hIFNε treatments of 250-1000 IU/ml. Graphs represent the mean cell index +/-SD, measured at 30 min intervals normalized post treatment time as deduced from RTCA software. Data is representative of three independent biological experiments, performed in technical quadruplicates.

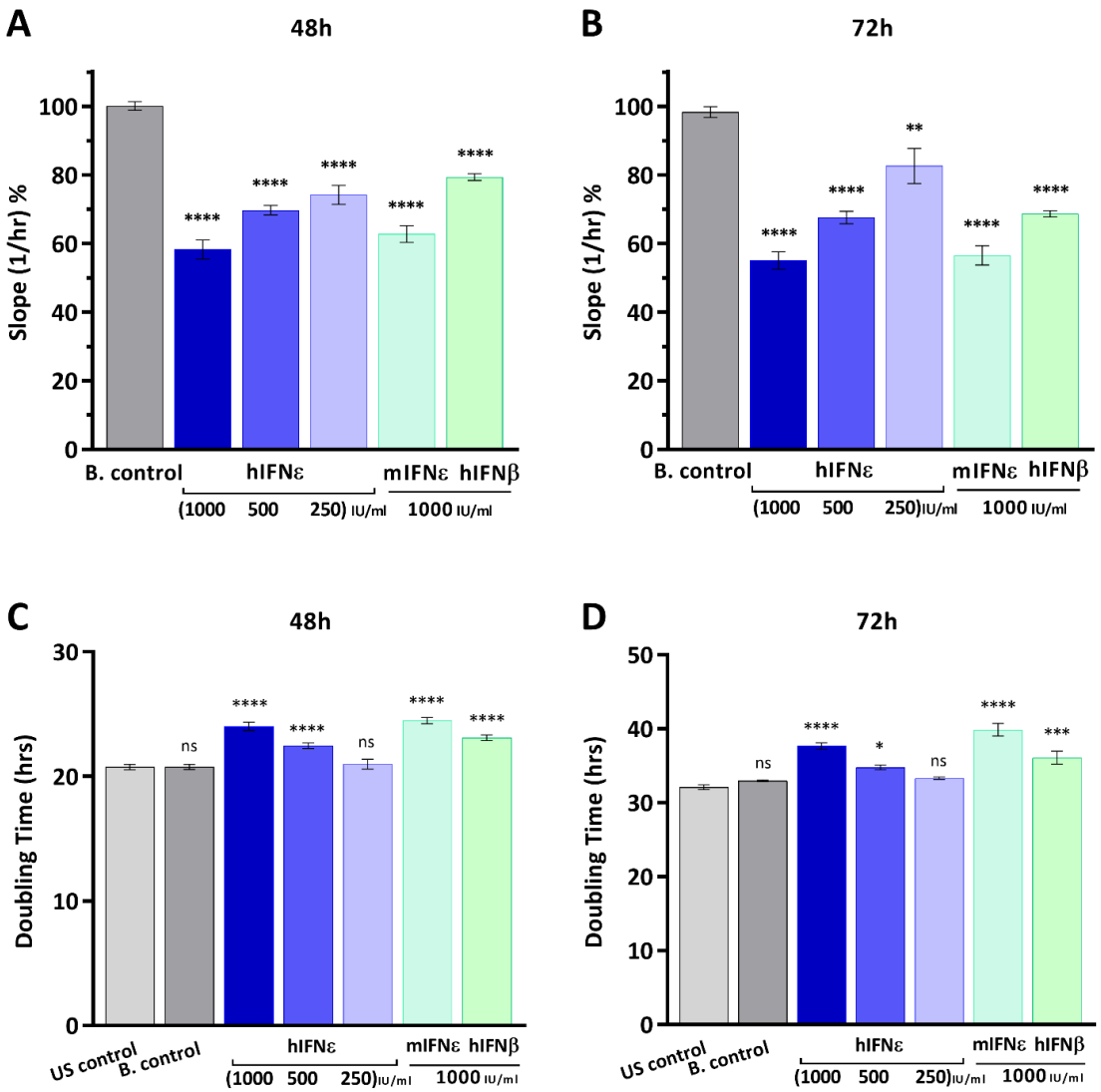

Figure 21. IFNε anti-proliferative effects on grade III derived endometrial cancer cells AN3CA quantified.

*Graphs show data quantified at 48 hrs (A, C) and 72 hrs(B,D) time point stimulations with recombinant hIFNε (250-1000 IU/ml); hIFNβ, mIFNε B.control (buffer control), (1000 IU/ml); and US control (unstimulated control), by xCELLigence Real-Time measurements of AN3CA endometrial cells. Data (A, B) show dose dependent decreases in AN3CA proliferation rates upon IFNε treatment expressed as slope (1/hrs) % relative to US control. Graphs (C, D) demonstrate increases in doubling time of AN3CA cells treated with type I IFNs. Data is representative of mean ± SEM, from three independent biological experiments, performed in technical quadruplicates. Statistical analysis was performed using one-way ANOVA with Fisher's LSD multiple comparisons test, (*P<0.05, **P<0.01, ***P<0.001, ****P<0.0001).*

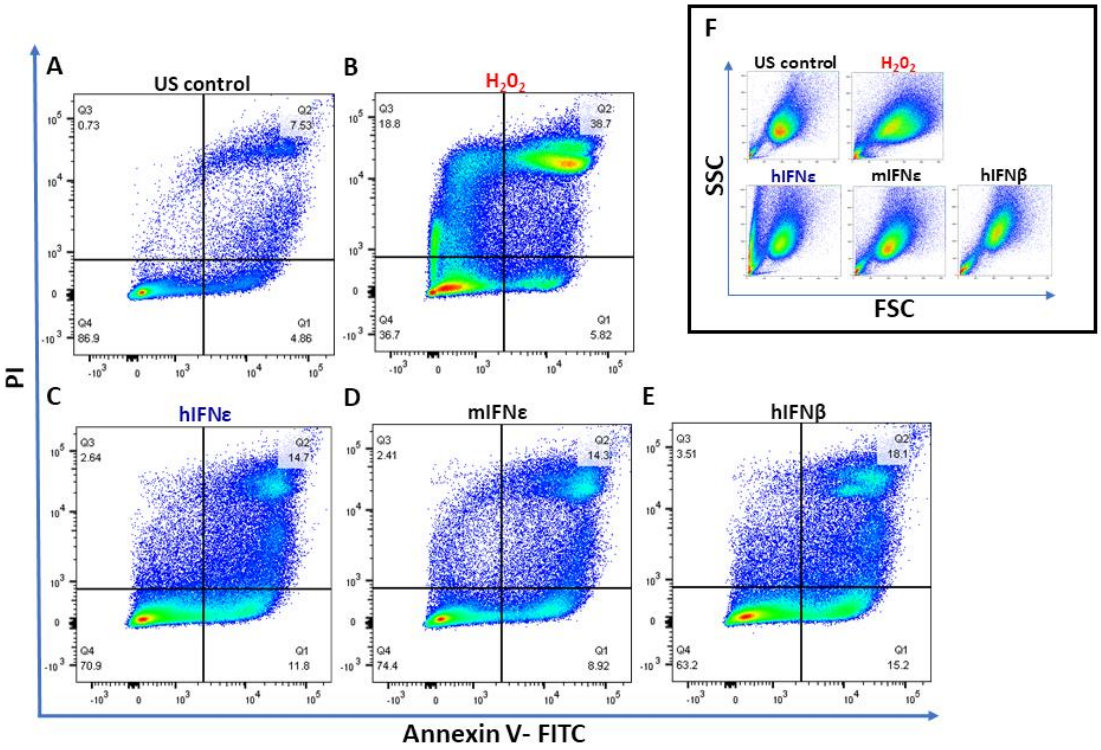

Figure 22. Apoptotic effects of type I IFN on FRT epithelial cells.
Scatter plots are representative of annexin V-FITC and PI stain as measured by FACS analysis of Ect1 (ectocervical cells) treated with 1000 IU/ml of hIFNε (C), mIFNε(D) and hIFNϐ [(Rebif®), E] for 72 hrs and compared to US control [(unstimulated control), A] as well as 5mM H_2O_2, [(positive control of apoptosis), B]. Plots demonstrate shift towards an apoptotic morphology Ect1 cells stimulated with type I IFNs. Representative side scatter (SSC) and forward scatter plots (FSC) indicate that type I IFN treatment of Ect1 cells alters their size and granularity consistent with the state of cellular apoptosis. Data is representative of mean ± SEM, from three independent biological experiments in technical triplicates.

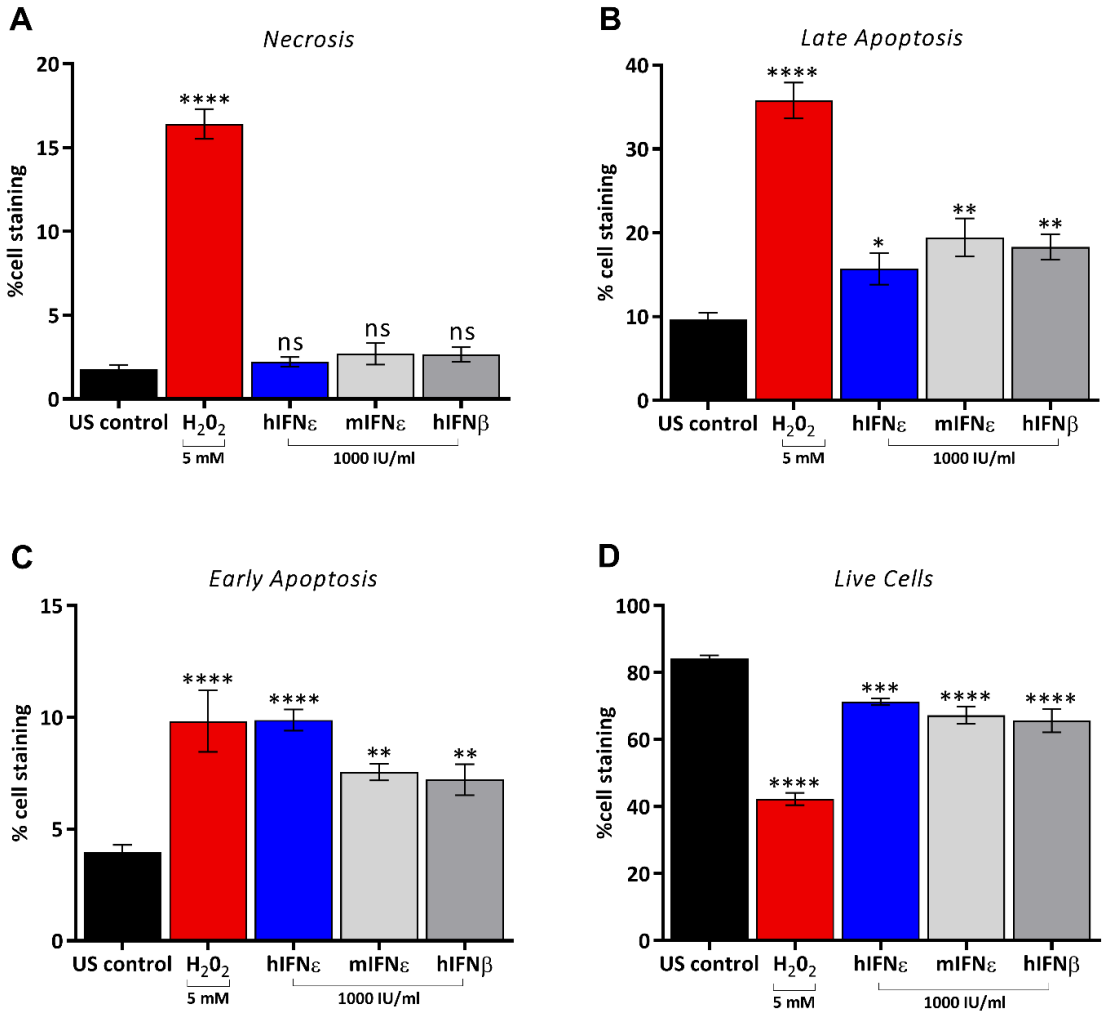

Figure 23. Induction of apoptosis by IFNε in FRT epithelial cancer cells.
*Graphs show quantitative data of cell staining % as measured by FACS analysis in the necrotic phase [annexin V- FITC $^{-}$/PI $^{+}$, (A)], late apoptosis [annexin V-FITC $^{+}$/PI $^{+}$, (B)], early apoptotic phase [annexin V-FITC $^{+}$/PI $^{-}$, (C)] and live cells [annexin V-FITC $^{-}$/PI $^{-}$, (D)]. Data is representative of mean ± SEM, from three independent biological experiments, in technical triplicates. Statistical analysis was performed using one-way ANOVA, Holm-Sidak's multiple comparisons test, (*P<0.05, **P<0.01, ***P<0.001, ****P<0.0001).*

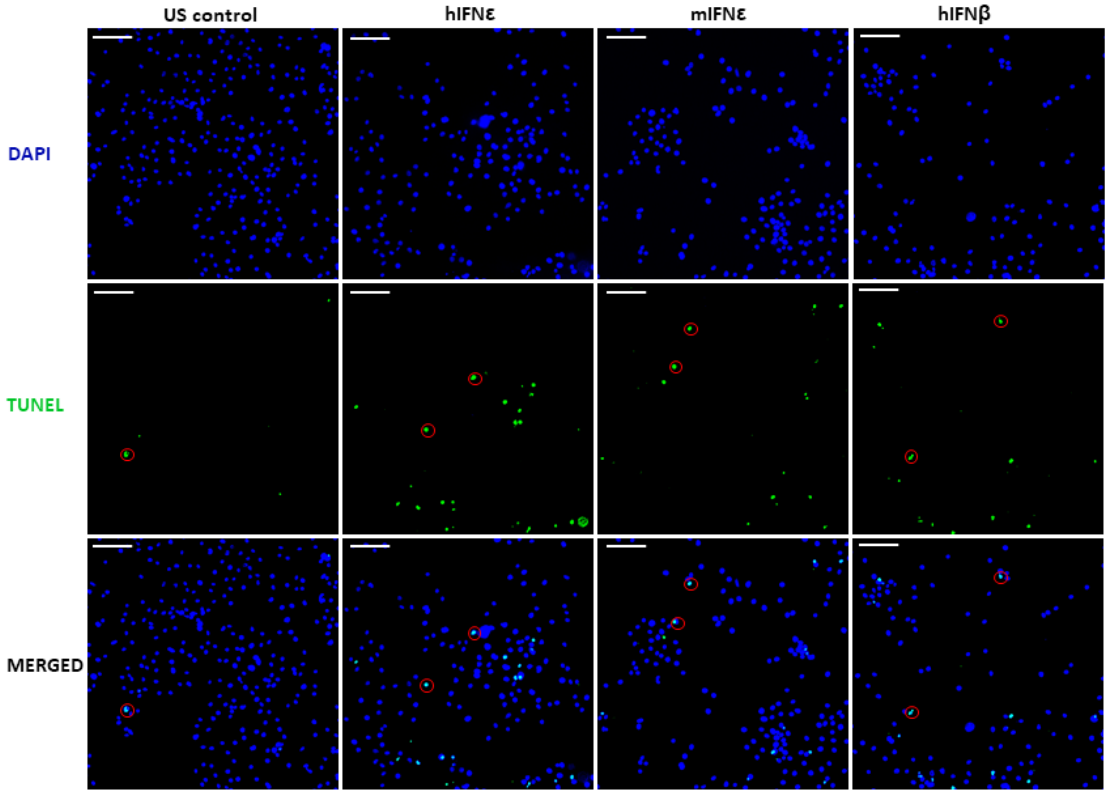

Figure 24. Type I IFNs induce DNA fragmentation of epithelial cancer cells.
Ect1 cells treated for 96 hrs with r-hIFNε, r-mIFNε and r-hIFNβ (1000 IU/ml) and compared to US control (unstimulated control), were subjected to TUNEL staining. Representative images showing TUNEL-positive cells (green fluorescence), DAPI staining (nuclear stain, blue fluorescence), as well as merged Images (composite of TUNEL-positive cells and DAPI stained cells) using a 10 x objective. Red circle specifies TUNEL-positive cells. Imaging was generated by Cellomics Arrayscan, high-throughput imaging system (Cellomics Scan software v7.6.2.1). Data is representative of mean ± SEM, from three independent biological experiments in technical triplicates. Scale bar is equivalent to 51 µm.

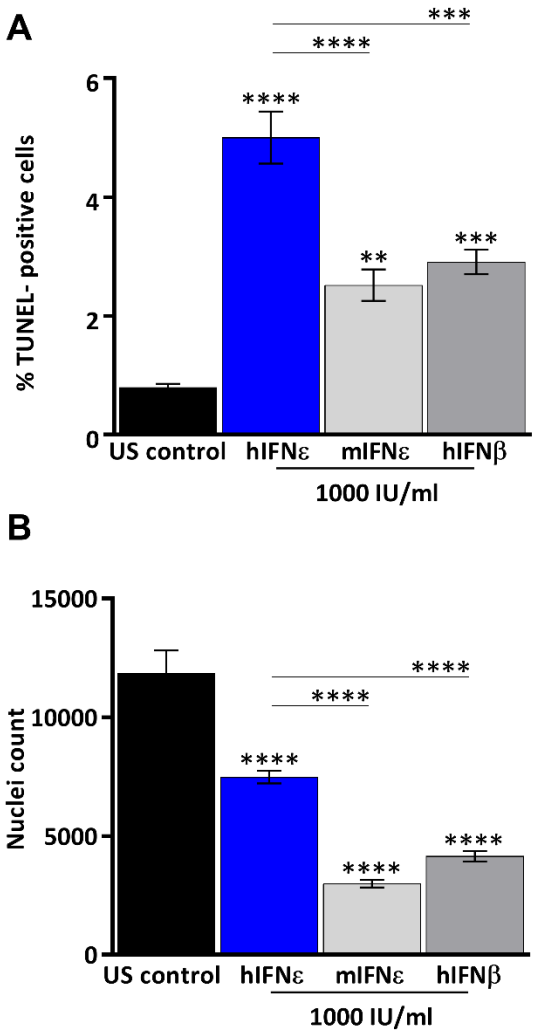

Figure 25. Quantification of IFNε induced DNA fragmentation in epithelial cancer cells.

*Ect1 cells treated for 96 hrs with hIFNε, mIFNε and h IFNβ (1000 IU/ml) and compared to US control (unstimulated control), were subjected to TUNEL staining. Quantification of TUNEL-positive cells was deduced by Cellomics Arrayscan, high-throughput imaging system. Graphs denote data % TUNEL-positive cells (A) and nuclei count (B) as acquired by Cellomics Scan software v7.6.2.1, with a 10 x objective of 49 fields. Data is representative of mean ± SEM, from three independent biological experiments in technical triplicates. Statistical analysis was performed using one-way ANOVA, with Tukey's multiple comparisons test, (*P<0.05, **P<0.01, ***P<0.001, ****P<0.0001).*

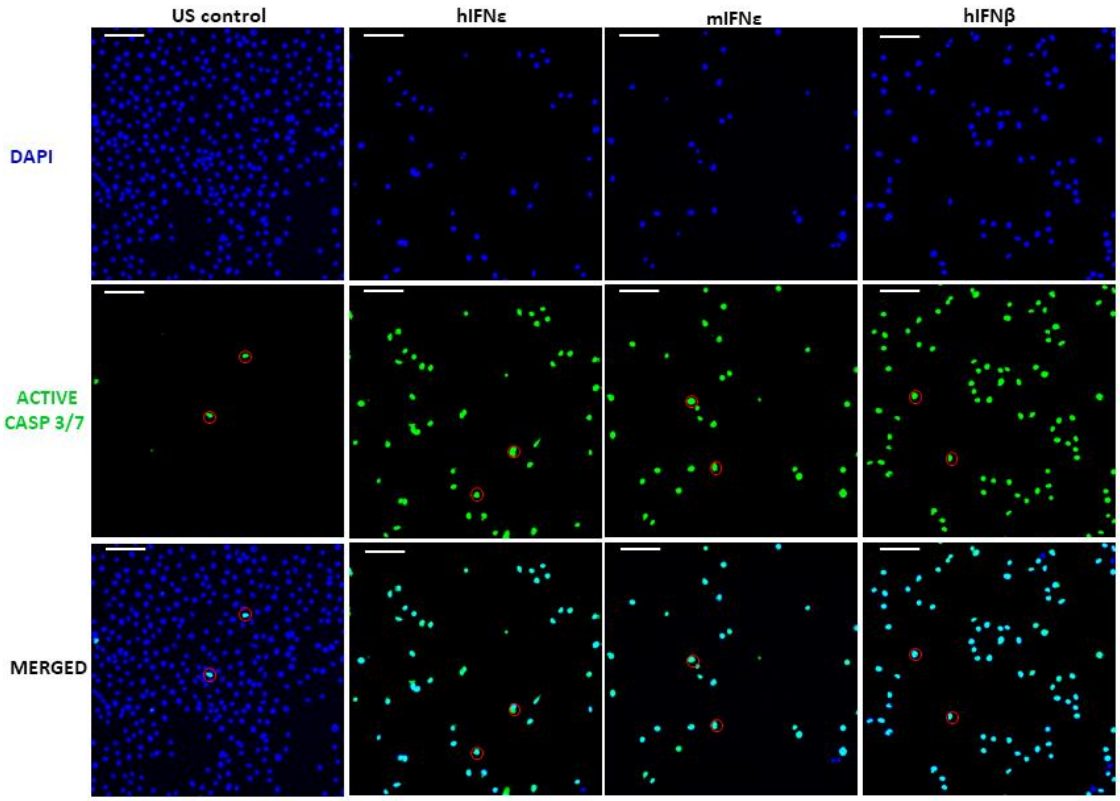

Figure 26. Type I IFN increase of Caspase-3/7 activity in epithelial cancer cells.
Ect1 cells treated for 72 hrs with hIFNε, mIFNε and hIFNβ (1000 IU/ml) and compared to US control (unstimulated control), were stained with CellEvent Caspase-3/7 Green Detection Reagent. Representative images showing active Caspase-3/7 positive cells (green fluorescence), DAPI staining (nuclear stain, blue fluorescence), as well as merged Images using a 10 x objective. Apoptotic cells with active Caspase-3/7 are circled in red. Imaging was generated by Cellomics Arrayscan, high-throughput imaging system (Cellomics Scan software v7.6.2.1). Data is representative of mean ± SEM, from three independent biological experiments in technical triplicates. Scale bar is equivalent to 51µm.

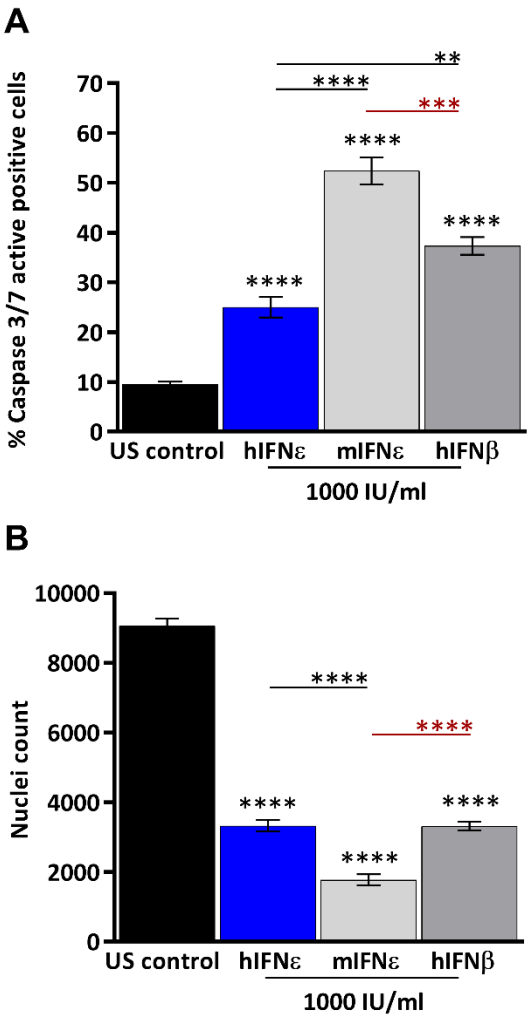

Figure 27. IFNε activation of Caspase-3/7 in epithelial cancer cells quantified.
*Ect1 cells treated for 72 hrs with hIFNε, mIFNε and h IFNβ (1000 IU/ml) and compared to US control (unstimulated control), were stained with CellEvent Caspase-3/7 Green Detection Reagent. Quantification of active Caspase- 3/7 positive cells was deduced by Cellomics Arrayscan, high-throughput imaging system. Graphs denote data % Caspase- 3/7 active positive cells (A) and nuclei count (B) as acquired by Cellomics Scan software v7.6.2.1, with a 10 x objective of 49 fields. Data is representative of mean ± SEM, from three independent biological experiments in technical triplicates. Statistical analysis was performed using one-way ANOVA, with Tukey's multiple comparisons test, (*P<0.05, **P<0.01, ***P<0.001, ****P<0.0001).*

Chapter 5

Integrated Discussion and Conclusions

"Science is beautiful when it makes simple explanations of phenomena or connections between different observations. Examples include the double helix in biology and the fundamental equation of physics".

-Stephen Hawking

Chapter 5: Integrated Discussion and Conclusions

Tumourigenesis involves the acquisition of multiple processes associated with cellular transformation, uncontrolled proliferation, invasion and metastasis (**Chapter 1,** p2). These processes under normal physiological conditions are tightly regulated by **cytokines** and are essential for maintaining homeostasis. However dysregulated cytokine signalling can lead to the pathogenesis of cancer. When aberrantly expressed, the TGF-β family member of growth factors Nodal can display pro-tumourigenic properties (**Chapter 1,** p41). In contrast cytokines exhibiting anti-tumourigenic properties can also be dysregulated as a mechanism to promote malignancy and this includes the type I IFN family protein, IFNε. This thesis intends to shed some light as to how these two cytokines are utilized to favour tumourigenesis, or alternatively to protect against cancer development.

5.1 The expression profile of Nodal signalling components in Normal vs Cancerous Human Endometrium

This thesis aimed to identify the expression patterns of Nodal signalling cohorts in human cycling endometrium and in endometrial cancer tissues (**Chapter 2,** p100).

5.1.1 Cyclical expression of nodal signalling components in human endometrium

Prior to elucidating the involvement of Nodal pathway in endometrial cancer, this thesis sought to examine expression of Nodal and Cripto in normal human endometrial tissue. This is the first study to detect **Nodal**, and co-receptor **Cripto**, co-localized within the

normal endometrium across the menstrual cycle of healthy non-pregnant women (**Chapter 2,** p 100).

In particularly, we found that Nodal and Cripto proteins are co-expressed at high levels in both stromal and epithelial (glandular and luminal) cells during the proliferative phase of the menstrual cycle. Expression of both Nodal and Cripto in glandular epithelium was maintained at steady-state levels across the cycle, and significantly decreased within the stromal compartment of the mid secretory phase. Whereas Lefty expression was primarily restricted to glandular epithelium and surrounding stroma during the late secretory and menstrual phases, confirming previous studies (1). These results suggest that Nodal signalling is tightly regulated throughout the menstrual cycle. With Lefty confining signals during the menstrual and late secretory phases, whereas in the absence of Lefty's antagonism **Nodal** is unrestricted to interact with **Cripto** and mediate Smad **signalling** during the **proliferative phase**. These results suggest that Nodal signalling could play important roles in remodelling events that occur within the proliferative phase of the menstrual cycle.

A limitation of this study is that due to time constraints we did not examine expression of activin receptors, essential in mediating the Smad signalling pathway. However, a previous study carried out by Jones et al., (2002), detected activin receptors within the human endometrium (2). Furthermore, activin shares these receptors and functionality has been previously validated within the endometrium (2, 3). Considering these observations, we postulated that Nodal's cognate receptors might also be present in this tissue.

According to Jones et al., (2002), expression of activin receptors (ALK4, ActRII/B) was demonstrated with in endometrial stromal cells across the cycle, with the highest levels detected in the early secretory phase (2). Whilst neither luminal or glandular epithelium

where found to express activin receptors at any stage of the cycle (2). These observations in addition to our findings collectively suggest that Nodal is secreted from the luminal and glandular epithelium cells and that Nodal does not function in an autocrine manner within the epithelial compartment. It is also likely that Nodal acts in a paracrine manner with signalling occurring within the **stroma** as well as within the **endometrial lumen**.

We subsequently observed **co-localization** of **Nodal** and **Cripto** in **blood vessels** and in endometrial **spiral arterioles.** Whereas Lefty was expressed within the stroma surrounding spiral arterioles, in line with previous reports that detected Lefty in endothelial cells lining the uterine spiral arterioles. Due to the pro-angiogenic properties attributed to Nodal, these results may indicate that Nodal signalling could be involved in **angiogenic processes** occurring in the cycling endometrium and are controlled by the inhibition of Lefty (4).

Nodal functionality within the endometrial stoma can be deduced from the well characterized morphogenic properties exhibited during embryonic development (5-7). Given that the endometrium is a highly regenerative tissue, we postulated that Nodal may mediate cellular proliferation, migration and wound healing, as these activities have been clearly validated during embryogenesis (8, 9). Furthermore, as Nodal has recently been identified as a key regulator of adult stem cell maintenance, it could be speculated that it mediates plasticity and pluripotency of the specialized progenitor stem cell niche identified by Gargett *et al.*, (2008) to drive endometrial regeneration (9-11). However additional studies are required to further illuminate activities mediated by Nodal within the endometrium.

Furthermore, we also detected, Nodal pro-protein in human **uterine fluid**, indicating that it is secreted into the lumen of the uterus implicating that it may also be important

in fertilization and pregnancy. Previous studies, according to Ma *et al.,* (2001) suggest that Nodal facilitates placentation as well as regulating trophoblast differentiation (12). Recent studies have since confirmed that Nodal plays important roles in murine placentation and in maintenance of full-term pregnancy (13). In this study conditional knockout mice lacking Nodal specifically in the reproductive tract, showed defective maternal-foetal interface and disturbed placentation accompanied by preterm birth and foetal loss (13).

5.1.2 Nodal is positively corelated with human endometrial cancer aggressiveness

Following elucidation of Nodal signalling components within the cycling endometrium, we next examined their expression patterns during the progression of endometrial cancer. This is the first study to detect the overexpression of **both Nodal and Cripto** in **human endometrial cancer** (**Chapter 2,** p100).

We observed that Nodal and Cripto are both localized primarily within the glandular epithelial tumour cells, and to a lesser extent in stromal cells. We also found that Nodal and Cripto staining intensities increased dramatically in the histological transition from Grade 1 to Grades 2 and 3 within the epithelial tumour compartment of the endometrium. Strikingly, Lefty expression was low in Grade 1 endometrial carcinoma, whilst absent in Grades 2 and 3. These results suggest that both **Nodal** and **Cripto** are **aberrantly overexpressed during the progression of endometrial cancer** and that Nodal signalling is **unrestricted** by Lefty antagonism. This correlates with previous as well as recent observations detecting high levels of Nodal or Cripto expression in patients from various different types of malignancies including melanoma, breast, colon, non-small cell-lung, testicular, gastric, pancreatic, cervical squamous, ovarian, oesophageal

squamous, and hepatocellular (14-26). Our study further suggests that **expression of Nodal and Cripto positively correlates with human endometrial carcinoma aggressiveness** an observation that is supported by a significant body of evidence to concur in multiple cancer types (as mentioned above) (25-34). More importantly, expression of Nodal or Cripto has also been shown to be associated with poor patient survival rates and this may also apply to endometrial cancer (17, 18, 24, 26, 32-38). However, the vast majority of studies examine the pro-tumourigenic properties of either Nodal or Cripto independently. Our findings provide an advantage over other studies by identifying both Nodal and Cripto as diagnostic markers of endometrial cancer progression and, potentially, as molecular targets for the treatment of these aggressive carcinomas. It is crucial to concurrently examine co-receptor Cripto and Nodal as they are both tumourigenic factors.

Our findings implicate that **re-emergence** of **both Nodal and Cripto** as well as **deregulated Nodal signalling** may contribute to the **progression of endometrial cancer**. Subsequent studies have shown that oncogenic transformation processes also recruit the embryogenic properties of Nodal by promoting proliferation, EMT (epithelial-mesenchymal transition), migration, invasion, angiogenesis, plasticity and stem cell maintenance, to aid malignant transformation and progression (4, 20, 31, 36, 39-43). Based on the expression patterns of Nodal, Cripto and Lefty (inhibitor) across the cycling endometrium, our study may implicate involvement of Nodal signalling to facilitate cellular proliferation necessary for remodelling process occurring within the proliferative phase of the menstrual cycle. Whilst high levels of Lefty expressed during the late secretory and menses phases, would be consistent with reduced Nodal signalling and cellular growth suppression. In contrast it appears that this tight regulation of Nodal signalling is lost in the carcinogenic endometrial epithelium, as

reported in our study, associated with increased expression of both oncogenic Nodal and Cripto proteins as well as loss of Lefty antagonism.

Consistent with previous studies demonstrating that Nodal is crucial in promoting cellular growth in melanoma and breast cancer cells, we postulated that our findings may also be in support of Nodal's **pro-proliferative** roles in endometrial cancer (27, 39, 40, 44). In addition, we speculate that Nodal signalling may also be facilitating **angiogenic** processes during endometrial cancer progression, as reported to occur in breast cancer development (4, 45). Nodal signalling is an important regulator of stem cell switching and plasticity, to promote cancer stem cell (CSC) in driving invasive breast and pancreatic cancer phenotypes (32, 43, 46, 47). As a stem cell niche exists within the endometrium, it could be speculated that unrestricted Nodal signalling could regulate these populations by giving rise to **CSCs** to further sustain aggressive endometrial malignancies (11).

5.2 Targeted Nodal signalling in Cancer cells

Following observations of Nodal and Cripto re-activation in endometrial cancer as well as positive correlations with tumour aggressiveness, we hypothesized that dysregulated Nodal signalling is associated with cancer pathogenesis and progression. Thus, we examined the effects of Nodal signalling blockade on cancer cell phenotypes (**Chapter 3,** p112).

5.2.1 Cripto MAbs block Nodal signalling

We established a Nodal dependent Smad 2/3 functional assay using the NTERA 2-D1 (testicular teratocarcinoma) cellular model as these cells express essential signalling

components, including receptors, and are responsive to Nodal dependent Smad 2/3 signalling. In this assay 6E10 and 3D1 Cripto MAbs significantly suppressed Nodal induced luciferase activity in a dose dependent manner. Essential for canonical Nodal signalling is the co-receptor Cripto which binds to Nodal and facilitates association of Nodal with its signalling receptors type II (ActRII/B) and type I (ALK4) to mediate the Smad signalling cascade (refer to **Chapter 1**, p26) (48-51). We have thus identified 3D1 and 6E10 anti-Cripto MAbs as potent neutralising antibodies that exhibit specificity in blocking Nodal-mediated Smad 2/3 signalling, without affecting activities of other TGF-β ligands.

5.2.2 Reversal of tumourigenic phenotypes by Cripto MAb treatment

Utilizing anti-Cripto MAb treatment we sought to block Nodal signalling in cancer cells and examine the *in vitro* anti-cancer effects (**Chapter 3,** p112).

5.2.2.1 6E10 antibody suppresses cancer cell growth

Uncontrolled cellular growth is a key hallmark of tumourigenesis (**Chapter 1,** p2). Therefore, pinpointing the specific molecular mechanisms that contribute to this oncogenic characteristic is essential to further the understanding of cancer biology (52). Subsequently, our study examined the effects of Nodal signalling blockade on cancer cell proliferation. MAb treatment of highly aggressive NTERA 2-D1 (testicular teratocarcinoma) cells profoundly suppressed proliferation with both neutralising antibodies 3D1 and 6E10. Additionally, anti-proliferative effects were observed using the conformational specific 6E10 antibody in LNCaP, Du 145, PC-3 (metastatic prostate); C8161 (melanoma); KGN (granulosa ovarian); cancer cells. The observed growth

suppression was relative to Cripto/Nodal expression levels of these cells. A previous finding has also similarly detected that anti-Cripto antibody treatment mediated growth suppression of Du 145 and PC-3 cells (53). Subsequently, it has been recently shown that overexpression of Nodal in LNCaP cells enhanced cancer cell growth (54). These data suggest that Nodal signalling may facilitate cancer cell proliferation.

5.2.2.2 6E10 antibody suppresses cancer cell migration

Our previous findings positively corelated expression of Nodal and Cripto with endometrial cancer aggressiveness (**Chapter 2,** p100). Cancer progresses and increases in aggressiveness, with the acquisition of migratory properties to disseminate into neighbouring sites and distant tissues (**Chapter 1,** p2). We subsequently examined the effects of Nodal blockade on the metastatic potential of cancer cells (**Chapter 3,** p112). In this study, *in vitro* anti-migratory effects exhibited by 6E10 MAb treatment paralleled the anti-proliferative properties, reflecting cellular expression status of Nodal/Cripto. Strikingly, 6E10 MAb treatment of highly metastatic NTERA 2-D1 (testicular) and LNCaP, PC-3 (prostate); cancer cell lines, significantly suppressed cellular migration in a dose dependent manner. These results correlate with additional *in vivo* and *in vitro* studies confirming Nodal signalling as an important mediator of cancer cell metastasis and invasion (20, 25, 28, 39, 40, 54, 55).

5.2.2.3 6E10 antibody suppresses Nodal mediated Smad signalling

Furthermore, our study showed that 6E10 MAb treatment of NTERA 2-D1 abrogated Smad 2/3 phosphorylation levels, implicating involvement of Smad activation pathway, in Nodal-mediated signalling activities. Therefore, we postulate the anti-proliferative and anti-migratory cellular effects of 6E10 antibody treatment are mediated by reduced

Smad signalling. However non-canonical as well as alternative Cripto signalling pathways may also be important in cancer cell development.

Other studies have also utilized anti-Cripto MAbs to target Nodal activities, in both *in vivo* and *in vitro* cancer models with promising anti-tumour effects (53, 56-59). Unfortunately, the BIIB015 MAb developed by Kelly, *et al*., (2011), has been withdrawn from phase I clinical trials due to insufficient efficacy (59). Recently, Focà A, *et. al.,* (2015) observed reduced vascular formation of melanoma and breast cancer cells using anti-Nodal MAbs to block Nodal signalling (72, 73). However, this antibody cannot target Nodal-independent pathways including soluble Cripto alternative signalling.

It is important to further consider alternative Cripto signals independent of Nodal/Smad signalling, which can also drive oncogenic events. As such, Cripto can independently interact with cytostatic TGF-β ligands (TGF-β1, activin A/B) and inhibit their activities, to further amplify anti-apoptotic or pro-cell survival mechanisms (60). Additionally, Cripto can activate c-src/MAPK/PI3K/Akt, pathways associated with pro-proliferative, pro-survival and pro-migratory cellular activities by interacting with either Glypican-1 and associated lipid raft signalling; or by GRP78 (15, 61). The anti-tumourigenic 6E10 and 3D1 anti-Cripto MAbs presented in the current study were demonstrated to specifically block the Nodal/Smad cascade. We further postulate that, 6E10 and 3D1 could potentially target the alternative non-canonical Nodal/Smad-independent signalling mechanisms mediated by Cripto, however this should be further validated. Therefore, we propose that 6E10 MAb treatment would be advantageous compared to the anti-Nodal antibodies suggested in other studies for anti-cancer immunotherapy applications.

Apart from the time constraints that restricted further validation of the aforementioned MAbs effects on alternative Cripto signalling, additional **study limitations** include reagent constraints. As such the 3D1 MAb clearly demonstrated positive *in vitro* anti-tumour properties however due to restricted supply we could not further include this antibody in our experimentation. Furthermore, at the time of conducting this study we did not have access to endometrial cancer cell lines to incorporate in our studies. Finally, we experience some technical difficulties in the detection of Cripto and Nodal protein in cancer cell lines by Western Blotting. As such, Nodal was particularly difficult to detect as this protein is highly unstable and this may be due to it trafficking cellular kinetics. Whereas Cripto was detected but only in cell lines which overexpressed it. These difficulties were overcome by using qRT-PCR as measures of Nodal and Cripto transcript expression levels. Alternatively, an ELISA method could have been developed for the detection of Nodal/Cripto protein levels in cells, if there was more time available.

5.3 The anti-tumourigenic roles of Interferon Epsilon in FRT Cancer

Apart from the tumour promoting Nodal/TGF-β signalling, another family of cytokines the interferons, may also contribute to the pathogenesis of female reproductive malignancy when their signalling is dysregulated (**Chapter 1,** p47). Our lab has demonstrated that in contrast to conventional type I IFNs, IFNε is constitutively expressed by both murine and human epithelial cells within the FRT and is hormonally regulated, exclusively within the endometrium (**Chapter 1,** p62) (62, 63). In addition, IFNε exhibits prophylactic roles within the FRT against sexually transmitted infections (63).

5.3.1 IFNε regulates Apoptotic and Cell survival ISGs

In a previous study, our group identified IFNε to be expressed within the vagina, cervix, uterus, and ovaries of the mouse, whilst expression in human was only examined in the endometrium (63). For this reasoning, we selected human epithelial cancer cells lines from the lower FRT VK2 (vaginal), Ect1 (ectocervical), End1 (endocervical); as well as the upper FRT RL95-2 (grade II-derived), AN3CA (grade III-derived), endometrial cancer cells; for analysis (**Chapter 4**, p 171) . Following validation of IFN type I receptor mRNA present in all cells, we examined responsiveness to recombinant interferon stimulation by monitoring ISG induction. In this study we observed that interferon responsiveness was depended upon cell type specificity, and that all FRT cell lines were sensitive to both IFNε and IFNβ stimuli. Thus, corroborating that IFNε exerts its actions via the canonical IFN type I signalling pathway, as previously demonstrated by our group (63, 64). However, in this study we also observed that lower FRT cells VK2, Ect1 and End1 were more sensitive to both IFNε and IFNβ stimulations and required lower dosage, compared to upper FRT RL95-2 and AN3CA endometrial cancer cells, which required a longer incubation period and higher dosage. This differential IFN activation maybe reflecting the anatomical cell origins. It could be postulated that epithelial cells derived from the lower FRT are highly susceptible to infections requiring immediate activation of the immune system via type I IFN signalling compared to the relatively sterile upper FRT endometrial epithelium (65). This could suggest an inherent regulatory mechanism to avoid excessive inflammatory signals with in the FRT epithelium.

Given that our cellular models are responsive to interferon stimulation we next sought to investigate regulation of IFNε on survival and apoptotic associated ISGs. Interestingly, IFNε **downregulated anti-apoptotic and pro-survival** (*BCL-2, CDC20*) ISGs in Vk2, End1, RL95-2, and AN3CA cells. In contrast, IFNε significant **upregulated pro-apoptotic** ISGs (*TAP1, OAS2, ISG12A)* in VK2, Ect1, End1, RL95-2, and AN3CA cancer cells (66-68). More

importantly, this data emphasizes the ability of IFNε to elicit anti-tumourigenic effects in endometrial as well as lower FRT carcinoma cells to modulate transcription of cell survival and apoptotic ISGs via IFN type I signalling.

Additionally, in this study we also observed that IFNε transcript levels were extremely low in ECC-1 (grade I -derived), RL95-2 (grade II -derived), or undetected in AN3CA (grade III -derived) endometrial cancer cells compared to VK2, Ect1 and End1 cells of lower FRT origin exhibiting relatively lower tumourigenic properties. Subsequent evidence indicates that IFNε is down regulated in fallopian tissues of ovarian cancer patients compared to healthy controls (Marks *et al.,* unpublished). According to this preliminary observation, we speculate that down regulation of IFNε may be associated with the pathogenesis of endometrial cancer. However, this is yet to be further investigated.

5.3.2 IFNε Suppresses FRT Cancer Cell Proliferation

Having confirmed that IFNε regulates apoptotic and cell survival ISGs we also examined the effects of IFNε on cellular growth. In this study we observed that IFNε treatment significantly reduced both cell viability and proliferation of VK2 and Ect1 epithelial cells in parallel to IFNβ treatment. These results are comparable with previous studies demonstrating that *in vitro* IFNβ treatment supressed melanoma and hepatocellular carcinoma cellular growth (69, 70). Our findings suggest that IFNε may play key anti-proliferative roles within the **lower FRT epithelium** and reactivation of IFN signalling may be of therapeutic importance for the treatment of vaginal and cervical cancers.

Concurrently, we also observed that IFNε greatly **reduced cellular growth** of **high grade endometrial cancer cells** RL95 (grade II-derived) and AN3CA (grade III-derived). Whereas **IFNβ was considerably less effective than IFNε** in suppressing proliferation

rates of these endometrial cancer cell lines. A previous study utilizing combination therapy of IFNβ expressing stem cells with subsequent 5-fluorocytosine administration demonstrated a 50-60% tumour growth suppression of endometrial xenografts (71). Our data identifies IFNε as an essential regulator of proliferation within the endometrial epithelium. However, as IFNε is confirmed in the present study to elicit a greater reduction in endometrial cancer cell proliferation compared IFNβ, we anticipate that it may also provide increased therapeutic benefits for endometrial cancer.

5.3.3 IFNε Induces Cancer Cell Apoptosis

Classical type I interferons such as IFNα and IFNβ, exhibit pro-apoptotic properties and have been successfully utilized in anti-cancer therapies (72, 73). We therefore examined the effects of IFNε on cancer cell apoptosis. We demonstrated by FACS analysis of Ect1 (ectocervical) cells, that IFNε induces **early** and **late apoptotic events** without affecting necrosis. Induction of apoptosis was comparable amongst IFNε and IFNβ treatments. In addition, we confirmed significant **increase in active Caspase-3/7** upon IFN stimulation of Ect1 cells. This suggests that IFNε leads to activation of Caspase-3/7 essential in **early apoptotic events**. Furthermore, the pro-apoptotic effects of IFNε were also confirmed by an **increase of TUNEL positive cells** upon stimulation of Ect1 cells. This evidence further indicates that IFNε also induces **late apoptotic events** accompanied by **DNA fragmentation**. This is the first study providing important insights into the mechanisms employed by IFNε to elicit pro-apoptotic activities in cancerous epithelial cells.

This study was performed initially using r-mIFNε, prepared by our group, to examine gene induction and establish cell responsiveness to interferon stimulations, as this was the only currently available recombinant IFNε preparation in our laboratory, at that time. The biological effects of IFNε were assessed using a newly developed r-hIFNε

preparation that generated by our group. As this preparation was initially in limited supply (due to technical purification difficulties), ISG gene expression with r-hIFNε was only validated for one cell line (preliminary data not shown) as there were no noticeable differences in ISG induction between the human and the murine preparations. Even though type I IFNs do not normally display cross-species activities, r-hIFNε has been shown by our group to induce antiviral activity of human lymphocyte cells (64). We thus anticipate that this does not constitute a significant **limitation** of this study as it would be expected to see similar ISG induction profiles amongst r-mIFNε and r-hIFNε stimuli in our FRT cancer cell line models. Due to time constraints, we analysed a small cohort of ISGs (out of 3000 known to be regulated by interferons). Nevertheless, our results demonstrate regulation of classical ISGs and more importantly modulation of genes that may promote apoptosis or halter survival mechanisms. Hence this is also not regarded as an important **study limitation**.

We examined endogenous expression of mRNA levels of *IFNAR1* and *IFNAR2 signalling* receptors as well as IFNε in our cellular models (**Chapter 4**, Figure 1). These results could have been complemented with analysis of protein levels, however due to time restrictions this was not carried out. As this project aimed to examine the anti-tumourigenic effects of IFNε on FRT epithelial cells (see **Chapter 1**, p 71) the omission of protein expression levels was **not a significant oversight** of the study. All cell lines (VK2, Ect1, RL95-2, AN3CA) responsive to IFNε stimulation as monitored by qRT-PCR modulation of ISGs (see Figures 2, 3, 4, 5, 9, 10, 11, 12, Chapter 4), also exhibited anti-proliferative responses to IFNε treatment (see **Chapter 4**, Figures 14 - 21).

Subsequently we studied responsiveness to recombinant interferon stimulation by monitoring ISG induction in FRT cells. In these experiments the ECC-1 cells showed moderate responsiveness to interferon stimulation for 3 hrs (**Chapter 4**, Figure 8). As these cells are of endometrial origin, we could postulate that a more appropriate

interferon stimulation time frame of 24 hrs, would allow for increased ISG regulation, as observed for the other endometrial cancer cell lines RL95-2 and AN3CA utilised in this study. However due to **time constraints** the aforementioned experiment as well as anti-proliferative and anti-apoptotic assays on ECC-1 endometrial cancer cells were omitted from this thesis.

5.4 Future Directions

To further unravel important aspects linking deregulated Nodal signalling with cancer progression we propose several future studies emanating from this PhD thesis. To additionally contribute to the Nodal /Cripto diagnostic and prognostic values associated with endometrial cancer, as suggested by evidence presented in **Chapter 2** (p100) of this thesis, clinical analysis of serum/plasma samples from human endometrial cancer patients would be required. Plasma/serum samples from this cohort would be analysed to determine Nodal and Cripto expression levels compared to healthy controls.

In addition, it was clearly illustrated in this thesis that both Nodal and Cripto are expressed in a tightly regulated pattern across the cycling endometrium **(Chapter 2,** p100). As expression levels of both Nodal and Cripto are high during the proliferative phase and lower during the secretory phase of the menstrual cycle this suggests that oestrogen may be promoting their expression within the endometrial epithelium. Thus, it would be important to investigate hormonal induction of both Cripto and Nodal by examining the effects of oestrogen, progesterone or androgens on their expression status.

As the monoclonal antibody 3D1, was demonstrated to suppress *in-vitro* cancer cell growth, similar to 6E10, it should be generated from hybridoma cells, purified and further analysed in functional assays (**Chapter 3,** 112). It would also be very interesting to perform biochemical studies on both neutralising 6E10 and 3D1 anti-Cripto MAbs discussed in **Chapter 3** (p112) of this thesis, to decipher the exact Cripto binding sites that these antibodies recognize. MAb epitope mapping ELISA experiments may be carried out using overlapping peptides generated across the Cripto molecule. Such peptides could be manufactured on a solid-phase support, cleaved and biotinylated for

capture onto streptavidin plates, and screened for their ability to bind to the Cripto monoclonal antibodies.

In addition, our findings clearly illustrated suppression of cancer cell proliferation upon 6E10 and 3D1 MAb treatment. However, is this associated with cellular apoptosis or cytostatic processes? To answer these questions, 6E10 and 3D1 MAb treatments should be assessed in apoptotic experiments including TUNEL and Caspase-3/7 assays to determine *in vitro* induction of apoptotic events. Moreover, the *in vitro* effects of 6E10 and 3D1 MAbs on alternative Cripto signalling independent to the Nodal Smad cascade would also add value to the characterization of these antibodies.

Subsequent *in vivo* experiments utilizing endometrial cancer mouse model xenografts may further evaluate the potential of 6E10 and 3D1 MAbs in cancer immunotherapy. In these experiments appropriate human endometrial cancers should be selected to express both Cripto and Nodal oncoproteins, as well as being responsive to 6E10/3D1 MAb growth inhibition. These endometrial cancer xenografts would be employed to assess the effects of Cripto monoclonal antibodies on tumourigenesis, metastasis and angiogenesis, which would greatly complement the results obtained in this PhD. Furthermore, these xenografts could also be used to examine combination therapy of 6E10/3D1 MAb with other anti-cancer compounds, even potentially IFNε, as a novel endometrial cancer treatment.

In **Chapter 4** (p171) of this thesis, we demonstrated the *in vitro* anti-tumourigenic roles of IFNε. This warrants further investigation to examine protein expression levels of IFNε within human endometrial cancer tissue using immunohistochemical techniques. It would be also useful to examine the protein expression of type I IFN receptors (IFNAR1/ IFNAR2) in order to draw conclusions regarding IFNε signalling within these endometrial cancer specimens in comparison to healthy controls. Furthermore, endometrial cancer

cell lines described in this thesis (**Chapter 4,** p171) could be further employed in mouse model xenografts to examine the *in vivo* anti-cancer effects of administered IFNε.

5.5 Conclusions and Significance

Evidence presented in this thesis assigns to the embryonic morphogen Nodal novel regulatory roles within the cycling human endometrium consistent with remodelling events that occur during the proliferative phase of the menstrual cycle. This PhD thesis also elucidated for the first time that expression of both Nodal and Cripto cytokines positively correlated with the degree of endometrial cancer aggressiveness, in the absence of antagonist Lefty. Our findings strongly support the hypothesis that dysregulated Nodal signalling may facilitate pathogenesis and progression of endometrial cancer, concurrent with previous evidence involving other types of highly invasive human malignancies among melanoma, breast and pancreatic.

Additionally, this thesis characterized 6E10 anti-Cripto MAb, as a neutralising antibody that specifically blocks Nodal signalling. More importantly 6E10 MAb treatment dramatically suppressed proliferation and migration of Nodal/Cripto expressing cancer cells in a Smad signalling dependent manner *in-vitro*. The translational significance of these findings collectively would implicate Nodal and Cripto oncoproteins as potential diagnostic and prognostic biomarkers of endometrial malignancy, which in line with subsequent studies, could also be extended to a wide variety of different cancer types. Moreover, this thesis also highlights Nodal signalling as an attractive target for endometrial cancer therapeutic interventions. More importantly, 6E10 monoclonal antibody could be utilized as a potential immunotherapeutic anti-cancer agent.

Subsequent findings of this thesis also indicate that IFNε transcript is undetected or of low level in endometrial cancer cells, compared to epithelial cells of lower FRT origin. In addition, IFNε stimulation of cancer cells lead to down-regulation of anti-apoptotic and up-regulation of pro-apoptotic ISGs. Interestingly, IFNε treatment significantly suppressed cancer cell proliferation and induced *in vitro* epithelial cell apoptosis. Collectively these results support our hypothesis that IFNε exhibits anti-tumour actions, similar to other type I IFN family members.

In fact, the unique properties of IFNε render it particularly pertinent to endometrial cancer treatments as well as other FRT cancers. Although current IFN type I exhibited potent anti-cancer properties they are regarded as unfavourable long-term treatments due to detrimental side effects [9,10]. Whilst IFNε is constitutively expressed within the FRT, it is speculated that it may be well tolerated in this region. This thesis characterized important *in vitro* anti-cancer properties of IFNε in highly aggressive endometrial cancer cells. This data further supports the potential use of IFNε as a possible therapeutic agent in endometrial cancer. However, the potential of IFNε in therapeutic development of endometrial cancer would require further investigation.

Collectively the results of this thesis have illustrated the detrimental effects of deregulated signalling of Nodal and IFNε cytokine pathways. We speculate that integration of Nodal blockade via 6E10 MAb, with concomitant stimulation of anti-cancer, type I IFN signalling by IFNε treatment may provide increased therapeutic benefits as an adjuvant endometrial cancer treatment. As both Nodal and IFNε display essential roles in the healthy cycling endometrium, it would be anticipated that the suggested novel combination therapy would have limited side effects for the treatment of endometrial cancer.

5.6 References

1. Tabibzadeh S, Mason JM, Shea W, Cai Y, Murray MJ, Lessey B. Dysregulated expression of ebaf, a novel molecular defect in the endometria of patients with infertility. The Journal of clinical endocrinology and metabolism. 2000;85(7):2526-36.

2. Jones RL, Salamonsen LA, Findlay JK. Activin A promotes human endometrial stromal cell decidualization in vitro. The Journal of clinical endocrinology and metabolism. 2002;87(8):4001-4.

3. Jones RL, Stoikos C, Findlay JK, Salamonsen LA. TGF-β superfamily expression and actions in the endometrium and placenta. Reproduction. 2006;132(2):217-32.

4. Quail DF, Walsh LA, Zhang G, Findlay SD, Moreno J, Fung L, et al. Embryonic protein nodal promotes breast cancer vascularization. Cancer Res. 2012;72(15):3851-63.

5. Conlon FL, Lyons KM, Takaesu N, Barth KS, Kispert A, Herrmann B, et al. A primary requirement for nodal in the formation and maintenance of the primitive streak in the mouse. Development. 1994;120(7):1919-28.

6. Schier AF, Shen MM. Nodal signalling in vertebrate development. Nature. 2000;403(6768):385-9.

7. Schier AF. Nodal signaling in vertebrate development. Annual review of cell and developmental biology. 2003; 19:589-621.

8. Shen MM. Nodal signaling: developmental roles and regulation. Development. 2007;134(6):1023-34.

9. Zhang YQ, Sterling L, Stotland A, Hua H, Kritzik M, Sarvetnick N. Nodal and lefty signaling regulates the growth of pancreatic cells. Developmental dynamics: an official publication of the American Association of Anatomists. 2008;237(5):1255-67.

10. Heemskerk I, Warmflash A. Pluripotent stem cells as a model for embryonic patterning: From signaling dynamics to spatial organization in a dish. Developmental Dynamics. 2016;245(10):976-90.

11. Gargett CE, Chan RW, Schwab KE. Hormone and growth factor signaling in endometrial renewal: role of stem/progenitor cells. Molecular and cellular endocrinology. 2008;288(1-2):22-9.

12. Ma GT, Soloveva V, Tzeng SJ, Lowe LA, Pfendler KC, Iannaccone PM, et al. Nodal regulates trophoblast differentiation and placental development. Developmental biology. 2001;236(1):124-35.

13. Park CB, DeMayo FJ, Lydon JP, Dufort D. NODAL in the uterus is necessary for proper placental development and maintenance of pregnancy. Biol Reprod. 2012;86(6):194.

14. Dublin E, Bobrow L, Barnes D, Gullick W. Amphiregulin and cripto overexpression in breast cancer relationship with prognosis and clinical and molecular variables. International journal of oncology. 1995;7(3):617-22.

15. Bianco C, Strizzi L, Normanno N, Khan N, Salomon DS. Cripto-1: an oncofetal gene with many faces. Current topics in developmental biology. 2005; 67:85-133.

16. Gong YP, Yarrow PM, Carmalt HL, Kwun SY, Kennedy CW, Lin BP, et al. Overexpression of Cripto and its prognostic significance in breast cancer: a study with long-term survival. European journal of surgical oncology: the journal of the European Society of Surgical Oncology and the British Association of Surgical Oncology. 2007;33(4):438-43.

17. Strizzi L, Postovit L-M, Margaryan NV, Lipavsky A, Gadiot J, Blank C, et al. Nodal as a biomarker for melanoma progression and a new therapeutic target for clinical intervention. Expert review of dermatology. 2009;4(1):67-78.

18. Hooijkaas AI, Gadiot J, van Boven H, Blank C. Expression of the embryological morphogen Nodal in stage III/IV melanoma. Melanoma research. 2011;21(6):491-501.

19. Pilgaard L, Mortensen JH, Henriksen M, Olesen P, Sorensen P, Laursen R, et al. Cripto-1 expression in glioblastoma multiforme. Brain pathology (Zurich, Switzerland). 2014;24(4):360-70.

20. Duan W, Li R, Ma J, Lei J, Xu Q, Jiang Z, et al. Overexpression of Nodal induces a metastatic phenotype in pancreatic cancer cells via the Smad2/3 pathway. Oncotarget. 2015;6(3):1490-506.

21. Xu CH, Cao L, Wei Y, Yu LK. Serum cripto-1 as a clinical marker for lung cancer. The International journal of biological markers. 2015;30(4): e369-73.

22. Spiller CM, Gillis AJ, Burnet G, Stoop H, Koopman P, Bowles J, et al. Cripto: Expression, epigenetic regulation and potential diagnostic use in testicular germ cell tumors. Mol Oncol. 2016;10(4):526-37.

23. Liu Q, Cui X, Yu X, Bian B-S-J, Qian F, Hu X-g, et al. Cripto-1 acts as a functional marker of cancer stem-like cells and predicts prognosis of the patients in esophageal squamous cell carcinoma. Molecular Cancer. 2017;16(1):81.

24. Zhang H, Zhang B, Gao L, Zhang L, Zhu K, Cheng R, et al. Clinical significance of cripto-1 expression in lung adenocarcinoma. Oncotarget. 2017;8(45):79087-98.

25. Karkampouna S van der Helm D, Gray PC, Chen L, Klima I, Grosjean J, et al. CRIPTO promotes an aggressive tumour phenotype and resistance to treatment in hepatocellular carcinoma. The Journal of pathology. 2018;245(3):297-310.

26. Xu CH, Chi CZ, Zhang Q, Wang YC, Wang W, Yuan Q, et al. Diagnostic and prognostic value of serum Cripto-1 in patients with non-small cell lung cancer. The clinical respiratory journal. 2018.

27. Kenney NJ, Adkins HB, Sanicola M. Nodal and Cripto-1: embryonic pattern formation genes involved in mammary gland development and tumorigenesis. Journal of mammary gland biology and neoplasia. 2004;9(2):133-44.

28. Quail DF, Siegers GM, Jewer M, Postovit L-M. Nodal signalling in embryogenesis and tumourigenesis. The International Journal of Biochemistry & Cell Biology. 2013;45(4):885-98.

29. Li P, Sun D, Li X, He Y, Li W, Zhao J, et al. Elevated expression of Nodal and YAP1 is associated with poor prognosis of gastric adenocarcinoma. Journal of cancer research and clinical oncology. 2016;142(8):1765-73.

30. Oliveira-Nunes MC, Assad Kahn S, de Oliveira Barbeitas AL, TC ES, Dubois LG, Ventura Matioszek GM, et al. The availability of the embryonic TGF-beta protein Nodal is dynamically regulated during glioblastoma multiforme tumorigenesis. Cancer Cell Int. 2016; 16:46.

31. Postovit LM, Seftor EA, Seftor RE, Hendrix MJ. Influence of the microenvironment on melanoma cell fate determination and phenotype. Cancer Res. 2006;66(16):7833-6.

32. Bodenstine TM, Chandler GS, Reed DW, Margaryan NV, Gilgur A, Atkinson J, et al. Nodal expression in triple-negative breast cancer: Cellular effects of its inhibition following doxorubicin treatment. Cell cycle (Georgetown, Tex). 2016;15(9):1295-302.

33. Strizzi L, Margaryan NV, Gerami P, Haghighat Z, Harms PW, Madonna G, et al. Translational significance of Nodal, Cripto-1 and Notch4 in adult nevi. Oncology Letters. 2016;12(2):1349-54.

34. Mahmoudian RA, Abbaszadegan MR, Forghanifard MM, Moghbeli M, Moghbeli F, Chamani J, et al. Biological and Clinicopathological Significance of Cripto-1 Expression in the Progression of Human ESCC. Reports of biochemistry & molecular biology. 2017;5(2):83-90.

35. Hueng DY, Lin GJ, Huang SH, Liu LW, Ju DT, Chen YW, et al. Inhibition of Nodal suppresses angiogenesis and growth of human gliomas. Journal of neuro-oncology. 2011;104(1):21-31.

36. Kirsammer G, Strizzi L, Margaryan NV, Gilgur A, Hyser M, Atkinson J, et al. Nodal signaling promotes a tumorigenic phenotype in human breast cancer. Seminars in Cancer Biology. 2014; 29:40-50.

37. Wang J-h, Wei W, Xu J, Guo Z-x, Xiao C-z, Zhang Y-f, et al. Elevated expression of Cripto-1 correlates with poor prognosis in hepatocellular carcinoma. Oncotarget. 2015;6(33):35116-28.

38. Sampath K, Robertson EJ. Keeping a lid on nodal: transcriptional and translational repression of nodal signalling. Open Biology. 2016;6(1):150200.

39. Topczewska JM, Postovit LM, Margaryan NV, Sam A, Hess AR, Wheaton WW, et al. Embryonic and tumorigenic pathways converge via Nodal signaling: role in melanoma aggressiveness. Nat Med. 2006;12(8):925-32.

40. Postovit L-M, Margaryan NV, Seftor EA, Kirschmann DA, Lipavsky A, Wheaton WW, et al. Human embryonic stem cell microenvironment suppresses the tumorigenic phenotype of aggressive cancer cells. Proceedings of the National Academy of Sciences. 2008;105(11):4329-34.

41. McAllister JC, Zhan Q, Weishaupt C, Hsu MY, Murphy GF. The embryonic morphogen, Nodal, is associated with channel-like structures in human malignant melanoma xenografts. Journal of cutaneous pathology. 2010;37 Suppl 1:19-25.

42. Bodenstine TM, Chandler GS, Seftor RE, Seftor EA, Hendrix MJ. Plasticity underlies tumor progression: role of Nodal signaling. Cancer metastasis reviews. 2016;35(1):21-39.

43. Gong W, Sun B, Sun H, Zhao X, Zhang D, Liu T, et al. Nodal signaling activates the Smad2/3 pathway to regulate stem cell-like properties in breast cancer cells. American journal of cancer research. 2017;7(3):503-17.

44. Hendrix MJC, Seftor EA, Seftor REB, Kasemeier-Kulesa J, Kulesa PM, Postovit L-M. Reprogramming metastatic tumour cells with embryonic microenvironments. Nature Reviews Cancer. 2007; 7:246.

45. Bianco C, Strizzi L, Ebert A, Chang C, Rehman A, Normanno N, et al. Role of human cripto-1 in tumor angiogenesis. J Natl Cancer Inst. 2005;97(2):132-41.

46. Meyer MJ, Fleming JM, Ali MA, Pesesky MW, Ginsburg E, Vonderhaar BK. Dynamic regulation of CD24 and the invasive, CD44posCD24neg phenotype in breast cancer cell lines. Breast Cancer Res. 2009;11(6): R82.

47. Lonardo E, Frias-Aldeguer J, Hermann PC, Heeschen C. Pancreatic stellate cells form a niche for cancer stem cells and promote their self-renewal and invasiveness. Cell cycle (Georgetown, Tex). 2012;11(7):1282-90.

48. Gritsman K, Zhang J, Cheng S, Heckscher E, Talbot WS, Schier AF. The EGF-CFC protein one-eyed pinhead is essential for nodal signaling. Cell. 1999;97(1):121-32.

49. Yan YT, Gritsman K, Ding J, Burdine RD, Corrales JD, Price SM, et al. Conserved requirement for EGF-CFC genes in vertebrate left-right axis formation. Genes & development. 1999;13(19):2527-37.

50. Minchiotti G, Manco G, Parisi S, Lago CT, Rosa F, Persico MG. Structure-function analysis of the EGF-CFC family member Cripto identifies residues essential for nodal signalling. Development. 2001;128(22):4501-10.

51. Yeo C, Whitman M. Nodal signals to Smads through Cripto-dependent and Cripto-independent mechanisms. Molecular cell. 2001;7(5):949-57.

52. Hanahan D, Weinberg RA. The Hallmarks of Cancer. Cell. 2000;100(1):57-70.

53. Xing PX, Hu XF, Pietersz GA, Hosick HL, McKenzie IF. Cripto: a novel target for antibody-based cancer immunotherapy. Cancer Res. 2004;64(11):4018-23.

54. Lawrence MG, Margaryan NV, Loessner D, Collins A, Kerr KM, Turner M, et al. Reactivation of Embryonic Nodal Signaling is Associated with Tumor Progression and Promotes the Growth of Prostate Cancer Cells. The Prostate. 2011;71(11):1198-209.

55. Lee CC, Jan HJ, Lai JH, Ma HI, Hueng DY, Lee YC, et al. Nodal promotes growth and invasion in human gliomas. Oncogene. 2010;29(21):3110-23.

56. Adkins HB, Bianco C, Schiffer SG, Rayhorn P, Zafari M, Cheung AE, et al. Antibody blockade of the Cripto CFC domain suppresses tumor cell growth in vivo. J Clin Invest. 2003;112(4):575-87.

57. Hu XF, Li J, Yang E, Vandervalk S, Xing PX. Anti-Cripto Mab inhibit tumour growth and overcome MDR in a human leukaemia MDR cell line by inhibition of Akt and activation of JNK/SAPK and bad death pathways. British journal of cancer. 2007;96(6):918-27.

58. Bianco C, Salomon DS. Targeting the embryonic gene Cripto-1 in cancer and beyond. Expert Opin Ther Pat. 2010;20(12):1739-49.

59. Kelly RK, Olson DL, Sun Y, Wen D, Wortham KA, Antognetti G, et al. An antibody-cytotoxic conjugate, BIIB015, is a new targeted therapy for Cripto positive tumours. Eur J Cancer. 2011;47(11):1736-46.

60. Klauzinska M, Castro NP, Rangel MC, Spike BT, Gray PC, Bertolette D, et al. The multifaceted role of the embryonic gene Cripto-1 in cancer, stem cells and epithelial-mesenchymal transition. Semin Cancer Biol. 2014; 29:51-8.

61. Kelber JA, Panopoulos AD, Shani G, Booker EC, Belmonte JC, Vale WW, et al. Blockade of Cripto binding to cell surface GRP78 inhibits oncogenic Cripto signaling via MAPK/PI3K and Smad2/3 pathways. Oncogene. 2009;28(24):2324-36.

62. Bourke NM, Achilles SL, Huang SU, Cumming HE, Papageorgiou I, Gearing LJ, Thakore S, Mangan NE, Mesiano S, Hertzog PJ. Human IFNε: Spaciotemporal expression, hormone regulation and innate immunity in the female reproductive tract. bioRxiv. October 16, 2018.

63. Fung KY, Mangan NE, Cumming H, Horvat JC, Mayall JR, Stifter SA, et al. Interferon-epsilon protects the female reproductive tract from viral and bacterial infection. Science. 2013;339(6123):1088-92.

64. Stifter SA, Matthews AY, Mangan NE, Fung KY, Drew A, Tate MD, et al. Defining the distinct, intrinsic properties of the novel type I interferon, epsilon. Journal of Biological Chemistry. 2017.

65. Wira CR, Rodriguez-Garcia M, Patel MV. The role of sex hormones in immune protection of the female reproductive tract. Nat Rev Immunol. 2015;15(4):217-30.

66. Grommé M, Neefjes J. Antigen degradation or presentation by MHC class I molecules via classical and non-classical pathways. Molecular Immunology. 2002;39(3):181-202.

67. Zhou A, Paranjape J, Brown TL, Nie H, Naik S, Dong B. Interferon action and apoptosis are defective in mice devoid of 2[prime]5[prime]-oligoadenylate-dependent RNase L. EMBO J. 1997;16:6355-63.

68. Rosebeck S, Leaman DW. Mitochondrial localization and pro-apoptotic effects of the interferon-inducible protein ISG12a. Apoptosis: An International Journal on Programmed Cell Death. 2008;13(4):562-72.

69. Ethiraj P, Veerappan K, Samuel S, Sivapatham S. Inhibitory effects of interferon-β on hepatocellular carcinoma HepG2 via Akt/STAT phosphorylation. Fundamental & Clinical Pharmacology. 2015;29(3):278-85.

70. Krasagakis K, Garbe C, Kruger S, Orfanos CE. Effects of Interferons on Cultured Human Melanocytes In Vitro: Interferon-Beta but Not -Alpha or -Gamma Inhibit Proliferation and All Interferons Significantly Modulate the Cell Phenotype. Journal of Investigative Dermatology. 1991;97(2):364-72.

71. Yi BR, Kim SU, Choi KC. Additional effects of engineered stem cells expressing a therapeutic gene and interferon-beta in a xenograft mouse model of endometrial cancer. International journal of oncology. 2015;47(1):171-8.

72. Chawla-Sarkar M, Lindner DJ, Liu YF, Williams BR, Sen GC, Silverman RH. Apoptosis and interferons: role of interferon-stimulated genes as mediators of apoptosis. Apoptosis. 2003; 8:237-49.

73. Clemens MJ. Interferons and apoptosis. J Interferon Cytokine Res. 2003; 23:277-92.

Appendices

"The more you know, the more you know you don't know."

-Aristotle

Appendices

Appendix A (Chapter 3)

Electrophoresis and Western Blotting Solutions

RIPA buffer

790 mg of Tris base (50 mM), (Sigma Aldrich, Merk)
75 ml MQ water
900 mg NaCL (150 nM), (Sigma Aldrich, Merk) dissolve by stirring and adjust pH to 7.4
10 ml nonyl-phenoxypolyethoxylethanol (NP-40, 10%), (Sigma Aldrich, Merk)
2.5 ml sodium deoxycholate (0.25%), (Sigma Aldrich, Merk)
Add MQ water to a final volume of 100 ml.

2x SDS-PAGE loading buffer

4 % SDS (MP Biomedicals)
10 % β-mercaptoethanol (BioRad)
20 % glycerol, (Sigma Aldrich, Merk)
0.004 % bromophenol blue, (Sigma Aldrich, Merk)
0.125 M Tris-HCL (Sigma Aldrich, Merk)

SDS polyacrylamide gels

	4 % Stacking gel	**12 % Running gel**
Milli-Q water	1.6 ml	1.2 ml
30% Acrylamide (Biorad)	0.5 ml	3 ml
Gel buffer	1.25 ml	2.5 ml
20% Glycerol (Sigma Aldrich, Merk)	0.5 ml	1 ml
10% APS	15 µl	30 µl
TEMED (Biorad)	5 µl	10 µl

Gel buffer

36.33 g Tris base (Sigma Aldrich, Merk)
0.3 g SDS (MP Biomedicals)
Dissolve in 100 ml of MQ water and adjust pH to 4.5

APS 10%

1 g APS (Sigma Aldrich, Merk)

Dissolve in 10 ml of dH_2O

Top Running buffer

24.2 g Tris-HCL (Sigma Aldrich, Merk)

35.59 g Tricine (Sigma Aldrich, Merk)

2 g SDS (MP Biomedicals)

Dissolve in 2 L of MQ water

Bottom Running buffer

48.44 g (MP Biomedicals)

Dissolve in 2 L of MQ water

Transfer buffer

25 mM Tris-HCL

192 mM glycine

10% methanol

TBS (10×)

146.1 g NaCL

30.3 g Tris base

Dissolve in 1L of MQ water and adjust pH to 7.5

TBS (1×)

900 ml MQ water

100 ml TBS (10×)

TTBS (Tris-buffered saline containing 0.05% Tween-20)

500 ml TBS (1×)

250 µl Tween-20 (Sigma Aldrich, Merk)

5% BSA/TTBS (Western Blotting Blocking Buffer)

5 g BSA (Sigma Aldrich, Merk)

100 ml TTBT

Filter mixture through 0.22 micron filter

1% BSA/TTBS (Western Blotting Antibody Buffer)

1 g BSA (Sigma Aldrich, Merk)

100 ml TTBT

Filter mixture through 0.22 micron filter

Appendix B (Chapter 3)

Agarose Gel Electrophoresis Methodology and Solutions

RT-PCR products were visualised by electrophoresis on a 1.5% agarose gel. 5 µl of sample product was combined with 3 µl of loading dye and loaded onto the gel. Band sizes were directly compared with the 1Kb Plus DNA Ladder (Invitrogen, LifeTechnologies, Thermo Fisher Scientific). Electrophoresis was carried out in TBE buffer, for 40 mins at 100 V using the BioRad Laboratories apparatus. The gel was then imaged on a GelDoc (Ultraviolet Transilluminator; Bioimaging Systems).

1.5% Agarose gel

To 3.0 g agarose (Invitrogen, LifeTechnologies, Thermo Fisher Scientific) 200 ml of buffer TBE were added and heated for 2 mins, in a microwave (800W). The mixture was allowed to cool for 5 mins, before adding SYBR Safe DNA gel stain (Invitrogen, LifeTechnologies, Thermo Fisher Scientific) to a final dilution of 1:30 upon gentle mixing. The gel was then poured into a sealed cassette, fitted with 10/20 lane comb and allowed gel to set at room temperature, for 30 mins.

TBE buffer

1 g APS (Sigma Aldrich, Merk)

54 g Tris-base (Sigma Aldrich, Merk)

27.5 g Boric Acid (BHT)

3.74 g EDTA disodium salt (Sigma Aldrich, Merk),

Dissolve in 1L MQ water

Loading buffer

4 M urea

50% sucrose

50 mM EDTA pH 8.0

some bromophenol blue

Appendix C (Chapters 3, 4)

General Tissue Culture Methods

All cell lines were propagated in 25 cm^2 or 75 cm^2 polystyrene tissue culture flasks (BD Falcon) in a 5% CO_2 humidified incubator at 37°C. All tissue culture procedures were performed in specialised laminar flow hoods designated for tissue culturing, under sterile conditions. Cells were cultured in complete media as specified in **Chapter 3** (p116-119) and **Chapter 4** (p176)**,** for each cell line. Mycoplasma testing of all cell lines was performed by the Laboratory and Technical Services at Hudson Institute for Medical Research using MycoAlert PLUS Mycoplasma Detection Kit (Lonza). Authentication and identification of cell lines as indicated in **Chapter 4** (p176) was performed by short tandem repeat profiling analysis carried out by the Medical Genomics facility at Monash Health Translational Precinct (refer to Appendix D and E, p265-278).

Thawing of frozen cells

Cryotubes containing frozen cells were removed from liquid nitrogen storage and thawed immediately in a water bath at 37°C. The cell suspension was transferred immediately to a sterile centrifuge tube containing 9 ml of the appropriate prewarmed complete media and centrifuged at 180 x g for 5 mins. The supernatant was discarded, and the cell pellet was gently resuspended in 1 ml of complete media and transferred to a 25 cm^2 (BD Falcon) tissue culture flask supplemented with prewarmed complete medium. The cells were established in culture by incubation in a 5% CO_2 humidified, 37°C incubator. The media was replenished after 24 hrs and the cells returned to the incubator. The cells were further maintained in culture depending on the experimental requirements and cell confluency, with complete media replenishing or subcultivation performed every 2-3 days.

Passaging of Monolayer Cell Culture

Adherent cell lines were passaged every 2-4 days upon reaching 70-80% confluency. Media was then aspirated, and the cells were washed with 10 ml sterile PBS (Gibco, Life Technologies). The cells were incubated at 37°C, 5% CO_2 for 2-4 mins as required to detach from the culture substratum, by addition of 1-2 ml of TrypLE (Invitrogen, LifeTechnologies, Thermo Fisher Scientific Life Technologies, Thermo Fisher Scientific). This was confirmed by microscopic examination followed by gentle tapping of the flask to facilitate cell dislodgment. Trypsinization was then inactivated by addition of 5-8 ml of complete media (containing 10% FCS) followed by centrifugation at 180 x g for 5 mins, and removal of the supernatant. The cell pellet was resuspended in prewarmed complete media and transferred to a new 75 cm^2 flask (BD Falcon) at the appropriate subcultivation ratio which was specifically determined for each cell line.

Freezing of cells

Cells were cultured to 70-80 % confluency, trypsinised and then pelleted at 180 x g for 5 mins. The cell pellet was gently dislodged by tapping, and the cells were resuspended in freezing media [90 % v/v FCS (Gibco, Life Technologies), 10 % v/v DMSO (Sigma Aldrich, MERK). The cells were then aliquoted into cryovials (Greiner Biosciences), transferred to a Mr. Frosty™ Freezing Container (Invitrogen, LifeTechnologies, Thermo Fisher Scientific Life Technologies, Thermo Fisher Scientific) and placed at 80°C for 24 hrs. Cells were subsequently transferred to liquid nitrogen for permanent storage.

Appendix D (Chapter 4)

The Gandel Charitable Trust Sequencing Centre

Cell Line Identification and Authentication Results

Client Name: Irene Papageorgiou
Date samples processed: 8th August 2016
Database search date: 9th August 2016

STR Profiling: PowerPlex HS16 System kit - Promega is used to amplify 15 loci and Amelogenin in a single tube and provides loci consistent with major worldwide STR databasing standards.

Database used for cell line identification: ATCC, DSMZ

- STR profiles of select human cell lines are offered through cell banks from Germany (DSMZ), ECACC (UK), Japan (JCRB and RIKEN) and USA/Europe (ATCC/LGC) offer public data. We provide the top three search results from the ATCC database

- The STR profile of a cell line sample being investigated should match with the reference STR profile for the same cell line at ≥80 % of alleles from the 8 core STR loci, provided that optimized validated kits and protocols are used.

Cell Line can be authenticated	A cell line can be considered to be authenticated when ≥80 % of the alleles in its STR profile match profiles from tissue or other cell line
Cell line is misidentified	A cell line is considered misidentified when ≥80 % of the alleles in its STR profile match a cell line in the database from a different donor. Similarly, a cell line is considered misidentified if it fails to match tissue or other cell line samples known to be come from the same donor.
Cell line nomenclature	A cell line knowledge base that can be accessed at http://clkb.ncibi.org has been created to determine if a given cell line name exists, and if it does, the number of different cell lines which have the same name.

References

1. ATCC SDO, Authentication of Human Cell Lines: Standardization of STR Profiling ATCC SDO document ASN-0002. Manassas, VA: ATCC Standards Development Organization, 2011.

Issue Date: 26.06.12 QS3-Cell line report-1

Sample Name	Unique Laboratory Number	Search results using ATCC database
IP-1	16-09485	Search returned 1 record from DSMZ dataset
IP-2	16-09486	Search returned 1 record from ATCC dataset as detailed below
IP-3	16-09487	Search returned 1 record from ATCC dataset as detailed below

Cell Line identified	IP-1 16-09485	DSMZ Number CRL-2923 ECC-1 (EnCA1)		
% match		100%		
PowerPlex® Loci				
D3S1358	16, 17			
TH01	9, 10	9, 10		
D21S11	28			
D18S51	12, 19			
Penta_E	11			
D5S818	10, 11	10, 11		
D13S317	9, 12	9, 12		
D7S820	9, 10	9, 10		
D16S539	9	9		
CSF1PO	11, 12	11, 12		
Penta_D	10, 11			
Amelogenin	X	X		
VWA	14, 17	14, 17		
D8S1179	13, 16			
TPOX	8	8		
FGA	21			

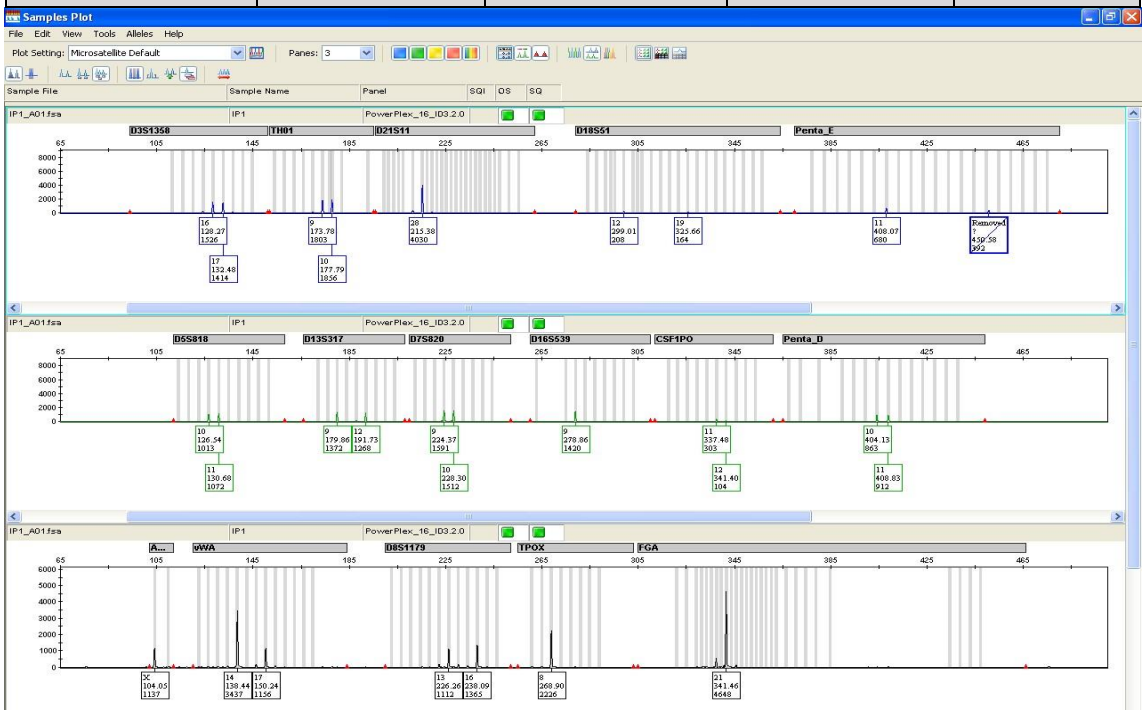

Cell Line identified	IP-2 16-09486	ATCC Number CRL-2616 VK2/E6E7		
% match		100%		
PowerPlex® Loci				
D3S1358	17			
TH01	7, 9.3	7, 9.3		
D21S11	29, 31.2			
D18S51	17, 19			
Penta_E	7, 8			
D5S818	9, 10	9, 10		
D13S317	9, 12	9, 12		
D7S820	10, 11	10, 11		
D16S539	9	9		
CSF1PO	10, 11	10, 11		
Penta_D	9, 12			
Amelogenin	X	X		
VWA	16	16		
D8S1179	12, 13			
TPOX	11	11		
FGA	19, 25			

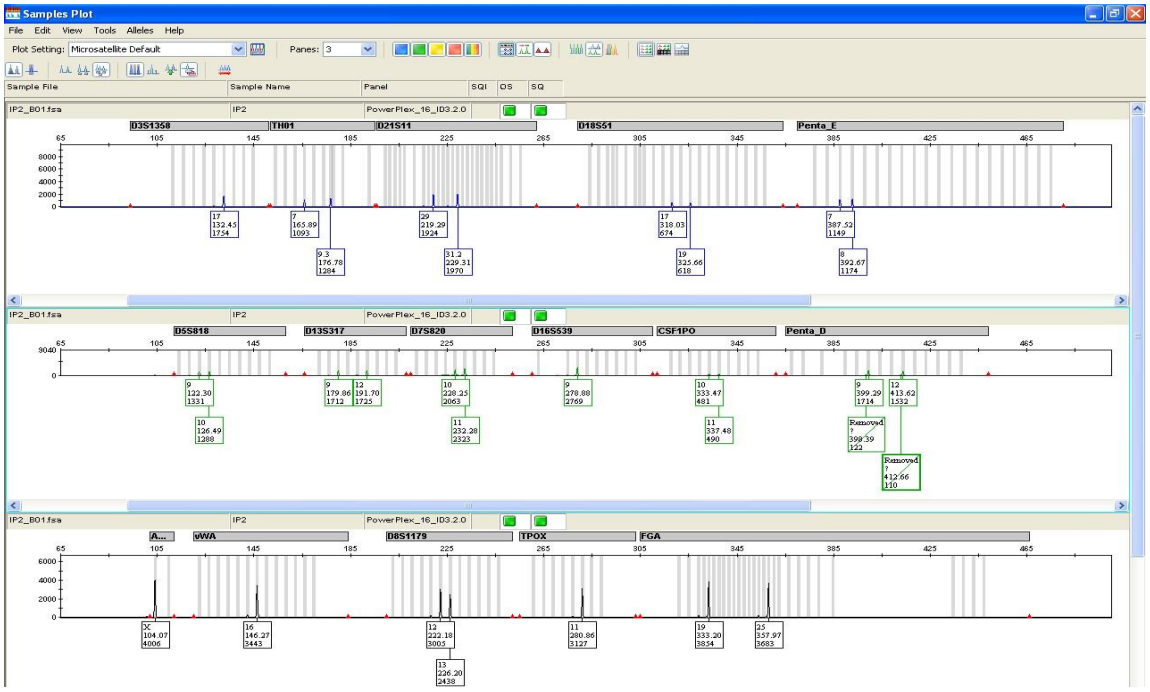

Cell Line identified	IP-3 16-09487	ATCC Number HTB-111 AN3CA		
% match		100%		
PowerPlex® Loci				
D3S1358	17			
TH01	9.3, 10	9.3, 10		
D21S11	29, 30			
D18S51	15, 18			
Penta_E	9, 16			
D5S818	11, 14	11, 14		
D13S317	12, 14	12, 14		
D7S820	7, 10,7.1	7, 10, 7.1		
D16S539	10, 14	10, 14		
CSF1PO	12, 14, 15	12, 14,15		
Penta_D	9, 11			
Amelogenin	X	X		
VWA	14, 20	14, 20		
D8S1179	12, 14			
TPOX	8, 10	8, 10		
FGA	22, 23			

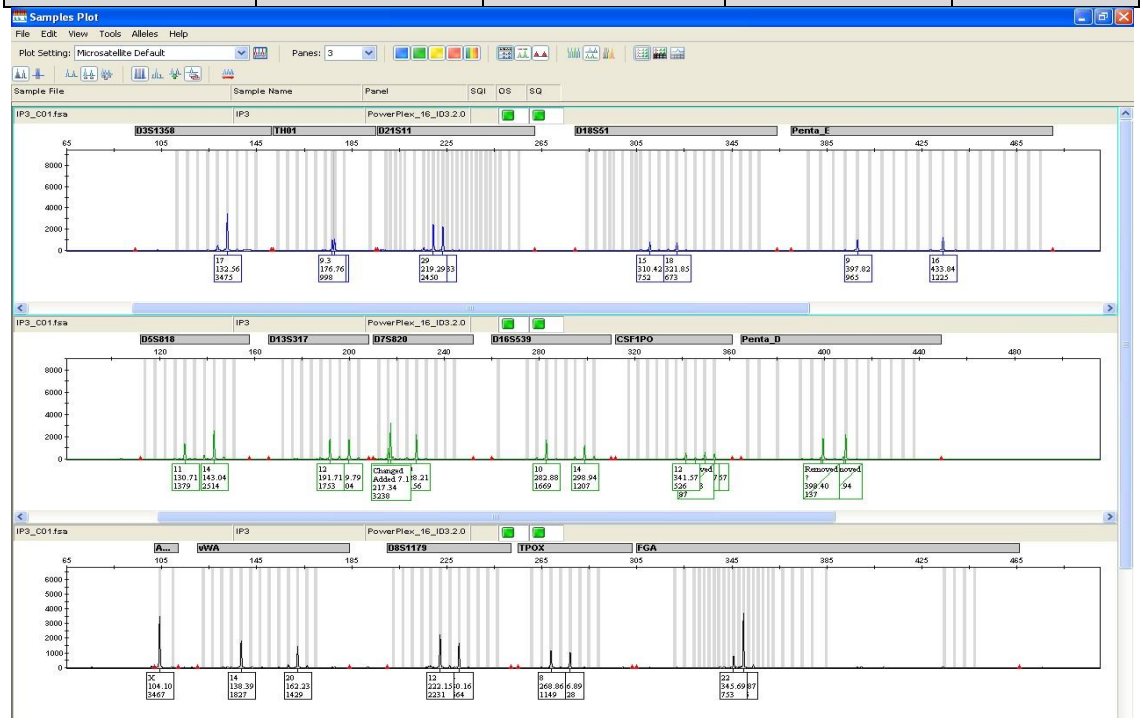

Office use only (Tick indicates checked and passes quality control)

□ Positive control -pass □ Negative control - pass □ Ladder - pass

□ PCR set up 08.08.2016 SR

□ Fragment Analysis 08.08.2016 SR

□ Database Search 09.08.2016 SR

□ Analysis to be checked by 09.08.2016 AG

Appendix E (Chapter 4)

The Gandel Charitable Trust Sequencing Centre

Cell Line Identification and Authentication Results

Client Name:	Irene Papageorgiou
Date samples processed:	03.02.2016
Database search date:	08.02.2016
STR Profiling:	PowerPlex HS16 System kit - Promega is used to amplify 15 loci and Amelogenin in a single tube and provides loci consistent with major worldwide STR databasing standards.

Database used for cell line identification: ATCC

- STR profiles of select human cell lines are offered through cell banks from Germany (DSMZ), ECACC (UK), Japan (JCRB and RIKEN) and USA/Europe (ATCC/LGC) offer public data. We provide the top three search results from the ATCC database

- The STR profile of a cell line sample being investigated should match with the reference STR profile for the same cell line at ≥80 % of alleles from the 8 core STR loci, provided that optimized validated kits and protocols are used.

Cell Line can be authenticated	A cell line can be considered to be authenticated when ≥80 % of the alleles in its STR profile match profiles from tissue or other cell line
Cell line is misidentified	A cell line is considered misidentified when ≥80 % of the alleles in its STR profile match a cell line in the database from a different donor. Similarly, a cell line is considered misidentified if it fails to match tissue or other cell line samples known to be come from the same donor.
Cell line nomenclature	A cell line knowledge base that can be accessed at http://clkb.ncibi.org has been created to determine if a given cell line name exists, and if it does, the number of different cell lines which have the same name.

References

1. ATCC SDO, Authentication of Human Cell Lines: Standardization of STR Profiling ATCC SDO document ASN-0002. Manassas, VA: ATCC Standards Development Organization, 2011.

Issue Date: 26.06.12 QS3-Cell line report-1

Sample Name	Unique Laboratory Number	Search results using ATCC database
Irene1_HEC-1A	16-01022	Cell line is cross-contaminated*
Irene2_HEC-1A	16-01023	Cell line is cross-contaminated*
Irene3_AN3-CA	16-01024	Cell line is cross-contaminated*
Irene4_RL95	16-01025	Search returned 1 records from ATCC dataset as detailed below
Irene3_Ishikawa	16-01026	Cell line is cross-contaminated*

Cell Line identified	Irene1_HEC-1A 16-01022			
% match				
PowerPlex® Loci				
D3S1358	15			
TH01	6,7			
D21IS11	30,31			
D18S51	16,21			
Penta_E	11,12,13			
D5S818	11,15			
D13S317	11			
D7S820	9,11			
D16S539	12			
CSF1PO	10,12			
Penta_D	9,12,13			
Amelogenin	X			
VWA	18,19			
D8S1179	13,14			
TPOX	8,11			
FGA	21,22			

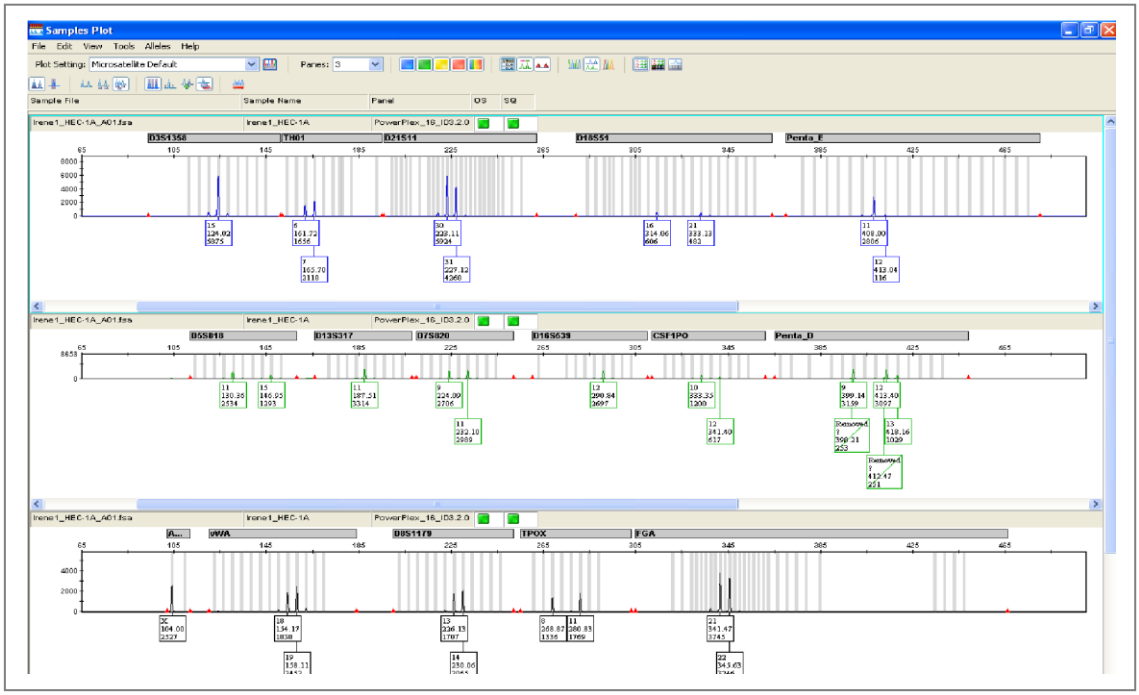

Cell Line identified	Irene2_HEC-1A 16-01023			
% match				
PowerPlex® Loci				
D3S1358	15,16,17			
TH01	6,7			
D21IS11	29,30,31			
D18S51	15,16,21			
Penta_E	9,11,16			
D5S818	11,14,15			
D13S317	11,12			
D7S820	9,10,11			
D16S539	10,12,14			
CSF1PO	10,12			
Penta_D	9,11,12,13			
Amelogenin	X			
VWA	14,18,19,20			
D8S1179	12,13,14			
TPOX	8,10,11			
FGA	21,22,23			

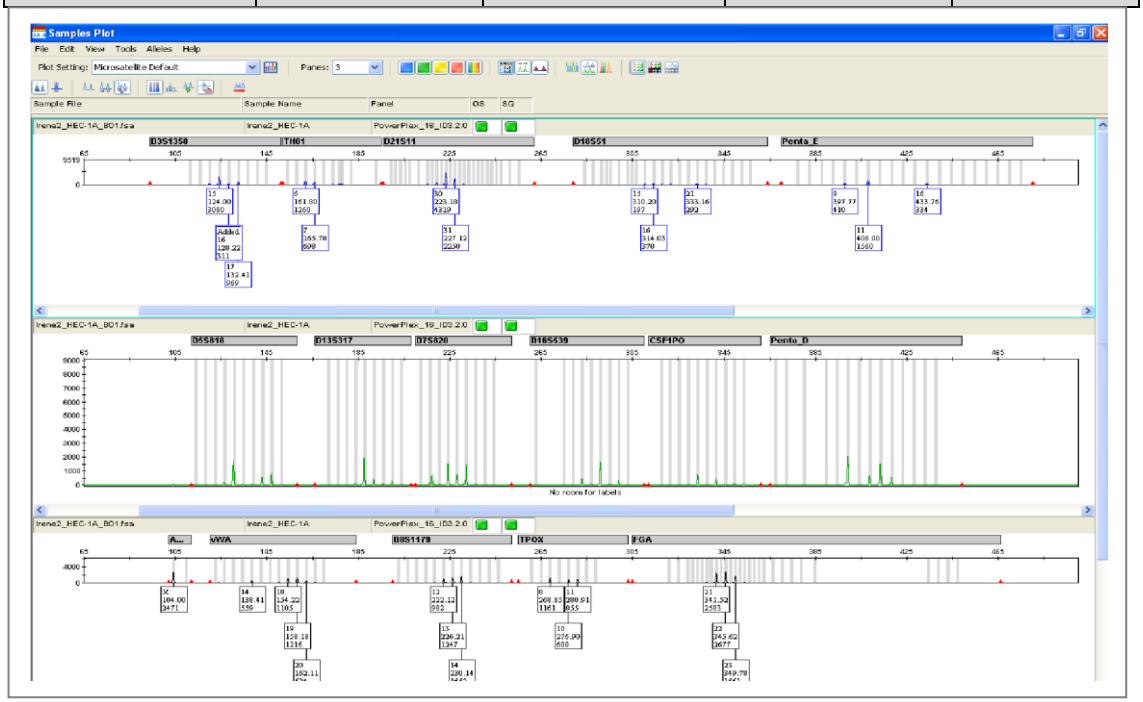

Cell Line identified	Irene3_AN3-CA 16-01024			
% match				
PowerPlex® Loci				
D3S1358	17			
TH01	9.3,10			
D21IS11	29,30			
D18S51	15,18			
Penta_E	9,16			
D5S818	11,14			
D13S317	12,14			
D7S820	7,7.1,10			
D16S539	10,14			
CSF1PO	12,13,14,15			
Penta_D	9,11			
Amelogenin	X			
VWA	14,20			
D8S1179	12,14			
TPOX	8,10			
FGA	22,23			

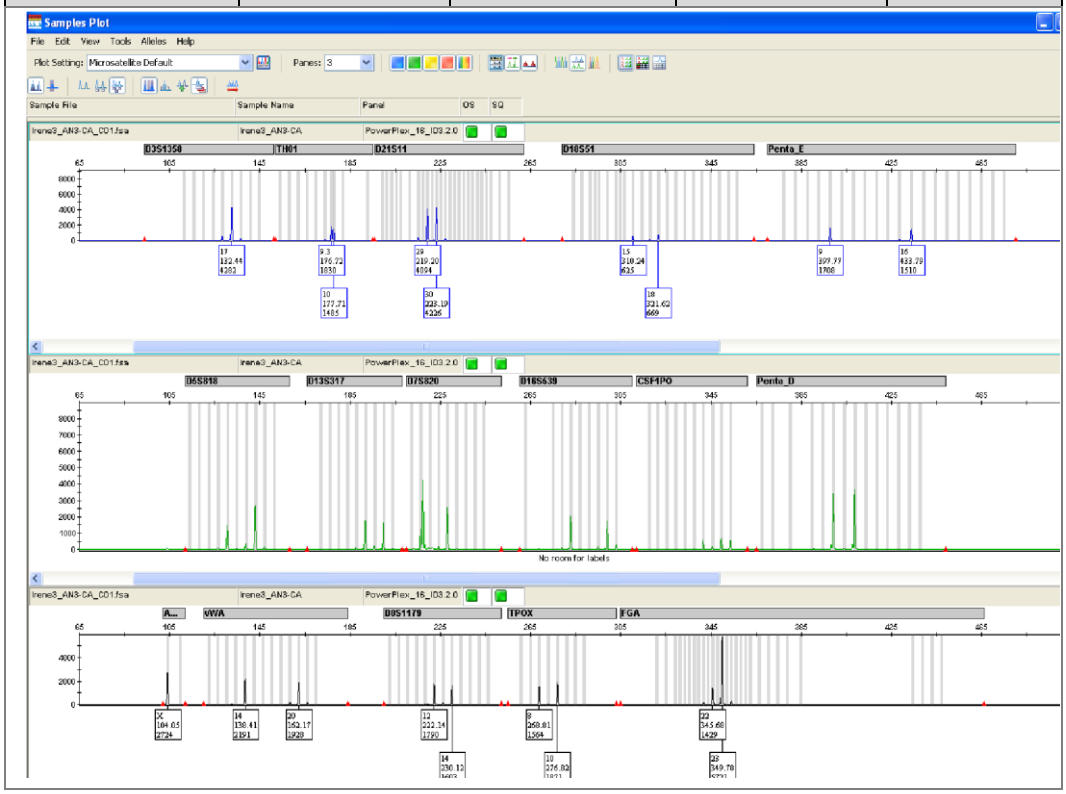

Cell Line identified	Irene4_RL95 16-01025	ATCC Number CRL-1671, RL95-2		
% match		100%		
PowerPlex® Loci				
D3S1358	14,16			
TH01	9,9.3	9,9.3		
D21IS11	28,29			
D18S51	10,14			
Penta_E	5,11			
D5S818	10,11	10,11		
D13S317	8,12	8,12		
D7S820	10	10		
D16S539	11,13	11,13		
CSF1PO	10,11	10,11		
Penta_D	9			
Amelogenin	X	X		
VWA	16,20	16,20		
D8S1179	10,14			
TPOX	8	8		
FGA	20,22			

Cell Line identified	Irene5_Ishikawa 16-01026			
% match				
PowerPlex® Loci				
D3S1358	16,17			
TH01	9,10			
D21IS11	27,28,29			
D18S51	12,19,20			
Penta_E	11,19			
D5S818	10,11			
D13S317	9,13			
D7S820	9,10			
D16S539	9			
CSF1PO	11,12			
Penta_D	10,11			
Amelogenin	X			
VWA	14,17			
D8S1179	12,16			
TPOX	8			
FGA	21			

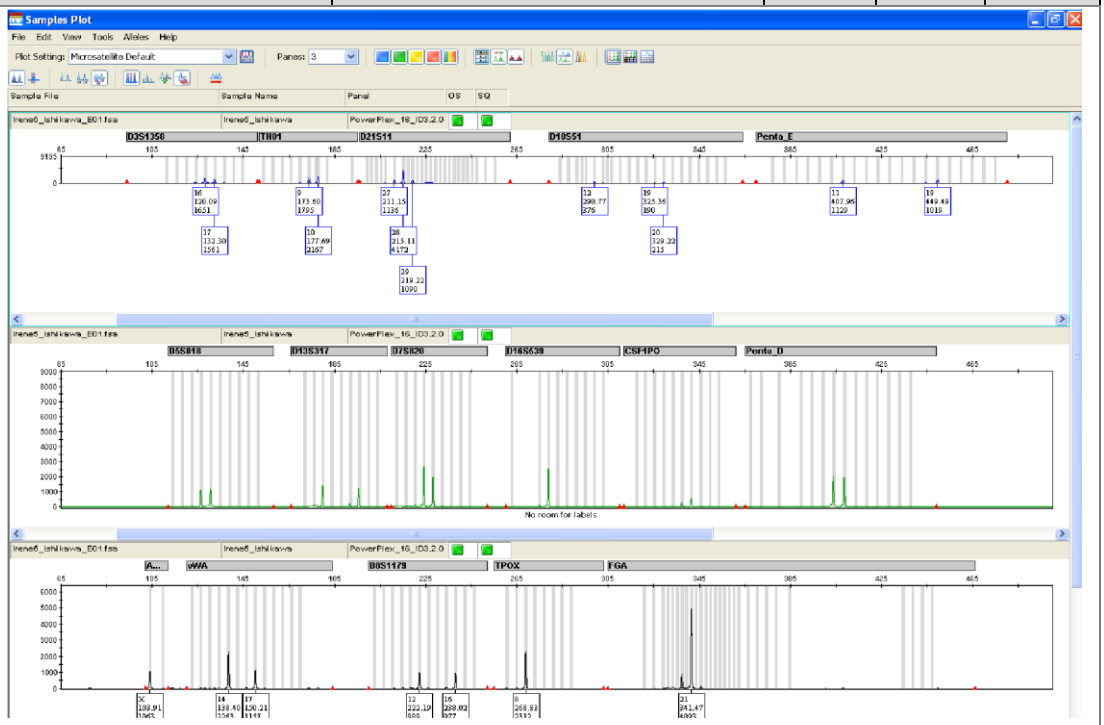

* **<<>> Cell line is cross-contaminated**
Cross-contamination involves the contamination of one human cell line with another during the expansion of a culture.
In its early stages, cellular cross-contamination results in a mixture; in its later stages, rapid growth of the contaminating cell line usually leads to an STR profile more consistent with misidentification.
Mixtures are unusual because the micro-environment of the culture usually favors the contaminating cell line.
However, in some cases the contaminated cell line is observed as distinct STR profiles along with the expected cell. The STR profile of a mixed cross-contaminated culture usually involves more than two alleles at three or more loci.

Ref: ATCC SDO, Authentication of Human Cell Lines: Standardization of STR Profiling ATCC SDO document ASN0002.
Manassas, VA: ATCC Standards Development Organization, 2011.

Office use only (Tick indicates checked and passes quality control)

☐ Positive control -pass ☐ Negative control - pass ☐ Ladder - pass

☐ PCR set up AG 03.02.16

☐ Fragment Analysis AG 03.02.16

☐ Database Search AG 08.02.16

☐ Analysis to be checked by AG 10.02.1